

5-2010

Performance of Nevada's aggregates in alkali-aggregate reactivity of Portland cement concrete

Mohammad Shahidul Islam
University of Nevada Las Vegas

Follow this and additional works at: <https://digitalscholarship.unlv.edu/thesesdissertations>



Part of the [Civil Engineering Commons](#), [Construction Engineering and Management Commons](#), and the [Structural Materials Commons](#)

Repository Citation

Islam, Mohammad Shahidul, "Performance of Nevada's aggregates in alkali-aggregate reactivity of Portland cement concrete" (2010). *UNLV Theses, Dissertations, Professional Papers, and Capstones*. 243. <http://dx.doi.org/10.34917/1452669>

This Dissertation is protected by copyright and/or related rights. It has been brought to you by Digital Scholarship@UNLV with permission from the rights-holder(s). You are free to use this Dissertation in any way that is permitted by the copyright and related rights legislation that applies to your use. For other uses you need to obtain permission from the rights-holder(s) directly, unless additional rights are indicated by a Creative Commons license in the record and/or on the work itself.

This Dissertation has been accepted for inclusion in UNLV Theses, Dissertations, Professional Papers, and Capstones by an authorized administrator of Digital Scholarship@UNLV. For more information, please contact digitalscholarship@unlv.edu.

PERFORMANCE OF NEVADA'S AGGREGATES IN ALKALI-AGGREGATE
REACTIVITY OF PORTLAND CEMENT CONCRETE

by

Mohammad Shahidul Islam

Bachelor of Science
Bangladesh University of Engineering and Technology, Bangladesh
1999

Master of Science
Texas A&M University-Commerce, USA
2003

A dissertation submitted in partial fulfillment
of the requirements for the

**Doctorate of Philosophy Degree in Civil and Environmental
Department of Civil and Environmental Engineering
Howard R. Hughes College of Engineering**

**Graduate College
University of Nevada, Las Vegas
May 2010**

Copyright by Mohammad Shahidul Islam 2010
All Rights Reserved



THE GRADUATE COLLEGE

We recommend the dissertation prepared under our supervision by

Mohammad Shahidul Islam

entitled

Performance of Nevada's Aggregates in Alkali-Aggregate Reactivity of Portland Cement Concrete

be accepted in partial fulfillment of the requirements for the degree of

Doctor of Philosophy in Engineering

Civil and Environmental Engineering

Nader Ghafoori, Committee Chair

Samaan Ladkany, Committee Member

Ying Tian, Committee Member

Pradip Bhowmik, Committee Member

Clay Crow, Graduate Faculty Representative

Ronald Smith, Ph. D., Vice President for Research and Graduate Studies
and Dean of the Graduate College

May 2010

ABSTRACT

Performance of Nevada's Aggregates in Alkali-Aggregate Reactivity of Portland Cement Concrete

by

Mohammad Shahidul Islam

Dr. Nader Ghafoori, Professor, Examination Committee Chair
Department of Civil and Environmental Engineering
University of Nevada, Las Vegas

Alkali-aggregate reaction (AAR) is a form of distress that occurs in concrete and results in serviceability problems, cracks, spalling, and other deterioration mechanisms. There are two categories of AAR, namely, alkali-silica reaction (ASR) and alkali-carbonate reaction (ACR). Alkali-silica reaction is one of the most recognized deleterious phenomena in concrete, and has been a major concern since its discovery in the 1940s. The reaction which occurs between reactive silica or silicates present in some aggregates and alkalis of Portland cement produces an alkali-silica gel that expands in the presence of moisture resulting in concrete cracks. ACR is also a chemical reaction between reactive carbonate rocks and the alkalis present within the cement paste. Alkali-carbonate reaction is not as well-spread as alkali-silica reaction.

The aim of the research study was to (1) examine the extent of the reactivity (expansion) of the aggregates quarried from fourteen different sources in the Southern and Northern Nevada, (2) investigate the ASR-induced losses in the unconfined ultimate compressive strength and stiffness of the concrete cylinders made with the trial aggregates, and (3) apply various mitigation methodologies to suppress the excessive expansion of the reactive aggregates.

The reactive aggregates were identified by conducting different accelerated laboratory testings; namely, ASTM C 1260, modified C 1293, and ASTM C 1105. Afterward, a number of mitigation techniques were employed to control the adverse effect of alkali-aggregate reactivity. The selected mitigation methodologies included the use of the (i) Class F fly ash as a partial replacement of Portland cement, (ii) lithium nitrate in the mixing water, and (iii) combined Class F fly ash and lithium nitrate. Four different dosages of Class F fly ash; namely, 15, 20, 25 and 30% by weight of cement replacement were considered. Up to six dosages of lithium nitrate resulting in the lithium-to-alkali molar ratio ($\text{Li}/(\text{Na}+\text{K})$) of 0.59, 0.74, 0.89, 1.04, 1.18 and 1.33 were used to suppress the excessive expansion of the reactive aggregates. For the third mitigation technique, a constant amount of lithium nitrate with a $\text{Li}/(\text{Na}+\text{K})$ molar ratio of 0.74 was combined with two dosages of Class F fly ash (15% and 20% by weight of cement replacement) to alleviate the excess expansion of the reactive aggregates that could not be controlled by the utilization of lithium nitrate with a $\text{Li}/(\text{Na}+\text{K})$ molar ratio of higher than 0.74.

The laboratory test results reveal that the ASR-induced expansions depend on the aggregate mineralogy, soak solution type and concentration, cement alkalis, and immersion age. The ASR classification of the trial aggregates based on the late-age failure criteria of the test specimens produces more reliable and consistent results when compared to those obtained from the early-age failure criteria. The study also shows that the loss in stiffness due to ASR is more severe than the loss in compressive strength at both early and late-immersion ages. The optimum dosages of Class F fly ash or lithium nitrate in suppressing ASR-induced excess expansions of the reactive aggregates at

different immersion ages varies depending on the aggregate mineralogy, ASR-induced expansion of untreated mortar bars, and the physio-chemical compositions of pozzolan or admixture used. The combined use of standard lithium nitrate dose (lithium-to-alkali molar ratio of 0.74) and a moderate amount (15%) of Class F fly ash (with a CaO content of 7.4% or less) as a partial replacement of Portland cement by weight is sufficiently effective in arresting the excess ASR-induced expansions of the investigated reactive aggregates at all selected immersion ages.

ACKNOWLEDGEMENTS

First and above all, I praise God, the almighty for providing me this opportunity and granting me the capability to proceed successfully.

I would like to express the deepest appreciation to my committee chair, Professor Nader Ghafoori, who continually and convincingly conveyed a spirit of adventure in regard to research and scholarship, and an excitement in regard to teaching. Without his guidance and persistent help, this dissertation would not have been possible. I also wish to extend my acknowledgement to my examination committee members, Dr. Samaan Ladkany, Dr. Ying Tian, Dr. Clay Crow, and Dr. Pradip Bhowmik for their guidance and suggestions.

I would like to acknowledge Nevada Department of Transportation (NDOT) for supplying materials and financial support throughout the research investigation. Thanks are extended to the Southern Nevada Aggregate Association (SNAA) that acted as a liaison between aggregate producers and researchers. Material contributions made by lithium, fly ash and cement producers are also acknowledged.

I thank Mr. Alan Sampson, the research shop technician, for providing unlimited assistance and technical supports during the experimental program. I wish to thank Mrs. Mary Barfield for reviewing my drafts and Mr. Patrick Morehead for being my teammates during the research work.

I need to express my gratitude and deep appreciation to my parents, Mr. Abdul Halim Mollah and Mrs. Mossammat Shamimatun, my brothers and sisters, my wife Mrs. Kamrun Nahar, my relatives and friends for their love and patience throughout my education.

TABLE OF CONTENTS

ABSTRACT.....	iii
ACKNOWLEDGEMENTS.....	vi
LIST OF TABLES.....	xiv
LIST OF FIGURES.....	xvii
CHAPTER 1 INTRODUCTION.....	1
1.1 Alkali-Aggregate Reaction.....	2
1.2 Historical Background of Alkali-Aggregate Reactivity.....	3
1.2.1 Alkali-aggregate reactivity in the United States.....	6
1.2.2 Alkali-silica reactivity in the State of Nevada.....	8
1.3 Alkali-Silica REACTION.....	11
1.3.1 Introduction.....	11
1.3.2 The mechanisms of alkali-silica reactivity	12
1.3.2.1 The chemical reactions due to ASR.....	12
1.3.3 Formation of ASR gel.....	14
1.3.4 Development of ASR cracks	17
1.3.5 Common symptoms of ASR.....	18
1.3.5.1 Map or pattern cracks.....	18
1.3.5.2 Longitudinal cracks.....	19
1.3.5.3 Misalignment cracks	19
1.3.5.4 Exudation	19
1.3.5.5 Pop-out.....	20
1.3.5.6 Spalling	21
1.4 Factors Affecting Alkali-Silica Reaction	21
1.4.1 Reactive forms of silica in aggregates	21
1.4.2 Role of alkalis on alkali-silica reactivity	27
1.4.2.1 Portland cement.....	28
1.4.2.2 Pozzolanic materials.....	30
1.4.2.3 Aggregates.....	31
1.4.2.4 Chemical admixtures.....	31
1.4.2.5 Water	32
1.4.2.6 External sources	32

1.4.3	Role of sufficient moisture on alkali-silica reaction.....	32
1.4.4	Temperature.....	35
1.5	Testing for the Potential Alkali-Silica Reactivity of Aggregates.....	35
1.5.1	Petrographic examination of aggregates.....	35
1.5.2	Chemical tests.....	36
1.5.3	Expansion tests	36
1.5.3.1	ASTM C 227 (Mortar bar method).....	37
1.5.3.2	ASTM C 1260 (Accelerated mortar bar test).....	37
1.5.3.2.1	Modified ASTM C 1260	38
1.5.3.3	ASTM C 1293 (Concrete prism test)	43
1.5.3.3.1	Modifications of ASTM C 1293.....	44
1.6	Preventing ASR Expansion.....	46
1.6.1	Using non-reactive (innocuous) aggregates.....	47
1.6.2	Using mineral admixtures.....	48
1.6.2.1	Blending individual SCMs.....	48
1.6.2.1.1	Effects of fly ash.....	48
1.6.2.1.1.1	The advantages of fly ash	50
1.6.2.1.1.2	Studies on Class F fly ash to suppress ASR	52
1.6.2.1.2	Effects of slag	60
1.6.2.1.3	Effects of silica fume.....	61
1.6.2.1.3.1	Advantages of silica fume.....	62
1.6.2.2.3.2	Studies on silica fume to suppress ASR expansion	62
1.6.2.2	Ternary blends of SCMs	63
1.6.3	Using chemical admixtures.....	64
1.6.3.1	Mechanisms of lithium salts to suppress ASR.....	66
1.6.3.1.1	Lithium may alter ASR product compositions	67
1.6.3.1.2	Lithium may reduce silica dissolution.....	68
1.6.3.1.3	Lithium may re-polymerize ASR gel	71
1.6.3.2	Studies on lithium salts to suppress ASR expansion	72
1.6.4	Combining SCMs and chemical admixtures to control ASR	79
1.6.5	Adding air entrainment.....	81
1.6.6	Adding steel fibers.....	82
1.7	Effects of ASR on Mechanical Properties of Concrete.....	82
1.8	Alkali-Carbonate Reaction.....	88
1.8.1	Introduction.....	88

1.8.1.1	Reactions caused by nondolomitic carbonate rocks.....	89
1.8.1.2	Reactions caused by moderate or highly dolomitic carbonate rocks.....	89
1.8.1.3	Reactions caused by impure dolomite rocks.....	89
1.8.2	The mechanisms of ACR (Dedolomitization reaction)	90
1.8.3	Rim-silification reaction	91
1.9	Factors Affecting Alkali-Carbonate Reactivity.....	92
1.10	Testing for the Potential Alkali-Carbonate Reactivity of Aggregates	93
1.12	Research Objectives	95
1.13	Research Significance.....	97

CHAPTER 2 MATERIALS PREPARATION AND

	EXPERIMENTAL PROGRAM	101
2.1	Experimental Program.....	101
2.2	Materials Preparation	101
2.2.1	Collecting aggregates.....	103
2.2.2	Washing and drying aggregates.....	103
2.2.3	Crushing aggregates.....	103
2.2.3	Crushing aggregates.....	104
2.2.4	Sieving aggregates	104
2.2.5	Grading aggregates	106
2.3	Aggregate Classifications Based on Mineralogy	106
2.3	Testing Materials.....	109
2.3.1	Sodium hydroxide pellet.....	109
2.3.2	Portland cement	110
2.3.3	Class F fly ash.....	110
2.3.4	Lithium nitrate	110
2.4	Testing Equipment	112
2.4.1	Concrete mixer.....	112
2.4.2	Length comparator.....	113
2.4.3	Flow table	113
2.4.4	Bar molds.....	114
2.4.5	Compressometer and concrete compression machine	115
2.4.6	Oven.....	117
2.4	Testing Methods and Experimental Programs	117
2.4.1	Assessing alkali-aggregate reactivity	117
2.4.1.1	Assessing alkali-silica reactivity.....	119

2.4.1.1.1	ASTM C 1260 and modified ASTM C 1260	119
2.4.1.1.2	Modified ASTM C 1293	122
2.4.1.2	Assessing alkali-carbonate reactivity.....	123
2.4.2	Loss of ultimate compressive strength and modulus of elasticity ...	125
2.4.3	Mitigating ASR-induced expansion	125
2.4.3.1	Use of Class F fly ash	126
2.4.3.2	Use of lithium nitrate to the mixture water	128
2.4.3.3	Use of combined Class F fly Ash and lithium nitrate	130
CHAPTER 3 IDENTIFICATION OF REACTIVE AGGREGATES.....		133
3.1	Determining ASR using ASTM C 1260 (Mortar Bar).....	133
3.1.1	Expansion Progression as Related to Soak Solution Concentrations	135
3.1.2	Alkali-silica reactivity of ASTM C 1260 for the 1N solution.....	138
3.1.3	Comparison of crushed coarse and fine aggregates reactivity.....	142
3.1.4	Determination of the failure criteria of ASTM C 1260 for the 0.5 and 0.25N solutions.....	145
3.1.5	Aggregate classifications based on the failure criteria of ASTM C 1260 for the 0.5N solution.....	150
3.1.6	Aggregate classifications based on the failure criteria of ASTM C 1260 in 0.25N Solution	153
3.1.7	Role of soak solution concentrations on the expansion of ASTM C 1260	155
3.1.7.1	Expansion ratio as related to solution strength and immersion age.....	157
3.1.7.2	Expansion of ASTM C 1260 for the three solution concentrations as presented in ternary diagram.....	160
3.1.7.3	ASR-induced cracks on the mortars as related to soak solution strength.....	164
3.1.8	Role of cement alkali on the expansion of mortar bars	164
3.1.8.1	ASR expansion as related to cement alkalis and immersion ages	166
3.1.8.2	Expansion of ASTM C 1260 as related to cement alkalis as presented in ternary diagram.....	171
3.1.8.2.1	1N NaOH soak solution.....	172
3.1.8.2.2	0.5N NaOH soak solution.....	173
3.1.8.2.3	0.25N NaOH soak solution.....	175
3.1.9	Summary alkali-silica reactivity of mortar bars made with three rates of cement alkali for the 1, 0.5 and 0.25N solutions.....	177

3.2	ASR Using Modified ASTM C 1293	181
3.2.1	Prisms Submerged in the 1N NaOH at 80°C (ASTM C 1293M1)..	182
3.2.1.1	Determination of the failure criteria of ASTM C 1293M1 .	184
3.2.1.2	ASR-induced cracks on the surface of alkali-cured prisms	186
3.2.2	Prisms submerged in the distilled water at 80°C (ASTM C 1293M2).....	190
3.2.2.1	Determination of the failure criteria of ASTM C 1293M2 .	190
3.2.3	Comparison of aggregate classifications based on the two modifications of ASTM C 1293	196
3.4	Concluding Remarks on the Alkali-Aggregate Reactivity	197
CHAPTER 4 LOSS IN MECHANICAL PROPERTIES DUE TO ASR		201
4.1	Loss in Ultimate Compressive Strength Due to ASR	202
4.1.1	Failure criteria due to loss in compressive strength.....	208
4.1.1.1	Failure criteria of the 28-day loss in compressive strength of alkali-cured cylinders.....	208
4.1.1.2	Failure criteria of the 6-month loss in compressive strength of alkali-cured cylinders.....	208
4.1.1.3	Failure criteria due to the loss in compressive strength of the alkali-cured cylinders between 28 days and 180 days.....	213
4.1.2	Trial aggregate classifications based on the proposed failure criteria of loss in compressive strength	214
4.2	Loss in Modulus of Elasticity Due to ASR	216
4.2.1	Determination of the failure criteria based on the loss in stiffness..	218
4.2.1.1	Failure criteria of 28-day loss in stiffness of alkali-cured cylinders.....	218
4.2.1.2	Failure criteria of the 6-month loss in stiffness of alkali-cured cylinders.....	220
4.2.1.3	Failure criteria of the loss in stiffness of the alkali-cured cylinders between the ages of 28 and 180 days	224
4.2.1.4	Alkali-silica reactivity of the trial aggregates based on the proposed failure criteria of loss in stiffness.....	224
4.5	Failure Mechanisms of Concrete Cylinders due to ASR	228
4.6	Aggregate Classifications Based on Eight Evaluation Methods	231
CHAPTER 5 CONTROLLING ASR EXPANSION.....		236
5.1	Blending Class F Fly Ash as a Partial Replacement of Portland Cement....	236
5.1.1	Introduction.....	236
5.1.2	ASR-induced cracks of the mortar bars as related to various fly ash dosages.....	244

5.1.3	Reduction in expansion of the mortar bars made with fly ash dosages	243
5.1.4	Effect of chemical compositions of Class F fly ash on ASR expansion.....	250
5.1.4.1	Effect of equivalent SiO_2 of the SCMs on ASR expansion	253
5.1.4.2	Effect of equivalent CaO content of the mortar bars on the ASR expansion	260
5.1.4.3	Effect of the ratio of equivalent CaO to equivalent SiO_2 of the mortar bars on ASR expansion	261
5.2	Adding Lithium Nitrate to the Mixing Water	264
5.2.1	ASR-related cracks as function of lithium dosages.....	270
5.2.1	Reduction in expansion of the lithium-bearing mortar bars	270
5.2.3	Analytical model to determine the optimum lithium dosages to control ASR.....	278
5.3	The Combined Use of Class F Fly Ash and Lithium Nitrate Salt.....	286
5.3.1	ASR expansion of the fly-ash and lithium-bearing mortar bars as related to the immersion ages.....	287
5.3.2	The reduction in expansion of the mortars containing fly ash, lithium, and the combined fly ash and lithium as related to the test durations.....	290
5.4	Comparison of the Three Mitigation Techniques in Suppressing ASR	298
CHAPTER 6 CONCLUSION AND RECOMMENDATION.....		301
6.1	Identification of Reactive Aggregates.....	301
6.1.1	ASR-induced expansions under ASTM C 1260 for the 1N solution	301
6.1.2	Influence of soak solution (NaOH) concentration on ASR-induced expansion	302
6.1.3	Influence of immersion age on the expansion of mortar bars under various soak solutions	305
6.1.4	Influence of cement alkalis on ASR-induced expansion.....	305
6.1.5	ASR-induced expansions under modified ASTM C 1293	306
6.1.6	Influence of aggregate mineralogies on ASR.....	307
6.2	Loss in Mechanical Properties due to ASR.....	307
6.3	Mitigating Techniques to Suppress ASR	309
6.3.1	Role of Class F fly ash on ASR expansions	310
6.3.2	Role of lithium salt in suppressing ASR.....	311
6.3.3	Role of combined fly ash and lithium nitrate to suppress ASR.....	312
6.3.4	ASR-related cracks of the fly ash and lithium bearing mortar bars	313

6.5 Recommendations for Future Studies	314
APPENDIX A CHAPTER 3 DATA..	315
APPENDIX B CHAPTER 4 DATA.....	329
APPENDIX C CHAPTER 5 DATA.....	332
APPENDIX D FIGURES.....	339
BIBLIOGRAPHY.....	343
VITA.....	361

LIST OF TABLES

Table 1.1	Minerals and rocks susceptible to ASR (Bérube & Fournier, 1993)	24
Table 1.2	Summary of findings on major rock types (mineralogy) susceptible to ASR	25
Table 1.3	The 14-day expansion criterion of the mortar bars for different soak solution strengths with corresponding $\text{Na}_2\text{O}_{\text{eq}}$ in the mortars	43
Table 1.4	Chemical information for Li^+ , Na^+	69
Table 1.5	Summary of findings on lithium salts in suppressing ASR expansion (Feng et al., 2005)	78
Table 1.6	Compressive strength and modulus of elasticity of normal and high strength concretes (Marzouk and Langdon, 2003)	86
Table 2.1	Crushed aggregate gradation for mortar bar specimens	106
Table 2.2	Coarse aggregate gradation for prism	106
Table 2.3	The identification, chemical composition and rock type of the selected aggregates	107
Table 2.4	The ASR reactivity of rock types used for research investigation	108
Table 2.5	Physico-chemical properties of Type V Portland cement	111
Table 2.6	Physico-chemical properties of Class F fly ash	111
Table 2.7	Physico-chemical properties of LiNO_3 solution	112
Table 2.8	ASTM C 1260 and its modifications for each rate of cement alkali	120
Table 2.9	Constituents and properties of mortar bars for ASTM C 1260 and modified C 1260	121
Table 2.10	Modifications of ASTM C 1293 with failure criteria	123
Table 2.11	Mixture constituents for concrete prisms and cylinders	124
Table 2.12	Mixture constituents of mortar bars containing Class F fly ash	127
Table 2.13	Lithium- to- alkali molar ratio (%Li dose) of mortars with corresponding soak solution's constituents	129
Table 2.14	Mixture constituents of mortars containing lithium nitrate for the aggregates quarried from Southern Nevada	130
Table 2.15	Mixture constituents of mortars containing lithium nitrate for the aggregates quarried from Northern Nevada	131
Table 2.16	Lithium nitrate and Class F dosage of mortars with corresponding soak solution's constituents	132
Table 2.17	Mixture constituents of mortars containing Class F fly ash and lithium nitrate	132
Table 3.1	Aggregate classifications based on ASTM C 1260 for the 1N Solution	140
Table 3.2	Statistical data for Equation 3.2, and the failure criteria of ASTM C 1260 for the 0.5N solution at various immersion ages	147
Table 3.3	Statistical data for Equation 3.3, and the failure criteria of the mortar bars for the 0.25N soak solution at various immersion ages	150
Table 3.4	Comparison of aggregate classifications based on the failure criteria of ASTM C 1260 for the 1 and 0.5N soak solutions at various immersion ages	152

Table 3.5	Comparison of aggregate classifications based on the failure criteria of ASTM C 1260 for the 1 and 0.25N soak solutions at various immersion ages	154
Table 3.6	Statistical data for Equation 3.4 and the failure criteria of the mortar bars prepared with 0.84% cement alkali	169
Table 3.7	Statistical data for Equation 3.4 and the failure criteria of the mortar bars prepared with 1.26% cement alkali	169
Table 3.8	Levels of alkali-silica reactivity of the selected aggregates	178
Table 3.9	Number of reactive aggregates (from the fourteen investigated aggregates) based on the suggested failure criteria.....	180
Table 3.10	Aggregate classifications based on the failure criteria of ASTM 1293M1 (prisms submerged in the 1N NaOH at 80°C).....	186
Table 3.11	Statistical data for Equation 3.7 and the failure criteria of water-cured prisms at various immersion ages	192
Table 3.12	Aggregate classifications based on the failure criteria of the water-cured prisms at 80°C (ASTM C 1293M2).....	193
Table 3.13	Comparison of aggregate classifications based on the failure criteria of modified ASTM C 1293	195
Table 3.14	Alkali-carbonate reactivity of the fourteen investigated aggregates	196
Table 3.15	Levels of alkali-aggregate reactivity of the investigated aggregates.....	198
Table 4.1	ASR classifications of the trial aggregates and percent loss in compressive strength.....	206
Table 4.2	Statistical parameters for Equation 4.1, and the failure criteria of the 6-month loss in compression strength of alkali-cured cylinders	210
Table 4.3	Statistical parameters for Equation 4.2, and the failure criteria due to the 6-month loss in compressive strength	212
Table 4.4	Loss in compressive strength (LICS) and aggregate classifications.....	215
Table 4.5	ASR classifications of the trial aggregates and percent loss in stiffness	219
Table 4.6	Statistical parameters for Equation 4.4, and the failure criteria of the 6-month loss in stiffness of alkali-cured cylinder.....	221
Table 4.7	Statistical parameters for Equation 4.5, and the failure criteria due to the 6-month loss in stiffness of alkali-cured cylinders	223
Table 4.8	Loss in stiffness (LIS) for each aggregate and the classification of ASR of the trial aggregate	225
Table 4.9	ASR classifications of the trial aggregates based on the loss in mechanical properties (compressive strength and stiffness).....	227
Table 4.10	ASR classifications of the trial aggregates based on rock mineralogy, the expansions of mortar bars at early and extended immersion ages and those of alkali-cured prisms at 28 days and extended immersion ages, loss in mechanical properties	234
Table 5.1	Minimum dosage of Class F fly ash to suppress ASR expansion	242
Table 5.2	$\text{SiO}_{2(\text{eq})}$, CaO_{eq} and $\text{CaO}_{\text{eq}}/\text{SiO}_{2(\text{eq})}$ of SCMs in the mortar bars	252
Table 5.3	The statistical data for Equation 5.6 for each trial reactive aggregate at various immersion ages.....	255
Table 5.4	The optimum fly ash content for the trial aggregates to suppress ASR expansion at the immersion age of 14 days	258

Table 5.5	The optimum analytical fly ash dosages to suppress ASR expansion at 28 days	258
Table 5.6	The optimum analytical fly ash dosages to suppress ASR expansion at 56 days	259
Table 5.7	Comparison between the experimental fly ash dosages (EFA) and the analytical fly ash dosages (AFA), evaluated by using the equivalent SiO_2 content of the mortar bar, to inhibit ASR at different immersion ages...	260
Table 5.8	Comparison between the experimental fly ash dosages (EFA), and the analytical fly ash dosages, evaluated by using the equivalent CaO content of the mortar bar, to inhibit ASR at the immersion ages of 14, 28 and 56 days	262
Table 5.9	Comparison between the optimum analytical fly ash dosage (AFA), evaluated by using the ratio of equivalent CaO to equivalent SiO_2 content of the mortar bars, and the experimental fly ash dosages (EFA) to inhibit ASR at the immersion ages of 14, 28 and 56 days	263
Table 5.10	Optimum analytical Class F fly ash dosage to suppress ASR expansion based on the equivalent SiO_2 , CaO and CaO/SiO_2 of the mixture at the extended failure criteria	264
Table 5.11	Optimum experimental lithium dosage to suppress ASR expansion at 14, 28 and 56 days	269
Table 5.12	Statistical data for Equation 5.13 at the immersion age of 14 days.....	280
Table 5.13	Statistical data for Equation 5.13 at the immersion age of 28 days.....	281
Table 5.14	Statistical data for Equation 5.13 at the immersion age of 56 days.....	281
Table 5.15	Statistical data for Equation 5.14 at various immersion ages	282
Table 5.16	Statistical data for Equation 5.15 at various immersion ages	282
Table 5.17	Statistical data for Equation 5.16 at various immersion ages	283
Table 5.18	Analytical lithium dosage to suppress ASR expansion below 0.10% at the immersion age of 14 days	283
Table 5.19	Analytical lithium nitrate dosage to suppress ASR expansion at the immersion age of 28 days	284
Table 5.20	Analytical lithium nitrate dosages to suppress ASR expansion at the immersion age of 56 days	284
Table 5.21	Optimum experimental and analytical lithium nitrate dosages to control ASR expansion at the immersion ages of 14, 28 and 56-days.....	286
Table 5.22	Regression parameters for Equation 5.17 at various immersion ages	296
Table 5.23	Minimum dosage of Class F fly ash, lithium nitrate, and the combination of fly ash and lithium nitrate at 14, 28 and 56 days.....	300

LIST OF FIGURES

Figure 1.1	Number of publications concerning alkali-aggregate reactivity and published year (Data retrieved from Diamond, 1992).....	6
Figure 1.2	Reported case of ASR in the United States (FHWA-RD-03-047, 2003)....	8
Figure 1.3	ASR cracks in the concrete of Hoover Dam (Hobbs, 1988)	10
Figure 1.4	Attack of alkali solution on lattice structure of aggregate.....	13
Figure 1.5	Ternary diagram plotted normalized compositions ASR products (Hanson et al., 2003).....	16
Figure 1.6	Typical symptoms of ASR	20
Figure 1.7	Effects of different siliceous rocks and mineral on the expansion of Portland cement mortar bars containing high-alkali cement (Blanks & Kennedy, 1955)	23
Figure 1.8	Silicon tetrahedron (silicate).....	26
Figure 1.9	Quartz (silica) structure	27
Figure 1.10	Effect of cement alkali on expansion using ASTM C 1293 (Thomas, 2002)	29
Figure 1.11	Effect of relative humidity on expansion using ASTM C 1293 (Pedneault, 1996)	33
Figure 1.12	The influence of water-to-cement ratio on the ASR expansion of concrete (Stark, 1995).....	34
Figure 1.13	Expansion of C 1260 for 1, 0.5 and 0.25N solutions (Shon et al., 2002). ..	40
Figure 1.14	Projected failure criterion to determine safe cement alkali level for deleterious aggregates (Stark, 1993).....	42
Figure 1.15	Effect of fly ash composition and replacement level on ASR expansion (Shehata & Thomas, 2000)	55
Figure 1.16	Effect of 14-day AMBT expansion and equivalent SiO ₂ content of the mortars (Malvar & Lenke, 2006)	57
Figure 1.17	Effect of equivalent CaO content on 14-day AMBT expansion (Malvar & Lenke, 2006)	58
Figure 1.18	Effect of normalized CaO _{eq} /SiO _{2(eq)} on 14-day expansion (Malvar & Lenke, 2006)	59
Figure 1.19	14-day expansion of AL quarry and (alkali+lime)/silica	60
Figure 1.20	Influence of LiNO ₃ at a molar ratio of 0.74 on ASR expansion (Ekolu et al., 2007).....	65
Figure 1.21	Concrete expansions (ASTM C 1293) vs. lithium-to-alkali molar ratios (Thomas et al., 2000)	77
Figure 1.22	Expansion of Placitas aggregate with lithium and fly ash (McKeen et al., 1998)	81
Figure 2.1	Flow chart of experimental program for alkali-aggregate detection and mitigation	102
Figure 2.2	Washing coarse aggregates.....	104
Figure 2.3	Rock crushers	105
Figure 2.4	Digital length comparator.....	114
Figure 2.5	Flow table	115
Figure 2.6	Compressometer	116

Figure 2.7	Fabricated oven along with the heating units and temperature controller	118
Figure 2.8	Mortar bars cured for 24 hours in a moisture room after casting	121
Figure 2.9	Mortar bars stored in NaOH solution at 80°C	122
Figure 2.10	Prisms stored in a moisture room for ASTM C 1105 test	125
Figure 2.11	Cylinders stored in a moisture room at a temperature of 20°C	126
Figure 2.12	Cylinders stored in 1N NaOH solution at a temperature of 80°C	126
Figure 3.1	Expansion of ASTM C 1260 for the 1N solution	135
Figure 3.2	Expansion of ASTM C 1260 for the 0.5N NaOH	136
Figure 3.3	Expansion of ASTM C 1260 for the 0.25N NaOH	137
Figure 3.4	The average expansion of the fourteen aggregates for the 1N solution at various immersion ages.....	139
Figure 3.5	The 14-day expansion of mortar bars prepared with.....	143
Figure 3.6	The mortar bars made with the innocuous aggregate (SN-A).....	144
Figure 3.7	The mortar bars made with the slowly reactive aggregate (NN-A)	144
Figure 3.8	The mortar bars made with the highly reactive aggregate (NN-C)	144
Figure 3.9	14-day expansion of the mortars for the 0.5 and 1N solutions.....	146
Figure 3.10	The expansion of the mortars for the 0.25 and 1N solutions.....	149
Figure 3.11	Effect of soak solution strength on ASR expansion at 14 days.....	156
Figure 3.12	Expansion ratio of the mortar bars for the 0.5 and 1N NaOH soak solutions	158
Figure 3.13	Expansion ratio of the mortars for the 0.25 and 1N NaOH.....	159
Figure 3.14	Influence of soak solution concentrations of ASTM C 1260 at 14 days	161
Figure 3.15	Influence of soak solution concentrations on 98-day ASR expansions of 0.42% cement alkali	163
Figure 3.16	Influence of soak solution concentrations of ASTM C 1260 on ASR-induced cracks for the NN-C aggregate group	165
Figure 3.17	Expansion of mortar bars made with SN-G aggregate and three rates of cement alkalis for the 1N solution.....	166
Figure 3.18	14-day expansion of mortar bars for the 1N solution as related to cement alkalis.....	167
Figure 3.19	Influence of cement alkalis for the three soak solution concentrations..	170
Figure 3.20	Influence of cement alkalis on the expansion of ASTM C 1260 for the 1N solution at the immersion age of 14 days.....	173
Figure 3.21	Influence of cement alkalis on the expansion of ASTM C 1260 for the 0.5N solution at the immersion age of 14 days.....	174
Figure 3.22	Influence of cement alkalis on the expansion of ASTM C 1260 for the 0.5N solution at the immersion age of 98 days.....	175
Figure 3.23	Influence of cement alkalis on the expansion of ASTM C 1260 for the 0.25N solution at the immersion age of 14 days.....	176
Figure 3.24	Influence of cement alkalis on the expansion of ASTM C 1260 for the 0.25N solution at the immersion age of 98 days.....	177
Figure 3.25	Expansion of alkali-cured prisms at 80°C (C 1293M1)	183
Figure 3.26	ASR expansion of alkaline-cured prisms at the immersion ages of 4, 8, 13 and 26 weeks.....	184
Figure 3.27	Prism containing innocuous aggregate (SN-A).....	187

Figure 3.28	Prism containing highly reactive aggregate (NN-B).....	187
Figure 3.29	Aggregates popped-out from the prism of highly reactive aggregate (SN-G).....	188
Figure 3.30	Expansion of concrete prisms submerged in water at 80°C.....	190
Figure 3.31	ASR expansion of water-cured prisms at the immersion ages of 4, 13 and 26 weeks.....	191
Figure 4.1	Stress-strain curve of the cylinders prepared with innocuous aggregate (SN-A).....	205
Figure 4.2	Stress-strain curves of the cylinders made with reactive aggregate (NN-C).....	207
Figure 4.3	The 6-month loss in alkali-cured compressive strength as related to the expansion of the mortar bars at 14 days.....	209
Figure 4.4	The 6-month loss in compressive strength of alkali-cured cylinder as related to the expansion of the alkali-cure prisms at 4 weeks.....	211
Figure 4.5	Loss in compressive strength of alkali-cured cylinders at 6 months and that of the alkali-cured cylinders between the ages of 28 days and 180 days	214
Figure 4.6	The 6-month loss in stiffness (alkali-cured vs. water-cured) as related to the expansion of the mortar bars at 14 days.....	221
Figure 4.7	The loss in stiffness at 6 months of alkali-cured cylinder as related to the expansion of the alkali-cure prisms at 4 weeks.....	223
Figure 4.8	The 6-month loss in stiffness of alkali-cured cylinders as related to the loss in stiffness of alkali-cured cylinders between the ages of 28 and 180 days	225
Figure 4.9	ASR-induced cracks on the surface of the 6-month alkali-cured cylinders made with the (a) innocuous aggregate (SN-E), (b) reactive aggregate (NN-C)	229
Figure 4.10	Failure mode of the 6-month alkali-cured cylinders prepared with the (a) the innocuous aggregate (SN-A), and (b) reactive aggregate (SN-G).....	231
Figure 5.1	Effect of Class F fly ash on the ASR expansion of SN-F aggregate.....	238
Figure 5.2	The 14-day expansion of mortar bars prepared with trial aggregates and various amounts of Class F fly ash dosages.....	239
Figure 5.3	The 28-day expansion of mortar bars prepared with trial aggregates and various amounts of Class F fly ash dosages.....	239
Figure 5.4	The 56-day expansion of the mortar bars prepared with trial aggregates and various amounts of Class F fly ash dosages.....	241
Figure 5.5	Influence of Class F fly ash dosages on ASR cracks	244
Figure 5.6	Reduction in expansion of the mortar bars made with SN-J aggregate and various rates of fly ash dosage	245
Figure 5.7	RIE of the test mortar bars prepared with the 15% fly ash	246
Figure 5.8	RIE of the test mortar bars prepared with the 30% fly ash	247
Figure 5.9	RIE of the test mortar bars made with various fly ash dosages at 14 days	248
Figure 5.10	RIE of the test mortar bars made with various fly ash dosages at 98 days	249

Figure 5.11	The average reduction in expansion (ARIE) of the mortar bars containing eight reactive aggregate and fly ash dosage.....	251
Figure 5.12	The 14-day expansion of the mortar bars made with the NN-D aggregate as related to the $\text{SiO}_{2(\text{eq})}$ of the specimen.....	254
Figure 5.13	The expansion of the untreated mortar bars and the slopes of Equation 5.6 at the immersion age of 14 days.....	256
Figure 5.14	The expansion of the untreated mortar bars and the intercept of Equation 5.6 at the immersion age of 14 days.....	256
Figure 5.15	Linear expansion of the mortar bars made with NN-B aggregate and various lithium dosages.....	265
Figure 5.16	The expansions of the mortar bars made with various lithium dosages at 14 days	266
Figure 5.17	The expansions of the mortar bars containing various lithium nitrate dosages at 28 days.....	267
Figure 5.18	The expansions of the mortar bars prepared with various lithium nitrate dosage at 56 days	268
Figure 5.19	ASR-related cracks on the lithium-bearing mortar bars made with the SN-G aggregate.....	271
Figure 5.20	The reduction in expansion of the mortar bars made with the NN-C aggregate and various lithium dosages	272
Figure 5.21	The reduction in expansion of the mortar bars treated with the lithium-to-alkali molar ratio of 0.59	274
Figure 5.22	The reduction in expansion of the mortar bars treated with the lithium-to-alkali molar ratio of 1.04	274
Figure 5.23	The reduction in expansion of the mortar bars made with various lithium dosages at 14 days	276
Figure 5.24	The reduction in expansion of the mortar bars containing various lithium dosages at 98 days	277
Figure 5.25	Average reduction in expansion of the seven reactive aggregates and various lithium dosages.....	278
Figure 5.26	The 14-day expansion of the mortar bars containing SN-F aggregate and various lithium dosages.....	279
Figure 5.27	Linear expansion of the SN-G aggregate containing fly ash and lithium nitrate individually and jointly.....	288
Figure 5.28	The expansion of the treated and untreated mortar bars made with the SN-G aggregate.....	290
Figure 5.29	Reduction in expansion of the mortar bars containing various mitigation techniques of suppressing ASR (14 days)	291
Figure 5.30	Reduction in expansion of the mortar bar containing NN-B aggregate treated with 15 and 20% fly ash, 100% Li, 15%FA+100%Li and 20%FA+100%Li at various ages	292
Figure 5.31	Reduction in expansion of the treated mortar bars at 98 days.....	293
Figure 5.32	The 98-day mortar bars made with NN-B aggregate, fly ash, lithium, and the combination of fly ash and lithium	295

Figure 5.33	Comparison of the results obtained from the experimental and analytical method for the mortar bars containing combined fly ash and lithium salt.....	297
Figure 5.34	The reduction in expansion of the treated mixtures at various immersion ages	300

This dissertation is dedicated to
my mother,
my sister Mahmuda Begum, and
my brothers Faruque Hossain and Wahidul Islam.

CHAPTER 1

INTRODUCTION

The rapid growth of the global population and increased urbanization during the 20th and 21st centuries has generated a high demand of new construction work. The abundance, availability and economy of materials used in cement-based concrete are a great concern for future construction. Since the end of the 19th century, a tremendous number of investigations have been conducted throughout the world on cement-based concrete and its characteristics in order to improve the strength and serviceability qualities of the materials used in concrete construction.

In the present day, concrete is the most widely-used construction material in the world. It consists of particles of aggregate, water, and a binding agent (cement and other cementitious materials). The reactions between aggregates and binding agents are extremely complex. Troublesome reactions can take place between the alkalis in the cement and calcium- and silica-rich minerals in the aggregates. Many natural aggregates contain a quantity of amorphous silica and carbonate, which both react with the alkalis of the mixture (Na and K, which usually come from cementitious materials). The reaction can cause deterioration expansion in concrete. This interaction is widely known as alkali-aggregate reaction (AAR).

AAR is a common cause of concrete cracking which can result in significant damage to concrete structures. The deterioration caused by alkali-aggregate reaction is fairly slow, but progressive. Generally, when the concrete reaches at the age of 5 to 10 years, cracking due to the AAR becomes visible. However, Tuscaloosa Lock in Alabama, Stewart Mountain Dam in Arizona and other structures were affected by AAR no earlier

than 30 years after the construction (Mather, 1999). Occasionally, ASR distress can also be seen in structures that are more than 100 years old and some structures that are only a few years old.

The structural behavior of concrete is affected by AAR. The durability, serviceability, and the safety of the installation in the long run can be impaired by AAR (Bach et al., 1993). AAR leads to concrete expansion, loss of strength, and stiffness which tends to deform the structures and disturb the internal force (Leger et al., 1996). For example, AAR damaged beams and slabs show more ductility and more expansive cracking before failure, and anchorage strengths of 20% to 30% than the corresponding undamaged specimens (Bach et al., 1993). Fifty-year-old concrete from Cabril Dam in Central Portugal was investigated by Fernandes et al. (2004) and found signs of deterioration of concrete due to the granite that was used as aggregate for the concrete.

By early detection of AAR, engineers and builders can save millions of dollars in repairs and rehabilitation costs, and increase the service life of existing structures through maintenance programs. Hence, necessary steps need to be executed to minimize severe forms of deterioration in the concrete caused by AAR.

The main factor in controlling or eliminating AAR reaction is through the choice of aggregates to be used for concrete construction. In the State of Nevada, a seismic region, it is very important to detect not only the reactive aggregates, but also the degree of reactivity as well.

1.1 Alkali-Aggregate Reaction

Alkali-aggregate reaction (AAR) is a chemical reaction between the reactive silica and carbonates contained in the aggregate and the alkalis present within alkali hydroxides

in concrete. Gel expansion causes cracking in the concrete. AAR is one of the most commonly recognized chemical durability problems and one of the most deleterious phenomena that concrete structures face.

The result of the AAR reaction produces an alkali-silicate or alkali-carbonate gel that absorbs water and increases in volume. If the gel is confined by the cement paste, it builds up pressure as it grows; which causes internal stresses that eventually crack the concrete. The failure occurs in the form of overall cracking throughout the structure manifested at the surface as extensive map cracking or pattern cracking. Generally, it is not possible to estimate the deleterious effects from the knowledge of the quantities of the reactive materials used in the concrete alone.

Depending on which minerals are involved, AAR is subdivided into alkali-silica reaction (ASR) and alkali-carbonate reaction (ACR). ASR develops by the aggregates containing reactive silica minerals, a common aggregate composition, while ACR develops by the specific composition of aggregates, dolomitic (calcium-magnesium carbonate), which is very rare. Worldwide, ASR is the more common form of AAR.

1.2 Historical Background of Alkali-Aggregate Reactivity

In the United States, many concrete structures built from the late 1920's to the early 1940's failed due to overall cracking throughout the structures. The destruction manifested at the concrete surface as extensive map cracking (pattern cracking), surface pop-outs, spalling and gel exuding from the cracks. In the late 1930's T. Stanton of the California Division of Highways identified the phenomenon and called it alkali-silica reactivity (ASR). Since then, it has been the subject of intense research. Sixty years after

its identification, ASR continues to be a major cause of concrete deterioration in the United States.

Blanks and Kennedy (1955) described some of the earlier ASR cases in the United States. According to the authors, deterioration was first observed in 1922 at the Buck hydroelectric plant on the New River (Virginia), 10 years after construction. Conducting petrographic studies of the concrete of this hydroelectric plant, R. J. Holden (1935) had concluded that the expansion and cracking of the structure were caused by chemical reaction between the cement and phyllite rock used in concrete. Linear expansion in excess of 0.5 percent caused by the alkali-aggregate reaction had been detected in concrete.

Published reports on concrete deterioration due to alkali-aggregate reaction show that alkali-aggregate reactivity is widespread all over the world. Since chemical reactions are a function of temperature, in colder countries such as Denmark, Germany, and England, it was first thought that the alkali-silica reaction in these countries was not a concern. Subsequent experience with certain alkali-reactive rocks has shown that the assumption was incorrect.

After the identification of ASR in 1940, the next couple of decades produced a few cases of deleterious alkali-aggregate reaction. Researchers, therefore, decreased the study of AAR reaction. However, by the early of 1970's, the number of deleterious structures (highways, hydraulic structures and concrete buildings) increased significantly across the world, and the engineers decided to re-evaluate AAR. Since then, extensive research on the alkali-aggregate reaction was carried out at many laboratories in the world, first in the United States, and later in Europe, Canada and Asia. The reasons for the AAR reactions

and the parameters influencing them have hence been determined. Tests have been devised to detect these reactions and mitigation techniques have been suggested to eliminate or control the reactions.

ASR has already been identified as a problem in concrete structures in Australia, China, India, Korea, Hong Kong, France, Germany, Iran, Italy, Norway, South Africa, Turkey, Brazil and other places of the world. The deterioration of several concrete structures in more than fifty countries has been attributed to AAR.

As the problems had spread across the world, a group of RILEM technical committee (RILEM TC-106) was formed in 1988 to develop internationally approved methods for identifying the alkali-reactivity of aggregates. The committee conducted a survey of sixteen countries including the United States, the United Kingdom, Australia, and Germany.

A large number of studies have been conducted to investigate both the fundamental and practical aspects of AAR. Diamond (1992) provided an excellent overview of the literature pertaining to alkali-aggregate reactions from 1940 to 1991. It has been shown that the number of published papers has been increasing substantially over the past two decades (Figure 1.2). In fact, this proves an intense awareness of concrete durability problems as related to AAR. In response to these concerns, since 1974, research scientists and practitioners have met on regular occasions in a series of international conferences to present their latest work and to discuss the areas that require further research. The last meeting, the 13th ICAAR (International Conference on Alkali-Aggregate Reaction) was successfully held in Trondheim, Norway on June 16-21, 2008. Through these scientific

exchanges, engineers, researchers and builders will be able to implement new techniques in detecting ASR, and in minimizing the ASR-related damages as well.

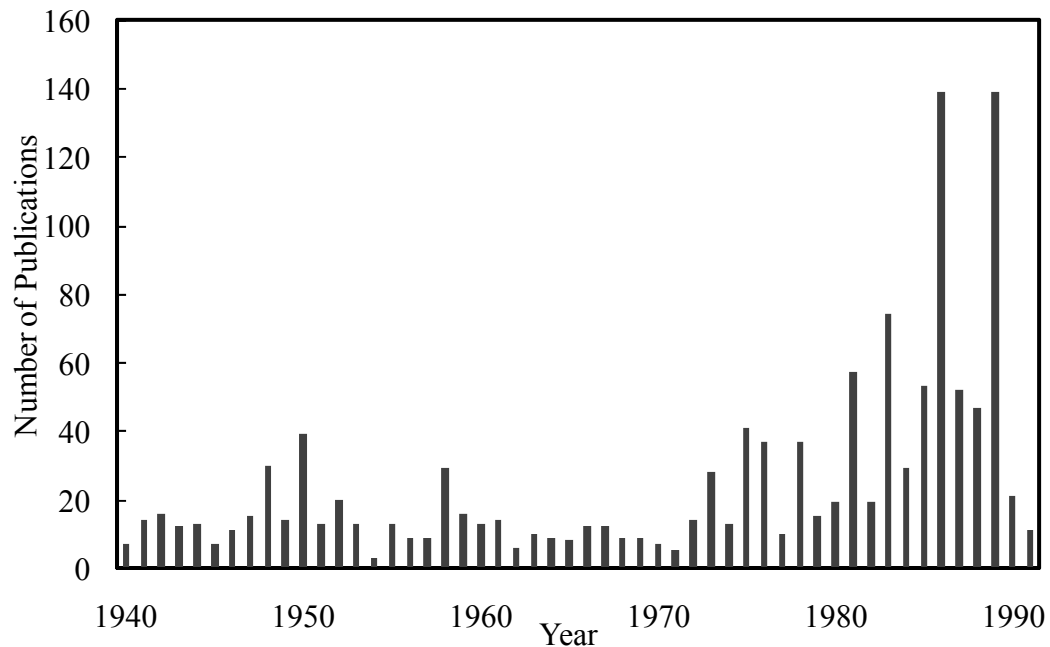


Figure 1.1: Number of publications concerning alkali-aggregate reactivity and published year (Data retrieved from Diamond, 1992)

An extensive review of international experience with ASR is presented by Touma et al. (2001). A historical survey of AAR across the United States and in the State of Nevada is described below:

1.2.1 Alkali-aggregate reactivity in the United States

Classic research by Stanton in the early 1940's correctly diagnosed the ASR failures as being due to the expansion caused by a chemical reaction between the alkalis contained in the cement paste and certain reactive forms of silica or carbonates present in the aggregates. It was only in the 1990's under the aegis of the American Association of State Highway and Transportation Officials (AASHTO) that an alkali-aggregate

reactivity Technology Implementation Lead States Team was established. In the early 2000's, AASHTO Lead States developed ASR Guide Specification including the basic ASR expansion test in concrete (ASTM C 1293).

As part of a Strategic Highway Research Program study, Stark (1993) conducted ASTM C 227 and ASTM C 289 tests for assessing the ASR of the aggregates quarried from sixteen different locations in the United States. Based on the test results and field performance of the aggregates, Stark (1993) mentioned that a rapid and more reliable ASR test procedure was needed as those tests were inadequate for detecting slowly reactive aggregates. Hooton (1996) strengthened the ideas of Stark and appended that ASTM C 1260-94 (CSA A23.2-25A-M94) and ASTM C 1293-95 (CSA A23.2-25A-M94) were gaining popularity.

Lane (1994) investigated a major cause of the deterioration of several concrete structures in Virginia. Among 13 aggregates studied with ASTM C 1260 test, 12 were claimed reactive. In 1996, Leming and coworkers investigated 22 highway structures in North Carolina. They concluded that ten had experienced extensive damage and were likely to see more damage due to ASR.

In 1998, the Federal Highway Administration offered the survey of alkali-silica reactivity in all the states that were primarily conducted by State transportation agencies. The survey was involved primarily in detecting, identifying, mitigating, and avoiding ASR in concrete structures and roadways. The studies found that ASR was generally evident in 35 states. The severity and availability of ASR within such large number of States turned it a national concern. A reported case of the ASR in the United States is shown in Figure 1.2.

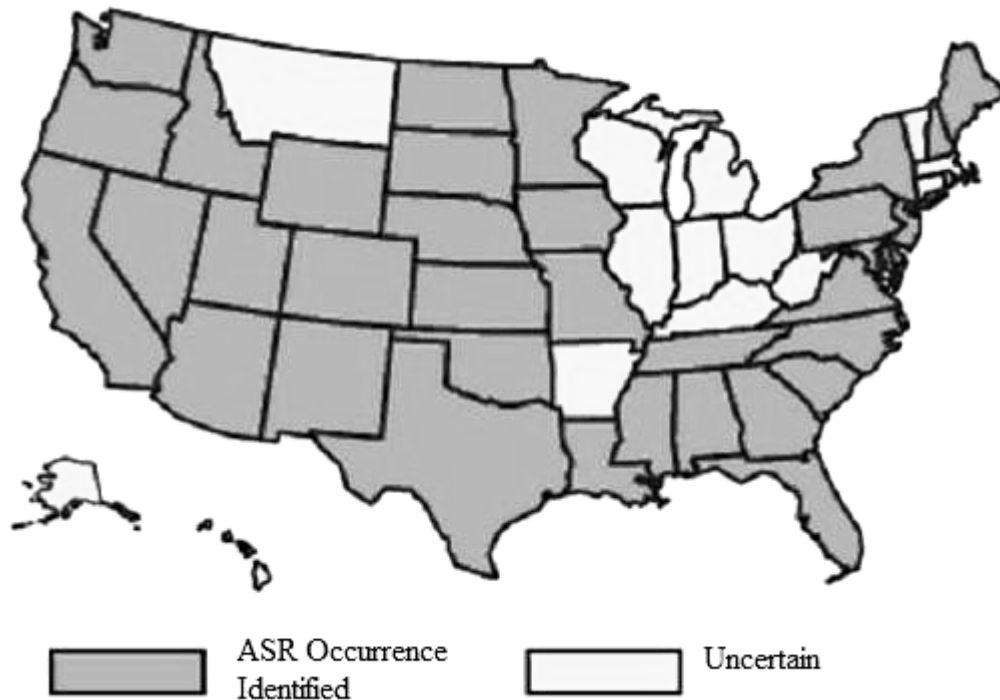


Figure 1.2: Reported case of ASR in the United States (FHWA-RD-03-047, 2003)

A total of 44 pages were included to review the selected research in North America summarizing the latest developments in the field of aggregate testing for potential ASR and ASR-mitigation methods in Research Report ICAR - 301-1f by Touma et al. (2001).

1.2.2 Alkali-silica reactivity in the State of Nevada

Due to lack of sufficient moisture, a necessary constituent for alkali-silica reaction to proceed, Nevada was expected not to be an ASR-affected state of the United States. During the winter in Northern Nevada, the temperature falls below the freezing point; whereas, the temperature of Southern Nevada remains above the freezing point. For this reason, the potential structural failure due to AAR problems is rapidly expanding to a

great extent in northwestern region, and to a lesser extent in the southern region of Nevada.

In 1993, the Nevada Department of Transportation (NDOT) recognized ASR-affected concrete pavement sections on Interstate 80 near Winnemucca, Nevada. NDOT brought them to the attention of the Federal Highway Administration (FHWA) under the Strategic Highway Research Program (SHRP) for the identification and possible mitigation of the distressed pavement. After conducting several tests, the distress was affirmed as ASR-damaged. A LiOH solution, high molecular weight methacrylate resin, and poly-siloxane resin were used to mitigate the existing pavement.

As shown in Figure 1.3, map cracks were observed in the concrete of Hoover Dam, the second highest dam in the country and the world's largest concrete structure, located in the border of Nevada and Arizona (Hobbs, 1988). As the research becomes more extensive on alkali-silica reaction, the number of ASR-affected structures and reactive aggregates in Nevada are getting higher. For example, Wang and Gillott (1993) found Nevada's opal reactive.

NDOT was also involved in the High Performance of Concrete Initiative (HPCI) Program in 2000. As a part of this program, Will (2000) investigated high-performance concrete prepared with aggregates obtained from three quarries (Vega, Paiute, All-Lite) in Northern Nevada. According to Will's findings, based on ASTM C 1260 results, All-Lite aggregate was the only aggregate that exhibited good performance on alkali-silica reactivity, and the remaining two aggregate groups, Paiute and Vega, caused severe damages in the form of cracking.



Figure 1.3: ASR cracks in the concrete of Hoover Dam (Hobbs, 1988)

Touma et al. (2001) conducted a variety of experiments on aggregates obtained from fourteen different producers all over the United States to cover the complete spectrum of ASR activity. Results obtained from ASTM C 1260 and ASTM C 1293 showed that Rilite aggregate group acquired from Nevada was potentially reactive. Petrographic analysis confirmed that this aggregate contained reactive minerals and was considered to be potentially deleterious. The mineralogy of the aggregate was natural siliceous and glassy.

Adams (2004) studied the potential alkali-silica reactivity of four aggregates acquired from Northern Nevada. This investigation gave an idea on the level of ASR of the selected aggregates; Rocky Ridge aggregate had a low level of potential ASR reactivity, All-Lite aggregate had a slightly higher level, Paiute aggregate had an even higher level, and Hidden Canyon aggregate had a severe level of ASR reactivity. A number of

photographs of ASR affected structures, captured from Northern Nevada, were documented.

1.3 Alkali-Silica Reaction

1.3.1 Introduction

Alkali-silica reaction is one of the most recognized deleterious phenomena in concrete and has been a major concern since its discovery in the 1940s. The reaction occurs between the reactive silica or silicates present in some coarse and fine aggregates and hydroxyl ions of the alkalis, which mainly come from the cementitious materials of the mixture. This produces an alkali-silica gel that expands in the presence of moisture resulting in concrete cracks, spalling and other deterioration mechanisms. This deleterious reaction is the most common form of alkali-aggregate reaction.

The problem of alkali-silica reactivity may appear to be similar to the other deterioration processes that cause damage to concrete. ASR is a time-dependent occurrence; it occurs during the service life of a structure, gives visible external warnings of internal damage, and generally appears to be harmless to the useful life of a structure. Although the actual number of structures affected by ASR is few and far between, experience has shown that, when considered in the context of concrete construction globally, the effects of ASR can be severely detrimental to concrete structures, affecting strength, stiffness, serviceability, safety, and stability.

The effects of the alkali-silica reactivity usually do not appear for a fixed number of years after construction, 5-15 years is perhaps most common, but some reported examples have exhibited distress at 30-50 years post construction. Certainly, more structures begin to show signs of ASR-related deterioration in the coming decades.

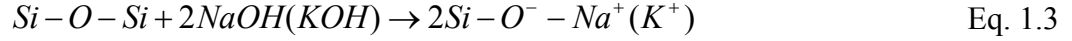
1.3.2 The mechanisms of alkali-silica reactivity

The chemistry of ASR has been thoroughly described in many studies during the last several decades. Among them, the most important are Swenson (1940), Glasser (1992), and Swamy (1992). Helmuth and Stark (1992) observed that the alkali-silica reaction results in the production of a two component gel; one component is a non-swelling calcium-alkali-silicate-hydrate [C-N(K)-S-H] and the other is a swelling alkali-silica-hydrate [N(K)-S-H]. When the alkali-silica reaction occurs in concrete, some non-swelling C-N(K)-S-H component is always produced. The reaction will be safe if only this type of product is formed, but unsafe if both gels form. The swelling reaction mechanism develops between alkali hydroxides and siliceous materials in the concrete aggregate. Generally, the ASR mechanism can be divided into two phases: (1) the chemical reaction, and (2) distress arising from the chemical reaction.

1.3.2.1 The chemical reactions due to ASR

The chemical reaction of ASR is a multi-stage process. The process starts with the reactive silica on the surface of the aggregate particles in a high alkaline (high pH) solution. The reaction occurs at the interface of the aggregate and the alkaline solution. The hydroxyl ions (OH^-) attack the stronger siloxane bridge (Si-O-Si), which generally forms a poor crystallized silica network. Siloxane bonds are broken and replaced by silanol bonds, seen in Equations 1.1 and 1.2. The negative charge created by the breakdown is balanced by the positively charged alkali ions, such as Na^+ or K^+ , as seen in below (Eq. 1.3).





As the reaction proceeds, alkali hydroxides penetrate into the siliceous particle, thus loosening the lattice structure. In well-crystallized silica (such as quartz), the breakdown of the lattice structure by alkali hydroxides is almost impossible. On the contrary, cryptocrystalline and amorphous silica are more susceptible to attack because of an untied and disordered lattice structure and increased surface area. Figure 1.4 shows the breakdown of the silica lattice due to alkali-silica attack. In the case of non-reactive quartz, the alkali ions cannot penetrate the well-ordered crystal lattice.

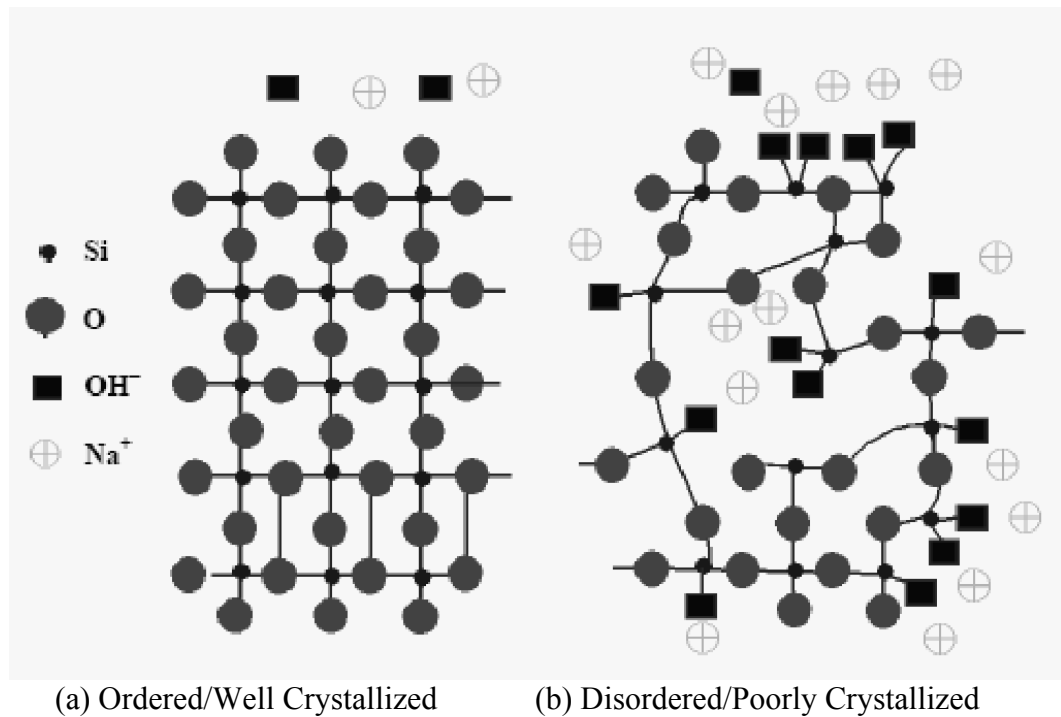


Figure 1.4: Attack of alkali solution on lattice structure of aggregate
(FAA AC 150/5380-8, 2004)

Mass transport is also an essential feature to ASR reaction. Aggregate particles consisting of SiO_2 are thermodynamically unstable in the cement environment. The

reaction, or series of reactions, is accompanied by mass transport of OH and alkali ions. The cement hydration products and aggregate particles are in intimate contact with pore fluid which serves as the main agent of transport (Swamy, 1992).

Since the gel is restrained by the surrounding mortar, an osmotic pressure is generated by the swelling. Once that pressure is larger than the tensile strength of the concrete, cracks occur, leading to additional water permeation through migration, absorption and additional gel swelling. The presence of gel does not always coincide with distress, and thus, does not necessarily indicate destructive ASR. The formation of alkali-silica gel leads to a developing expansion of the material. The rate of the expansion depends on the chemical composition and the available alkali content of the cement matrix (Pietruszek, 1996).

Some alkali-silica gels expand very little or not at all. If a gel is low-swelling, it will neither expand much nor create cracking problems in the concrete. High-swelling gel may cause pressures exceeding the tensile strength of concrete, which results in huge expansion and severe cracking. The rate of migration of pore fluids to the reaction site and temperature also influence swelling pressures. Consequently, the presence of gel must be linked to destructive cracking for a positive identification of harmfully expansive ASR.

1.3.3 Formation of ASR gel

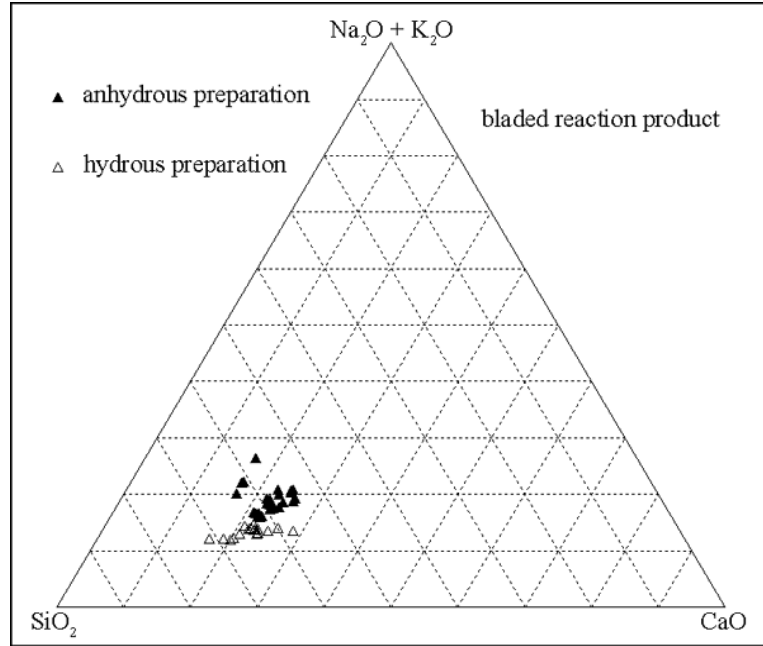
The types of alkali-silica reaction gel vary significantly in composition, depending on the nature of the alkali pore fluids, the nature of the particular form of reactive silica, the temperature of the reaction, and the concentration of reactants (Swamy, 1992). ASR gel consists of a complex mixture of alkali-rich and calcium-rich phases, which appear to be

the basis for considering gels of various components (Helmuth & Stark, 1992; and Diamond, 2000). The main compositions of alkali-silica gel usually include significant amounts of SiO_2 , Na_2O and K_2O , and CaO (Tambelli et al., 2006); however, other mineralogies do play a consistent role.

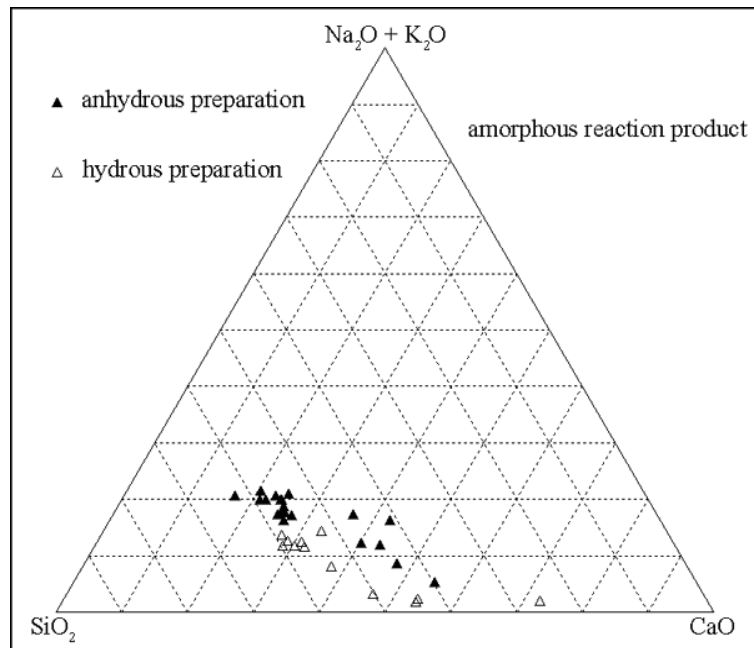
Hanson et al. (2003) studied two different ASR-product morphologies in the concrete: a porous bladed reaction product and a dense, amorphous reaction product. The chemical compositions of both products are composed of mainly SiO_2 , CaO , $\text{Na}_2\text{O}_{\text{eq}}$ (i.e. Na_2O and K_2O) and are presented in ternary diagrams as shown in Figure 1.5. The same conclusion was drawn by Sims (1992).

The ASR gel is transparent and its viscosity varies; some gels have sufficient fluidity to flow along the cracks and partially fill the voids in the concrete, while others are half-filled voids with the orientation of the gravity. Typically, gels carbonate with time and exposure to air, becoming white and hard with desiccation cracks similar to those observed in thin layers of dried mud. Drying of the gel often on the surface of a concrete also renders it less visible (Swamy, 1992).

Most researchers agree that ASR gels are responsible for expansion and the resulting damage in concrete. The formation of the gel is not deleterious. The deterioration of the concrete structure is due to the water absorption by the gel and its expansion. As the tensile strength of the system is exceeded, cracks will form and propagate. There is not a preferential direction for cracks to propagate, and the sites of crack initiation are randomly distributed in the specimen; therefore, map cracking will be characteristic of ASR deterioration. The sites of the cracks are determined by the location of the reacting silica on the aggregates and the availability of the OH^- vicinity.



(a) Bladed ASR product



(b) Amorphous product

Figure 1.5: Ternary diagram plotted normalized compositions ASR products (Hanson et al., 2003)

1.3.4 Development of ASR cracks

The pattern of cracking due to alkali-silica reactivity is generally different from that caused by thermal stress or drying shrinkage. The thermal cracking occurs at an early age mainly in the vertical direction of the structure. On the other hand, cracks due to alkali-silica reactivity occur mainly in the horizontal direction (with some cases in the axial direction) and increases with age.

In the case of reinforced concrete, ASR cracks develop in the direction of the main reinforcing bars (Nishibayashi et al., 1992). For instance, cracking in a beam or column takes place mainly in the axial direction. Fewer cracks occur in the perpendicular direction because compressive stress is developed in the concrete as a result of restraint from expansion by the reinforcing bar. On the other hand, at portions of concrete with little/no reinforcement (i.e. at the free end of a beam or abutment, on the surface of a sea defense structures or in a concrete block, etc.), the crack pattern due to ASR is irregular or map-like. However, a concrete section exposed to direct sunshine and rain generally has more cracks than the sheltered part of the same structure.

Different patterns of ASR-induced cracks and micro-structural features are observed in different types of reactive materials. As the reaction starts to take place, some cracks develop at the outer zone of the reactive aggregate due to the tension created by ASR gel. As the reaction takes place, the reactive grains are dissolved from the inside and an alkali gel is formed within the grains. In such a situation, it will take some time to initiate the reaction process. The reaction processes depend on the level of reactivity of the aggregates (Swamy, 1992).

1.3.5 Common symptoms of ASR

The cracks of hardened concrete may be associated with a number of factors, such as drying shrinkage, thermal stresses, corrosion of reinforcement, weathering, externally applied loads, and deleterious chemical reactions, etc. (Fournier & Bérubé, 1993). The occurrence of reaction products (gel) in micro-cracks is the main diagnostic symptom confirming that ASR has occurred.

ASR is most-reliably recognized with a petrographic analysis (ASTM C 856) of a core sample. Examination of a thin section of concrete under the petrographic microscope is probably one of the most widely used techniques for assessment of ASR in concrete. The test can easily detect whether any of the aggregate particles have clarified rims, peripheral cracks, or radial cracks that extend into the concrete.

ASR is a distress observed in any Portland cement structures caused by the cracking throughout the structures. Common symptoms of ASR-affected structures, as shown in Figure 1.6, are discussed below (Kosmatha et al., 2002; Sarkar et al., 2004; and Thomas et al., 2007).

1.3.5.1 Map or pattern cracks

The ASR-related cracks first form in a three- or four-pronged star pattern resulting from the expansion of gel around a reacting aggregate particle beneath the surface of the concrete, with the cracks relieving the stress due to the local expansion. As other particles react, more cracks develop until they join up to form the ‘map cracking.’ The bleaching or discoloration often associated with these cracks is probably due to the strong alkali solutions which permeate along them, killing and bleaching lichen and fungus growths which occur in the vicinity of the crack on the surface of the concrete.

This type of crack is never distributed uniformly on the surface of a pavement. Its pattern can vary from a few cracks to isolated areas of pattern cracking to fairly severe, closely spaced extensive map cracking. Additionally, the crack density on the surface may vary. The cracks show preferred orientation if expansion is restrained in one direction. When the interconnected cracks make a rectangular piece, then the cracks are referred to as block or rectangular cracks.

1.3.5.2 Longitudinal cracks

If a concrete element is sufficiently affected by alkali-silica reaction severe enough to cause cracking, but is under pre-existing stress, then cracks orientated with respect to the stress directions will develop. An example that illustrates longitudinal cracking is that of a bridge support column, with the load of the bridge deck on the column being sufficient to induce vertical cracking in the column. This particular column was eventually removed from the bridge and cut into sections. Once the loading was removed, map cracking developed on the surface of the column as the alkali-silica reaction continued.

1.3.5.3 Misalignment cracks

Since deleterious effects due to alkali-silica reactivity are largely the result of expansion within concrete elements in the structure, and since these effects are usually uneven in their severity, dimensional misalignments are a typical feature of the reaction. In many case studies, certain concrete pours are more severely affected than others.

1.3.5.4 Exudation

Exudation is the presence of a gel discharged through cracks and other openings in the concrete. When the gel interacts with the atmosphere in the presence of sufficient moisture, it takes on a white appearance. ASR gel exudation is not very common.

1.3.5.5 Pop-out

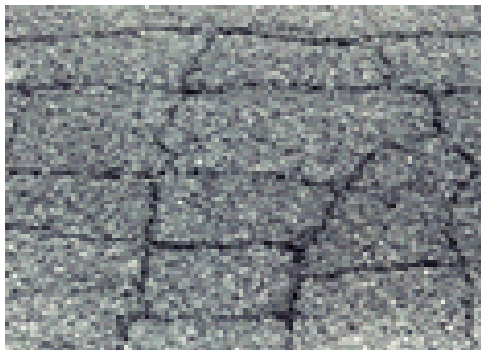
Pop-outs are cone-shaped depressions that break the surface of the concrete due to swelling of the gel. Aggregate pop-out is not a typical ASR indicator, and can also occur due to frost action on shale particles or porous chert particles.



Map cracks



Map or pattern cracks



Block cracks



Exudation



Pop-out



Blow-up/buckling

Figure 1.6: Typical symptoms of ASR

1.3.5.6 Spalling

Spalling itself is actually the deterioration of the concrete causing chunks of the concrete to separate from the concrete structure. It is not a typical ASR symptom.

Crushing of concrete at joints, misalignment of adjacent section, and discoloration around cracks has also been seen in ASR-affected concrete pavements and structures. Three additional symptoms of ASR are: D-cracking, closing of joints and crushing/spalling of concrete around joints.

1.4 Factors Affecting Alkali-Silica Reaction

The mechanisms of ASR expansion are quite complex. It is extensively accepted that three main components are essential for ASR-induced damage in concrete structures: (i) reactive forms of silica in aggregates, (ii) sufficient alkalis, and (iii) sufficient moisture. The ongoing process of ASR will only stop when one of the above reacting substances is used up.

1.4.1 Reactive forms of silica in aggregates

A reactive aggregate is mainly responsible for supplying the silica or silicate that is needed to form ASR in concrete. Reactive aggregates exposed to a highly alkaline pore solution tend to break down, which creates silica. Subsequently, the silica reacts with the alkali-hydroxides (sodium and/or potassium) in concrete to form ASR gel.

The potential reactivity of aggregates depends on many factors, such as aggregate mineralogy, degree of crystallinity, and solubility of the silica in high-pH concrete pore solution (Folliard et al., 2005). The internal grain size of the aggregate is also a major important factor in ASR expansion; since it is inversely related to the surface area of the silica available for alkali attack. Fine aggregate is more susceptible to ASR because of its

higher surface area (Baronio, 1987; and Hobbs, 1988). The porosity of the aggregate also increases the rate and extent of reactivity. Fine and coarse aggregates containing more than the following quantities of constituents are considered potentially reactive (ACI 221, 1998):

- a. Opal – 0.50% (by mass)
- b. Chert or Chalcedony – 3.0%
- c. Tridymite or Cristobalite – 1.0%
- d. Optically strained or microcrystalline quartz – 5% (as found in granites, granite gneiss, graywacks, argillites, phyllites, siltstones, and some natural sands and gravels)
- e. Natural volcanic glasses – 3%

The amount of reactive silica is also a crucial factor for alkali-silica reaction. Figure 1.8 illustrates the ASR-related expansion as a function of a particular reactive silica content, which typically varies from 2 to 10%, but can be as high as 100%.

The rocks and reactive minerals that are susceptible to alkali-silica reaction are illustrated in Table 1.1. The table highlights two groups of rocks, and their main differences in the crystalline structure of mineral constituents. The first set of rocks has a lack of minerals with a crystalline structure. As the structure of these rocks is in disarray, it creates channels and holes in the structure providing pathways for reactive ion migration in a greater surface area on which the reaction can occur. As a result, all rocks of this category are extremely reactive (Bérube & Fournier, 1993; and Thomas et al., 2007). The second category of rocks contains minerals with a crystalline structure. The level of ASR of this group of rocks ranges from mild to very reactive (Bérube &

Fournier, 1993; and Thomas et al., 2007). However, it does not represent that the rocks or minerals shown in Table 1.1 are always prone to ASR or that other rocks or minerals not listed in the table are completely immune from the adverse effects of ASR.

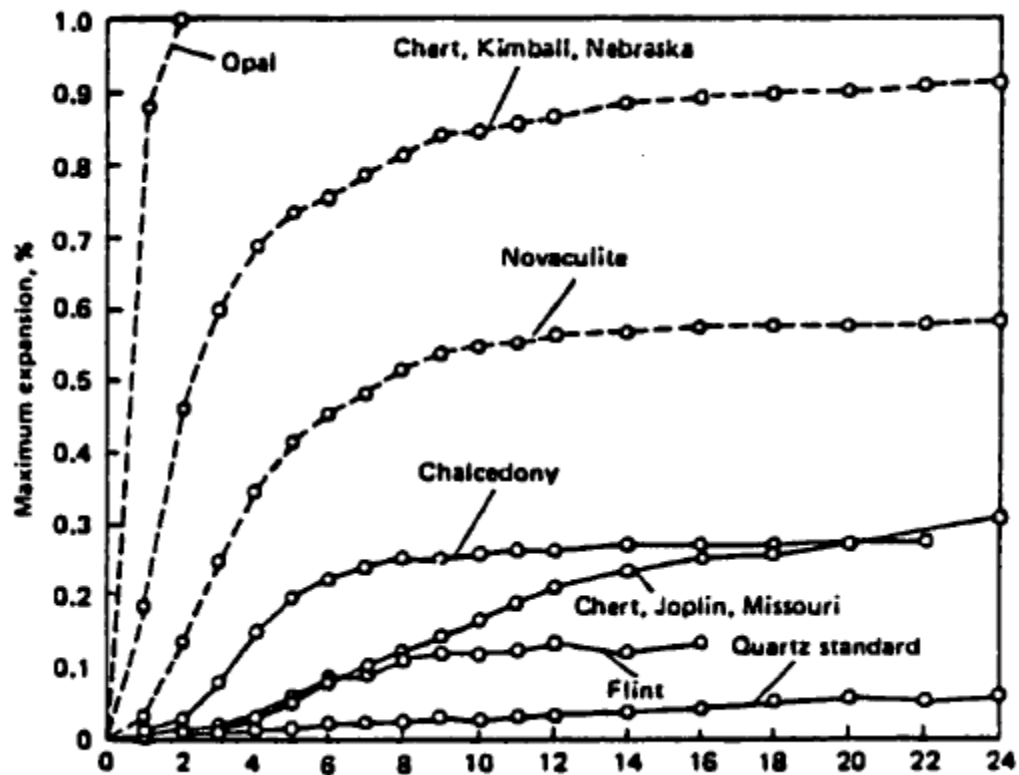


Figure 1.7: Effects of different siliceous rocks and mineral on the expansion of Portland cement mortar bars containing high-alkali cement (Blanks & Kennedy, 1955)

There are wide varieties of rock types used as aggregates in concrete construction. Table 1.2 outlines a summary of findings on major rock types susceptible to alkali-silica reaction. Based on the findings in Tables 1.1 and 1.2, andesite, basalt, decite, dolomitic-limestone, chert, opal, pyrex glass, quartz, rhyolite, and silicious rocks are prone to alkali-silica reactions. On the other hand, the mono-minerals dolomite and limestone

rocks, which often do not contain reactive minerals, are not prone to alkali-silica reaction (Stark, 1993). However, if limestone is partially replaced by dolomite rock, the resulting dolomite-limestone rock can be treated as innocuous provided that it does not contain a variety of other reactive minerals.

Table 1.1: Minerals and rocks susceptible to ASR (Bérube & Fournier, 1993)

Category (1)	Alkali-reactive poorly crystalline or metastable silica minerals, and volcanic or artificial glasses (Classical alkali-silica reaction)
Reactants	Opal, tridymite, cristobalite; volcanic glasses; artificial glasses, beekite
Rocks	Opal such as shales, sandstones, silicified carbonate rocks, some cherts, flints, and diatomite Volcanic rocks, such as rhyolites, dacites, latites, andesites, and their tuffs, perlites, obsidians; some basalts
Category (2)	Alkali-reactive quartz-bearing rocks
Reactants	Chalcedony; cryptocrystalline to microcrystalline quartz; quartz with deformed crystal lattice, rich in inclusions, intensively fractured or granulated; poorly crystalline quartz at grain boundaries; quartz cement overgrowths (in sandstones)
Rocks	Cherts, flints, quartz veins, quartzites, quartz-arenites, quartzitic sandstones which contain microcrystalline to cryptocrystalline quartz and/or chalcedony Volcanic rocks such as that in category (1) but with devitrified, cryptocrystalline to microcrystalline groundmass Micro-granular to macro-granular silicate rocks of various origins which contain microcrystalline to cryptocrystalline quartz: a) Metamorphic rocks: gneisses, quartz-mica schists, quartzites, hornfelses, phyllites, argillites, slates; b) Igneous rocks: granites, granodiorites, charnockites; c) Sedimentary rocks: sandstones, greywackes, siltstones, shales, siliceous limestones, arenites, arkoses; Sedimentary rocks (sandstones) with epitax

The volume of reactive silica needed to produce deleterious effects is very small (Swamy, 1992), and the quantity varies on the rock types and reactive minerals (ACI,

1998). An aggregate used in concrete might contain a small proportion of reactive silica as an original, primary or secondary constituent, which may not be determined by the chemical compositions. Considering rock type as only criterion for an aggregate's potential for ASR might lead to an erroneous result. Additionally, the mineralogy of aggregate is quite unable to offer the extent of the reactivity of an aggregate. Therefore, standard laboratory test results are only needed to classify ASR of an aggregate but also the extent of reactivity.

Table 1.2: Summary of findings on major rock types (mineralogy) susceptible to ASR

Rock Types	Research Investigations	ASR Type
Andesite	Tuthill, 1982; Swamy, 1992; Bérube & Fournier, 1993; Touma et al, 2001; Bian et al, 2003; Adam, 2004; Thomas et al., 2007; Ikeda et al., 2008	Reactive
Basalt	Lane, 1994; Adam, 2004; Korkanç and Tuğrul, 2005	Reactive
Chert	Stark, 1993; Lane, 1994; Touma et al, 2001	Reactive
Dacite	Tuthill, 1982; Swamy, 1992; Bérube & Fournier, 1993; Hooton & Rogers, 1993; Touma et al., 2001, Thomas et al., 2007	Reactive
Dolomite	Banahene, 1991; Hooton & Rogers, 1993; Stark, 1993	Innocuous
Dolomitic-limestone	Banahene, 1991; Deng et al., 1993; Lane, 1994; Milanesi et al., 1994	Reactive
Limestone	Stark, 1993; Jensen, 1996; McKeen et al., 1998; Touma et al., 2001	Innocuous
Opal	Ohama et al, 1989; Bérube and Fournier, 1993	Reactive
Pyrex glass	McCoy and Caldwell, 1951; Rogers and Hooton, 1991; Lane, 1994; Ekolu, 2004	Reactive
Quartz	Touma et al., 2001; Stark, 1993; Lane, 1994; Mo et al, 2003 ; Adam, 2004	Reactive
Rhyolite	Touma et al., 2001; Adam, 2004	Reactive
Silicious aggregate	Hooton and Rogers, 1993; Fournier et al., 1994; Berra et al., 2003	Reactive

1.4.1.1 Microstructures of silica and silicate

The reactivity of silica depends on the crystal structure of the silica rather than its chemical composition. Silica exists in either a crystalline or a non-crystalline state. The expansion of the concrete depends on the type, size, and the amount of aggregates containing reactive silica present in the concrete mixture (Broekmans, 1999). In order to provide a better understanding of alkali-silica reactions, the structures of silica need to be reviewed.

The basic structure of silicate, as depicted in Figure 1.8, is a silicon tetrahedron which consists of one center silicon atom, Si^{+4} , bonded with four oxygen atoms, one in each corner of the silicate (Leming, 1996; and Touma et al, 2001). The tetrahedron can be formed singly or in multiples with rings, chains, sheets or frameworks. A crystalline silicate structure can be formed by the repetition of the silicon tetrahedron in an oriented manner of three-dimensional space (Prezzi et al., 1997; and Touma et al., 2001).

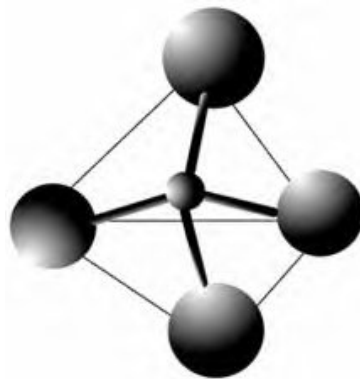


Figure 1.8: Silicon tetrahedron (silicate)

In the quartz (SiO_2) structure, as shown in Figure 1.9, the silica is completely crystalline. Each silicon tetrahedron is linked by oxygen ions, where each oxygen ion is

bonded to two silicon ions in order to achieve electrical neutrality. On the surface, however, unsatisfied negative charges develop because the structure is linked with three oxygen atoms instead of four oxygen atoms. Such structures are chemically and mechanically stable, impermeable, and react only on the surface (Leming, 1996).

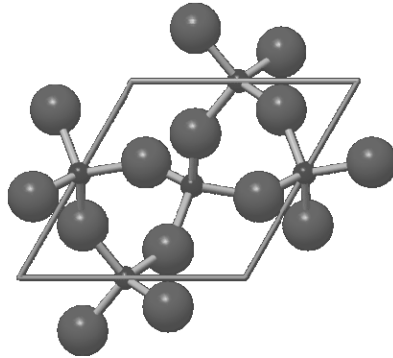


Figure 1.9: Quartz (silica) structure

Due to the lack of an ordered pattern, amorphous silica has holes (porous) in the network where electrical neutrality is unsatisfied, thus creating a large surface area for the alkali-silica reactions to take place. The more amorphous the silica is present in the aggregate, the more ASR-related reactions take place. Certain volcanic aggregates contain glassy materials formed by the rapid cooling of melted silica that prevents it from crystallization, and renders it very reactive (Leming, 1996).

1.4.2 Role of alkalis on alkali-silica reactivity

Concrete consists of infinite pores that are often filled with solution containing alkalis (Na^+ , K^+) and hydroxyl (OH^-) ions. The alkali level in the pore solution must be higher in order to raise ASR expansion. The amount of alkalis, in cement or concrete, is expressed

by sodium oxide equivalent, which is calculated by equation 1.4, as the percent of Na₂O plus 0.658 times the percent of K₂O.

$$Na_2O_{eq} = Na_2O + 0.658K_2O \quad \text{Eq. 1.4}$$

The major sources of alkalis in the concrete can be found from any of the following sources.

1.4.2.1 Portland cement

All ingredients of concrete contribute the total alkali content of concrete, and among all the sources, Portland cement contributes the largest amount of alkalis. Alkalis in the Portland cement range from 0.2 to 1.1 percent and reside in the pore solution of concrete (Folliard et al., 2003). There is an abrupt change upward from about 0.4% to about 1.2% Na₂O_{eq} in the alkali content of the available cement (Mather, 1999). The alkalis produce an inherently high pH (normally from 13.2 to 14) in the pore solution by associating hydroxyl ion (OH⁻) concentration. An effective way of preventing ASR-induced damages is not only to control cement alkalis, but also the total alkali content of the concrete mixture.

Limiting cement alkalis below 0.60% Na₂O_{eq} is unlikely to prevent the occurrence of ASR (Stanton, 1940). The lowest recommended value of alkali content of cement is 1.8 kg/m³ Na₂O_{eq} for the structures with a relatively high risk level of alkali-silica reaction to provide a safety factor from the potential contribution of alkalis (Fournier and Bérubé, 2000). Canadian Standards Association (CSA) recommends the limit for the concrete alkali content ranging from 1.8 to 3.0 kg/m³ Na₂O_{eq} depending on the degree of reactivity of the aggregates, exposure conditions, and the proposed life of the concrete structures (Fournier et al., 1999, 2000).

Ramachandran (1997) also studied the effect of various percentage of alkali content of cement on the linear expansion of mortar bar specimens. The study demonstrated that ASR-induced expansion increased with an increase in cement alkali. The expansion of the prisms (ASTM C 1293) as related to the cement alkali is illustrated in Figure 1.10. The data shows that the concrete containing less than $3.0 \text{ kg/m}^3 \text{ Na}_2\text{O}_{\text{eq}}$ is generally resistant to excessive expansion of 0.04% at 2 years. Touma et al. (2001) clarified the influence of cement alkali on the levels of alkali-silica reactivity. The results of their investigation concluded that highly reactive aggregates showed expansions at $\text{Na}_2\text{O}_{\text{eq}}$ content as low as 0.50%, and innocuous aggregates showed innocuous behavior at $\text{Na}_2\text{O}_{\text{eq}}$ content as high as 0.90% in the Portland cement. The idea demonstrates that altering cement alkalis does not impact the level of the alkali-silica reactivity of an aggregate.

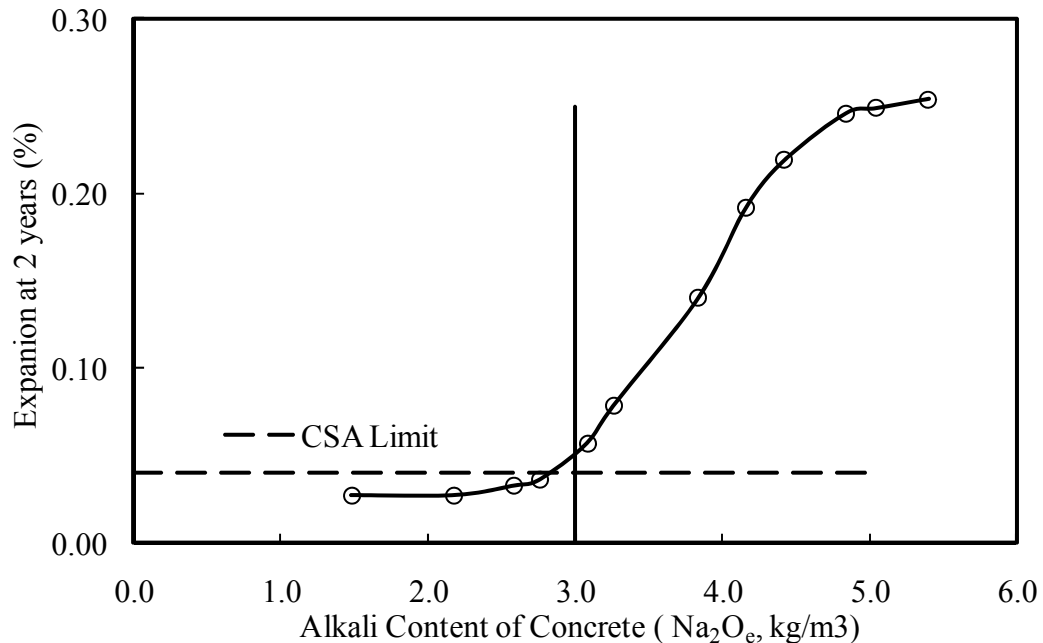


Figure 1.10: Effect of cement alkali on expansion using ASTM C 1293 (Thomas, 2002)

Shon et al. (2002) performed the ASTM C 1260 test by using the storage concentrations of 1N, 0.50N and 0.25N NaOH and the cement alkalis of 0.51% and 0.58% $\text{Na}_2\text{O}_{\text{eq}}$. The results obtained from the study showed that low-alkali cement generally resulted in slightly lower expansion than the high-alkali cement.

The fineness of Portland cement also affects the expansion caused by ASR. The finer cement releases alkalis faster, thus, inducing expansion faster. Fournier and Bérubé (1991) and Berra et al. (1998) observed higher expansion in the accelerated mortar bar method with the highest blaine values. Their results also indicated that the fineness effect is limited when using moderately reactive aggregate.

Bektas et al. (2008) studied the influence of different fineness levels of Portland cement on ASR expansion of moderately and highly reactive aggregates using low and high alkali clinker in a storage solution of 0.5N and 1N NaOH. Cement alkali content did not significantly affect the expansion of the mortar bars made with the moderately reactive aggregate, but tended to have significant effect on the expansion of the mortar bar containing highly reactive aggregates.

1.4.2.2 Pozzolanic materials

A pozzolan is a siliceous or siliceous and aluminous material which reacts with lime released from cement hydration, forming a compound possessing cementitious properties. Pozzolanic materials are typically used as a cement replacement or a part of cementitious material to modify or improve concrete properties, and occasionally used for economical consideration.

Common pozzolanic materials used in concrete include fly ash, silica fume and ground granulated blast furnace slag (GGBFS). These materials consume alkalis when

they react with lime. Addition of pozzolans to concrete results in a reduction of alkali content which yields reducing ASR expansion (Xu et al., 1995). A pozzolanic reaction reduces the permeability of concrete and absorbs some alkali ions, and alkali-silica reaction that consumes most of the available alkali ions (Xu et al., 1995). Thus, the concrete is protected from the reaction between alkalis and aggregates.

1.4.2.3 Aggregates

Some aggregates can release alkalis, thus increasing the alkali content of the mixture (Stark & Bhatti, 1986; and Thomas et al., 1992). For an example, aggregate containing feldspars, micas, glass, and glass rock release alkalis in concrete. For certain aggregates, the amount of released alkalis is equivalent to 10 percent of Portland cement alkalis under severe conditions. A significant amount of alkalis can also be supplied with time by aggregates to the concrete pore solution, particularly by feldspar-rich aggregates, such as granite, which are often used in concrete (Bérubé et al., 2002). Additionally, if sea-dredged aggregates are used in the mixture, the additional alkalis lead to the concrete mixture resulting in ASR expansion. Therefore, the alkalis produced by the certain types of aggregates provide an additional source for further ASR.

1.4.2.4 Chemical admixtures

Admixtures are chemical agents that are added to concrete during the mixing state. Chemical admixtures include accelerators, water reducers (or plasticizers), super plasticizers, retarders, air-entrainers, etc. Some of the admixtures contain sodium and potassium compounds that also contribute to the alkalis in concrete.

1.4.2.5 Water

Water may contain a certain amount of alkalis. The total alkali content of a given mixture may also be increased from the external sources, such as seawater, ground water, and water from industrial process. Nixon and Sims (1992) confirmed that seawater increases the OH^- concentration in the pore solution, which resulted in higher ASR-induced expansion.

1.4.2.6 External sources

External alkalis may increase ASR expansion, especially when concrete is cracked or highly permeable. A common source of external alkalis is deicing salts. In recent years, the use of deicer salts has increased significantly, which can provide vast amounts of alkalis, producing in excessive ASR-induced expansion.

1.4.3 Role of sufficient moisture on alkali-silica reaction

Alkali-silica reactivity requires water to initiate the reaction. Water is an essential for the 'carrier' of alkali cations and hydroxyl ions, and is absorbed by the gel which is the essential element in developing pressures to crack the concrete. Sufficient moisture is necessary to induce pressure on gels, which are formed by the alkali-silica reaction that leads to expansion, and cracking of the aggregate, and surrounding paste. Concrete mixtures involved in highly reactive aggregates and high-alkali cements have shown little or no expansion in a dry environment. Likewise, the concrete structure with a large amount of local moisture typically results in more expansion.

The effects of alkali-silica reaction vary directly with the percentage relative humidity (RH) of the concrete. The swelling of the gel occurs at a RH higher than 80%, although it can be formed in a lower humidity (Helmuth, 1993; and Pedneault, 1996). Limiting the

moisture content to less than 70% relative humidity, can reduce ASR-induced damage (Swamy, 1992). Figure 1.11 shows that concrete specimens that maintained in an environment with less than 80% relative humidity did not undergo significant expansion. Therefore, higher humidity can increase moisture absorption and thus, impacts on the severity of ASR distress. However, it is practically possible to limit the moisture exposure for exterior structures. Providing proper drainage facilities through low-permeability concrete will enhance the durability.

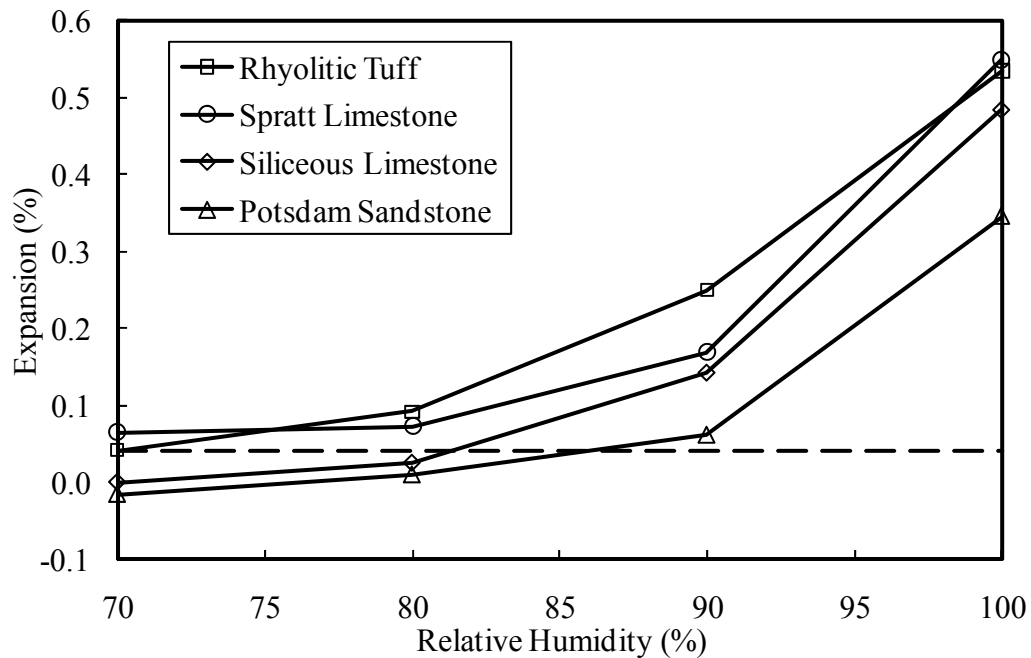


Figure 1.11: Effect of relative humidity on expansion using ASTM C 1293 (Pedneault, 1996)

ASR expansion increases an increased amount of mixing water, provided that all other factors in a given mixture remain constant (Stark, 1995). Altering water-to-cementitious materials ratio (w/cm) in mortar bars affects the alkali concentration of the

pore solution. Results obtained from Figure 1.12 found that reducing the w/cm of the concrete mixture results in less expansion than that of the higher w/cm concretes.

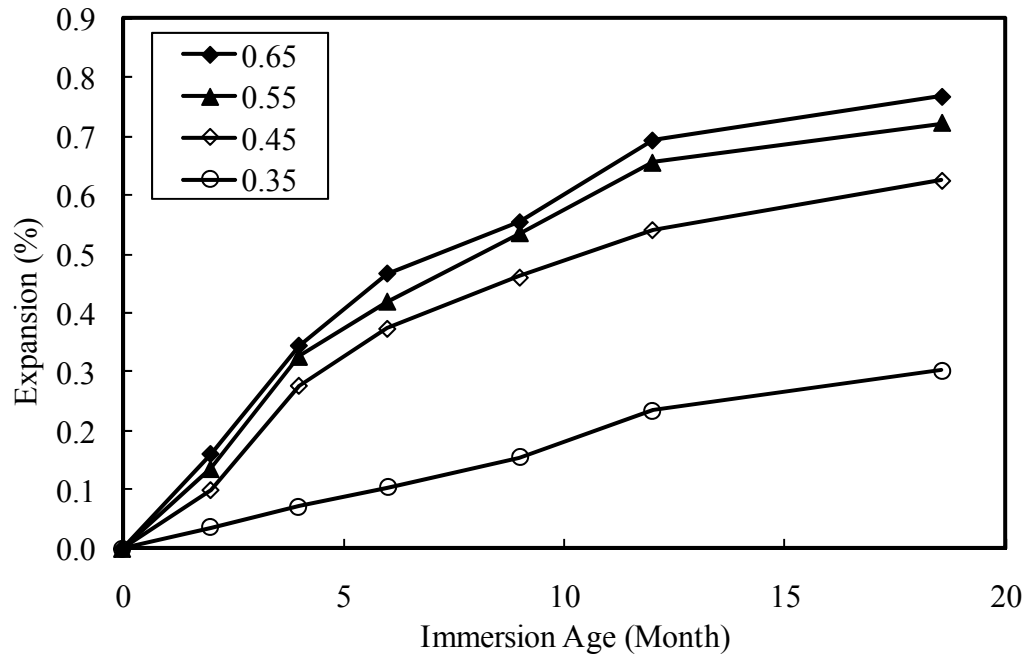


Figure 1.12: The influence of water-to-cement ratio on the ASR expansion of concrete (Stark, 1995)

Reducing the permeability of concrete is a more feasible approach to reducing the deleterious effects of ASR (ACI 221, 1998). Decreasing the w/cm ratio in concrete results in a high cement content (i.e. high alkali content), and a reduced pore space which affects the expansion rate (ACI 221, 1998; and Shon et al., 2002). As such, one approach to suppress ASR expansion is to add silica fume or other supplementary cementitious materials to the concrete mixture. Applying a protective coating over concrete is another solution to minimize contact with moisture though the procedure can be costly.

1.4.4 Temperature

Structures in warmer exposures are more susceptible to alkali-silica reactivity than those in colder exposures. For the majority of aggregates, higher temperatures also mean larger ultimate expansions. The effect of high or low temperatures on ultimate expansion is aggregate-dependent, with most aggregates more reactive more at higher temperatures (Mindess et al., 2002).

1.5 Testing for the Potential Alkali-Silica Reactivity of Aggregates

Several ASTM standards have been used in assessing alkali-aggregate reactions and their potential for deleterious expansion in concrete; each has its limitations. The methods are classified into three major groups:

- a. Petrographic examination of aggregates
- b. Chemical tests
- c. Expansion tests

1.5.1 Petrographic examination of aggregates

ASTM C 295, “Petrographic examination of aggregates for concrete,” is one of the most reliable indicators of the potential for deleterious ASR. Petrographic evaluation provides useful information about the types and amounts of minerals present in an aggregate, and can be used to identify a wide range of reactive components. This test is highly recommended for use in conjunction with other tests and field performance evaluations. This is a very quick method and its findings greatly depend on the experience and capabilities of the petrographer examining the aggregate. It is recommended that petrographic examination together with ASTM C 1260 jointly appear to the most reliable indicators of potential for deleterious ASR. Information from

petrographic analysis aids in determining which accelerated testing method should be used to further evaluate the alkali-silica reactivity of an aggregate.

Petrographic examination requires interpretation. While conducting the test, small amount of certain important components can readily be missed, especially with an aggregate such as opal (Nixon & Sims, 1996). A few aggregates, on the other hand, can be classified as deleterious reactive even with a good service record, because they contain minerals that have been known to be reactive in other situations (Touma et al, 2001).

1.5.2 Chemical tests

Chemical tests are also used to identify the potential reactivity of aggregates. Among them, ASTM C 289, “Potential reactivity of aggregates (Chemical Method),” is one of the well known chemical tests. This test evaluates aggregate reactivity by measuring the amount of dissolved silica and the reduction of alkalinity in the reaction of the alkali solution by immersing finely crushed aggregate in concentrated sodium hydroxide and heating it under pressure for 24 hours. This test is found to have several problems in its testing procedures. Many aggregates, in the presence of carbonate rock components, are not adequately identified using this test.

1.5.3 Expansion tests

In the expansion tests, mortar bars or concrete prisms are made with an aggregate to be investigated. The specimens are then put into a specified condition and the expansion of the specimens is measured at specific time intervals. Expansion tests are performed to identify alkali-silica and alkali-carbonate reactions.

1.5.3.1 ASTM C 227 (Mortar bar method)

Since the 1950s, ASTM C 227 method has been the most widely used ASR test method in the United States (Touma et al., 2001). The method is used to determine the susceptibility of cement aggregate combination to alkali silica reaction by means of measuring the change in length of mortar bars made using the proposed combinations of materials for a job. The mortar bar specimens have an aggregate-to-cement ratio of 2.25 and are exposed to 100% relative humidity at 38°C. ASTM C 227 indicates that the expansion is considered excessive if it exceeds 0.05% at 3 months or 0.10% at 6 months. The presence of wicks inside the storage containers largely affects the results. It was found that the wicks promote the leaching of alkalis from mortar bars, causing lower expansions (Bérubé & Fournier, 1993).

The ASTM C 227 test has been declared unreliable (Touma et al., 2001). The method is not suitable for identifying slowly reactive aggregates, and should not be used to predict the potential alkali-silica reactivity of aggregates.

1.5.3.2 ASTM C 1260 (Accelerated mortar bar test)

ASTM C 1260 referred as the accelerated mortar bar test (AMBT) was developed by Oberholster and Davies (1986) at the National Building Research Institute in South Africa. The test has been adopted by various countries, including the United States (by ASTM and AASHTO) and Canada. This is a recommended test method for assessing ASR. ASTM C 1260 is recognized as a very severe test method because of the extreme test conditions such as highly alkaline storage solution and high temperature. The test requires only 16 days in deciding the level of reactivity, compared to one year for the concrete prism test (ASTM C 1293). As the specimens are exposed to the 1N NaOH

solution, the alkali content of the cement is not a significant factor in affecting expansion (ASTM C 1260).

The test is also reliable for evaluating the effectiveness of cementations materials. Aggregates found innocuous with ASTM C 1260 are very likely to perform well in the field. There is a general agreement by most researchers that the 14-day expansion of ASTM C 1260 under the 1N NaOH solution of less than 0.10% is an indication of innocuous aggregate and more than 0.20% is regarded as highly reactive aggregates. The expansion between 0.1% and 0.2% is either slowly reactive or inconclusive, and more likely depends on prism test, aggregate type or field performance. The average coefficient of variation of a multi-laboratory study at 14 days was found to be about 15% (Rogers, 1999). Additionally, slowly reactive aggregates continue to expand rapidly beyond 14 days, which is a marginal time for evaluating the reactivity. To minimize the associated problems, additional expansion limits of 0.33% at 28 days and 0.48% at 56 days were proposed by Hooton (1991), and Rogers and Hooton (1993).

1.5.3.2.1 Modified ASTM C 1260

ASTM C 1260 can be modified by (i) changing the normality of the alkaline solution, (ii) varying the water-to-cementitious materials ratio, (iii) altering the alkali content of cement, and (iv) extending the duration of the test.

Van Aardt and Visser (1982) investigated the influence of different alkali (sodium hydroxide) concentrations, namely, 0.25N, 0.5N, 0.75N, 1N, 2N and 4N solutions on the ASR-related expansion of the prisms. Results showed that prisms cured in the 2N and 4N NaOH solutions initially expanded more quickly than those for the reduced concentrations but the expansion stabilized at a value below that obtained for the 1N

solution. Overall, the specimens for the 1N NaOH showed the maximum expansion at 14 days.

After exploring ASR expansion of six aggregates under the three different concentrations of soak solution, namely 0.5N, 1.0N and 1.5N, Davies and Oberholster (1986) proposed the 1N NaOH as the optimum solution since it produced higher expansion than that obtained for the 1.5N solution. The study conducted by Fournier and Bérubé (1991) generated conflicting results; higher expansion occurred for the 1.5 N soak solution over the 1N soak solution. Due to the complex mechanisms of ASR expansion and the sensitive chemical equilibriums, each individual case would be different (Bektas et al., 2008).

Touma et al. (2001) performed the ASTM C 1260 test along with its modifications, using the different solution strengths and cement alkalis, such as 1N NaOH with 1.50% $\text{Na}_2\text{O}_{\text{eq}}$ cement alkali, 0.75N NaOH with 1.15% $\text{Na}_2\text{O}_{\text{eq}}$ cement alkali, 0.5N NaOH with 0.81% $\text{Na}_2\text{O}_{\text{eq}}$ cement alkali, and 0.25N NaOH with 0.46% $\text{Na}_2\text{O}_{\text{eq}}$ cement alkali. Results indicated that as the solution normality decreased the expansions decreased progressively. Because reducing the soak solution's normality results in a progressive reduction of OH^- concentration, which leads to reduction in concrete expansion (Stark, 1993).

In 1994, Johnston modified the ASTM P 214 (equivalent method to ASTM C 1260) test to use different concentrations of NaOH solution to explore the feasibility of using two different base strengths to better predict reactivity. The 14-day expansion of one aggregate under the 1N, 0.5N and 0.25N NaOH solutions was recorded as 0.312%, 0.072% and 0.004%, respectively. Additionally, for this particular source, the 14-day

expansion under the 1N NaOH soak solution was 4.33 and 78 times that under the 0.5N and 0.25N NaOH soak solutions, respectively.

Shon et al. (2000) evaluated the functionality of ASTM C 1260 after modifying some of the important test parameters, such as water-to-cement ratio (w/c), normality of soak solution, test duration, and alkali content of cement. The results of their study are presented in Figure 1.13. The cement alkali, w/c, and soak solution concentrations had adverse effects on ASR-generated expansion. The authors also demonstrated that the 28-day expansion of mortar bars under the 0.5N NaOH solution was comparable or slightly higher than the 14-day expansion under the 1N NaOH. A suggestion was also proposed to extend the testing period to 28 days in order to obtain a more reproducible expansion.

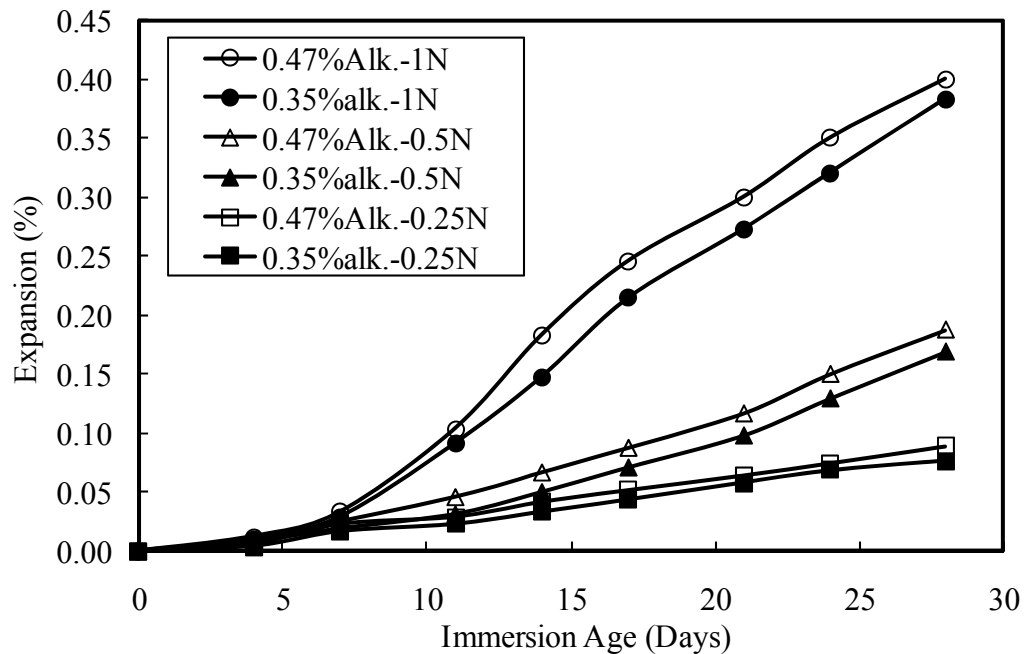


Figure 1.13: Expansion of C 1260 for 1, 0.5 and 0.25N solutions (Shon et al., 2002)

Stark (1993) studied various levels of normality in order to determine the safe cement alkali below which the aggregates do not exhibit deleterious expansions. A relationship between the alkali content of cement and soak solution normality was correlated. Helmuth (1992) developed a linear regression equation based on the published data that related cement alkali level to solution normality in a hydrated cement paste of a given water-cement ratio, as seen in Equation 1.5.

$$[\text{OH}^-] = 0.339 \frac{\text{Na}_2\text{O}}{w/c} + 0.022 \pm 0.06 \text{ moles/L} \quad \text{Eq. 1.5}$$

Where:

$[\text{OH}^-]$ corresponds to NaOH Normality

Na_2O = equivalent Na_2O of the Portland cement in percent

w/c = water-to-cement ratio

Using Equation 1.5, the relationships of OH^- concentration between the soak solution and cement alkali at a given water-to-cement ratio is linearly proportional. To obtain the correlation among solution normalities, cement alkali, and ASR expansion, several series of rapid immersion tests were conducted using the NaOH solution concentrations of 1.0, 0.70, 0.52, 0.35 and 0.18N with various cement alkalis.

Figure 1.14 illustrates that the failure criteria of 0.02% expansion occurs for solution normalities of less than about 0.60N, which corresponds to a cement alkali level of about 0.82 percent $\text{Na}_2\text{O}_{\text{eq}}$ at a water-cement ratio of 0.50. The failure criterion admittedly is based on very limited data and is slightly conservative (Stark, 1993). Figure 1.14 also depicts that virtually no expansion would develop for 0.35N and 0.18N solution, while in reality, this behavior is non-existent. Stark (1993) suggested that aggregates showing 14-day expansions higher than 0.08% are considered reactive, whereas those lower than 0.08% are considered innocuous. It is also recommended that the failure criteria must be

adjusted progressively downward from 0.08% for the 1.0N to a minimum of about 0.02% as solution normality decreases to about 0.6N (Fig. 1.14).

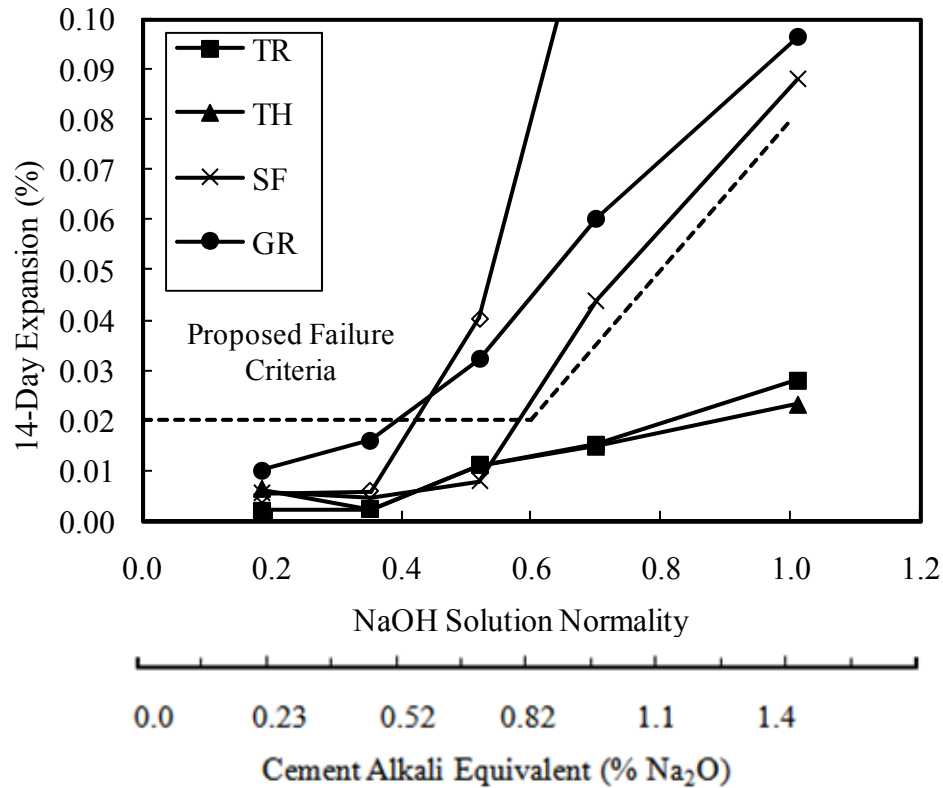


Figure 1.14: Projected failure criterion to determine safe cement alkali level for deleterious aggregates (Stark, 1993)

Table 1.3 shows the failure limits of the mortar bars made with three dosages of cement alkalis for the three different soak solution concentrations. The proposed failure criteria performed well except for the 0.25N solution, for which the procedures were very conservative and would result in a worst-case scenario (Touma et al., 2001).

Several studies (Xu et al., 1995; and Touma et al., 2001) have documented the effectiveness of ASTM C 1260 for predicting the potential alkali reactivity of aggregates

and for investigating the efficacy of mitigation alternatives by the use of mineral admixtures, pozzolans and chemical admixtures.

Table 1.3: The 14-day expansion criterion of the mortar bars for different soak solution strengths with corresponding $\text{Na}_2\text{O}_{\text{eq}}$ in the mortars (Shon et al., 2004)

Normality	1N	0.5N	0.25N
Corresponding $\text{Na}_2\text{O}_{\text{eq}}$ content (%)	1.5	0.81	0.44
14-day expansion criterion (%)	0.10	0.04	0.02

1.5.3.3 ASTM C 1293 (Concrete prism test)

ASTM C 1293, “Determination of length change of concrete due to alkali-silica reaction,” was adopted by ASTM in 1995 from Canadian Standards Association (CSA A23.2-14A). The method is generally considered the most accurate and effective test in predicting the field performance of aggregates. Concrete prisms are cast, cured for 24 hours at 23°C, and then stored over water (100% RH) at 38°C. Expansion measurements are taken at regular intervals, and when testing plain concrete (without SCMs or chemical admixtures), the test is typically run for one year. When testing SCMs or lithium compounds, the test is typically carried out for two years.

Among the ASR assessing test methods, ASTM C 1293 is generally considered to be more representative of field performance and provides an accurate reactivity of the suspicious aggregates. The only disadvantage of this method is that it takes more than six months before obtaining the initial test result and runs for a year or more. This method is less conservative than the ASTM C 1260 (AMBT) test and more likely for assessing slow reacting aggregates.

1.5.3.3.1 Modifications of ASTM C 1293

As ASTM C 1293 requires a long time to determine ASR of an aggregate, modifications of ASTM C 1293 test are being used to show the same results in a shorter span of time. Modifications of ASTM C 1293 can be made by (i) changing the solution type and/or solution strength, (ii) altering curing environment, and (iii) changing the duration of the test. Touma et al. (2001) slightly modified the procedure of ASTM C 1293 in the following three ways:

- a. The specimens were submerged in the 1N NaOH solution at an elevated temperature of 80°C. The proposed failure criterion for this modification was 0.040% expansion at the immersion age of 4 weeks. This is the most accelerated modification of ASTM C 1293.
- b. The specimens were submerged in the 1N NaOH solution at 38°C. The proposed failure criterion for this modification was 0.040% expansion at 26 weeks.
- c. The specimens were stored over water at 60°C. The proposed failure criterion for these procedures was 0.040% expansion at 3 months of testing.

Results obtained from the above modifications of ASTM C 1293, Touma et al. (2001) revealed that (i) concrete prisms cured in the 1N NaOH solution at 80°C was found too severe, (ii) those cured over water (100% RH) in sealed containers with wicks at 60°C resulted in almost identical results as the standard ASTM C 1293 with some minor exceptions. The concrete prism test was shown very much dependent on the immersion conditions and test duration.

Bérubé and Frenette (1994) conducted concrete prism test prepared with two highly alkali-silica reactive aggregates under the 1N NaOH solution at two distinct temperatures

of 80°C and 38°C, and in water at 80°C. Results obtained from the study indicated that (i) prisms immersed in water gave very low expansion as a result of alkali dilution and consequent pH reduction in the pore solution; (ii) prism testing in the 1N NaOH at 80°C showed the most rapid testing procedure due to the initial concrete alkali content, and this modification is unreliable for determining the potential alkali-reactivity of aggregates, and (iii) testing in the 1N NaOH at 38°C appeared to be the most promising procedure, compared with the concrete prism test (CSA A23-2-14A, testing in air at 100% RH) and the test duration can be reduced from 1 year to 6 months.

Folliard et al. (2004) studied the use of two accelerated versions of ASTM C 1293, storing prism specimens above water at the temperatures of 60°C and 49°C, with the standard testing at 38°C to assess alkali-silica reactivity. The overall findings show that the typical long-term expansions measured at 60°C are significantly less than those measured at 49°C and 38°C. This reduction in expansion is shown to be mainly caused by increased specimen drying out of the prisms and increased alkali leaching at higher temperatures, as well as changes in pore solution composition.

Currently, ASTM C 1260 and ASTM C 1293 are the two recommended tests for assessing ASR in the USA and Canada. ASTM C 1293 generally is considered to be more representative of field performance due to concrete specimen and the curing environment. To supplement these tests, a petrographic evaluation (ASTM C 295) is also suggested, but not required.

Clearly, an ideal test method for predicting the alkali-silica reactivity of aggregates does not exist (Touma et al., 2001; Nixon and Sims, 1996). As such, a comprehensive

evaluation of test methods is needed for aggregates having known alkali-silica reactivity ranging from innocuous to highly reactive.

1.6 Preventing ASR Expansion

An engineering technique is to take the steps to avoid excessive expansion due to ASR before the structure is built (Bérubé & Fournier, 1993; and Mather, 1999). Therefore, appropriate precautions are typically taken before concrete is placed for building any structures. Additionally, concrete producers need to analyze the cementitious materials and aggregates, and ultimately choose a control strategy that optimizes effectiveness and decreases ASR effects. However, special requirements are not needed if the aggregate is not susceptible to alkali-silica reactive based on the testing or historical background.

Avoiding reactive aggregates is not always possible from a practical or an economical perspective. The understanding of the chemistry governing ASR reactions allows the development of approaches that could help in safely using the potentially reactive aggregates. Feasible mitigation techniques of alkali-silica reactivity are broadly encompassed as follows (Mather, 1999; Mindess et al., 2002):

- a. Decreasing the pH of the concrete's pore solution to suppress the initial silica solubility
- b. Reducing the free alkali (sodium and potassium) present to restrict ASR gel formation
- c. Reducing the permeability of the concrete to restrict water ingress, hence preventing the gel expansion.

A variety of available materials can be used to implement the mitigation techniques in order to suppress ASR-induced damage. Using the standard tests to demonstrate effectiveness in controlling ASR, the following materials and approaches should be considered in designing concrete mixtures. The options are not listed in priority and, although usually not necessary, they can be used in combination with one another.

1.6.1 Using non-reactive (innocuous) aggregates

Using a non reactive aggregate (avoiding a reactive aggregate) in concrete is certainly the most obvious method of preventing ASR-induced damage. The level of reactivity primarily depends on the type and amount of the reactive silica in the aggregate. To identify the reactivity of the aggregates, one must perform ASTM C 1260 and ASTM C 1293 tests, ensuring good quality control, and well-documented preferably, field performance. The failure limit of ASTM C 1260 of 0.10% expansion at 14 days in some cases has led to costly failures in the field, such as Denver International Airport and Hartsfield International Airport (Stokes, 2006). In the Northwest Mountain Region of the US, the failure requirement is brought down between 0.080% and 0.10% at 28 days (U.S. DOT, FAA, 150/5370-10B, 2006).

There is a small risk of ASR even when the aggregate sources have been shown to be non-reactive by testing, therefore, some agencies still specify that additional precautions be taken (e.g., use of SCM or limiting the alkali content of the concrete). Moreover, in some locations non-reactive aggregates may be limited, and potential reactive aggregates can be used safely when appropriate preventive measures are taken.

1.6.2 Using mineral admixtures

Supplementary cementitious materials (SCMs) are a siliceous or siliceous and aluminous material. When used with Portland cement, they contribute the hardened properties of concrete through hydraulic activity, pozzolanic activity, or both. The use of SCMs to reduce ASR-induced expansion is allowed by many countries of the world. The most common reasons for using SCMs are the performance-enhancing aspects. The advantages of using SCMs include not only ASR mitigation, but also improve resistance to durability related problems of concrete, such as sulfate attack, corrosion of reinforcing steel, and freezing and thawing. The typical examples of SCMs are fly ash, ground granulated blast furnace slag (GGBFS) and silica fume etc. Most of the SCMs are industrial by-products with less or no direct energy-related costs, while the Portland cement is the most expensive component of concrete, as it is a highly energy-intensive material. The amount of required SCMs for ASR mitigation varies according to its source, the type of aggregate, the type of pozzolan, the amount of alkalis, the environmental and service conditions for the intended concrete and the geometry of the structure (Adams & Stokes, 2002; and Folliard et al., 2003).

1.6.2.1 Blending individual SCMs

1.6.2.1.1 Effects of fly ash

Fly ash is the most widely used supplementary cementitious material in concrete. Use of fly ash in concrete started in the United States since 1930's, and currently more than 50% of the concrete placed in this country contains fly ash (PCA, 2000). Fly ash is a by-product of the combustion of pulverized coal in electric power-generating plants. Fly ash is collected by removing the particles from the combustion air-stream exiting the power

plant. The major constituents of fly ash are glass containing silica, alumina, iron, and calcium; while the minor constituents are magnesium, sulfur, sodium, potassium and carbon (Detwiler et al., 1996). As power plants change fuel sources and methods of burning, the composition of the fly ash and its ability to control ASR also changes (Hudec & Banahene, 1993). The influence of other factors of fly ash is noted below:

Classifications of fly ash

Two major types of fly ashes, Class F and Class C, are specified in ASTM C 618 on the basis of their chemical compositions resulting from the type of coal burn. Class C fly ash is often high-calcium (10% to 30%) ashes with carbon content of less than 2%, and is normally produced from the burning of sub-bituminous coal and lignite. In contrast, Class F fly ash is generally low-calcium (less than 10%) ashes with carbon contents of less than 5%, and is normally produced from bituminous coal. Performance properties between Class C and F ashes vary depending on the chemical and physical properties of the ash and how the ash interacts with Portland cement in the concrete. Class C fly ash usually has cementitious properties in addition to pozzolanic properties due to free lime, while Class F fly ash only reacts with the by-products formed when cement reacts with water. All fly ashes used in the United States before 1975 were Class F. The efficiency of fly ash to control ASR affects on the following parameters:

Fineness

ASR expansion can be prevented by utilizing pozzolans of fine particles. Ultra fine fly ash (UFFA) with particle sizes of approximately 3 microns is shown to be very effective. On the other hand, the effectiveness of silica fume in suppressing ASR is due to its fine particle sizes (around 0.1 microns).

Mineralogy

The characteristic of a fly ash depends on its chemical compositions. As the chemical compositions vary from ash to ash, their reaction properties change, as do their prevention capacities with regard to ASR expansion. The chemical constituents of a fly ash, such as CaO , SiO_2 , Na_2O , K_2O , Al_2O_3 , MgO , Fe_2O_3 and SO_3 , significantly influence expansion due to ASR reactions (McKeen et al., 1998; and Malvar et al., 2002).

Influence of fly ash Amount on ASR Expansion

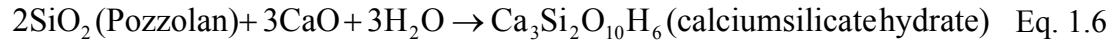
In suppressing ASR expansion for a given aggregate, the amount of required fly ash varies depending on the Portland cement, the type of fly ash, and the desired effects on concrete. In general, Class F fly ash has been found to be more effective in mitigating ASR than Class C fly ash (Bleszynski, 1997), requiring 15 to 30 percent, by mass of cementitious material compared to greater than 30 percent, by mass of cementations material, respectively (ACI 1998). Both types of fly ash are dependent on the lime created during hydration and are never used in lieu of cement entirely.

1.6.2.1.1.1 The advantages of fly ash

Fly ash is one of the most commonly used SCMs because of its economical, technical and ecological benefits. The contributions of fly ash in concrete are described below:

Concrete durability and strength

The main benefit of fly ash in concrete is that it not only reduces the amount of non-durable calcium hydroxide (lime), but in the process converts lime into calcium silicate hydrate (CSH) over time as shown in Equation 1.6. CSH is the strongest and most durable portion of the paste in concrete, which increases the compressive strength of concrete with an increase in immersion age.



Concrete workability

The “ball-bearing” effect of fly ash particles creates a lubricating action (concrete flow) when concrete is in its plastic state. Fly ash contributes 30% more volume of cementitious paste than cement alone. The amount of sand required in the fly ash concrete to produce a certain level of workability is much less than that of the concrete with no fly ash. The workability due the fly ash concrete offers less effort in placement and less energy in pumping, and response better in vibration when filling complicated forms to achieve a sharp and clear architectural design (RILEM 7, 1990).

Concrete durability

One of the important aspects of concrete durability is its impermeability. Fly ash concrete creates more durable CSH as it fills capillaries and bleeds water channels occupied by water-soluble lime (calcium hydroxide). The long term effects of pozzolanic actions of fly ash are decreased permeability and a reduced rate of ingress water and corrosive chemicals, thus, protecting steel reinforcement from corrosion and Portland cement concrete from expansion.

Sulfate attack

Fly ash ties up free lime, which combines with sulfates to create destructive expansion. In general, the chemistry of Class F ashes is proven to be more effective over Class C ashes in mitigating sulfate, mild acid, seawater, and deterioration in concrete (RILEM 7, 1990).

Heat of hydration in Concrete

The hydration of cement, which is as an exothermic reaction, generates heat very quickly and causes the concrete temperature to rise, thus, accelerate the setting time and gain in strength. In many applications, the rapid heat gain increases the chances of thermal cracking which leads to reduce concrete strength and durability. The damaging effects of thermal cracking can easily be solved in replacing large percentages of cement with fly ash.

Protects the environment

Fly ash has a positive impact in enhancing the environment by (i) decreasing landfill disposal as one-third produced fly ash is recycled, and (ii) decreasing CO₂ emission by replacing Portland cement by fly ash.

1.6.2.1.1.2 Studies on Class F fly ash to suppress ASR

Using coal ash from power plants as a substitute for a portion of the Portland cement in concrete is one simple and economical way of minimizing ASR-related damage. The optimal proportion of fly ash in the mixture varies depending on the fly ash type (Class F or Class C), alkali content, its fineness, and other factors.

Calcium hydroxide is considered to be an integral constituent of ASR. Fly ash consumes Ca(OH)₂, which is a factor to influence expansion due to alkali-silica reaction, to reduce damaging expansion (Bleszynski et al., 1998). Calcium hydroxide reaction extent depends on fly ash type in complex ways (Wang, 2007). Additionally, the alkali content of the fly ash must be controlled, and it has been found that Class C fly ash may release a larger portion of their total alkalis into the concrete (Lee, 1989). High CaO fly ashes are generally less effective in controlling alkali silica reactivity and up to 60%

replacement is required to control expansion due to ASR (Thomas et al., 1999). Typically, adequate protection is attained by replacing 15 to 20% and 35 to 40% of cement replacement by a Class F and Class C fly ash, respectively.

Shon et al. (2004) studied the effectiveness of several Class C and Class F fly ashes in controlling expansion due to alkali-silica reactivity (ASR) based on the modifications of ASTM C 1260 test. Three different strengths of NaOH solution (1N, 0.5N, and 0.25N) were used with high and low alkali cement in the mortar bars with 20 and 35% Class C and F fly ash replacements by mass of cement. The other factors included extended immersion age of 28 days. Test results confirmed that Class F fly ash is more effective than Class C fly ash in controlling the expansion of ASTM C 1260.

Bleszynski's (1997) studied lime content of fly ash and level of replacement influenced its ability to mitigate expansion due to ASR. Results showed that decreasing lime contents and increasing replacement levels resulted reductions in expansion and pore solution alkalinity. Taha and Nounu (2008) included that the hydration products of low Ca/Si ratio of the low lime ashes can effectively bond the alkalis in the hydration products and C–S–H structure compensates the lack of calcium in concrete. Therefore, the alkalis will not be free to contribute in the ASR reaction.

In the three provinces of Canada, Manitoba, Saskatchewan, and Alberta, about 80% to 90% of the concrete produced contains fly ash in the range of 10% to 40% by mass of cement depending on the application. Only few cases of ASR-induced structures are reported in that region. On the other hand, replacing 25% to 27% and 25% to 30% of Portland cement (by mass) with Class F fly ash in the States of New Mexico and

California, respectively, was found to mitigate ASR. Low fly ash replacements, on the other hand, did not mitigate the AAR expansion (Monteiro et al., 1997).

At present, high-volume fly ash mixtures are not explicitly used for any purpose, because ACI International's code 318 (building code requirements for structural concrete) specifies a maximum fly ash replacement volume of 25% for concrete exposed to deicing chemicals. Clearly, high-volume fly ash concretes are, in fact, appropriate for many applications where durability and ASR resistance are critical and high early strength is not required.

Shehata and Thomas (2000) conducted experiments on concrete prisms and mortars containing reactive aggregates and six chemical compositions of fly ash and different levels of Portland cement replacements by weight. Results showed that the bulk chemical composition of the fly ash provided a reasonable indication of its performance in physical expansion tests. They concluded that for a given fly ash replacement level, the expansion increased as the calcium or alkali content of the ash increased or its silica content decreased (Fig. 1.15).

Predominantly, CaO and $\text{Na}_2\text{O}_{\text{eq}}$ compositions of fly ash make a significance difference in its influence on expansion due to ASR (McKeen et al., 1998; and Shehata and Thomas, 2000) and play an important role in mitigation ASR expansion. A pessimum effect (i.e. more expansion instead of less) has been observed with an increase in CaO content in fly ash (Malhotra et al., 1994; and Rogers et al., 2000). A 15% cement replacement is adequate only if the fly ash has less than 2% CaO and less than 3% total alkali or 30% fly ash replacement if the CaO content is less than 10% and the total alkali content is less than 3%.

However, it is recommended that fly ash with a maximum CaO content of 8% be used (State-of-the-Art, TR-2195-SHR, 2001). As a result, natural pozzolanic materials with low lime (<2% CaO) and low total alkali content (<3%) are very efficient against ASR when replacing a 15% Portland cement by weight or a 30% fly ash replacement if CaO and total alkali content are less than 10% and 3%, respectively. A maximum CaO content between 8% and 10% can be allowed if the amount of cement replacement is at least 30%. As a result, fly ash with more than 10% CaO is inappropriate for mitigation ASR.

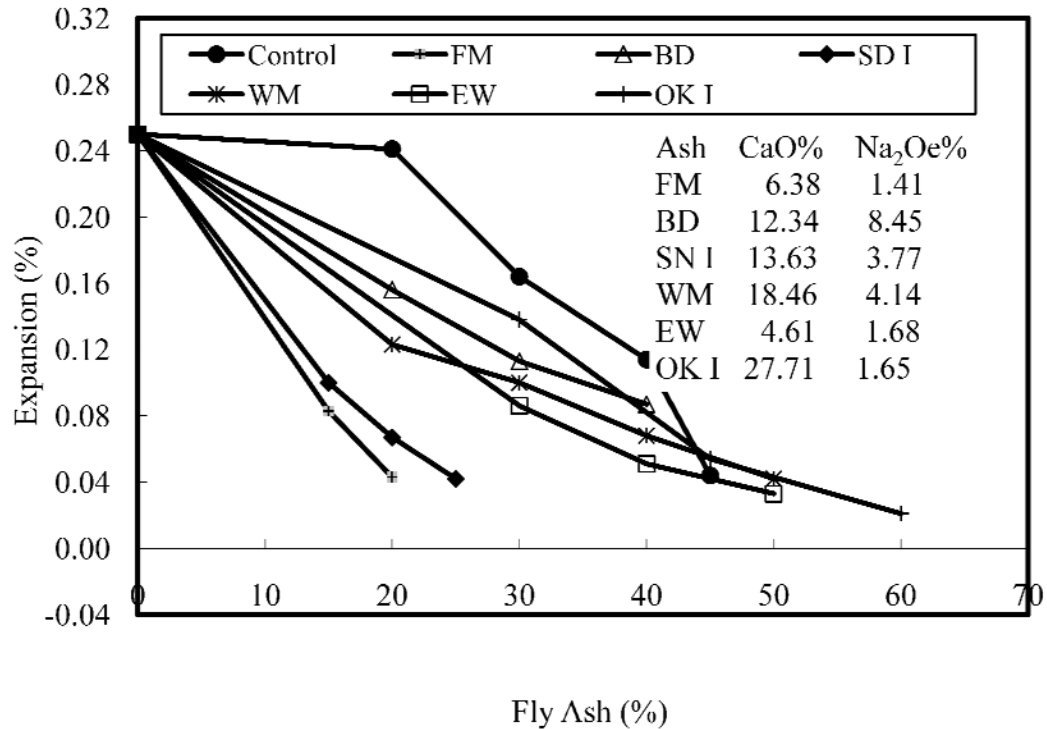


Figure 1.15: Effect of fly ash composition and replacement level on ASR expansion (After Shehata and Thomas, 2000)

1.6.2.1.1.3 Evaluation of pozzolanic activity

Fly ash is proven to be somewhat variable in its effectiveness, principally because its composition depends on the coal properties from which it is derived (Hudec & Banahene 1993). The compositional characteristics of Class F fly ash, when an adequate amount of Portland cement is replaced by fly ash, make a significant difference in its influence on expansion due to ASR (McKeen et al., 1998). There are three characteristics of a fly ash that determine its efficiency in preventing ASR expansion (Malvar & Lenke, 2005): fineness, mineralogy and chemistry. The fineness of fly ashes is one of the important physical properties that affecting pozzolanic activity (Berube, 1995). Finer pozzolans are more efficient in reducing ASR expansion. The mineralogy of the fly ashes varies from ash to ash, so does its effectiveness in suppressing alkali-silica reactivity.

The chemical constituents of a fly ash are divided into two groups based on its capacity to control ASR-induced expansion: the constituents that increase expansion, such as CaO, Na₂O, K₂O, MgO, and SO₃, and those that reduce expansion, such as SiO₂, Al₂O₃, and Fe₂O₃ (Malvar et al., 2001).

Constituents that take place in pozzolanic reaction reducing expansion

The sequence in which the constituents of SCMs are beneficial in reducing ASR is SiO₂ > Al₂O₃ > Fe₂O₃. These constituents act the pozzolanic reaction either in acid or in alkalis. They are replaced and combined to their SiO₂ equivalents [SiO_{2(eq)}] (Malvar & Lenke, 2006), as shown in Equation 1.7.

$$\text{SiO}_{2\text{eq}} = \text{SiO}_2 + 0.589\text{Al}_2\text{O}_3 + 0.376\text{Fe}_2\text{O}_3 \quad \text{Eq. 1.7}$$

The influence of equivalent SiO₂ content of a given mixture on ASR expansions has shown a strong inverse correlation with a R² value of 0.7834, as shown in Figure 1.16,

which is better than any previous correlation with a single component of SiO_2 ($R^2 = 0.741$), Al_2O_3 ($R^2 = 0.604$), and Fe_2O_3 ($R^2 = 0.131$) in reducing ASR expansion (Malvar & Lenke, 2005, 2006).

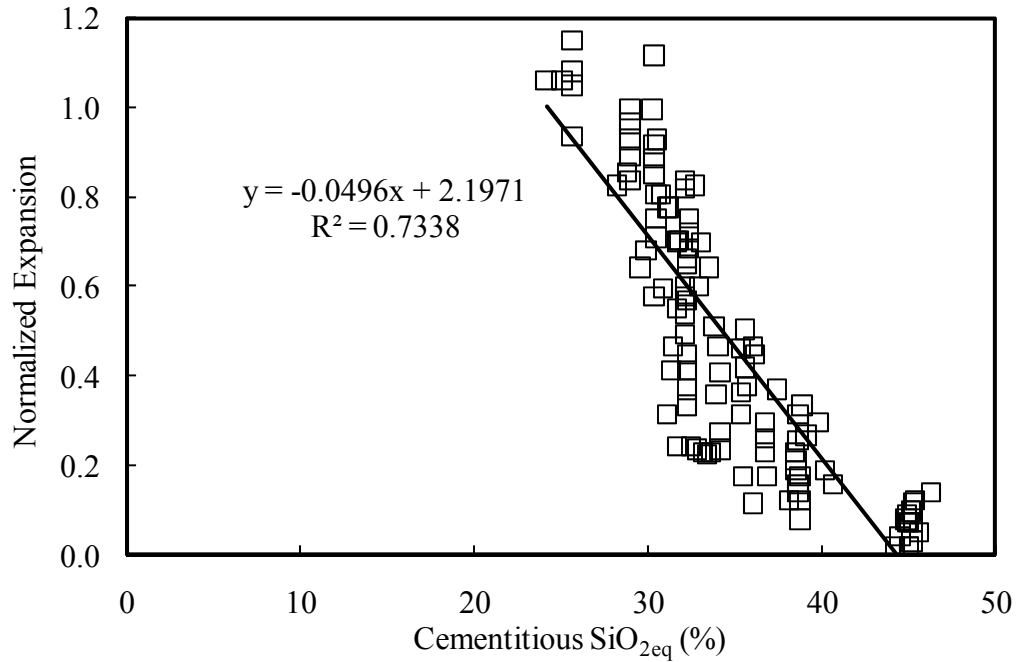


Figure 1.16: Effect of 14-day AMBT expansion and equivalent SiO_2 content of the mortars (Malvar & Lenke, 2006)

Constituents that take place in pozzolanic reaction promoting ASR expansion

Calcium oxide is the major constituent of fly ash that induces ASR expansion most, and other deleterious constituents are $\text{Na}_2\text{O}_{\text{eq}}$, MgO , and SO_3 . These constituents are also replaced by their CaO molar equivalents of a test mixture (Malvar & Lenke 2006), as shown in Equation 1.8.

$$\text{CaO}_{\text{eq}} = \text{CaO} + 0.905\text{Na}_2\text{O}_{\text{eq}} + 1.391\text{MgO} + 0.700\text{SO}_3 \quad \text{Eq. 1.8}$$

ASR expansion is often correlated to CaO content of SCMs. The relationship between the normalized 14-day expansion and CaO_{eq} of the mixture, as shown in Figure 1.17,

represented a better correlation (with a R^2 value of 0.78) than any previous correlation with a single constituent of CaO with a R^2 of 0.7143, $\text{Na}_2\text{O}_{\text{eq}}$ with a R^2 of 0.0251, MgO with a R^2 of 0.055, SO_3 with a R^2 of 0.05, in promoting ASR expansion (Malvar & Lenke, 2005, 2006).

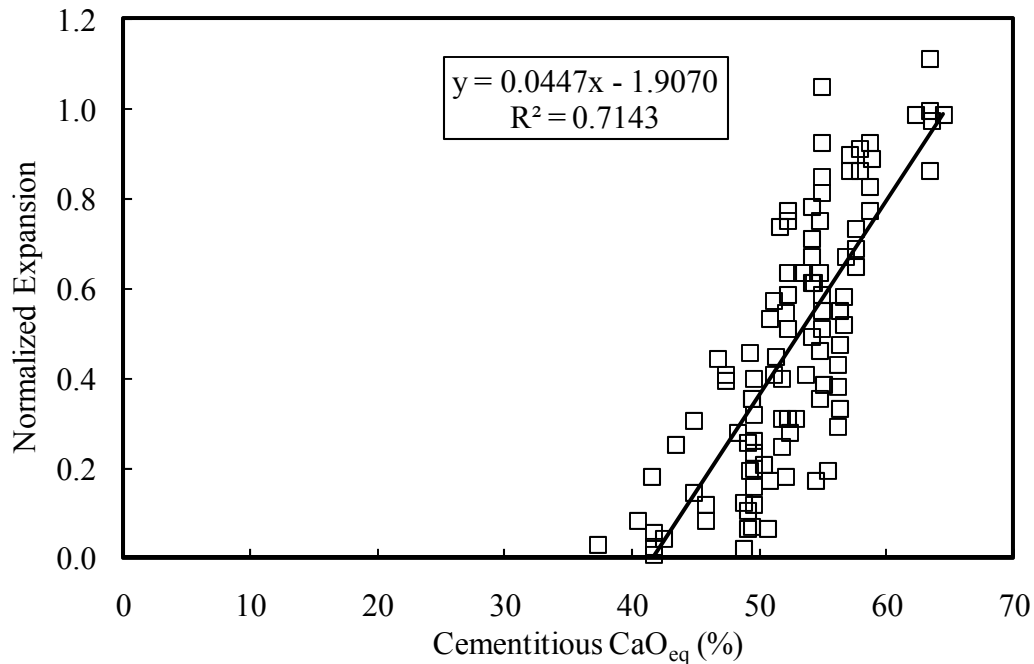


Figure 1.17: Effect of equivalent CaO content on 14-day AMBT expansion (Malvar & Lenke, 2006)

Malvar and Lenke (2006) also analyzed the 14-day expansion over the ratio of CaO_{eq} to $\text{SiO}_{2(\text{eq})}$ of the concrete mixture. The expansion was shown a better influence of the $\text{CaO}_{\text{eq}}/\text{SiO}_{2(\text{eq})}$ of SCMs, as shown in Figure 1.18, which showed an improved R^2 value of 0.83 (Malvar & Lenke, 2006) as compared to with just CaO_{eq} ($R^2 = 0.78$) and $\text{SiO}_{2(\text{eq})}$ ($R^2 = 0.7834$) of the concrete mixture.

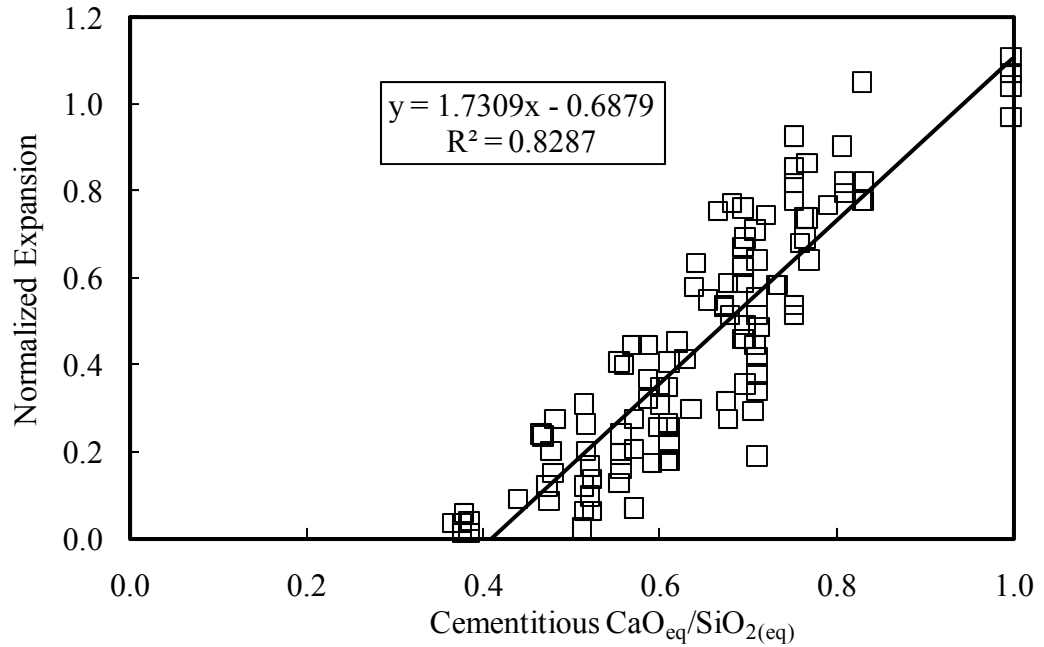


Figure 1.18: Effect of normalized $\text{CaO}_{\text{eq}}/\text{SiO}_{2(\text{eq})}$ on 14-day expansion (Malvar & Lenke, 2006)

McKeen et al. (1998) studied the amount of equivalent alkalis plus lime divided by the amount of silica $[(a+l)/s]$ for the total cementitious materials on the 14-day expansion of mortar bars. The results are presented in Figure 1.19, which suggests that the expansion was a function of $(a+l)/s$ of mixture. The quantity of $[a+l]/s$ required to reduce the expansion of the mortar bars made with reactive aggregates to 0.10% was related to the control expansion of the reactive aggregates. The analysis was effective for blending Class F fly ash only, not Class C or the combination of both. Based on the results, the authors contemplated a setting value of $[a+l]/s$ at 1.45 was required to suppress ASR expansion of all four investigated reactive sources with the specified cement and Class F fly ash.

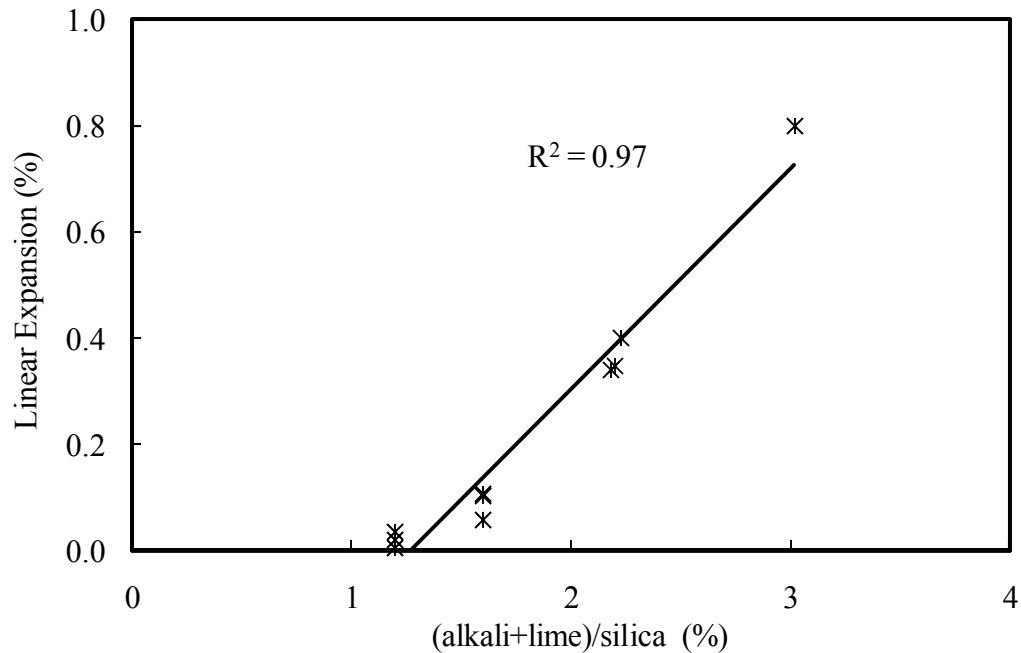


Figure 1.19: 14-day expansion of AL quarry and (alkali+lime)/silica of the cementitious materials (McKeen et al., 1998)

1.6.2.1.2 Effects of slag

Ground granulated blast furnace slag (GGBFS) is a non-metallic product consisting essentially of silicates and aluminosilicates of calcium and other bases that are developed in a molten condition simultaneously with iron in a blast furnace. GGBFS consumes alkalis in the hydration process, thus reducing the total alkalis in the concrete. As a result, only a reduced amount of alkalis are present for ASR reaction. Additionally, slag cement also reduces the pore liquid, which is one of the three influential parameters for alkali-silica reactivity.

Normally, a higher dosage of slag is required to reduce ASR-related expansion than fly ash. In general, slag cement replacement of 25 to 70% of the Portland cement in a concrete mixture would result in effective mitigation of ASR, depending on the Portland cement, the slag cement, and the reactivity of the aggregate used (Malvar et al., 2002).

The ACI 233R (1995) guide indicates a minimum of 40% cement replacement with GGBFS is needed to mitigate ASR. A significant reduction in expansion of the concrete was observed when 50% Portland cement was replaced with slag, and the alkali level of that dosage of slag was not a contributory factor (Hester et al., 2005).

1.6.2.1.3 Effects of silica fume

Silica fume is very fine non-crystalline silica produced in electric arc furnaces as a by-product of the production of element silicon or alloys containing silica (ACI 116R). The particle size of silica fume is extremely small, with more than 95% of the particles being less than one micro meter. The potential for the use of silica fume in concrete has been established since the 1940s (Holland, 2005).

Silica fume creates millions of very small particles in a concrete mixture that fill in the spaces between coarse and fine particles as well as in the spaces of cement particles. This phenomenon is referred as particle packing or micro-filling. Though silica fume has no ability to react like cement, its micro-filler effect would enhance the significant improvements in the nature of the concrete. Both physical and chemical properties of silica fume are influenced by its size (Holland, 2005).

The high amorphous silicon dioxide content makes silica fume a very pozzolanic material in concrete. Silica fume reacts with the calcium hydroxide, a byproduct leased by the hydration process, to form an additional binder material (calcium-silicon-hydrate), which is very similar to the calcium silicate hydrate formed from the Portland cement. The additional binders develop the hardened properties of concrete.

1.6.2.1.3.1 Advantages of silica fume

Silica fume is used in concrete because it significantly improves the fresh and hardened properties of concrete. Fresh concrete made with silica fume is more cohesive and therefore less prone to segregation than concrete without silica fume. Silica-fume concrete requires very low water content because of its high surface area. There will be no bleeding in most concrete when silica fume content is reached to about 5%.

Silica fume produces concrete with a very high compressive strength and modulus of elasticity. The contribution of silica fume is to reduce the permeability of the concrete, an important factor of concrete, is directly related to its durability (Holland, 2005). Moreover, additional abrasion resistance can also be controlled with the use of higher silica fume in the concrete.

1.6.2.2.3.2 Studies on silica fume to suppress ASR expansion

Silica fume has not been used as frequently as fly ash and slag to mitigate ASR. Short-term use of condensed silica fume in sufficient amounts is considered effective in suppressing concrete expansion due to alkali-silica reactivity (Bérubé, 1993). However, a low level of silica fume replacement (4%) shows no differences in expansion of concrete prism up to a year (Boddy et al., 2000). Silica fume at a dosage of 10% has been proven to reduce the expansion to a level as compared to that of 20% Class F Fly ash (Touma et al., 2001).

For highly reactive aggregates, the amount of silica fume (10%) required to control ASR may be in excess of the typical dosage used in concrete construction, making it difficult for use in field applications, mainly due to workability concerns, high water and super plasticizer demand, and shrinkage problems (Folliard, 2003). To overcome those

difficulties, it is generally more effective to use silica fume in conjunction with other SCMs, such as fly ash or slag. This combination reduces the required dosages of silica fume with improvement in constructability attributes. The combination of blending more than one cementitious material in the concrete, known as ternary blends, are discussed in the next section.

1.6.2.2 Ternary blends of SCMs

The concept of ternary blends, combination of two or more SCMs in concrete, has been well accepted in recent years due to the economical aspects and technical benefits, such as workability, early strength development, and durability properties. The ternary blends of SCMs are also very effective in controlling ASR, and in reducing quantities of each SCMs than the usually amount of the individual cementitious material. For instance, 4 to 6% of silica fume in conjunction with moderate dosages of slag (20 to 35 percent) or any types of fly ash (C or F) has shown to be very effective in controlling highly reactive aggregates (Shehata & Thomas, 2002). Another research study (Thomas et al., 1999) demonstrated that the combinations of 3 to 5% silica fume and 20 to 30% fly ash with high CaO content showed satisfactory performances in both ASR and sulfate expansion tests.

When considering ternary blends to control ASR, the combining two or more SCMs must reduce the quantities and increase the durability that otherwise would be used individually. The durability properties of the ternary concrete are never critically affected by heat curing even at high curing temperatures (Ekolu, 2004). The combination of silica fume and slag, on the other hand, reduced high-range water reducer dose and increased

resistance to ASR expansion and chloride ingress than the use of one of these materials alone (Bleszynski et al., 2002).

Shehata and Thomas (2002) investigated the effects of cementitious materials containing Portland cement, silica fume and fly ash on the expansion caused by alkali-silica reaction. Results showed that practical levels of silica fume with low-, moderate- or high-calcium fly ash are effective in maintaining the expansion below the 0.04% after 2 years for prism specimens. The results showed that the pastes containing silica fume yielded pore solutions of increasing alkalinity at ages beyond 28 days, while these containing ternary blends maintained the low alkalinity of the pore solution throughout the testing period up to 2/ 3 years.

1.6.3 Using chemical admixtures

Some chemical admixtures, such as lithium salts and air-entrainment, are capable of controlling the excessive expansion of reactive aggregates caused by alkali-silica reactivity. Though air-entrainments are primarily used to enhance concrete durability, they also suppress ASR-induced expansion and cracks (Hobbs, 1988). Conversely, lithium-bearing salts are used only to inhibit ASR without altering the physical properties of concrete. The idea was first reported in 1951 (McCoy and Caldwell). For the next 40 years, a few studies were conducted on the effectiveness of lithium-bearing compounds to control ASR. However, in the past two decades, the researchers have demonstrated renewed interests in lithium as an admixture in new concrete to control ASR.

Lithium is an alkali metal found in Group IA of the periodic table and has an atomic number of 3 (Folliard et al., 2003). It is a soft, silver-white metal with light density (Thomas, 2007). The normal properties of lithium are parallel to those of K and Na

because they are in the same alkali-metal group. The cation radius of lithium is smaller, and the electric charge density is higher compared to that of K^+ and Na^+ . Lithium is a purely unstable metal and can easily react to moisture because it has one electron in its outer shell (Thomas, 2007). Stable lithium compounds – lithium carbonate, lithium chloride, and lithium nitrate – can be manufactured for commercial use. Lithium-based admixtures are promising alternatives to conventional methods for preventing or mitigating ASR (Folliard et al., 2003).

Figure 1.20 illustrates the expansion of the mortar bars made with the Placitas and quartz aggregates due to alkali-silica reactivity. As can be seen, the expansion of the untreated specimen is suppressed with the use of lithium-to-alkali molar ratio of 0.74. The untreated mortar bars expand with an increase in immersion age, while the specimens treated with lithium salt produce a very small expansion throughout the test.

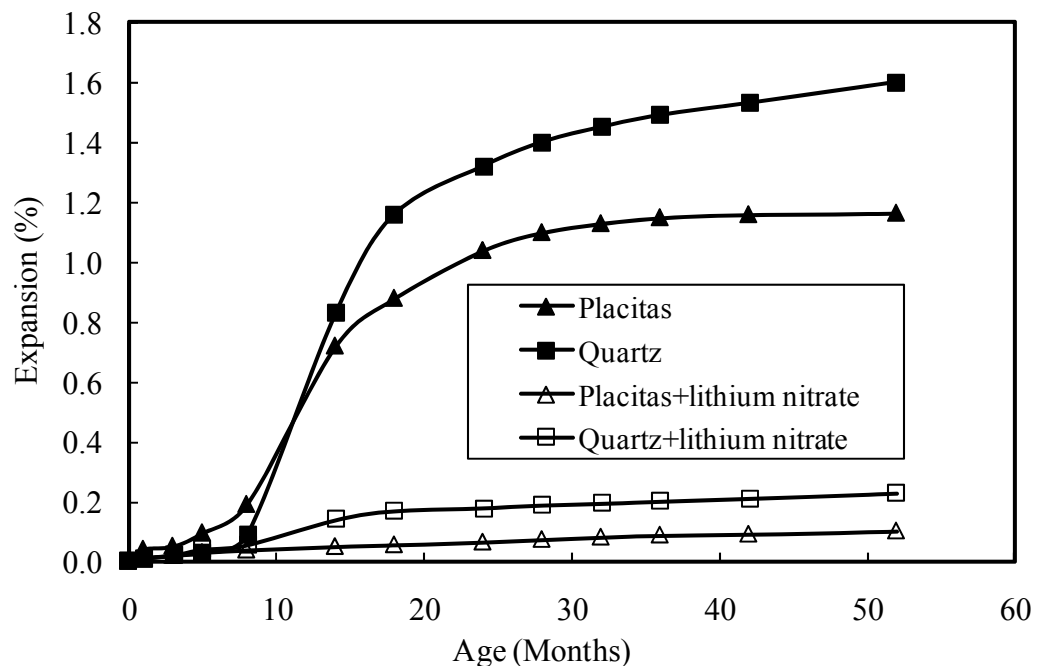


Figure 1.20: Influence of $LiNO_3$ at a molar ratio of 0.74 on ASR expansion (Ekolu et al., 2007)

Several national and local specifications have included lithium technologies as a tool for combating ASR due to its availability of a range of products and custom-tailored to specific applications. On the whole, lithium admixtures offer the following benefits to concrete (Adams & Stokes, 2002):

- a. Permit the use of local and cost-effective aggregates
- b. Increase the life span of concrete structures
- c. Lithium nitrate admixtures are safe, easy to handle, and environmentally benign,
- d. Lithium nitrate and glass-based admixtures have no significant effect on other concrete properties

The main application for lithium in the construction industry is in the formulation of chemical admixtures for concrete, such as LiNO_3 , Li_2CO_3 , LiOH , and Li_2SO_4 . These types of admixtures are used in the formulation of set accelerators for calcium-aluminate-cement concrete, and lithium hydrate and lithium nitrate have been used to control ASR in Portland cement concrete.

1.6.3.1 Mechanisms of lithium salts to suppress ASR

Lithium does not react with concrete in the same manner as pozzolanic materials. The mechanisms by which the lithium salts reduce ASR expansion are still unclear. A better understanding of the mechanisms will help significantly in identifying the effectiveness of a particular lithium salt, its dosage and predicted the duration of its control on ASR expansion. The following mechanisms by which lithium react with ASR have been proposed by many researchers (Folliard et al., 2003; Feng et al., 2005; Mo et al., 2008; and Taha & Nounu, 2008):

- a. Lithium may alter ASR product compositions

- b. Lithium may reduce silica dissolution
- c. Lithium may decrease the repolymerization of silica and silicates

Each of the above mentioned mechanism is discussed below.

1.6.3.1.1 Lithium may alter ASR product compositions

The most commonly recognized mechanism by which lithium compounds suppress ASR expansion was first proposed by Lawrence and Vivian (1961). The mechanism is the ability of lithium to change the reaction compositions. Lawrence and Vivian studied the reactions of three different alkali solutions (NaOH, KOH, and LiOH) and a mixture of these with reactive silica. The researchers illustrated that in the presence of lithium, a lithium silicate forms by ASR, and this product is less soluble and more stable than the ASR product. They proposed that due to gel stability and non-expansive behavior, the resulting LiOH silica complex might form an insoluble surface layer around the silica protecting from further attack by the alkalis in the concrete. The studies conducted by Ramyar et al. (2004), and Kawamura and Koderia (2005) strengthened Lawrence and Vivian (1961)'s observation and they added that massive reaction products formed in the vicinity of aggregate or in thick layers.

Sakaguchi et al. (1989) and Stark (1992) empowered the idea of Lawrence and Vivian's proposal on lithium-silica gel composition. A non-swelling dissolved product, lithium silicate gel, was produced at the interface of the aggregates. In the presence of sufficient concentration of lithium, a lithium-alkali (possibly calcium) silicate, which is crystalline (Mo et al., 2005), forms at the interface of the aggregates (Sakaguchi et al., 1989). Thus, in the presence of lithium salt, reactive aggregates have little or no influence on expansion (Stark, 1992; Sakaguchi et al., 1999; and Mo et al., 2005). The study of

Diamond and Ong (1992) showed that the amount of lithium present in the gel product increased in proportion to the amount of sodium and potassium present.

Collins et al. (2004) observed a sharp decline in dissolved Na and Li concentrations over the first 24 hours of curing, which indicated that the alkalis were bound within the reaction products. Collins and his co-workers also noticed that the formation of a crystalline product at the paste-aggregate interface as early as 1 day of curing by laser scanning confocal microscopy (LSCM). The form of reaction product, whether crystalline or gelatinous, significantly depends on the lithium dosage and may also vary with the location and time (Ramyar et al., 2004; and Mo et al., 2005). Analyzing the direct results of significant crystalline products in the lithium-bearing specimens in suppressing ASR by SEM, Mo et al. (2005) observed that large amount of Ca and Si in the crystalline product but less K than that in a typical ASR gel.

Kawamura and Fuwa (2003) revealed that massive ASR gels existed in relatively wide cracks within reactive aggregate particles with LiOH dosage of 0.3% and 0.5% mortars which showed great expansions. Conversely, no gel was observed in mortars with greater than the threshold dosage level of a lithium salt. The results also showed that the average CaO/SiO₂ ratio in ASR gels decreased with increasing amount of added lithium salts. The addition of relatively small amounts of LiOH and Li₂CO₃ resulted in increased expansion, and that the composition of ASR gels became homogeneous at a high dosage level.

1.6.3.1.2 Lithium may reduce silica dissolution

The mechanism of silica dissolution is not so much controlled by alkalis, but rather by dissolved OH-ions breaking silica bonds which recombine with alkali-ions present in

the concrete (Broekmans, 1999). The rate of silica gel dissolution in aqueous alkali metal hydroxides depends on the type of alkali metal hydroxide in solution (Wijnen et al., 1989). The rate of dissolution depends on the radius of the hydrated ion, which, in fact, is important in determining the extent of chemical reaction of alkali-silica reactivity. The silica dissolution rate of three alkali-hydroxides increases in the following order (Lawrence & Vivian, 1961; Sakaguchi, 1989; and Wijnen et al., 1989):



Wijnen et al. (1989) proposed that the rate of silica dissolution decreased with increasing hydrated ion radius of the alkali metal cations in solution surrounding a silicate surface. Table 1.4 shows ionic and hydrated ionic radius of KOH, NaOH and LiOH. It can be declared that lithium decreases with the rate of silica dissolution, which resists the rate of gel formation. Results obtained from Lawrence and Vivian (1961), Wijnen et al. (1989) and Broekmans (1999) demonstrated that among three alkali-hydroxides, LiOH, NaOH, and KOH, the rate of silica dissolution is the slowest for LiOH and fastest for KOH. Collins et al. (2004) suggested that dissolution of silica and the behavior of Na appeared to be rate-limited by diffusion into and out of the thick bed of silica gel and the reaction products.

Table 1.4: Chemical information for Li^+ , Na^+ and K^+ ions (Feng et al., 2005)

Ions	Valence	Ionic radius (nm)	Hydrated ionic radius (nm)
Li	1	0.060	0.34
Na	1	0.095	0.276
K	1	0.133	0.232

Collins (2002) studied the silica gel in model pore solution, and he found out the silica concentration in solution decreased with increasing lithium concentration over a period from 1 hour to 28 days. Sakaguchi (1989) pointed out that the concentrations of lithium near the silica, with compared to alkalis, sodium and potassium, decreased the rate of dissolution (the rate of formation of the expansive product), confirming the lithium-silica reaction is more favorable than the sodium-silica or potassium-silica reaction. Lawrence and Vivian's study (1961) showed that increasing LiOH concentrations up to 2N LiOH equivalent in 2N NaOH solution resulted in a greatly decreased tendency for NaOH to react with silica gels.

The study performed by Collins et al. (2004) improved the understanding of mechanism by which lithium salts mitigate ASR. In their study, three lithium additives, LiOH, LiCl and LiNO₃, at various dosages were used. The effect of lithium additives on ASR was assessed using mortar bar expansion testing and measured the change in concentrations of Si, Na, Ca, and Li at different times from slurries of silica gel and alkali solution. Collins et al. (2004) concluded the following findings:

- a. The trend of dissolved Si concentration decreased with an increase in lithium in slurries prepared with LiCl and LiNO₃ could be due to lithium suppressing silica dissolution or promoting precipitation of a silica containing reaction product.
- b. In contrast to slurries prepared with LiCl and LiNO₃, slurries prepared with LiOH showed an increase in silica dissolution with a corresponding increase in additive amount.

Qi and Wen (2004) have proved above findings with lithium hydroxide that reduces the dissolution of silica by forming a lithium silicate layer on the surface of reactive

aggregates. Research studies demonstrated that lithium salts decrease pH of the pore solution (Diamond, 1999; and Bérubé et al., 2004), and silica dissolution controls by pH of the pore solution (Broekmans, 1999). The structure of the silica governs the rate and/or amount of dissolution. Poorly crystalline or amorphous silica is much more prone to ASR than well-crystallized or dense forms of silica, because that the solubility of amorphous silica increases significantly with pH (Tang and Su-fen, 1980). The dissolution rate of well-crystallized or dense forms of silica only occurs at very slow rate at the surface.

1.6.3.1.3 Lithium may re-polymerize ASR gel

Kurtis et al. (2000, 2003) first proposed this theory. They claimed that the suppressive effect of lithium on ASR-related expansion not only depended on the quantity of dissolved silica but also the attributed to the limitation of ASR gel re-polymerization. Their investigations of ASR gel in simulated pore solutions with and without lithium salts (LiNO_3 , LiCl , and LiOH), in which transmission soft X-ray microscopy was employed to image the changes in gel microstructure. The gel obtained from an ASR affected structure was exposed to the NaOH alone and NaOH with LiCl solutions. In the presence of NaOH solution alone, the ASR gel is partially dissolved and repolymerized as a potentially expansive gel. While in the presence of LiCl , a significant dissolution of the original gel particles was observed, but the repolymerization into an expansive gel was decreased as compared to the reaction of the ASR gel in the presence of NaOH solution alone. The results of the study revealed that lithium might limit the repolymerization of ASR gel, which can effectively control the expansion caused by alkali-silica reactivity. It should also be noted that the observations are based on one particular lithium salt. The situation may be different for other lithium salts.

In summary, lithium forms an alkali-silica gel that is non-expansive. Lithium silicates, a product generated by the reaction with lithium and silica comes from aggregate, are less water-soluble and do not absorb water as much as sodium or potassium silicates do. While the reaction of lithium with the ASR reaction product appears permanent, there should be sufficient lithium present in the pore solution to protect against future attack by any alkalis remaining in the concrete mixture.

1.6.3.2 Studies on lithium salts to suppress ASR expansion

The efficacy of lithium salts in suppressing excessive ASR-related expansion strongly depends on the nature of aggregate, form of lithium, the amount of alkalis and supplementary cementitious materials present in the concrete (Bérubé et al., 2004; and Feng et al. 2005). The expansion of concrete prepared with an aggregate depends on the amount of lithium relative to the amount of alkalis present in the mixture. For expressing the lithium dosage, this has led to the use of lithium-to-alkali molar ratio ($[Li]/[Na+K]$) in the mixture, where $[Li]$ is the number of lithium moles, and $[Na+K]$ is the sum of the sodium and potassium moles present in the mixture.

McCoy and Caldwell (1951) were the first researchers to identify lithium compounds as effective admixtures in controlling ASR. Four types of lithium compounds were employed, such as $LiCl$, Li_2CO_3 , LiF , $LiNO_3$ and Li_2SO_4 , and the results indicated that the lithium-to-alkali molar ratio of 0.74 was sufficient to restrain ASR expansion efficiently.

The standard lithium dose (sometimes referred 100%Li) is the amount of lithium admixture that supplies enough Li ion to achieve a lithium-to-alkali molar ratio of 0.74. The dose refers as approximately 4.6 liters of Li admixture for every kg of sodium

equivalent supplied by the cementitious materials. It is generally considered that with lithium-based salts, partial substitution of lithium ions for potassium or sodium ions occurs in the ASR gel. The ratio of Li^+ ions to ordinary alkali ions incorporated within the gel is a function of their relative proportions in solution. Inadequate dosages results increase rather than decrease in expansion (Diamond, 1999). Adding only half of the required quantity of lithium to a concrete mixture shows little or no reduction in ASR expansion (Lumley, 1997). However, the effectiveness of lithium treatments is related to a high relative proportion of lithium to the other cations in solution (Kawamura & Fuwa, 2003; and Lumley, 1997). In general, the $\text{Li}:(\text{Na}+\text{K})$ of 0.74 is adequate to suppress excessive ASR expansion for most aggregates (McCoy & Caldwell, 1951; Blackwell, et al., 1997; Thomas, 2000; Federal Highway Administration, 2003; Ekolú et al., 2007; and Millard & Kurtis, 2008). However, some highly reactive aggregates require substantially more dosage (Folliard et al., 2006), and some less reactive aggregates may need less (Touma et al., 2001; Lane, 2002; and Collins et al., 2004).

Previous studies illustrated that about half of the lithium added in the mortar bars to suppress ASR-induced expansion is absorbed by the hydrating cement and the uptake of lithium by C–S–H, and the remaining half is available for the suppressive purpose (McKeen et al., 1998; Bérubé et al., 2004; Feng et al., 2005; and Li, 2005). Therefore, the expansion of the untreated mortar bars under the 1N NaOH solution showed much higher than that of the specimens treated with the lithium solution (McKeen et al., 1998; Touma et al., 2001; and Li, 2005). Touma et al. (2001) demonstrated that the expansion of mortar bars made with 75% and 100% lithium merged closer as the time progressed (Touma et al., 2001). To prevent excessive leaching effect of lithium salts from the bars into the

surrounding solution, the ASTM C 1260 test was modified by adding lithium into the soak solution to maintain the same lithium-to-alkali molar ratio in the mortar bars and the soak solution (Stokes, 1993; Berra et al., 2003; Folliard et al., 2003; Collins et al., 2004; and Li, 2005).

Hudec and Nana (1993) studied an extensive number of lithium-bearing components in order to mitigate ASR expansion. Their investigations showed that all lithium bearing-specimens produced better results than an untreated specimen except for the lithium acetate and lithium carbonate, which showed had no effect on the expansion caused by ASR. Additionally, their studies proved that lithium hydroxide was effective for all aggregate types, whereas lithium nitrate showed most effective for all sources except for some aggregates.

McKeen et al. (1998) studied the evaluation of three lithium nitrate dosages, namely 75, 100 and 125% of the manufacturer's recommended dosage (that corresponded to lithium-sodium molar ratio of 0.55, 0.74 and 0.93), on ASR expansion of three severe reactive aggregates. Based on the failure criteria of AASHTO T 303 at 14 days, the above mentioned three lithium dosages were not adequate in holding back the excessive expansion below 0.1%. Lane (2002) demonstrated that the effective lithium-to-alkali molar ratio of 0.925 was showed to be effective for the less accelerated concrete prism tests. Recently, Ekolu et al. (2007) proved that the incorporation of lithium nitrate in a proportion of 0.74 was effective for controlling alkali-silica reaction and delayed ettringite formation concretes.

Ramyar et al. (2004) studied ASR-induced expansion of mortar bar specimens incorporated with Class C fly ash, lithium carbonate, and lithium fluoride. The expansion

of fly-ash treated mortar bars showed significant increase in expansion after 28 days, while the expansion of lithium treated specimens remained nearly constant beyond 28 days. This phenomenon confirmed that lithium-bearing specimens showed no expansion tendency after a certain period of immersion age.

Feng et al. (2005) studied the influence of the eleven distinct lithium salts, namely LiF, LiCl, LiBr, LiOH, LiOH.2H₂O, LiNO₃, LiNO₂, Li₂CO₃, Li₂SO₄, Li₂HPO₄, and Li₂SiO₃, in suppressing ASR expansion in new concrete. The findings showed that all lithium salts were effective in suppressing ASR at the appropriate dosages; however, LiNO₃ appeared to be the most effective. The minimum dosage (lithium-to-alkali molar ratio) to inhibit ASR expansion was found in the range of 0.72 – 0.93 for the LiNO₃, and 0.67 – 1.20 for the remaining lithium salts.

Tremblay et al. (2007) studied the use of LiNO₃ to control ASR expansion of twelve reactive aggregates. Of the aggregates tested, the study showed that the standard LiNO₃ dosage of 0.74 was adequate in suppressing excessive expansion of six aggregates. Three aggregates required a higher LiNO₃ dosage of 0.75 to 1.04, whereas the expansions of the remaining three aggregates were not inhibited even with the use of lithium to alkali molar ratio of 1.11.

A recent study on the influence of Li₂CO₃ against alkali-silica reactivity of two reactive aggregates was executed by Mo et al. (2008). Results showed that the most highly reactive source, having a control expansion of 1.205%, was effective to inhibit ASR to the extent of 93-95% by adding Li₂CO₃ at the lithium-to-alkali molar ratio ranging from 0.3 to 0.9. On the other hand, the least reactive aggregate, required Li/(Na+K) molar ratio of 0.9 to inhibit ASR expansion from 0.126% (control) to

0.048%. The study conferred a clear idea that lithium compounds were found to be more effectiveness with some extremely reactive aggregates, but relatively less effectiveness with some other less reactive ones.

Reactive aggregates were tested with lithium-based admixtures which extracted lithium in the pore solution of pastes and mortars over time, and the rate of the expansion decreased with increases in immersion age (Hester et al., 2005).

The addition of ASR-inhibiting compound, lithium hydroxide, had shown to be effective on highly reactive aggregates (Stark et al. 1993). Adding LiOH with n (Li)/(Na) of molar ratio with alkali content of the mortars declines the expansion (Xiang-yin et al., 2003). When LiOH.H₂O was used as an admixture, a molar ratio of 0.9 was sufficient to completely suppress ASR. However, using required amount of lithium hydroxide has a duplex effect; can suppress ASR expansion and induce ACR expansion (Quin, 2002). The use of LiOH in reducing ASR is less efficient than that of lithium nitrate (Fig. 1.21).

Table 1.5 outlines a summary of findings on the lithium dosages in suppressing alkali-silica reactivity of various aggregate types. As can be seen, the required lithium-to-alkali molar ratios to suppress ASR-induced expansions vary in a large extent depending on aggregate reactivity and mineralogy, alkali content of the mixtures, water-to-cement ratio and the type of lithium salts used. Based on the past research investigations, a wide range of lithium-to-alkali molar ratios that was shown effective for suppressing ASR were suggested. They were: 0.60 – 0.90 (Collins et al., 2004); 0.6 - 1.0 (Mo et al., 2003 and Hester et. al, 2005); 0.72 – 0.92 (Feng et al., 2005); 0.74-0.93 (McKeen et al., 1998; and Fournier et al., 2004), and 0.74 – 1.04 (Tremblay et al., 2007).

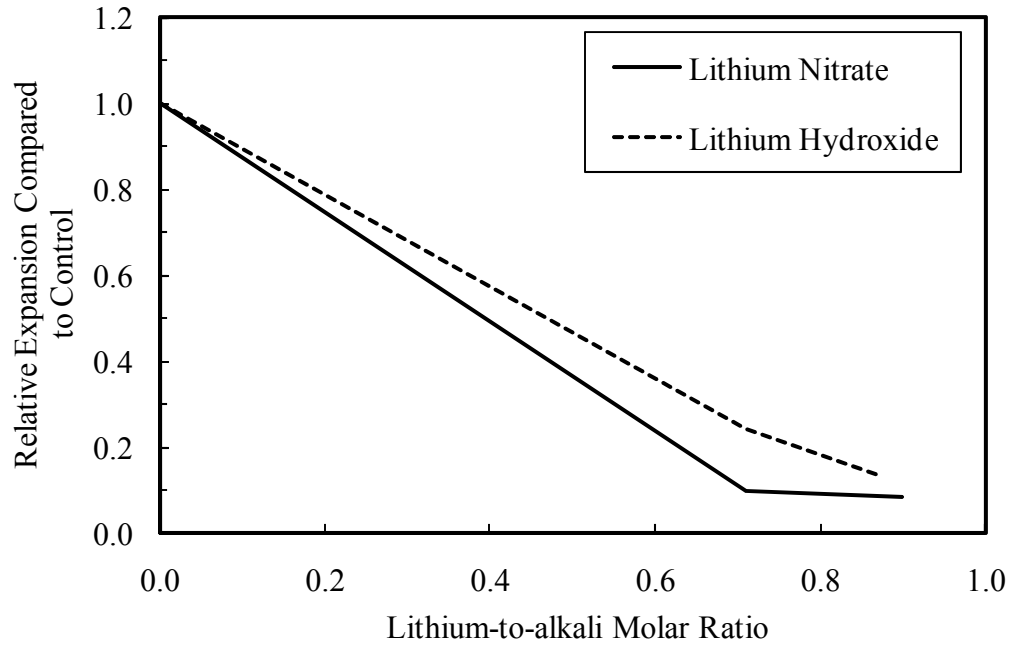


Figure 1.21: Concrete expansions (ASTM C 1293) vs. lithium-to-alkali molar ratios (Thomas et al., 2000)

The American Association of State and Highway Transportation Officials (AASHTO) recommends lithium nitrate over other lithium salts. Moreover, a number of State Departments of Transportation has approved the product in mitigating alkali-silica reactions of fresh concrete.

Lithium nitrate, a fully soluble neutral salt, does not generate significance increase in OH ion concentration, and thus, reduce ASR-induced expansion efficiently (Diamond, 1999). Lithium nitrate can be used to control ASR-induced damages in new and existing concrete structures. Moreover, lithium admixtures make the concrete easy to use in real world situations (Johnston et al., 2003).

Table 1.5: Summary of findings on lithium salts in suppressing ASR expansion (Feng et al., 2005)

Research work	ASTM Standard	Reactive aggregate	W/C by mass	Total Na ₂ O _{eq} %, by mass	Lithium salt(s) studied	Minimum lithium to alkali molar ratio
McCoy and Caldwell (1951)	C 227	Pyrex glass	-	1.15	LiCl, LiF, Li ₂ CO ₃ , Li ₂ SiO ₃ , Li ₂ SO ₄ , LiNO ₃	0.74
Sakaguchi et al. (1989)	C 227	Pyrex glass Andesite sand	0.55	0.8-1.0 1.2	LiOH·H ₂ O, LiNO ₂ , Li ₂ CO ₃ LiOH·H ₂ O	0.90 0.90
Stark (1992)	C 227	Andesite	-	-	LiF, Li ₂ CO ₃	0.67 (LiF), 0.92 (Li ₂ CO ₃)
Stark et al. (1993)	C 1293	Rhyolite Granite genesis	-	-	LiOH·H ₂ O	0.75-1.0 (LiOH)
Diamond and Ong (1992)	C 227	Cristobalite Beltane opal	0.485 0.485	1.0 1.0	LiOH LiOH	1.2 (Cristobalite, more for opal)
Durand (2000)	C 1293	Sudbury Potsdam Sherbrooke	0.405	0.88-1.25	LiOH·H ₂ O, LiF, Li ₂ CO ₃ , LiNO ₃	With Sudbury: 0.72 for LiNO ₃ , 0.82 for others
Lane (2000, 2002)	C 1260 & C 1293	Pyrex glass Quartz	0.45	0.75-1.25	LiOH·H ₂ O, LiNO ₃	0.925 for LiNO ₃
Lumley (1997)	C 1293	Cristobalite	0.5	0.86-1.13	LiOH·H ₂ O, LiF, Li ₂ CO ₃	0.62
Thomas et al. (2000)	C 1293	UK aggregates	-	-	LiOH·H ₂ O, LiNO ₃	0.74 for LiNO ₃ 0.85 for LiOH · H ₂ O
Collins et al. (2004)	C 227	Borosilicate glass	0.37	1.0	LiOH, LiCl, LiNO ₃	0.6 for LiOH, 0.9 for LiCl 0.8 for LiNO ₃
Kawanura et al. (2003)	C 227	Calcined flint	0.55	1.12	LiOH, Li ₂ CO ₃	0.75 M
Ohama et al. (1989)	Autoclave	Opaline amorphous silica	0.63- 0.78	2.0	LiOH·H ₂ O, LiF, Li ₂ CO ₃	0.5% wt for LiF 0.7% wt for LiOH.H ₂ O
Bian et al. (1995)	Autoclave	Andesite sand	0.5	0.5-3.5	LiF, LiCl, LiBr, LiNO ₃ , Li ₂ SO ₄ , Li ₂ CO ₃ LiH ₂ PO ₄	0.80
Mo et al. (2003)	Autoclave	Microcrystalline Quartz	-	1.5-3.0	LiOH·H ₂ O	≥ 0.3 for Na ₂ O _{eq} ≤ 2.5% ≥ 0.6 for Na ₂ O _{eq} = 3.0 %

Among all lithium salts, the reasons of lithium nitrate perform the best results in controlling ASR are as follows:

- a. It is non-toxic and safer to handle than other forms of lithium salts
- b. It does not exhibit a pessimum effect at lower dosages (ACI 221, 1998).
- c. It reduces expansion more efficiently than any other lithium compounds, because lithium nitrate does not convert hydroxide in the pore solution, therefore, it does not raise pore solution pH resulting in inducing ASR expansion (Thomas et al., 2000; Folliard et al., 2003; and Millard & Kurtis, 2008).
- d. Using lithium salt as an admixture in new concrete has no undesired impact on fresh properties, such as air content, slump, setting time, or hardened properties of concrete, such as strength, drying shrinkage, permeability, and resistance to freezing and thawing (Lane, 2002).
- e. Lithium-bearing specimens show no expansion tendency after four months of immersion (Ramyar et al., 2004).

Lithium dosages can be lowered when it is used in combination with suitable pozzolans. The combined use of lithium and SCMs (especially fly ash or slag) is recommended to reduce economical impact lithium salt, and to produce low-permeable concrete that is more resistant to ASR and other deterioration mechanisms (Folliard et al., 2003).

1.6.4 Combining SCMs and chemical admixtures to control ASR

A combination of lithium nitrate and moderate amounts of fly ash can control ASR expansion efficiently, when either the LiNO_3 or fly ash individually is unable to suppress expansion completely (McKeen et al., 1998; Folliard, 2003; and Johnston et al., 2003).

This technique requires less lithium, thereby reduces cost, and less fly ash, thereby increases the early strength development. Recent studies (Johnston et al., 2003; Stark, 1993; Taha & Nounu, 2008) confirmed the positive effect of combining lithium compounds and fly ash to keep the properties of concrete without sacrificing ASR-induced damages. ASR expansion controlled by fly ash alone may sometimes require higher dosages that impact significantly on the early strength of concrete. Secondary cementitious materials (mainly fly ash or slag) can be added with lithium salts for being economical as well as low permeable concrete (Federal Highway Administration, 2003).

McKeen et al. (1998) studied the combined effects of lithium nitrate and Class F fly ash on ASR expansion. In their study, the three dosages of Class F fly ash (12%, 24% and 36%) with low CaO content of 2.81% as a partial replacement of Portland cement by weight combined with the three dosages of lithium nitrate (75%, 100% and 125%) were used to reduce the expansion of the mortar bars made with three reactive aggregates. The ASR expansion of the test mortar bars is presented in Figure 1.23. Of the 27 aggregate-lithium-fly ash combinations, the study showed that the 14-day expansions of the 24 combinations were below 0.1% with the mutual effect of 75% lithium nitrate and 12% class F fly ash. McKeen et al. concluded that a combination of lithium nitrate at the manufacturer's recommended dosage (lithium to alkali molar ratio of 0.74 or 100% lithium) plus Class F fly ash at a minimum of 15% by weight of total cementitious materials would mitigate ASR expansion of most reactive aggregates.

As a part of SHRP program, in 1997, a section of the Lackawanna Valley Highway was constructed using reactive greywacke aggregate, high alkali cement and various preventive measures in suppressing ASR-induced damages. A total of the eleven

preventive techniques were conducted to restrain ASR expansion. They were: adding LiOH dosages at Li/(Na+K) molar ratios of 0.75, 1.0, and 1.25; blending slag replacement at a rates of 25%, 40%, 50%; blending Class F fly ash replacements of 15%, 20% and 25%; using low-alkali cement of 0.37% $\text{Na}_2\text{O}_{\text{eq}}$; and a combination of 15% Class F fly ash with a Li/(Na+K) molar ratio of 0.74. The combined effect of pozzolan and chemical admixture showed most effective to reduce the expansion of the untreated mortar bars from 0.432% to 0.008% (Folliard et al., 2003).

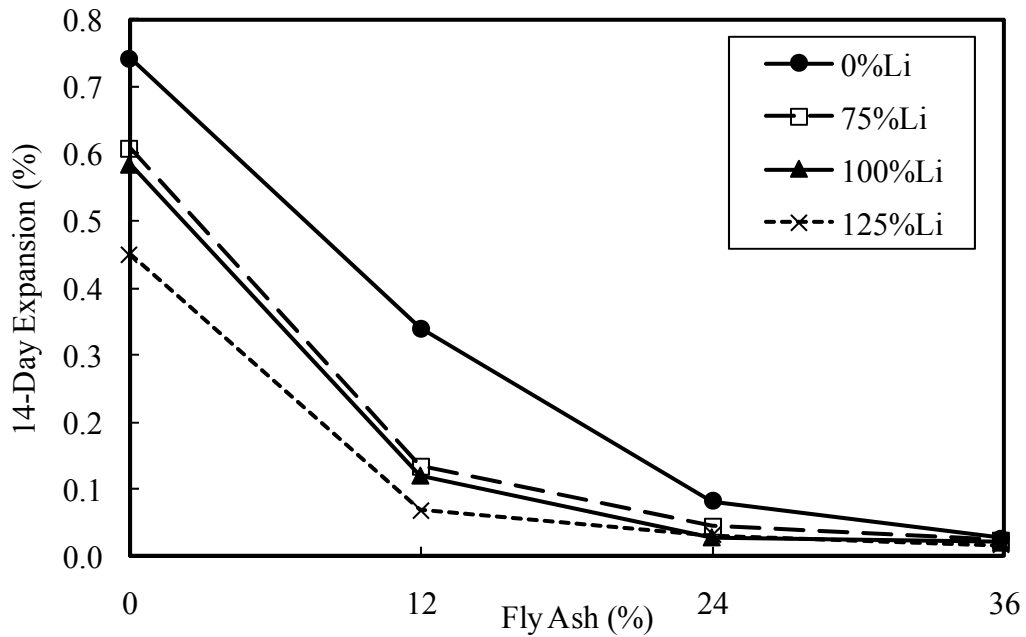


Figure 1.22: Expansion of Placitas aggregate with lithium and fly ash (McKeen et al., 1998)

1.6.5 Adding air entrainment

ASR-induced expansion is disrupted by the use of air-entrained concrete. It was reported that adding 4% entrained air to concrete reduced the ASR expansion by 40% (Jensen et al., 1984). The expanding gel in the mortar bars made of reactive aggregate is

filled by the voids in the concrete, reducing the internal pressure created. The influence of air content on ASR expansion indicates that the higher air content results in lower expansion (Hobbs, 1988). Air entrainment with silica fume reduces the expansion by about 50% of the expansion of the mortar bars when silica fume is used only (Wang & Gillott, 1989).

1.6.6 Adding steel fibers

A new approach in mitigating damages caused by alkali-silica reactivity is fiber-reinforcement, adding fibers to a concrete mixture, in which the reinforcement is distributed more uniformly than that of the tradition bars. Past investigations showed that adding fibers to a mixture had a positive effect in reducing the effects of ASR such as expansions and cracks (Turanli et al., 2001; Yi & Ostertag, 2005; and Bektas et al., 2006). Bektas et al. (2006) studied five dosages of steel fibers; namely, 0, 1, 3, 5 and 7% of mortar volume, on ASR-related expansions. The specimens containing 7% steel fibers exhibited the least expansions of 0.08% at 14 days and 0.11% at 30 days while the unreinforced specimens revealed the highest expansions of 0.35% at 14 days and 0.49% at 30 days.

1.7 Effects of ASR on Mechanical Properties of Concrete

Alkali-silica reactivity has a distinct affect on the mechanical properties of concrete, mainly from micro-cracking mechanisms. ASR-related damage can result in loss of unconfined compressive strength, stiffness, and tensile strength. The total losses in the engineering properties of concrete affected by ASR depends on the physical and chemical characteristics of the aggregates (Swamy & Al-Asali, 1989; and Giaccio et al., 2008), and

the size of the aggregates and the kinetics (rate) of the reaction (Giaccio et al., 2008) of the reactive aggregate present in concrete.

Once alkali-silica reaction takes place at the micro-structural level, the compressive strength of concrete initiates to decrease. Thus, the effect of ASR on the compressive strength of a concrete is a function of time (Clay, 1989; Swamy, 1992; Jones & Clark, 1997; and Ahmed et al., 2003). Excluding the level of reactivity and the progression of immersion age, the losses in compressive strength and stiffness is also a function of mix design, type of aggregate, and storage conditions. It has also been shown that compressive strength is extremely sensitive to restraint perpendicular to the direction of stress. However, restraint perpendicular to the direction of loading has a significant effect on the apparent compressive strength (Jones & Clark, 1997).

Alkali-silica reactivity has a distinct impact on the unconfined compressive strength of concrete. Clayton (1990) conducted cube compression and tall prism compression tests of concrete made with reactive aggregate. A 30% loss in compressive strength of the unrestrained specimen was observed at the immersion age of 28 days. The Canadian Standards Association (CSA, 2000) indicated that a reduction in the unrestrained compressive strength of concrete can be as high as 60% due to ASR related deterioration. It can be concluded that ASR has a significant strength reducing effect on the unrestrained concrete.

Compared to the unrestrained concrete, the restrained concrete suffered from ASR acts differently. The swelling pressure exerted by ASR plays a role of prestressing effects in restrained concrete in a bi-axial or tri-axial state of stress that retains most of its compressive strength (Blight, 1996). As a result, restraint concrete reduces the damage to

the concrete and increases the residual mechanical properties (IStructE, 1992). Due to the restrained behavior of the structures, practically a reduction of 20% compressive strength is likely to occur (Swamy, 1992). A significant increase in the mechanical characteristics of the confined alkali reactive specimens were shown in comparison with the non-confined specimens (Mohammed et al., 2006). The confined specimens not only resisted compressive stresses four to five times as high as non-confined specimens, but also stress-strain curves followed a linear evolution while non-confined specimens seemed to behave like powdery materials.

Monette et al. (2000) investigated the impact of ASR expansion on the mechanical properties of the materials under different loading conditions. Their study demonstrated that the loading conditions did not have a significant effect on the initial stiffness and the ultimate load carrying capacity of the reinforced concrete beam. The researchers also found that the compressive strength of the plain concrete cylinders was not affected by ASR but the stiffness was significantly affected by ASR-induced reaction.

Past investigations showed that the compressive strength was little affected during the early stages of the reaction (Nixon & Bollinghaus, 1985; Swamy & Al-Asali, 1989; and Monette et al., 2000). However, it became an indication when the cracking became severe at later stages (Nixon & Bollinghaus, 1985) and the loss in compressive strength could be as high as 40 to 60% (Swamy, 1992).

Using opal and fused silica reactive constituents, Swamy and Al-Asali (1986, 1988) conducted the behavior of the mechanical properties of concrete on alkali-silica reaction. Results obtained from their study showed that the tensile and flexural strengths were substantially more affected by ASR than the compressive strength. The tensile to

compressive strength ratio was reduced by almost 45% at an ASR expansion of 0.1%, and by almost 60% at an expansion of 0.3% (Sims, 1992). Moreover, a substantial reduction in modulus of elasticity was observed as ASR expansion increased.

Nishibayashi et al. (1992) studied the compressive strength and young's modulus of ASR-affected concrete cores. Results obtained from their research indicated that the mechanical properties of concrete went down due to the alkali-silica reactivity. Taking concrete cores from ASR-affected structures in Japan, Okado (1989) found a reduction in compressive strength. After a decade, the compressive strength of the same structure was found in 13% reduction (Ono, 2000), claiming claimed that ASR indicated a loss in compressive strength. However, a number of past investigations (Ahmed et al., 2003; and Monette et al., 2000) disputed the idea; they stated that compressive strength was not a good indicator of ASR. Additionally, they included that the static modulus of elasticity was a sensitive and reliable indicator of the deterioration of concrete due to the harmful reactions of ASR.

Recently, Gibergues-Carles et al. (2008) investigated the compressive strength of four reactive aggregates with or without mitigating techniques. After 34 weeks of immersion at 60°C and 100% RH, the concrete specimens prepared from both mixtures were subjected to compressive strength test. The results concluded that the compressive strength of concretes was affected by ASR.

The failure mechanisms of concrete in compression test are clearly affected by ASR. As a result, the shape of the stress–strain curves reflects the presence of internal fissures. The growth and the propagation of matrix cracks tend to start earlier due to defects produced by ASR. The period of stable cracks propagation is less affected than that of

unstable crack growth which is widely extended. The capability of controlling crack propagation decreases leading to premature failure. Even so, it can significantly reduce the bond and bearing strength of reinforced concrete that leads in increasing the deflections of the overall structure (Kapitan, 2006).

Marzouk and Langdon (2003) studied the effect of alkali-silica reactivity of mechanical properties of normal and high strength of concrete. After the initial 28 days of water cured, in their study, the specimens were equally divided and submerged in sodium hydroxide solution at 80°C for a period of 12 weeks. Results obtained from the tests are shown in Table 1.6. Table 1.6 shows that (a) the normal strength specimens containing the potentially reactive aggregate exposed to the sodium hydroxide solution experienced more losses in mechanical properties than that of the specimens made of moderate ASR reactive aggregate, (b) the high strength concrete exposed to the alkaline solution experienced less losses in mechanical properties for both of the specimens containing highly and moderately reactive aggregates.

Table 1.6: Compressive strength and modulus of elasticity of normal and high strength concretes (Marzouk & Langdon, 2003)

Aggregate	Curing Age	Normal Strength Concrete				High Strength Concrete			
		Cured in Water		Exposed to 1N NaOH		Cured in Water		Exposed to 1N NaOH	
		f'_c (MPa)	E_c (GPa)	f'_c (MPa)	E_c (GPa)	f'_c (MPa)	E_c (GPa)	f'_c (MPa)	E_c (GPa)
Highly reactive	28 Days	41.25	39.14	41.25	39.14	77.70	30.59	77.70	30.59
	12 Weeks	46.60	28.78	30.42	-	95.59	35.67	79.98	25.97
Moderately reactive	28 Days	47.98	33.46	47.98	33.46	74.52	31.75	74.52	31.75
	12 Weeks	57.93	53.95	48.70	23.04	93.64	44.17	91.69	37.28

f'_c : ultimate compressive strength of concrete, E_c : secant modulus of elasticity

Alkali-silica reaction in concrete reduces the young's modulus of concrete significantly (IStructE, 1992; Jones & Clark, 1997; Monette et al., 2000; Tarek et al., 2003; and Giaccio et al., 2008). The reduction is mainly due to micro-cracking, rather than the expansion as the losses in engineering properties do not occur at the same rate or in proportion to the expansion (Swamy & Al-Asali, 1989). Rivard & Ballivy (2005) emphasized that surface cracking did not seem to have a significant effect on the modulus of elasticity. Recently, Giaccio et al. (2008) revealed that the period of stable crack propagation was less affected than the period of unstable crack growth which was widely extended, showing that the capability of controlling crack propagation decreased leading to premature failure. However, it could significantly reduce the bond and bearing strength of reinforced concrete that leads in increasing the deflections in the overall structure (Kapitan, 2006).

ASR effect is more severe on all of the mechanical properties of concrete except for the compressive strength (Haha, 2006). Losses in elastic modulus are observed between 20% and 50% for the expansion of 0.10 to 0.30% (Rotter, 1996). With regard to mechanical characteristics of materials, modulus of elasticity is sensitive to variations in the ratio of crystalline and non-crystalline parts in the structures, while strength is comparatively insensitive to such variation (Kobayashi et al., 1993). ASR often reduces the elastic modulus of concrete core samples by a significant amount. In actual structures it does not necessarily cause a large increase in deflections. ASR-affected structures with adequate confinement subjected to large axial loads are likely to retain most of their capacity. In controlling the ASR expansion as well as maintaining structural integrity reinforcement was found very effective (Fan & Hanson, 1998).

Finally, it can be concluded that the reduction in compressive strength is not as significant as young's modulus (Swamy & Al-Asali, 1986, 1989; and Tarek et al., 2003).

1.8 Alkali-Carbonate Reaction

1.8.1 Introduction

Alkali-carbonate reaction (ACR) occurs between some argillaceous dolomite limestone aggregates and the alkalis in cement in the humid conditions. This phenomenon was first discovered by Swenson (1957). Though the mechanism of ACR is not fully recognized, a general agreement is accompanied the reaction as a dedolomization (Hardley, 1961; Walker, 1974; and Poole, 1981). The alkali-carbonate reaction is not as well understood as alkali-silica reaction is.

Reactive rocks usually contain larger crystals of dolomite scattered in and surrounded by a fine-grained matrix of calcite and clay. Calcite is one of the mineral forms of calcium carbonate; dolomite is the common name for calcium-magnesium carbonate. Argillaceous dolomitic limestone contains calcite and dolomite with appreciable amounts of clay, and it may contain small amounts of reactive silica. Alkali reactivity of carbonate rocks is not usually dependent on clay mineral composition. According to Swenson and Gillott (1967), and Ozol (1994), aggregates have potential for expansive ACR if the following lithological characteristics exist:

- a. Clay content or insoluble residue content, in the range of 5% to 25%
- b. The ratio of calcite-to-dolomite is approximately equal to 1
- c. Increase in the dolomite volume up to a point at which interlocking texture becomes a restraining factor

- d. Small size of the discrete dolomite crystals suspended in a clay atmosphere

Alkali-aggregate reactions of carbonate rocks, collectively termed as alkali carbonate reactions, can be subdivided into three reactions that form various rims, and these are discussed as follows.

1.8.1.1 Reactions caused by nondolomitic carbonate rocks

This type of reactive rocks contained little or no dolomite (Mather et al., 1965; and Buck, 1965). The reaction rims are visible along the cross sections of aggregate particles. The rim zone dissolves more quickly than the interior of the particle. The reaction, therefore, is not harmful to concrete.

1.8.1.2 Reactions caused by moderate or highly dolomitic carbonate rocks

This phenomenon was first reported by Tynes et al. (1966). The reaction rims are still visible on the cross sections of the aggregate particles. Etching in that cross section area with acid, the rims and the interior of the particle dissolved concurrently. No researches have been showed that this reaction was damaging to concrete.

1.8.1.3 Reactions caused by impure dolomite rocks

The impure dolomite rocks have a characteristic texture and composition. The impure dolomitic limestone, composed of large dolomite crystals in a fine-grained calcite and clay matrix, aggregate particles may develop silica-enriched rims.

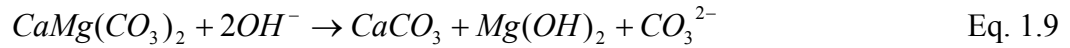
Two types of reactions have been developed with impure dolomite rocks, such as a) dedolomization reaction which describes the mechanisms of alkali-carbonate reaction and b) rim-silification reaction.

1.8.2 The mechanisms of ACR (Dedolomitization reaction)

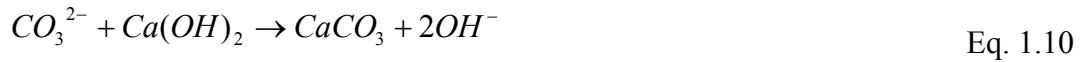
Dedolomitization, or the breaking down of dolomite, is normally associated with harmful expansion of concrete, caused ACR in concrete (Hardley, 1961). Magnesium hydroxide and brucite are formed as a by products of the reaction. Dedolomitization reaction follows the following equation (Ozol, 1994). This reaction and subsequent crystallization of brucite may cause considerable expansion. The deterioration caused by ACR is similar to that caused by ASR; however, ACR is relatively rare because aggregates susceptible to this phenomenon are less common.

The mechanism of alkali-carbonate reaction describes several different reactions which may take place between carbonate rock aggregate particles and the cement paste of Portland cement concrete. In general, the dedolomitization reaction can be viewed as a two-step process:

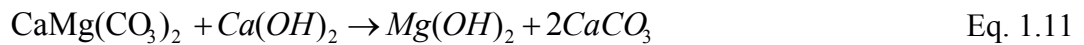
In the first step of dedolomitization, pore solution with high a pH break down dolomite to form calcite, brucite and carbonate ions:



In the second step, excess carbonates in solution react with lime to produce additional calcite and regenerate the hydroxides that drive the first step of the reaction series:



The next reaction will proceed until either dolomite or Portlandite is exhausted:



According to Tang et al. (1986), expansion was due to a combination of migration of alkali ions and water molecules into the restricted space and the growth and rearrangement of the dedolomitization products. Lu et al. (1992) concluded that the

dedolomitization reaction and consequent crystallization of brucite and calcite might cause significant expansion. In general, dedolomitization is a prerequisite to other expansion (Tang et al., 1994), though it's causes expansion directly or indirectly.

The volume change due to the reaction has little effect on the total volume of the concrete. Considerable expansion occurs locally, however, at the rims and in the zones surrounding reactive aggregate particles. This action often leads to a loss of bond between aggregate particles and cement paste. Typically, micro-fractures originate at the reactive rims, radiate into the aggregate particles and propagate through the paste.

1.8.3 Rim-silification reaction

This reacttion is not solely responsible for damaging concrete. The reaction is characterized by enrichment of silica in the borders of reacted particles (Bisque & Lemish, 1958). The reacted area is seen as a raised border at the edge of the cross section. Reaction rims, in that case, are visible before the concrete surfaces are etched.

Carbonate rocks that contain dolomite, calcite, and insoluble material in the proportions that cause either the dedolomitization or rim-silification reactions are relatively rare in nature as major constituents of the whole product of an aggregate source (Engineering and Design Manual, 1994).

1.8.4 Symptoms of ACR

ACR affected structural member are easily recognized in the field due to the differential volume changed. Expansion is indicated by map or pattern cracking on the surface of a structural member of joints, offsets, misalignments or rotations of structural members, concrete crushing and pavement blowups. Conversely, ACR can be pinpointed as the cause of expansion only through petrographic examination (ASTM C 865).

Following criteria are indicated by the petrographic examination:

- a. Loss of bond between the aggregate particles and cement paste
- b. Calcium-rich rims found around dolomitic aggregate particles and calcium-rich deposits in cracks
- c. If argillaceous dolomitic limestone aggregate particles are present, brucite in cracks voids and paste.

1.9 Factors Affecting Alkali-Carbonate Reactivity

ACR is relatively rare because aggregates susceptible to this reaction are usually unsuitable for use in concrete for other reasons; strength potential, etc. Argillaceous dolomitic limestone contains calcite and dolomite with appreciable amounts of clay and can contain small amounts of reactive silica. Alkali reactivity of carbonate rocks is not usually dependent on clay mineral composition. Aggregates have potential for expansive ACR if the following lithological characteristics exist (Kosmatka et al., 2002):

- a. Clay content, or insoluble residue content, in the range of 5% to 25%
- b. Calcite-to-dolomite ratio of approximately 1:1
- c. Increase in the dolomite volume up to a point at which interlocking texture becomes a restraining factor
- d. Small size of the discrete dolomite crystals suspended in a clay matrix

Maximum size of the reactive aggregate influences the amount and extent of reactivity. Alkali-carbonate reaction is also affected by pore solution alkalinity. ACR can occur in a solution with a relatively low pH. As the pH of the pore solution increases, potential for the alkali-carbonate reaction increases. During the ACR, calcium hydroxide produced by Portland cement hydration can combine with sodium carbonate to form

more sodium hydroxide and calcium carbonate. This reaction not only regenerates alkali, but also reduces the concentration of carbonate ions and aggravates the dedolomitization reaction. Low-alkali cements and mineral admixtures even at high levels are thus ineffective at reducing ACR to acceptable limits.

1.10 Testing for the Potential Alkali-Carbonate Reactivity of Aggregates

ASTM C 1105, “Standard test method for length change of concrete due to alkali-carbonate rock reaction,” is to evaluate of length change measurements of concrete prisms of an aggregates potential to be alkali-carbonate reactive. If ASTM C 295 indicates that an aggregate is potentially alkali-carbonate reactive, ASTM C 1105 should be conducted. It is recognized as the best indicator of potentially deleterious expansion due to carbonate aggregate in concrete (ACI 1998). This test calls for three concrete specimens to be fabricated using the aggregate under evaluation and the job cement, if possible. The specimens are kept in moist storage and their change in length is measured at 7, 28, and 56 days, and at 3, 6, 9, and 12 months. The failure limits of 0.015 percent at 3 months, 0.025% at 6 months, and 0.030% expansion at 1 year are considered indicative of a potentially deleteriously aggregate source.

1.11 Controlling Alkali-Carbonate Reaction

The nature, rate and effect on concrete of ACR depend on the mineralogy of the aggregate, climatic features such as temperature and availability of moisture, the permeability and porosity of the concrete, and the quantity of calcium hydroxide in the hardened concrete. Controlling these factors is the key in minimizing the deleterious effect of ACR on concrete structures. For aggregate selection, the following actions are taken:

1.11.1 Using non-dolomitic carbonate aggregate

To control ACR-induced expansion, non-reactive aggregate quarries are always to be selected. For screening the carbonate rocks, a petrographic examination of the aggregate, ASTM C 295 (Guide for Petrographic Examination of Aggregates for Concrete), should be used. If the petrographic examination shows positive result, then samples should be tested for length change as per ASTM C 586 (Rock Cylinder Method) or ASTM C 1105.

If the use of potentially reactive aggregate is not feasible, adding minimum aggregate size to the concrete mixture such a way that the amount of potentially reactive rock do not exceed 20% of either the course or fine aggregate, or 15% of both. The maximum size of the aggregate also affects its reactivity, with aggregate having a larger maximum size having the greater potential for deleterious reactivity (ACI 1998).

1.11.2 Controlling other factors

Pozzolans and low-alkali cement are generally not effective in controlling ACR expansion (Farny & Kosmatka, 1997). On the other hand, Ozol (1994) proposed that the most significant cement parameter to consider when the potential for ACR susceptibility exists is to minimize the total alkali content per unit volume of concrete, and not focus exclusively on the alkali content of the cement. If avoiding of potential reactive aggregate is not possible, the potential for deleterious ACR can be minimized by keeping the alkali content of cement as low as 0.40% (Mindess et al., 2002) for adequate protection.

Research conducted by Lu et al. (2006) showed that at the same molar concentration, sodium has the strongest contribution to expansion due to both ACR and ASR, followed by potassium and lithium. Nevertheless, preliminary evidence suggests that lithium-based

admixtures appear to control ACR although little research has been performed to support this finding. However, LiOH induces ACR expansion though it is very efficient to suppress ASR expansion (Lu et al., 2006). To prevent concrete deterioration due to ACR, Minghu et al. (1994) suggested maintaining the pH value of cement at a lower level than needed to prevent ASR. Thus the only method currently available to prevent ACR is to eliminate or significantly reduce the amount of reactive aggregate.

Once ACR initiates, the reaction continues until the reactants (dolomite and hydrated lime) are exhausted. For this reason, structures damaged by ACR can only be repaired by complete replacement of affected members.

1.12 Research Objectives

The objective of this experimental research program is to examine the extent of reactivity, in the form of expansion, of the aggregates acquired from the fourteen distinct quarries within the State of Nevada. The losses in the compressive strength and stiffness due to alkali-silica reactions are also evaluated. Additionally, a number of mitigation techniques, which were utilized to suppress the excessive expansion of the reactive aggregates, are studied. This research investigation includes a technical literature review, laboratory experimentations, discussions of results, and conclusions and recommendations. A summary of the experimental program is highlighted in a flowchart as documented in Figure 2.1. The presentation of this study is divided in six chapters and the chapter breakdown is described as follows:

Chapter 1 provides the background and a basic overview of alkali-aggregate reactivity (ASR/ACR), including history, gel formation, mechanisms of reactivity, crack development, and symptoms. It also discusses the factors affecting ASR/ACR and the

remediation of AAR-affected concretes. Research objectives and significance are presented as well.

Chapter 2 deals with the materials preparation and the experimental program used to identify and control ASR-induced expansion of reactive aggregates. The reactivity of the investigated aggregates obtained in the State of Nevada based on its chemical compositions (the mineralogy) is also pointed out. Testing methodologies, and matrix constituents and proportions are also discussed.

Chapter 3 presents the ASR-induced expansions of the ASTM C 1260 and modified ASTM C 1260, modified ASTM C 1293, and ASTM C 1105 tests. The extent of reactivity of each aggregate source based on the ASTM C 1260, while exposed to three different soak solution strengths in various immersion ages, is determined. The failure criteria of the ASTM C 1260 for the 0.25 and 0.5N soak solutions at different immersion ages are proposed. The influence of three dosages of cement alkalis on the expansion of the trial specimens using ASTM C 1260 is also studied. The soak solution strength and cement alkali at which ASR expansion of the trial aggregates executes reliable results are also proposed. Lastly, new ASR failure criteria based on the modified ASTM C 1293 are offered. Finally, the ASR classifications of the trial aggregates based on the adopted testing programs are compared.

Chapter 4 presents the ASR-induced loss in ultimate compressive strength and stiffness of the concrete cylinders made with the fourteen trial aggregates. The extent of reactivity of each aggregate source based on the loss in ultimate compressive strength and stiffness at the immersion ages of 28 and 180 days are also proposed. The relationships

among compressive strength/modulus of elasticity loss, ASR-related expansion, and the mineralogy of aggregate are also discussed.

Chapter 5 discusses the effectiveness of various mitigation techniques used in controlling the excessive expansion of the reactive aggregates. The three adopted remediation methods include: the utilization of Class F fly ash as a partial replacement of Portland cement, the addition of sufficient amount of lithium nitrate in the mixing water, and the use of combined Class F fly ash and lithium salt. The percent reductions in the expansion of the mortar bars containing various dosages of fly ash and/or lithium nitrate at different immersion ages are presented. The minimum amount of Class F fly ash and/or lithium nitrate required to inhibit ASR expansion of each reactive aggregate is determined.

Chapter 6 reports on the conclusions of the research investigation. Recommendations for the future related studies are also presented.

1.13 Research Significance

Alkali-aggregate reaction (AAR) can cause premature deterioration of concrete highways, bridges, runways, garages, parking lots, and other structures. A substantial loss in mechanical properties of concrete is experienced due to AAR-induced cracks and expansion. Identifying the susceptibility of an aggregate to the alkali-aggregate reaction prior to its use is one of the most efficient practices to prevent damage to concrete structures. While non-reactive aggregates are limited in some locations, reactive aggregates can be used safely when appropriate preventive measures are accounted for. Mitigating AAR-related problems permits the use of reactive aggregates that have

formerly been rejected, thus, not only enhancing substantial savings in repair and replacement costs, but also extending the life of concrete structures.

The use of the ASTM C 1260 and modified ASTM C 1293 tests in assessing the alkali-silica reactivity of an aggregate at the early-age immersion has been broadly reported. However, only a handful of studies has dealt with the failure criteria of ASTM C 1260 and ASTM C 1293M1 (prisms immerges in the 1N NaOH at 80°C) at the extended immersion ages. Additionally, the study on the influence of soak solution concentration and cement alkalis on the ASR-induced expansions of mortar bars at various immersion ages has been limited and inconclusive. Past investigations on the Nevada's aggregates in relation to alkali-aggregate reactivity were also limited in scope and confined to a few sources.

The study presented herein addresses the influence of the three soak solution concentrations (1, 0.5, and 0.25N) and three levels of cement alkalis on ASR-induced expansion of the mortar bars made with the fourteen selected Nevada's aggregates at 14, 28, 56, and 98 days. Moreover, the failure criteria of the mortar bars are proposed for not only 1N NaOH solution but also for 0.5 and 0.25N NaOH solutions at four distinct immersion ages. The ASR classifications of the trial aggregates are also compared among the suggested expansion limits of the mortar bars for the three solutions at 14, 28, 56 and 98 days.

Past studies also reported on the development of ASR expansion under ASTM C 1293M1. However, they were confined to the 4-week which classified some innocuous aggregates as reactive. This study proposes the extended failure limits of ASTM C 1293M1 at the immersion ages of 8, 13 and 26 weeks. Furthermore, the levels of ASR of

the trial aggregates based on the prescribed expansion limits are compared with the proposed failure criteria of mortar bars.

There exists a general agreement among the researchers that a substantial loss in compressive strength and stiffness of concrete is experienced due to the alkali-silica reactivity. However, past studies failed to establish limits on loss in strength and stiffness for which the ASR reactivity of an aggregate can be evaluated. This study proposes failure limits of loss in compressive strength and stiffness below which an aggregate behaves in an innocuous manner or is reactive otherwise. The evaluations are made from the statistical correlations of the fourteen selected aggregate groups with varying ASR-induced expansions.

This study also provides an insight in assessing the ASR of the trial aggregates on the basis of aggregate mineralogy, the expansion limits of mortar bars and prisms at early and extended immersion ages, and the loss in compressive strength and stiffness. The limitations of each evaluation method are also discussed.

Past studies on the impact of Class F fly ash or lithium nitrate in suppressing the alkali-silica reactivity were mostly confined to the test duration of 14 days and the aggregate types which produced a narrow range of ASR-induced expansions. This investigation enhances the previous research studies by utilizing various dosages of Class F fly ash or lithium nitrate contents for seven highly reactive aggregates having a large variation in their ASR-induced expansions. Unlike previous studies, this investigation extends the test duration from 14 days to 98 days in seeking a better understanding of the ASR-related expansions. The minimum required analytical fly ash dosages to suppress ASR expansions below the suggested expansion limits at 14, 28 and 56 days are

determined by utilizing the chemical compositions of the cementitious materials. The optimum analytical lithium dosages required for each trial aggregate at various ages are also determined and compared with the findings of the experimental tests.

Past investigations on the influence of combined fly ash and lithium nitrate in controlling the alkali-silica reactivity were mostly limited to the early immersion age of 14 days. This study highlights the effectiveness of the combined Class F fly ash and lithium in arresting the excess ASR-induced expansion, when compared with the individual effect of Class F fly ash or lithium, at the immersion ages of 14, 28 and 56 days. This investigation also presents statistical analyses in selecting the combined fly ash and lithium dosage that can effectively reduce ASR at the above- mentioned immersion ages.

In summary, through the identification of alkali-aggregate reactivity and suggested mitigation strategies, this study is expected to increase the aggregate sources that can be safely used in concrete construction, resulting in increased sales for producers and reduced costs for users without sacrificing the mechanical properties of concrete. Moreover, this investigation enhances the state-of-the-art knowledge of alkali-aggregate reactivity as affected by the aggregate type, cement alkali, immersion condition and duration, loss in strength and stiffness, and mitigation techniques.

CHAPTER 2

MATERIALS PREPARATION AND EXPERIMENTAL PROGRAM

The focus of this chapter is to present materials preparation, experimental programs, laboratory test procedures and equipments used during the investigation. Testing methodologies used to evaluate the reactive aggregates are also covered.

2.1 Experimental Program

The experimental program of this study was composed of three major phases. Phase I dealt with the preparation of testing materials, such as collecting, washing, drying, crushing, sieving and grading as per ASTM C 1260, ASTM C 1293 and ASTM C 1100. In the phase II, a variety of laboratory test methods, such as ASTM C 1260, Modified ASTM C 1293 and ASTM C 1105, were conducted to identify the reactive aggregates from the selected quarries. In the phase III, range of mitigation techniques; such as use of Class F fly ash, lithium nitrate, and combined fly ash and lithium nitrate; were used to control excess expansion of the reactive aggregates identified in the Phase II. The breakdown of each phase of the experimental program is shown in the following flow chart, and described in the later sections of this Chapter.

2.2 Materials Preparation

The steps involved in the preparation of the fourteen selected aggregates to produce AAR (ASR/ACR) test specimens, such as collecting, washing, crushing, sieving and grading aggregates are discussed below:

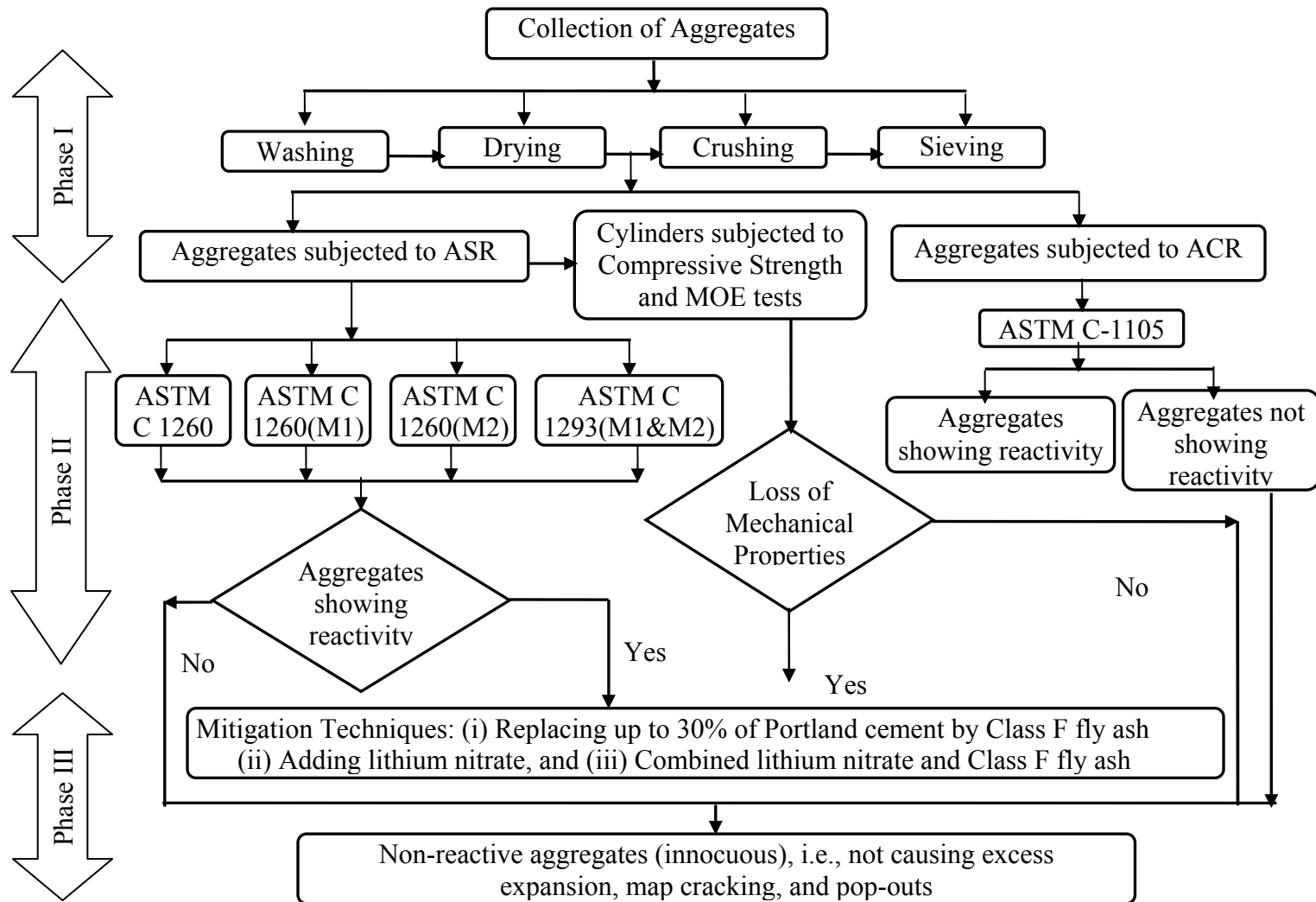


Figure 2.1: Flow chart of experimental program for alkali-aggregate detection and mitigation

2.2.1 Collecting aggregates

Sufficient amounts of coarse and fine aggregates were collected from fourteen different quarries within the State of Nevada. Ten sources were obtained from the Southern Nevada and four sources were from the Northern Nevada. The identification and the ASR reactivity of each trial aggregate based on its chemical composition (rock type) are described in Section 2.3.

2.2.2 Washing and drying aggregates

During the washing process, the coarse aggregates were first soaked in a bucket of water for about 15 minutes, and then placed on large trays and hand-washed with water sprays as shown in Figure 2.2. Once the dirt was washed off and the water running over the aggregates was clear, they were placed on aluminum trays and then put in the preheated oven at 100°C for 24 hours for all the moisture was dried off. Afterward, they were stored in clean and dry buckets for the crushing operation. Additionally, the fine aggregates were dried in the sun to remove excessive moisture if needed. Sufficient amounts of material from each of the quarries were prepared for the anticipated testing. During the washing process, the greatest care was taken to avoid any sort of contamination of the aggregates.

2.2.3 Crushing aggregates

Two rock crushers (a badger crusher and a cone crusher), shown in Figure 2.3, were used to crush the coarse aggregates to obtain the required amount of graded aggregates. The badger crusher crushes the aggregates into very fine particles; alternately, the cone crusher crushes the aggregates into different fractions although it is a time-consuming procedure. The cone crusher was used more often than the badger crusher because of its

capacity for crushing controlled sizes of aggregates. Once the aggregate was crushed, it was collected in a clean and dry bucket. The containers and rock crushers were wiped clean before and after crushing to avoid contamination.



Figure 2.2: Washing coarse aggregates

2.2.3 Crushing aggregates

Two rock crushers (a badger crusher and a cone crusher), shown in Figure 2.3, were used to crush the coarse aggregates to obtain the required amount of graded aggregates. The badger crusher crushed the aggregates into very fine particles; alternately, the cone crusher crushed the aggregates into different fractions. The cone crusher was used more often than the badger crusher because of the speed of operation and due to its capacity to crush aggregates in a specified size. Once the aggregate was crushed, it was collected in clean and dry buckets. The containers and rock crushers were wiped clean before and after crushing to avoid contamination.

2.2.4 Sieving aggregates

The aggregate gradation of the crushed aggregates was performed in accordance with ASTM C 136, “Sieve or screen analysis of fine and coarse aggregates.” The crushed

aggregates were sieved for the preparation of the specimens, the mortar bar and the prism specimens, as per the requirements of ASTM C 1260, ASTM C 1293 and ASTM C 1105. For the prisms (ASTM C 1293), the fractions into which the crushed sample had to be separated were ½ in., 3/8 in. and #4 sieve sizes. For the mortar bars (ASTM C 1260), the aggregates were separated into #8, #16, #30, #50, and #100 sieve sizes. The gradation of each aggregate source consisted of about four pounds of the crushed aggregate that was sieved for a period of 10 minutes. Repeated sieving was conducted until the source was exhausted completely.



a. Badger crusher



b. Cone crusher

Figure 2.3: Rock crushers

The separated fractions of aggregate were placed in plastic zipper bags and stored inside clean buckets. Lastly, the sieves were washed and dried before the next aggregate source was graded.

2.2.5 Grading aggregates

The coarse aggregates were graded into two major categories; finer coarse aggregate gradation and coarser coarse aggregate gradation. Finer aggregate gradation, shown in Table 2.1, was performed to prepare mortar bar specimens. The fineness modulus (FM) of the finer gradation of the coarse aggregate was 2.90. For the prism specimens, the coarser gradation of the coarse aggregate was graded as shown in Table 2.2.

Table 2.1: Crushed aggregate gradation for mortar bar specimens

Sieve Size		% Mass
Passing	Retained on	
4.75 mm (No. 4)	2.36 mm (No. 8)	10
2.36 mm (No. 8)	1.18 mm (No. 16)	25
1.18 mm (No. 16)	600 μ m (No. 30)	25
600 μ m (No. 30)	300 μ m (No. 50)	25
300 μ m (No. 50)	150 μ m (No. 100)	15

Table 2.2: Coarse aggregate gradation for prism and cylinder specimens

Sieve Size		% Mass
Passing	Retained on	
19.0 mm (3/4 in)	12.5 mm (1/2 in)	33
12.5 mm (1/2 in)	9.5 mm (3/8 in)	34
9.5 mm (3/8 in)	4.75 mm (# 4)	33

2.3 Aggregate Classifications Based on Mineralogy

This section deals with the identification and chemical composition (rock type) of the investigated aggregates used in the study. To protect the source of aggregates, an arbitrary designation of SN and NN was assigned to the aggregates quarried in the Southern and Northern Nevada, respectively. An additional letter was given to reflect the

source of aggregate. For an example, SN-G aggregate means the G quarry which is located in the Southern Nevada. The identification for each aggregate tested, as specified in Table 2.3, was used throughout the study to recognize the aggregate source. Rock types of the trial aggregates are then classified according to the geological nomenclature based on the compositional fields of the rocks in terms of total alkalis and silica content. The results are documented in Table 2.3.

Table 2.3: The identification, chemical composition and rock type of the selected aggregates

Agg. ID	Chemical Composition (%)								Rock Type
	SiO ₂	Al ₂ O ₃	Fe ₂ O ₃	CaO	MgO	Na ₂ O	K ₂ O	LOI	
SN-A	0.74	0.03	0.12	30.74	21.24	<0.01	0.03	46.5	Dolomite
SN-B	17.19	1.22	0.28	43.40	1.49	0.24	0.39	35.6	Limestone
SN-C	13.50	0.40	0.29	32.55	13.09	0.03	0.14	39.4	Dolomite-Limestone
SN-D	65.35	15.03	2.84	2.91	1.52	4.55	4.37	2.31	Dacite
SN-E	1.83	0.38	0.28	30.60	20.18	0.03	0.16	45.4	Dolomite
SN-F	63.09	11.50	3.48	6.92	1.97	2.34	3.28	6.43	Dacite
SN-G ^a	60.82	15.89	5.37	4.34	2.49	3.57	3.73	2.14	Andesite
SN-H	10.91	0.66	0.24	41.00	6.65	0.05	0.29	39.4	Limestone
SN-I	56.66	15.83	5.78	5.33	3.36	3.60	3.85	2.88	Basaltic-Andesite
SN-J ^a	68.00	15.48	2.86	1.14	0.94	4.52	5.40	0.63	Dacite
NN-A	61.17	16.82	5.64	4.88	2.28	3.54	1.92	2.2	Andesite
NN-B	59.33	17.15	5.83	5.30	2.54	3.76	2.68	1.83	Andesite
NN-C	52.50	18.45	8.35	8.36	4.59	3.74	1.22	0.98	Basaltic-Andesite
NN-D	64.14	17.01	4.20	4.16	1.76	4.23	2.54	0.92	Dacite

^aAggregate quarried from Nevada-Arizona border

It is well known that the most essential requirement for alkali-silica reaction in concrete to take place is a form of reactive silica of the aggregates present in concrete. However, all siliceous aggregates are not reactive. Damaging reactions can only occur if the rock contains sufficient quantities of the reactive silica. The volume of reactive silica needed to produce deleterious effects is very small (Swamy, 1992) and the quantity varies on the rock types, and the reactive minerals (ACI, 1998). The rock types of the investigated aggregates with their possible mineralogy are summarized in Table 2.4. Summary of the findings on the fourteen selected aggregates (mineralogy) susceptible to alkali-silica reaction is presented as well.

Table 2.4: The ASR reactivity of rock types used for research investigation

Rock Type	Minerals/Reactants	ASR Reactivity	Aggregate ID
Dolomite	Both mineral and rock; composed of calcium magnesium carbonate ($\text{CaMg}(\text{CO}_3)_2$)	Innocuous ^a	SN-A, SN-E
Limestone	Composed primarily of the mineral calcite (CaCO_3); may contain dolomite ($\text{CaMg}(\text{CO}_3)_2$) and aragonite (CaCO_3)	Innocuous ^b	SN-B, SN-H
Dolomite-limestone	Limestone partially replaced by dolomite	Reactive ^c	SN-C
Dacite	Opal, tridymite, cristobalite; volcanic glasses; artificial glasses, beekite	Reactive ^d	SN-D, SN-F, SN-J, NN-D
Andesite	Opal, tridymite, cristobalite; volcanic glasses; artificial glasses, beekite	Reactive ^e	SN-G, NN-A, NN-B
Basaltic-Andesite	Opal, tridymite, cristobalite; volcanic glasses; artificial glasses, beekite	Reactive ^f	SN-I, NN-C

^aBanahene, 1991; Hooton & Rogers, 1993; Stark, 1993

^bStark, 1993; Jensen, 1996; McKeen et al., 1998; Touma et al., 2001

^cBanahene, 1991; Deng et al., 1993; Lane, 1994; Milanese et al., 1994

^dTuthill, 1982; Swamy, 1992; Bérube & Fournier, 1993; Hooton & Rogers, 1993; Touma et al., 2001; and Thomas et al., 2007

^eTuthill, 1982; Swamy, 1992; Bérube & Fournier, 1993; Touma et al., 2001; Bian et al., 2003; Adam, 2004; Thomas et al., 2007; Ikeda et al., 2008

^fLane, 1994; Adam, 2004; Korkanç & Tuğrul, 2005

Table 2.4 shows that dacite (SN-D, SN-F, SN-J and NN-D), andesite (SN-G, NN-A and NN-B), and basaltic andesite (SN-I and NN-C) are found to be alkali-silica reactive. On the other hand, dolomite (SN-A and SN-E) and limestone (SN-B and SN-H) are not prone to ASR reactions if they are pure mono-minerals. If limestone is partially replaced by dolomite, dolomite-limestone rocks (SN-C) can be treated as reactive.

It is not sufficient to consider rock type as a criterion for an aggregate's potential for reactivity (Swamy, 1992). The mineralogy of aggregate is unable to prove the degree of ASR reactivity and ASR-induced damage. The standard tests are required to determine the extent of reactivity. In this research study, the ASTM C 1260 and modified ASTM C 1293 tests were conducted in assessing the ASR-induced expansion of the trial aggregates.

2.3 Testing Materials

2.3.1 Sodium hydroxide pellet

A sodium hydroxide (NaOH) pellet is a white particle approximately 4mm in diameter and 2mm in width. The weight of each particle is approximately 0.1 grams. Sodium hydroxide pellets are soluble, and generate heat when mixed with water. The containers of NaOH pellets were kept in a tightly closed container to prevent the conversion of NaOH to sodium carbonate by the CO₂ in air. Its purity was 99% (by acidimetry test) and among the other ingredients, sodium carbonate (Na₂CO₃) was 0.4%.

Sodium hydroxide was added to distilled water to prepare three different concentrations of soak solutions, such as 0.25N, 0.5N and 1N. Sodium hydroxide was also added in the mixing water to raise the cement alkali to the target level.

2.3.2 Portland cement

Portland cement primarily consists of calcium, silica, aluminum, and iron oxides. The calcium oxide and silica oxides are essential, whereas alumina and iron oxides are mainly used to decrease the temperature of manufacturing. Each of the principal compounds has an influence on the properties of Portland cement.

Type V Portland cement with alkali content of 0.42% $\text{Na}_2\text{O}_{\text{eq}}$ meeting the requirements of ASTM C 1507 was used in preparing the mortar, prism, and cylinder specimens. It had a very low C_3A composition, which accounts for its high sulfate resistance. The maximum content of C_3A allowed is five percent for Type V Portland cement. Another limitation is that the $(\text{C}_4\text{AF})+2(\text{C}_3\text{A})$ compositions cannot exceed twenty percent. Type V Portland cement is used in concrete that is exposed to alkali soil and ground water sulfates which react with (C_3A) causing disruptive expansion. The physico-chemical properties of the Portland cement utilized are presented in Table 2.5.

2.3.3 Class F fly ash

Class F fly ash with CaO content of 7.4% that complied with the requirements of ASTM C 618 was used in controlling the ASR expansion. Four different dosages of Class F fly ash as a partial replacement of Portland cement by weight were blended with cement. The physico-chemical properties of Class F fly ash are presented in Table 2.6.

2.3.4 Lithium nitrate

Lithium is a group IA element (alkali metal) in the periodic table that contains just a single valence electron. The lithium nitrate admixture used in this investigation is lithium based specially formulated admixture designed to control ASR in new and existing concrete. It is derived from the research conducted under the Strategic Highway Research

Project (SHRP). The physico-chemical properties of lithium nitrate used in this study are presented in Table 2.7.

Table 2.5: Physico-chemical properties of Type V Portland cement

Chemical Composition		Physical Properties	
Element	Percent	Specific Surface	
Metal Oxide		Blaine Fineness (cm ² /gm)	3760
		Soundness	
SiO ₂	21.0	Autoclave Expansion (%)	0.11
Al ₂ O ₃	3.6		
Fe ₂ O ₃	3.4	Air Content (%)	6.7
CaO	63.1		
MgO	4.7	Normal Consistency (%)	24.5
SO ₃	2.6		
Alkali Oxide		Time of Setting (min.)	
Na ₂ O _{equiv}	0.42	Initial Set	109
Phase Analysis		Final Set	212
C ₃ S	61	Min. Compressive Strength (psi)	
C ₂ S	15		
C ₃ A	4	1160 psi (3 days)	
C ₄ AF	10	2180 psi (7 days)	
Loss on ignition	1.3		
Insoluble residue	0.28		

Table 2.6: Physico-chemical properties of Class F fly ash

Chemical Composition		Physical Properties	
Element	Percent		
Metal Oxide		Specific gravity	2.26
SiO ₂	57.8	Retained on #325	19%
Al ₂ O ₃	21.7		
Fe ₂ O ₃	5.1	Water requirement	93%
CaO	7.4		
MgO	-	Autoclave expansion	0.01
Total alkali (Na ₂ O _{eq})	0.3		
Loss on ignition	0.2		
Moisture content	0.0		

Table 2.7: Physico-chemical properties of LiNO₃ solution

Physical Properties	
Appearance	Clear, water white to yellow solution
Odor	Odorless
Solubility in water	Soluble in any proportion
Oxidizing characteristic	Oxidizer
Chemical Properties	
pH	7-9.5 @ 25°C
Boiling point	110°C to 120°C
Specific gravity	1.2 to 1.3 g/cc at 25°C
Molecular weight	68.95
Chemical Compositions	
Lithium nitrate	30%
Water	70%

2.4 Testing Equipment

2.4.1 Concrete mixer

A concrete mixer is a device that homogeneously combines cement, aggregate such as sand or gravel, and water to form plastic concrete. An electric counter-pan mixer with a capacity of 1 ft³ (0.028 m³) and a speed of 15 rpm was used to blend the concrete constituents. A pan mixer was preferred because it is particularly efficient for mixing small quantities of concrete in a laboratory. The laboratory room condition was maintained at 25±5% relative humidity and a temperature of 71±3°F (20±1°C). Aggregates, cement, water, fly ash, lithium nitrate and soak solutions were kept in the same laboratory room to maintain consistency.

The mixing sequence for prism specimens consisted of: (i) adding the coarse aggregates with 1/3 of the water and mixing for one minute, (ii) adding the fine aggregates with another 1/3 of the mixing water and mixing for two minutes, (iii) adding Portland cement with the remaining 1/3 of the water and mixing for three more minutes.

The mixing sequence for mortar bar specimens consisted of: (i) placing all the mixing water in the pan, adding the cementitious materials and mixing for 45 seconds, (ii) adding the selected gradation of crushed aggregate and mixing for 30 seconds, (iii) scraping the paste from bottom of the pan, and mixing for additional 45 seconds.

2.4.2 Length comparator

The digital length comparator allows measurement of the changes in length of mortar bar and concrete prism specimens. ASTM C 490 is the standard practice for using that apparatus in determination of length change of hardened cement paste, mortar and concrete. Figure 2.3 shows the length comparator testing apparatus used in this study. The length change value for each bar was calculated to the nearest 0.0001 and the average of three to four samples was reported to the nearest 0.001. The calculation of the length change at any age was performed as follows:

$$\Delta L = \frac{L_x - L_i}{L_g} * 100 \quad \text{Eq. 2.1}$$

Where:

ΔL = change in length at x age, %

L_x = difference between the specimen and the reference bar readings at x age

L_i = difference between the specimen and the reference bar readings, usually taken before storing in the respective test environment

L_g = nominal gage length, or 10 in.

2.4.3 Flow table

The flow table, shown in Figure 2.5, provides an efficient means of determining the flow of cement pastes and hydraulic cement mortars. A specific volume of material was molded on the table of the flow mold. The mold was then removed and the table was subjected to a specific number of 1/2 in. (12.7 mm) drops using a crank handle. The

increase in average diameter of the sample, measured in mm, indicated the flow of cement mortar.



Figure 2.4: Digital length comparator

2.4.4 Bar molds

Bar molds produce standard sized specimens to evaluate potential deformation under different testing regimes. These are available in three types for 10 in. (25.4 cm) long bar specimens: the 1" single bar mold, 1"x1"x10", the 1" dual bar mold, two-1"x1"x 10", and the 3" single bar mold, 3"x3"x10". In this study, a dual bar mold with a 1 in² cross section and a single bar mold with a 9 in² cross section were used to produce mortar bars and prism specimens, respectively.



Figure 2.5: Flow table

2.4.5 Compressometer and concrete compression machine

Compressive strength is one of the most important physical properties used in design of concrete structure. A classic concrete compression machine (Model# MC-500CL) with a capacity of 500,000 pounds was used to evaluate the concrete compressive strength. The ASTM C 39, “Standard test method for compressive strength of cylindrical concrete specimens,” was used to evaluate the compressive strength of the concrete. Prior to testing, each specimen was capped with a thin layer of sulfur on both ends, as specified by ASTM C 617 “Standard practice for capping cylindrical concrete specimens.” This was done to make the ends of the specimen plane and perpendicular to the axis of loading. The surfaces of the upper and lower platens of the compression machine were wiped clean. As the upper platen was brought to bear on the top of the specimen, the

spherically seated platen was moved by hand and adjusted to seat uniformly over the specimen. The specimen was then subjected to uniaxial compression.

A compressometer was used to obtain the compressive modulus of elasticity. The procedure of ASTM C 469, “Standard test method for static modulus of elasticity and poisson’s ratio of concrete in compression” was used to perform the testing. Figure 2.6 shows a compressometer with a cylinder specimen. The compressometer consisted of two cast aluminum-magnesium alloy yokes, stainless steel control rods. The dial indicator had a range of ± 0.2 in. (5.08 mm) and an accuracy of 0.0001 in. (0.0025 mm). The top yoke was hinged and pivoted on a rod at the back end which provided an axial gage length of 2.0 in and a gage length of 5.25 inches.



Figure 2.6: Compressometer

2.4.6 Oven

The oven used in this study had inside dimensions of 12 ft (length) x 3.25 ft (wide) x 6.25 ft (height) as shown in Figure 2.7. The openings of the oven were kept in the longitudinal direction and three doors were installed on each longitudinal direction wall. The doors, walls, base, and roof were made of styrofoam with a thickness of 6 inches. To protect the oven from the environmental or any external sources, plywood was glued onto the exposed areas of the oven. The steel frames were installed to maintain the shape and stability of the oven.

The oven was built to maintain an inside temperature at $80 \pm 1^\circ\text{C}$. The oven was continuously monitored via a temperature control device with ten thermocouples placed inside the oven at different locations including three in the water containers. The average temperature of the thermocouples was recorded at 80°C and the maximum temperature difference among the thermocouples was less than 0.5°C .

2.4 Testing Methods and Experimental Programs

This section illustrates a review of the various laboratory tests used along with the experimental programs, which include (1) assessing reactive aggregates, (2) controlling the deleterious ASR expansion of reactive aggregates, and (3) evaluating loss in mechanical properties of concrete, such as compressive strength and modulus of elasticity due to ASR.

2.4.1 Assessing alkali-aggregate reactivity

In this study, two types of aggregate reactivity were tested, alkali-silica and alkali-carbonate reactivity. Their test procedures are described below:



(a) A view of laboratory assembled oven (volume capacity of 9 yd³)



(b) Heating unit (front portion)



(c) Temperature controller



(d) Specimen storage

Figure 2.7: Fabricated oven along with the heating units and temperature controller

2.4.1.1 Assessing alkali-silica reactivity

The following testing methods were conducted to determine the extent of alkali-aggregate reactivity.

2.4.1.1.1 ASTM C 1260 and modified ASTM C 1260

ASTM C 1260 is a recommended test method for assessing ASR. It is recognized as a very severe test method because of the extreme test conditions such as highly alkaline storage solution and high temperature. The test is considered as a screening tool for aggregates. Most researchers have agreed that this test is a good predictor of ASR; however, it may give overestimated results for some aggregates. It is emphasized that the modifications of ASTM C 1260 methodologies are suggested to improve the reliability and precision of the prediction. In addition to the standard testing, the influenced of the following variables were also investigated:

- a. Effect of the soak solution concentrations: 1N (standard) to 0.50N and 0.25N
- b. Impact of the cement alkalis: 0.42% (standard) to 0.84, 1.26 and 1.68% $\text{Na}_2\text{O}_{\text{eq}}$
- c. Influence of immersion age: 14 days (standard) to 98 days

Table 2.8 illustrates the details of ASTM C 1260 and modified ASTM C 1260 along with their recommended failure criteria.

The mixture constituents of mortar bars are tabulated in Table 2.9. The water-to-cementitious materials ratio (w/cm) was controlled at 0.47 to improve the consistency of the mixing procedures. The absorption and the moisture content were accounted in the mixture design. The mortar is mixed in accordance with the requirements of ASTM C 305. For each aggregate source, twelve mortar bars were cast from a 16-bar batch size, containing each level of cement alkali. Mortar bars were molded within a total elapsed

time of not more than 2 min and 15 sec after completing of the original mixing of the mortar batch. After 24 hours of moist curing, shown in Figure 2.8, the bars were demolded and initial readings were taken. Afterward, the specimens were stored in water at 80°C for 24 hours after which the zero readings were recorded. The twelve specimens were divided into three equal groups. Each group of specimens was submerged in NaOH solution of respective concentrations (1, 0.5, and 0.25N) in an air-tight plastic container, shown in Figure 2.9, and finally, the containers were kept in an oven maintaining temperature of 80°C. Subsequent readings were taken at the age of 3, 6, 10, 14 days of curing and after that one reading per week until the immersion age of 98 days was reached.

Table 2.8: ASTM C 1260 and its modifications for each rate of cement alkali

Testing Procedures of mortar bars (for all standards)					
<ul style="list-style-type: none"> - W/C = 0.47 - Specimens were immersed in NaOH solution at 80°C - Volume of solution to volume of mortar bars = 4.0 - Cement to graded aggregate ratio = 2.25 - Moisture and absorption of the aggregates were accounted for in mixture design 					
Variation of type	Solution normality	Typical test duration (Days)	Failure criteria (% expansion) at typical test duration		Adopted testing duration (Days)
			Slow Reactive Aggregate	Highly Reactive Aggregate	
Standard	1N	14	0.100 - 0.20% ^a	> 0.20% ^a	Up to 98
Modified I	0.5N	14	0.04 - 0.08% ^b	> 0.08% ^b	Up to 98
Modified II	0.25N	28	0.020 - 0.04% ^c	> 0.040% ^c	Up to 98

^aBased on ASTM C 1260

^bProposed by Stark (1993)

Table 2.9: Constituents and properties of mortar bars for ASTM C 1260 and modified C 1260

Agg. ID	Graded Agg. ^a (grams)	Absorption (%)	Cement ^a (grams)	W/C	Water ^{a,b} (grams)	Unit Weight (lb/ft ³)	Flow
SN-A	5280	1.00	2346.7	0.47	1150.5	103	135.5
SN-B	5280	1.20	2346.7	0.47	1161.4	79	130.7
SN-C	5280	2.18	2346.7	0.47	1214.3	79	129.7
SN-D	5280	1.91	2346.7	0.47	1184.2	81	131.4
SN-E	5280	1.20	2346.7	0.47	1386.5	109	130.5
SN-F	5280	1.70	2346.7	0.47	1189.5	83	130.1
SN-G	5280	3.30	2346.7	0.47	1256.0	75	130.1
SN-H	5280	1.67	2346.7	0.47	1185.3	91	129.7
SN-I	5280	4.02	2346.7	0.47	1300.6	71	129.8
SN-J	5280	3.48	2346.7	0.47	1171.9	74	129.5
NN-A	5280	5.87	2346.7	0.47	1386.5	74	128.5
NN-B	5280	2.80	2346.7	0.47	1228.6	68	132.7
NN-C	5280	3.12	2346.7	0.47	1146.5	55	129.5
NN-D	5280	1.75	2346.7	0.47	1178.3	67	130.2

^aWeights were calculated on a 16-bar batch basis

^bAggregate's absorption and moisture content were accounted in mixture design



Figure 2.8: Mortar bars cured for 24 hours in a moisture room after casting

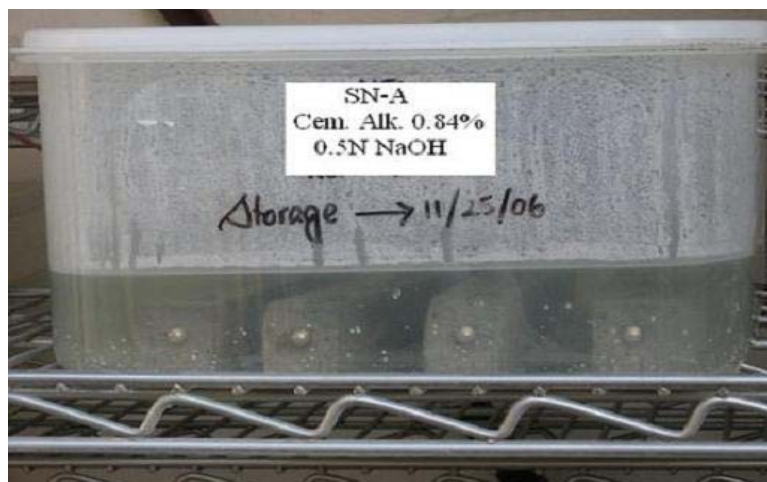


Figure 2.9: Mortar bars stored in NaOH solution at 80°C

2.4.1.1.2 Modified ASTM C 1293

The procedure of ASTM C 1293 was slightly modified to include the storage temperature of 80°C and the soak solutions of 1N NaOH and distilled water. The modified ASTM C 1293 tests were used to investigate the alkali-silica reactivity of the selected aggregates. The failure limits of the two modifications of ASTM C 1293 are shown in Table 2.10. The mixing constituents and proportions of the modified ASTM C 1293, which were also used to produce concrete cylinders, are shown in Table 2.11.

Concrete mixtures were prepared with a volume of 0.60 ft³ for each of the aggregate sources to cast six prism specimens. After 24 hours of moist curing, the prisms were demolded and initial readings were taken. The specimens were stored in water at 80°C for 24 hours, after which the zero readings were recorded. Afterward, the specimens were subjected to one of the following modified test conditions:

- a. Submerged in a 1N NaOH solution inside a 7.5-liter air-tight container at 80°C.

Two prisms of each aggregate source were stored in each of the containers. Using NaOH as a soak solution, this modification causes more accelerated. The

subsequent expansion readings were taken once at every week until the immersion age of 6 months.

- b. Submerged in distilled water inside a 7.5-liter air-tight container at 80°C. Two prisms of same aggregate source were stored in each of the containers. This modification does not generate accelerated results. The subsequent expansion readings were taken once a week for the first 3 months and bi-weekly for the remaining 3 months of immersion.

Table 2.10: Modifications of ASTM C 1293 with failure criteria

Properties of concrete prisms (for both modified methods)						
<ul style="list-style-type: none"> - W/C = 0.45 - Cement alkali content: 1.25% Na₂O_{eq} - Specimens submerged in solution at a temperature of 80°C - Volume of solution to volume of prism specimens = 2.0 - Cement content: 708 lb/yd³ - Aggregate's moisture content and absorption were considered in mixture design 						
Modifications of ASTM C 1293	Soak solution	Typical test duration	Failure criteria (% expansion) at typical test duration			Test duration (months)
			I	SR	HR	
ASTM C 1293M1	1N NaOH	28 days	< 0.04	0.04 - 0.08	> 0.08	6
ASTM C 1293M2	Distilled water	3 months	< 0.01	0.01 - 0.02	> 0.02	6

I = Innocuous (not reactive); SR = Slowly reactive; HR = Highly reactive

2.4.1.2 Assessing alkali-carbonate reactivity

ASTM C 1105 was conducted to evaluate the length change measurements of concrete prisms that may be potentially susceptible to alkali-carbonate reactivity. It is recognized as the best indicator of potentially deleterious expansion due to carbonate aggregate in concrete (ACI, 1998).

Table 2.11: Mixture constituents for concrete prisms and cylinders

Agg. ID	Aggregate Properties						Cement (lb/yd ³)	Water ^b (lb/yd ³)	Unit Weight ^c (lb/ft ³)
	Coarse Aggregate			Fine Aggregate					
	Absor. (%)	Specific Gravity	Unit Weight (lb/ft ³)	Absor. (%)	Specific Gravity	FM ^a			
SN-A	0.40	2.72	101.8	0.60	2.78	2.80	708	331.1	152.5
SN-B	1.40	2.62	94.26	2.0	2.57	2.74	708	338.5	148.2
SN-C	1.70	2.62	99.6	2.20	2.54	2.92	708	366.3	147.6
SN-D	1.40	2.54	94.3	2.00	2.51	2.78	708	358.6	144.8
SN-E	1.30	2.82	106.5	1.20	2.78	3.08	708	356.4	151.4
SN-F	1.09	2.68	104.5	1.81	2.62	1.81	708	354.2	149.8
SN-G	2.05	2.5	93.2	2.00	2.42	2.84	708	364.5	143.8
SN-H	0.96	2.57	94.3	1.20	2.58	2.87	708	342.4	146.0
SN-I	2.90	2.55	94.2	3.70	2.49	3.00	708	394.3	143.2
SN-J	2.75	2.49	92.4	1.10	2.61	2.86	708	368.3	142.7
NN-A	4.66	2.41	86.6	5.91	2.44	2.83	708	445.1	138.4
NN-B	2.58	2.52	95.2	2.60	2.55	2.53	708	376.8	144.4
NN-C	2.53	2.52	94.2	2.90	2.52	2.87	708	380.4	144.9
NN-D	1.0	2.65	95.3	1.30	2.58	2.99	708	345.5	144.2

^aFM = Fineness modulus^bAbsorption and moisture content of aggregates were accounted and w/c of 0.45^c1-day demolded unit weight

The mixture constituents of the prism specimens of ASTM C 1105 are shown in Table 2.11. Concrete mixtures with a volume of 0.3 ft³ were prepared for each of the aggregate quarries to cast three 3"x3"x11" specimens. The prisms were stored at 100% relative humidity at room temperature, shown in Figure 2.10. The change in length was measured in one week intervals for the first 3 months, in 2 weeks intervals for the next 3 months, and in 4 weeks intervals for the last 6 months.



Figure 2.10: Prisms stored in a moisture room for ASTM C 1105 test

2.4.2 Losses in ultimate compressive strength and modulus of elasticity

For each of the fourteen aggregate source, 0.75 ft³ of concrete was prepared in order to cast twelve 4"x8" cylinders. Their matrix constituents and proportions are shown in Table 2.11. After demolding, six cylinders were stored in the curing room of 100% RH at room temperature as shown in Figure 2.11, and the remaining were cured in 1N NaOH solution inside closed containers at a temperature of 80°C as shown in Figure 2.12. After 28 days of curing, three water-cured and three alkali-cured cylindrical specimens were subjected to uni-axial compression tests per requirements of the ASTM C 39 and ASTM C 469. The remaining six specimens were tested in the same manner when the specimens reached the age of 6 months.

2.4.3 Mitigating ASR-induced expansion

Three mitigation techniques were conducted to suppress the excess ASR-induced expansion of reactive aggregates. They are described as follows:



Figure 2.11: Cylinders stored in a moisture room at a temperature of 20°C



Figure 2.12: Cylinders stored in 1N NaOH solution at a temperature of 80°C

2.4.3.1 Use of Class F fly ash

The seven aggregates that showed excess reactivity based on ASTM C 1260 and modified ASTM C 1260 were investigated through the mitigation technique of incorporating Class F fly ash as a secondary cementitious material. In suppressing

expansion due to alkali-silica reaction (ASR), four dosages of Class F fly ash, namely 15, 20, 25 and 30%, as a partial replacement of Portland cement (by weight) with 0.42% $\text{Na}_2\text{O}_{\text{eq}}$ alkali content used. The mixing proportions of the mortar bars containing different levels of Class F fly ash are shown in Table 2.12.

Table 2.12: Mixture constituents of mortar bars containing Class F fly ash

Agg. ID	Fly Ash (%)	Graded Agg. ^a (gm)	Absorp- tion (%)	Cement ^a (gm)	Class F fly ash (gm)	W/C	Water ^{a,b} (gm)
SN-C	15	2310	2.18	872.7	154.0	0.47	531.3
	20	2310	2.18	821.3	205.4	0.47	531.3
	25	2310	2.18	777.0	256.7	0.47	531.3
	30	2310	2.18	718.7	308.0	0.47	531.3
SN-F	15	2310	1.70	872.7	154.0	0.47	520.4
	20	2310	1.70	821.3	205.4	0.47	520.4
	25	2310	1.70	777.0	256.7	0.47	520.4
	30	2310	1.70	718.7	308.0	0.47	520.4
SN-G	15	2310	3.30	872.7	154.0	0.47	555.5
	20	2310	3.30	821.3	205.4	0.47	555.5
	25	2310	3.30	777.0	256.7	0.47	555.5
	30	2310	3.30	718.7	308.0	0.47	555.5
SN-J	30	2310	4.02	718.7	308.0	0.47	569.0
	15	2310	3.48	872.7	154.0	0.47	556.5
	20	2310	3.48	821.3	205.4	0.47	556.5
	25	2310	3.48	777.0	256.7	0.47	556.5
NN-B	30	2310	3.48	718.7	308.0	0.47	556.5
	15	2310	2.80	872.7	154.0	0.47	542.1
	20	2310	2.80	821.3	205.4	0.47	542.1
	25	2310	2.80	777.0	256.7	0.47	542.1
NN-C	30	2310	2.80	718.7	308.0	0.47	542.1
	15	2310	3.12	872.7	154.0	0.47	545.4
	20	2310	3.12	821.3	205.4	0.47	545.4
	25	2310	3.12	777.0	256.7	0.47	545.4
NN-D	30	2310	3.12	718.7	308.0	0.47	545.4
	15	2310	1.75	872.7	154.0	0.47	515.5
	20	2310	1.75	821.3	205.4	0.47	515.5
	25	2310	1.75	777.0	256.7	0.47	515.5
	30	2310	1.75	718.7	308.0	0.47	515.5

^aWeights were calculated on 7-bar batch basis; ^bAbsorption and moisture were considered

To represent a better specimen, about half of each mixture was utilized to fabricate four specimens. For evaluating the effectiveness of different cementitious material combinations with a specific aggregate, ASTM C 1567 is a standardized modification of the mortar bar test, C 1260. The method entitled “Test method for determining the potential alkali-silica reactivity of combinations of cementitious materials and aggregate (Accelerated mortar-Bar method),” provides a quick answer regarding the prevention level of fly ash to be used with a specific aggregate. Mixing, curing, storage and testing procedures of ASTM C 1567 are the same as ASTM C 1260. Expansion readings were taken at the age of 0, 3, 6, 10 and 14 days of immersion, and one reading per week thereafter until the 98-day immersion age was reached.

2.4.3.2 Use of lithium nitrate to the mixture water

The experiments were comprised of four to six dosages of lithium nitrate, namely lithium-to-alkali molar ratios of 0.59, 0.74, 0.89, 1.04, 1.18 and 1.33, whose equivalent Li doses were 80, 100, 120, 140, 160 and 180%, respectively. The amount of lithium nitrate was calculated based on the alkali content of Portland cement and the amount of total cementitious materials in the concrete mixture. The dosages were assessed the sensitivity to low and high dosing of lithium nitrate admixture. The mixture water adjustment was calculated on the basis of $\text{H}_2\text{O}:\text{LiNO}_3$ equal to 70:30 to compensate for the water portion of the lithium dosage added to the concrete mixture. The desired dosage of lithium was added to the mixing water, and the amount of water contained in the mixture was removed from the calculated mixing water to maintain the target w/c ratio.

About half of the lithium added to suppress ASR-induced expansion is absorbed by the hydrating cement, and the uptake of lithium by C–S–H is more than that of sodium

and potassium (Feng et al., 2005). Hence, the remaining half of the lithium is available for the suppressive purpose. The lithium to alkali ratio of the soak solution would be about half of the initial ratio of the mortar bars (Bérubé et al., 2004). In order to minimize the leaching effect of lithium salt, ASTM C 1260 was modified by adding lithium into the soak solution to maintain the same lithium to alkali molar ratio in the mortar bars and the soak solution (Stokes, 1993; McKeen et al., 1998; and Folliard et al., 2003). The amount of lithium nitrate in the trial mixture and 1 liter of 1N NaOH solution is shown in Table 2.13.

Each 7-bar batch size mixture requires a total of 1026.7 grams of Type V Portland cement (0.84% alkali) and the target dosage of lithium nitrate. Mixing, curing, storage and testing procedures are same as ASTM C 1260 except for the soak solution concentration. The mixture constituents of mortar bars containing lithium nitrate are specified in Tables 2.14 and 2.15 for the aggregates quarried from the Southern and Northern Nevada, respectively.

Table 2.13: Lithium- to- alkali molar ratio (%Li dose) of mortars with corresponding soak solution's constituents

Lithium Mixture	Mortar Bar			1.0L of 1N soak solution			
	<i>Li</i>	Li dose (%)	LiNO ₃ ^a (gm)	<i>Li</i>	Water ^b (gm)	LiNO ₃ (gm)	NaOH (gm)
	<i>Na + K</i>			<i>Na + K</i>			
#1	0.59	80	37.78	0.295	952.50	67.93	40
#2	0.74	100	47.23	0.370	940.56	84.92	
#3	0.89	120	56.67	0.445	928.70	101.90	
#4	1.04	140	66.12	0.520	916.80	118.90	
#5	1.18	160	75.56	0.590	904.90	135.86	
#6	1.33	180	85.01	0.665	893.00	152.90	

^aThe amount of lithium was computed based on 0.84% cement alkali

^bDistilled water was added to prepare NaOH soak solution

Table 2.14: Mixture constituents of mortars containing lithium nitrate for the aggregates quarried from Southern Nevada

Agg. ID	$\frac{Li}{Na + K}$	Graded Agg. ^a (gm)	Absorption (%)	Cement ^a (gm)	LiNO ₃ ^a (gm)	Water in W/C LiNO ₃ (gm)	Mixture Water ^a (gm)
SN-C	0.59	2310	2.18	1026.7	37.78	26.45	504.8
	0.74	2310	2.18	1026.7	47.23	33.06	498.2
	0.89	2310	2.18	1026.7	56.67	39.67	491.6
	1.04	2310	2.18	1026.7	66.12	46.28	485.0
SN-F	0.59	2310	1.70	1026.7	37.78	26.45	494.0
	0.74	2310	1.70	1026.7	47.23	33.06	487.4
	0.89	2310	1.70	1026.7	56.67	39.67	480.8
	1.04	2310	1.70	1026.7	66.12	46.28	474.1
SN-G	0.59	2310	3.30	1026.7	37.78	26.45	523.1
	0.74	2310	3.30	1026.7	47.23	33.06	516.4
	0.89	2310	3.30	1026.7	56.67	39.67	509.8
	1.04	2310	3.30	1026.7	66.12	46.28	503.2
	1.19	2310	3.30	1026.7	75.56	52.89	496.6
	1.34	2310	3.30	1026.7	85.01	59.50	490.0
SN-J	0.59	2310	3.48	1026.7	37.78	26.45	530.0
	0.74	2310	3.48	1026.7	47.23	33.06	523.4
	0.89	2310	3.48	1026.7	56.67	39.67	516.8
	1.04	2310	3.48	1026.7	66.12	46.28	510.2
	1.19	2310	3.48	1026.7	75.56	52.89	503.6
	1.34	2310	3.48	1026.7	85.01	59.50	497.0

^aWeights were calculated on 7-bar batch basis

2.4.3.3 Use of combined Class F fly Ash and lithium nitrate

For the third ASR mitigation technique, a constant amount of lithium nitrate with a Li/(Na+K) molar ratio of 0.74 (standard lithium dosage) was combined with two dosages of Class F fly ash (15% and 20% by weight of cement replacement) to alleviate the expansion of five reactive aggregates.

When LiNO₃ salt is added to Class F fly ash, ASTM C 1260 (standard) has to be modified in order to eliminate the leaching effect of lithium salt into the soak solution. To

avoid the leaching lithium out of the specimens, lithium was added to the soak solution to maintain same lithium to alkali molar ratio of the mortar bars and the soak solution. The amount of sodium hydroxide, lithium nitrate and water in 1L of 1N NaOH soak solution with corresponding to half molar ratio of mortar bars is tabulated in Table 2.16.

Table 2.15: Mixture constituents of mortars containing lithium nitrate for the aggregates quarried from Northern Nevada

Agg. ID	$\frac{Li}{Na + K}$	Graded Agg. ^a (gm)	Absorption (%)	Cement ^a (gm)	LiNO ₃ ^a (gm)	Water in LiNO ₃ (gm)	W/C	Mixture Water ^{a,b} (gm)
NN-B	0.59	2310	2.80	1026.7	37.78	26.45	0.47	511.1
	0.74	2310	2.80	1026.7	47.23	33.06	0.47	504.5
	0.89	2310	2.80	1026.7	56.67	39.67	0.47	497.9
	1.04	2310	2.80	1026.7	66.12	46.28	0.47	491.2
	1.19	2310	2.80	1026.7	75.56	52.89	0.47	484.6
	1.34	2310	2.80	1026.7	85.01	59.50	0.47	478.0
NN-C	0.59	2310	3.12	1026.7	37.78	26.45	0.47	518.9
	0.74	2310	3.12	1026.7	47.23	33.06	0.47	512.3
	0.89	2310	3.12	1026.7	56.67	39.67	0.47	505.7
	1.04	2310	3.12	1026.7	66.12	46.28	0.47	499.1
	1.19	2310	3.12	1026.7	75.56	52.89	0.47	492.5
	1.34	2310	3.12	1026.7	85.01	59.50	0.47	485.9
NN-D	0.59	2310	1.75	1026.7	37.78	26.45	0.47	489.1
	0.74	2310	1.75	1026.7	47.23	33.06	0.47	482.5
	0.89	2310	1.75	1026.7	56.67	39.67	0.47	475.9
	1.04	2310	1.75	1026.7	66.12	46.28	0.47	469.3

^aWeights were calculated on 7-bar batch basis

^bAggregate's absorption and moisture content were accounted in mixture design

In order to create adequate representation of a typical concrete mixture, about half of each mixture was utilized to fabricate four specimens. Each 7-bar batch size mixture required a total of 1026.7 grams of cementitious materials (Portland cement and Class F fly ash) and constant lithium to alkali molar ratio of 0.74. Mixing, sampling, curing, storage and testing procedures were the same as ASTM C 1260 except for the soak

solution concentration. The constituents and proportions of the mortar bars containing lithium and Class F fly ash are shown in Table 2.17.

Table 2.16: Lithium nitrate and Class F dosage of mortars with corresponding soak solution's constituents

Mix	Mortar Bar		1.0 Liter of 1N NaOH solution				
	Molar ratio	Fly ash (%)	LiNO ₃ ^a (gm)	molar ratio	NaOH (gm)	LiNO ₃ (gm)	Water ^b (gm)
#1	0.74	15	40.14	0.37	40	84.92	940.56
#2	0.74	20	37.78	0.37			

^aWeights were calculated on 7-bar batch basis with 0.84% cement alkali

^bDistilled water was added to prepare NaOH soak solution

Table 2.17: Mixture constituents of mortars containing Class F fly ash and lithium nitrate

Agg. ID	Li-Na Molar Ratio	Class F Fly Ash (%)	Graded Agg. ^a (gm)	Absorption (%)	Cement ^a (gm)	Fly Ash (gm)	LiNO ₃ ^a (gm)	Water in LiNO ₃ (gm)	W/C	^{1,2} Water (gm)
SN-G	0.74	15	2310	3.30	872.7	154.0	40.2	28.10	0.47	560.7
		20	2310	3.30	821.3	205.4	37.8	26.50	0.47	562.3
SN-J	0.74	15	2310	3.48	872.7	154.0	40.2	28.10	0.47	568.1
		20	2310	3.48	821.3	205.4	37.8	26.50	0.47	569.8
NN-B	0.74	15	2310	2.80	872.7	154.0	40.2	28.10	0.47	547.8
		20	2310	2.80	821.3	205.4	37.8	26.50	0.47	549.5
NN-C	0.74	15	2310	3.12	872.7	154.0	40.2	28.10	0.47	556.2
		20	2310	3.12	821.3	205.4	37.8	26.50	0.47	557.9

^aWeights were calculated on 7-bars batch basis with 0.84% cement alkali

^bAggregate's absorption and moisture content were accounted in mixture design

CHAPTER 3

IDENTIFICATION OF REACTIVE AGGREGATES

The goal of this chapter is to evaluate the alkali-aggregate reactivity (AAR), alkali-silica reactivity (ASR) and alkali-carbonate reactivity (ACR), of the fourteen different aggregates quarried in the State of Nevada. Three accelerated tests were conducted to assess the potential reactivity of the trial aggregates. The mortar bar (ASTM C 1260) and concrete prism (ASTM C 1293 Modified) tests were used for assessing ASR, and the ASTM C 1105 standard was performed for evaluating ACR of each trial aggregate.

3.1 Determining ASR using ASTM C 1260 (Mortar Bar)

ASTM C 1260 is one of the most widely used standardized tests for assessing the potential alkali-silica reactivity of an aggregate. Due to the extreme nature of testing, high concentration (1N) of alkaline solution and an elevated temperature of 80°C, the method is known as an accelerated mortar bar test (AMBT). The test takes only 14 days (after submerging the specimens in alkali solution) to obtain the levels of alkali-silica reactivity of an aggregate, otherwise it would take 10 years or more to view the ASR effects in real time.

In addition to the standard ASTM C 1260 test, the modifications of ASTM C 1260 were also conducted by lowering the soak solution (NaOH) concentration from 1N to 0.5N and 0.25N, and elevating cement alkalis from 0.42% to 1.26% $\text{Na}_2\text{O}_{\text{eq}}$, and extending test duration from 14 to 98 days. The expansion readings of each mortar bar were taken at the immersion ages of 3, 6, 10 and 14 days, and, one reading per week thereafter until the immersion age had reached 98 days. The results of individual sample are documented in the Appendix A.

The trial aggregates were classified into two categories of alkali-silica reactivity, either innocuous or reactive, based on the 14-day failure criteria of ASTM C 1260 for the 1N soak solution. The aggregate producing the 14-day expansion of less than 0.10% was considered innocuous, designated by Group-A aggregates, greater than 0.20% was potentially (highly) reactive, and in between was declared as slowly reactive aggregate.

3.1.1 Expansion progression as related to soak solution concentrations

The ASR expansion of the mortar bars containing each trial aggregate for the 1N NaOH solution as a function of the immersion age is illustrated in Figure 3.1. As can be seen, the expansion of the test mortar bars increased with an increase in the test duration, and the expansion characteristics over the test duration varied depending on the aggregate source. It was shown that the expansion rates were faster and more extensive in the mortar bars containing reactive aggregates, having the 14-day expansions greater than 0.10%, than those cast with the innocuous aggregates. For the highly reactive aggregates, having the 14-day expansion greater than 0.20%, the most alkali-silica reactions occurred in the early stage of testing, and the reaction rate decreased with an increase in the immersion age. Conversely, the ASR-induced expansion of the innocuous aggregates was relatively slow throughout the test duration. In general, for the soak solution of 1N NaOH, a maximum increase in expansion was observed between the test durations of 14 and 28 days. A moderate increase in expansion was noted between the ages of 28 and 56 days, after which the specimens expanded slowly up to the test duration of 98 days. However, the progression in expansion also varied depending on the reactivity of an aggregate.

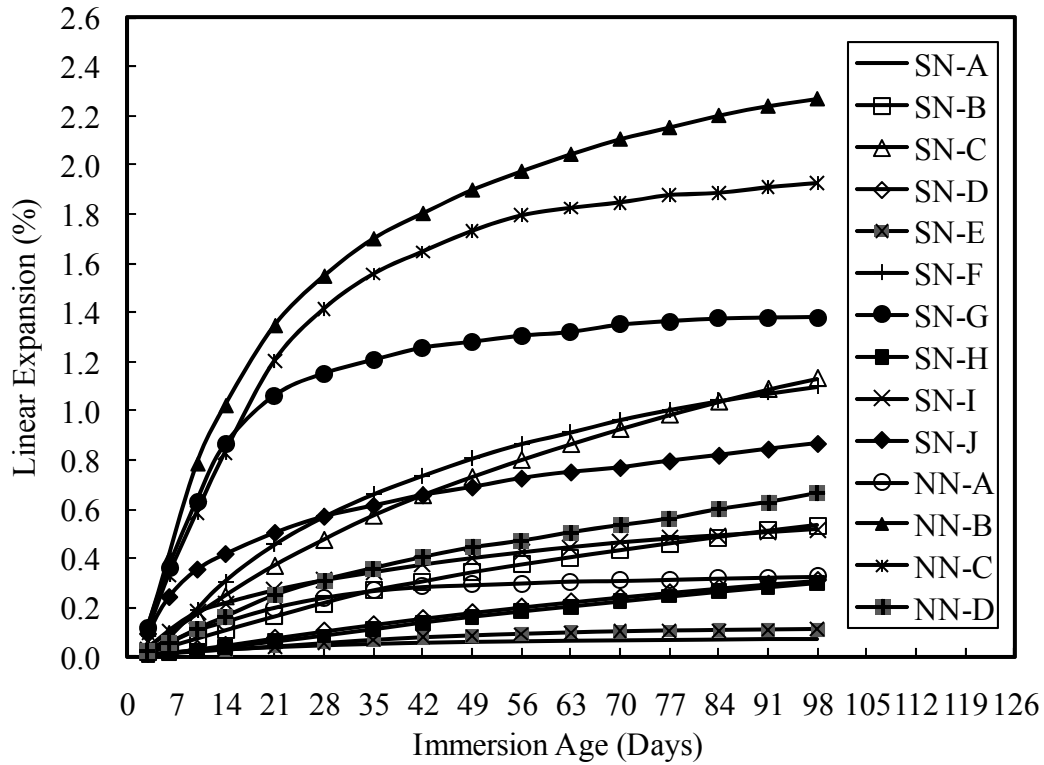


Figure 3.1: Expansion of ASTM C 1260 for the 1N solution

Figure 3.2 demonstrates the ASR-induced expansion of the mortar bars made with each trial aggregate for the 0.5N solution over the test duration of 98 days. As can be seen, the aggregates producing the 14-day expansions for the 1N solution of more than 0.40% the development of ASR expansion under the 0.5N solution over the test duration followed a similar pattern to that of for the 1N soak solution. A rapid increase in expansion was occurred between the immersion ages of 14 and 28 days, and the expansion rate decreased gradually thereafter. For the aggregates generating the 14-day expansions for the 1N solution in between 0.10 and 0.40%, designated by Group-C aggregates, the ASR-induced expansion for the 0.5N solution increased slowly until the test duration of 28 days, followed by a rapid increase between the immersion ages of 28 and 56 days, and a decreased rate of expansion between 56 and 98 days. However, in the

case of the innocuous aggregates, having the 14-day expansion for the 1N solution of less than 0.10%, the expansion increased slowly within a fairly constant rate throughout the 98-day test duration.

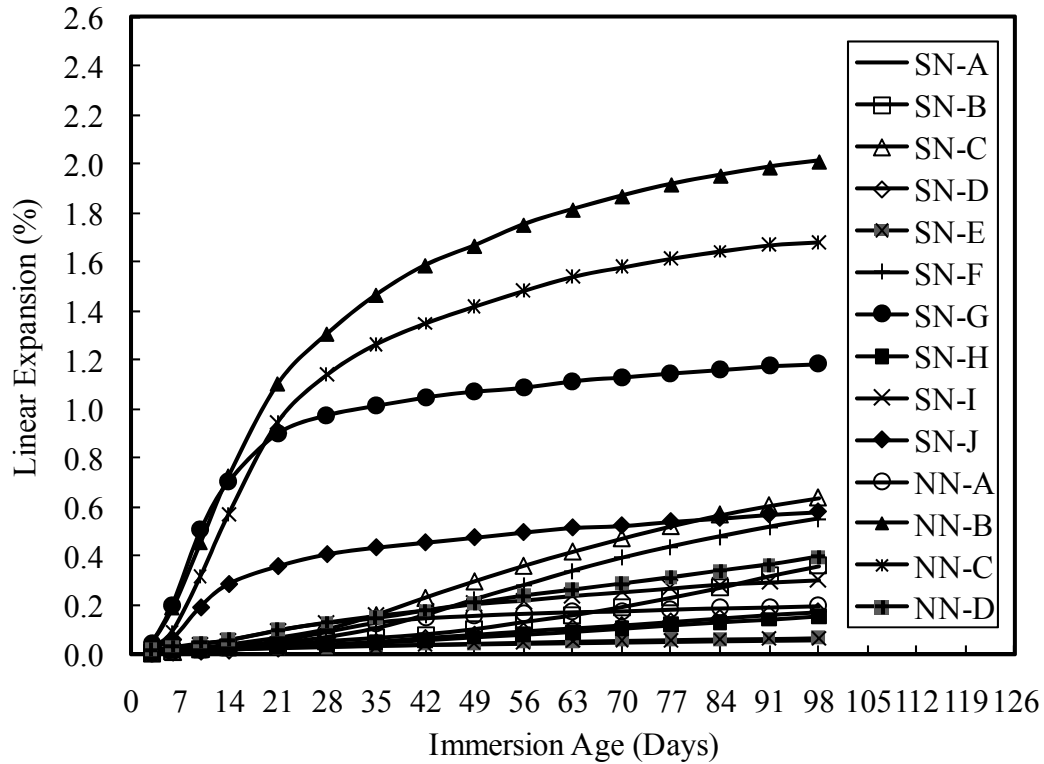


Figure 3.2: Expansion of ASTM C 1260 for the 0.5N NaOH

The progression in expansion of the trial aggregates for the 0.25N NaOH as related to the immersion age is shown in Figure 3.3. As can be seen, the ASR expansion for the 0.25N solution increased rapidly over the test duration of 98 days for the SN-G, NN-B and NN-C aggregate groups, all of which generating the 14-day expansions of more than 0.85% under the 1N solution. The expansions of the remaining eleven aggregate groups were slow till the immersion age of 28 days. A moderate growth in expansion was

observed during the test durations of 28 and 56 days, and the highest growth in expansion was detected between the immersion ages of 56 and 98 days.

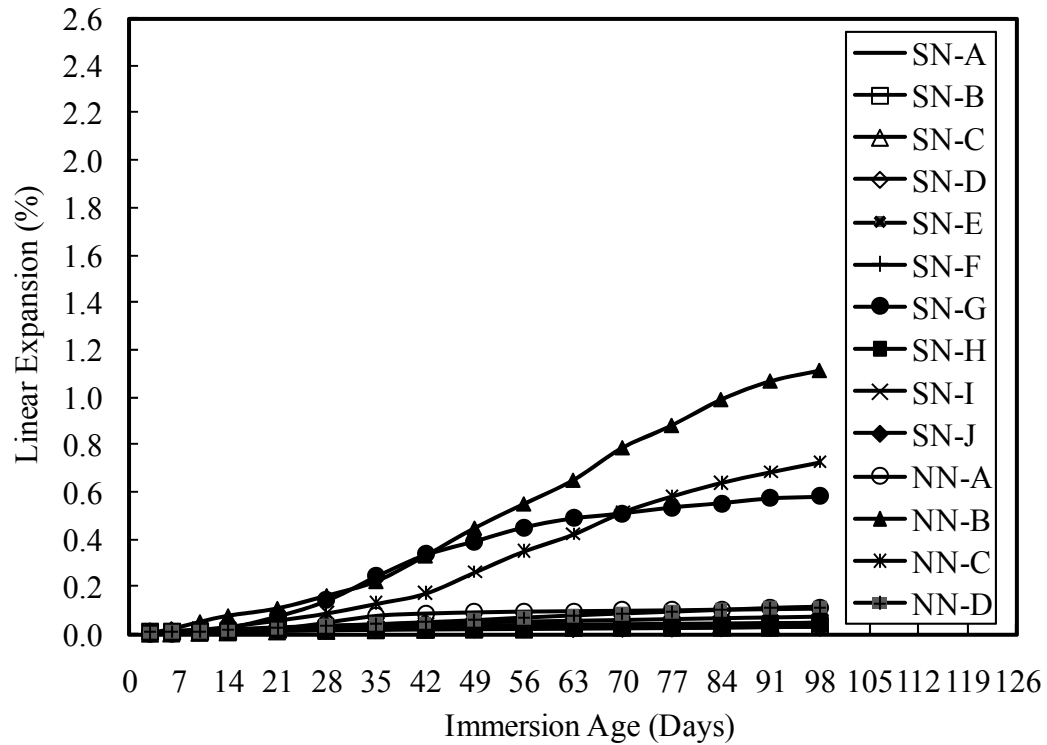


Figure 3.3: Expansion of ASTM C 1260 for the 0.25N NaOH

The study revealed that ASR expansion of each trial aggregate decreased with a decrease in soak solution concentration. The expansion of the mortar bars for the 1, 0.5 and 0.25N NaOH as related to the immersion age varied depending on the mineralogy of aggregates. For instance, some aggregates expanded rapidly at the early age of immersion, and the expansion rate decreased thereafter. Several aggregates expanded slowly throughout the test duration. The others expanded less initially and the expansion rate increased rapidly at a later age of immersion.

3.1.2 Alkali-silica reactivity of ASTM C 1260 for the 1N solution

Past investigations demonstrated that the 14-day failure limit of ASTM C 1260 of 0.10% was not capable of predicting the actual alkali-silica reactivity of some aggregates (Jin et al., 2000; FAA, 2006; and Lenke & Malvar, 2009). To examine the expressed concern associated with aggregate classifications based on the above-mentioned failure limit, this portion of the study investigate the expansion limits of the mortar bars made with different Nevada's aggregates under the 1N NaOH at the extended immersion ages of 28, 56 and 98 days.

The progression of the average ASR-induced expansion of the fourteen aggregate groups (AIE) for the 1N NaOH as related to different immersion ages is illustrated in Figure 3.4. The best fit curve that represented the correlation with a R^2 value of 0.997 between the AIE and the immersion age is shown in Equation 3.1. The value of Prob(F) of the regression curve and Prob(t) of the regression parameters a and b were zero. Equation 3.1 reported that the 14-, 28-, 56- and 98-day average expansions of the fourteen aggregates were 0.316, 0.495, 0.685 and 0.808%, respectively. It was shown that the AIE curve was 0.216 ($= 0.316\% - 0.10\%$) units more than the expansion limit at the immersion age of 14 days. Downward shifting of the AIE curve by 0.216 units for the remaining immersion ages established the corrected curve of the failure criteria for the extended immersion ages. The shifted AIE curve revealed the 28-, 56- and 98-day expansion limits of the mortar bars under the 1N NaOH soak solution of 0.28, 0.47 and 0.59%, respectively.

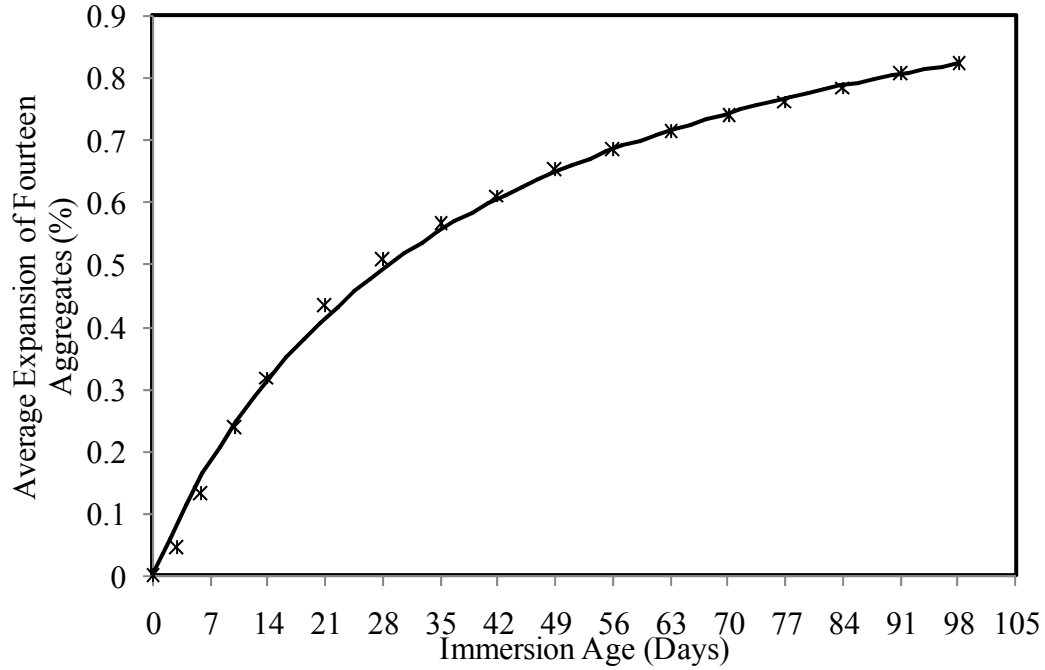


Figure 3.4: The average expansion of the fourteen aggregates for the 1N solution at various immersion ages

$$y = \frac{t}{(0.8897t + 31.9287)} \quad \text{Eq. 3.1}$$

where:

y is the average ASR expansion of the fourteen aggregates at t days

a and b are the regression parameters

It was concluded that the aggregates producing the 14-, 28-, 56- and 98-day ASR expansions of 0.10, 0.28, 0.47 and 0.59%, respectively, were considered potentially reactive, and those producing the expansions of less than the above mentioned four proposed expansion limits were considered innocuous. However, the aggregates generating the expansions of more than 0.10% at 14 days and less than 0.28% at 28 days, 0.47% at 56 days and 0.59% at 98 days were called marginally reactive. The classifications of the trial aggregates based on the above-mentioned suggested expansion limits at 14, 28, 56 and 98 days were evaluated. Additionally, the extended failure criteria

of the mortar bars of 0.33% at 28 days and 0.48% at 56 days, proposed by Hooton (1991), and Rogers and Hooton (1993), were also applied in the research investigation. Extrapolating the failure criteria of 0.10% at 14 days, 0.33% at 28 days and 0.48% at 56 days, the 98-day expansion limit of the mortar bars under the 1N NaOH was also determined, and utilized in classifying the aggregate reactivity. The results are documented in Table 3.1.

Table 3.1: Aggregate classifications based on ASTM C 1260 for the 1N Solution

Agg. ID	14-Day ^a (0.10%)	28-Day		56-Day		98-Day	
		0.28% ^b	0.33% ^c	0.47% ^b	0.48% ^c	0.59% ^b	0.57% ^d
SN-A	I	I	I	I	I	I	I
SN-B	SR	I	I	I	I	I	I
SN-C	HR	R	R	R	R	R	R
SN-D	I	I	I	I	I	I	I
SN-E	I	I	I	I	I	I	I
SN-F	HR	R	R	R	R	R	R
SN-G	R	R	R	R	R	R	R
SN-H	I	I	I	I	I	I	I
SN-I	HR	R	I	I	I	I	I
SN-J	HR	R	R	R	R	R	R
NN-A	SR	I	I	I	I	I	I
NN-B	HR	R	R	R	R	R	R
NN-C	HR	R	R	R	R	R	R
NN-D	SR	R	R	R	R	R	R

I = Innocuous, SR = Slowly reactive, R=Reactive, HR= Highly reactive

^aAggregates are classified as I, SR and HR based on ASTM C 1260

^bAggregates are classified as I and R based on the expansion limits proposed in this study

^cAggregates are classified as I and R based on the failure criteria proposed by Hooton (1991) and Rogers and Hooton (1993)

^d98-day expansion limit was determined by extrapolating the failure criteria of 0.10% at 14 days, 0.33% at 28 days and 0.48% at 56 days

As can be seen, the ASR classifications of the fourteen trial aggregates were perfectly matched based on the 28-, 56- and 98-day expansion criteria, proposed by Hooton (1991), and Rogers and Hooton (1993), and those proposed by Islam in this study. Three

aggregate groups (SN-B, SN-I and NN-A) were considered as reactive by the 14-day limit, whereas they were found to be innocuous by the limits of the 28, 56 and 98 extended ages. The levels of alkali-silica reactivity of the eleven of the fourteen aggregate groups produced similar results at all four distinct immersion ages.

Table 3.1 also demonstrates that, of the fourteen aggregates, the four aggregates (SN-A, SN-D, SN-E, and SN-H) displayed innocuous behavior, and the seven aggregate groups (SN-C, SN-F, SN-G, SN-J, NN-B, NN-C, and NN-D) were found to be reactive based on the failure criteria of mortar bars at the immersion ages of 14, 28, 56 and 98 days. It was also found that the aggregates having the 14-day expansion of more than 0.15% proved to be reactive at the extended immersion ages except for the SN-I aggregate. For instance, the mortar bars made with the SN-B and NN-A aggregates generating less than 0.15% expansion at 14 days were found to be innocuous based on failure criteria at 28, 56 and 98 days. Overall, the alkali-silica reactivity of the selected aggregates based on the extended immersion ages provided more consistent results than that obtained at the early immersion age.

Aggregates showing innocuous behavior based on all four suggested expansion limits at 14, 28, 56 and 98 days would probably have good performance characteristics in the field. Conversely, aggregates exceeding these expansion limits were considered reactive, and required corrective measures to control alkali-silica reactivity. The various mitigation techniques in suppressing ASR-induced expansion of the reactive aggregates, as identified by the mortar bar test at 14, 28, 56 and 98 days, are discussed in Chapter 5.

3.1.3 Comparison of crushed coarse and fine aggregates reactivity

The mortar bars containing fine aggregates of each aggregate source were evaluated in order to examine whether they could produce reliable results of ASTM C 1260, which required a specific gradation of crushed coarse aggregates. The 14-day expansion of the mortar bars made with fine aggregates was compared with that of crushed coarse aggregates of the same quarry. The results are shown in Figure 3.5. As can be seen, the mortar bars made with fine aggregates produced expansions that were marginally higher than those of the mortar bars cast with crushed coarse aggregate from the same source. Because the fine aggregates had a larger surface area than crushed coarse aggregates, more reactive silica surface was exposed to alkalis resulting in higher expansions. Although the difference in the expansion of both sets of mortar bars was marginal for all selected aggregate sources, the resulting levels of alkali-silica reactivity based on the 14-day failure criteria of ASTM C 1260 (innocuous, slowly reactive and highly reactive) remained identical. As a result, the use of fine aggregate, instead of graded crushed aggregate, reduces the effort needed for material preparation and the overall cost of experiment.

3.1.4 ASR-induced cracks on mortar bars for the 1N solution

The ASR-induced cracks formed on the surface of the test specimens were also carefully examined. Figures 3.6, 3.7 and 3.8 illustrate the ASR-related cracks on the surface of the mortar bars containing innocuous, slowly and highly reactive aggregates, respectively, as determined by ASTM C 1260 at 14 days. As seen in Figure 3.6, the mortar bars made with the innocuous aggregates showed no visible cracks even at the immersion age of 98 days. The specimens containing slowly reactive aggregates

experienced a limited number of random cracks (horizontal, longitudinal and map cracks) as illustrated in Figure 3.7. On the other hand, severe cracks (map cracks) were noted on the specimens prepared from the highly reactive aggregates as depicted in Figure 3.8. At the early age of immersion, tiny cracks were developed at the outer surface of the mortar bars containing reactive aggregates due to the tension exerted by the alkali-silica reactions. As the test duration prolonged, additional alkali-silica reactions took place resulting in an increase in expansion and surface cracking, a common symptom of ASR. In the case of the mortar bars made with NN-C aggregate, severe map cracking was observed at the immersion age of three days.

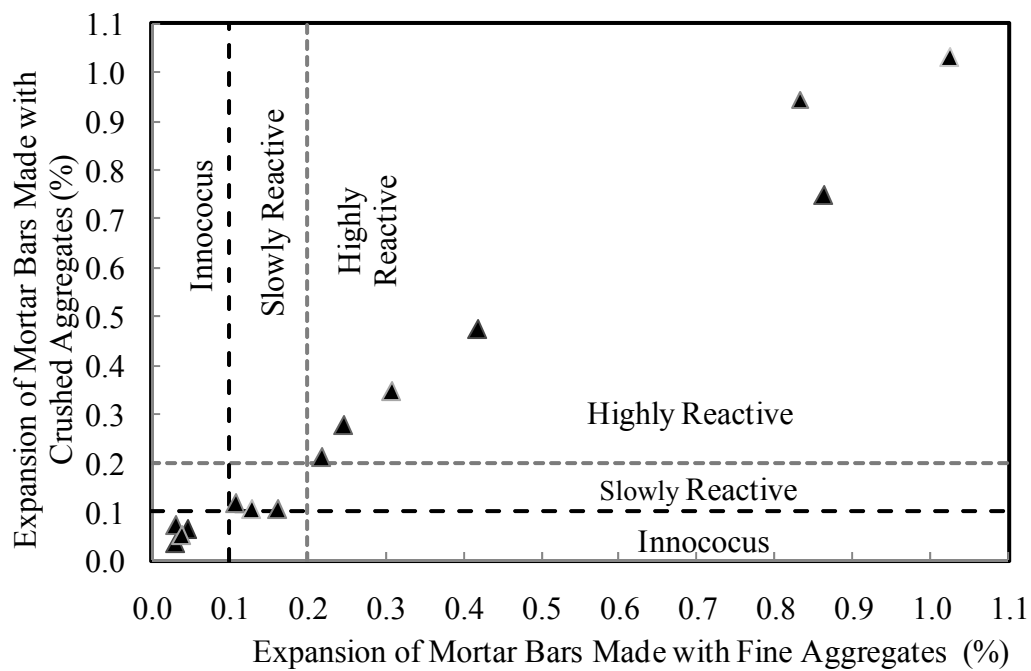


Figure 3.5: The 14-day expansion of mortar bars prepared with crushed coarse and fine aggregates



Figure 3.6: The mortar bars made with the innocuous aggregate (SN-A)



Figure 3.7: The mortar bars made with the slowly reactive aggregate (NN-A)

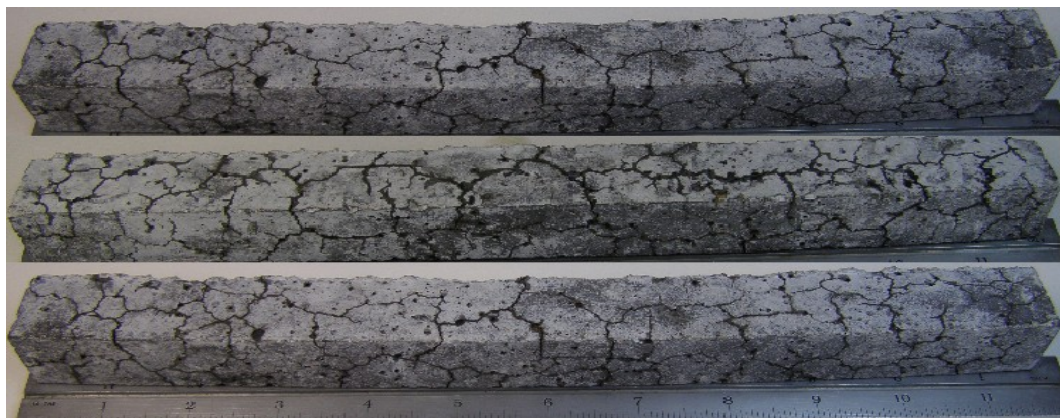


Figure 3.8: The mortar bars made with the highly reactive aggregate (NN-C)

It can be concluded that the progression of ASR-related cracks is directly linked to the increase in expansion of the test mortar bars. ASR-induced cracks are significantly affected by the type and the amount of reactive aggregates present in the mixture. The excessive expansion and related damages due to alkali-silica reactivity can be successfully eliminated by utilizing various mitigation techniques which will be discussed in Chapter 5.

3.1.4 Determination of the failure criteria of ASTM C 1260 for the 0.5 and 0.25N solutions

Past investigations (Van Aardt & Visser, 1982; Johnston, 1994; Touma et al., 2001a; and Shon et al., 2002), as well as this study revealed that the concentration of the sodium hydroxide solution can impact the ASR-based expansion characteristics. Hence, the failure limits of the mortar bars for the 0.5 and 0.25N solutions at various immersion ages were needed to be adjusted from those found for the standard solution (1N NaOH) at the corresponding immersion ages. To achieve the stated objective, correlations were developed between the expansion of the test mortar bars for the 1N and 0.5N and 0.25N solutions at the immersion ages of 14, 28, 56 and 98 days.

Figure 3.9 presents the 14-day expansion of ASTM C 1260 for the 0.5 and 1N solutions. The pattern that best fitted the experimental data is shown in Figure 3.9 and presented in Equation 3.2. Due to the variability of data, outliers significantly outside the trend line were removed from the regression analysis in order to produce a more suitable statistical correlation. Equation 3.2 also represents the most suitable relationship between the dependent and independent variables at the immersion ages of 28, 56 and 98 days. The statistical data for Equation 3.2, regression parameters a and b , Prob(t), Prob(F) and

coefficient of multiple determination (R^2), at the four distinct immersion ages are documented in Table 3.2. The most suitable predictions of the failure criteria of ASTM C 1260 for the 0.5N soak solution at the immersion ages of 14, 28, 56 and 98 days were determined by substituting the expansion limits of ASTM C 1260 for the 1N solution at the respective immersion ages in Equation 3.2. The results are also illustrated in Table 3.2.

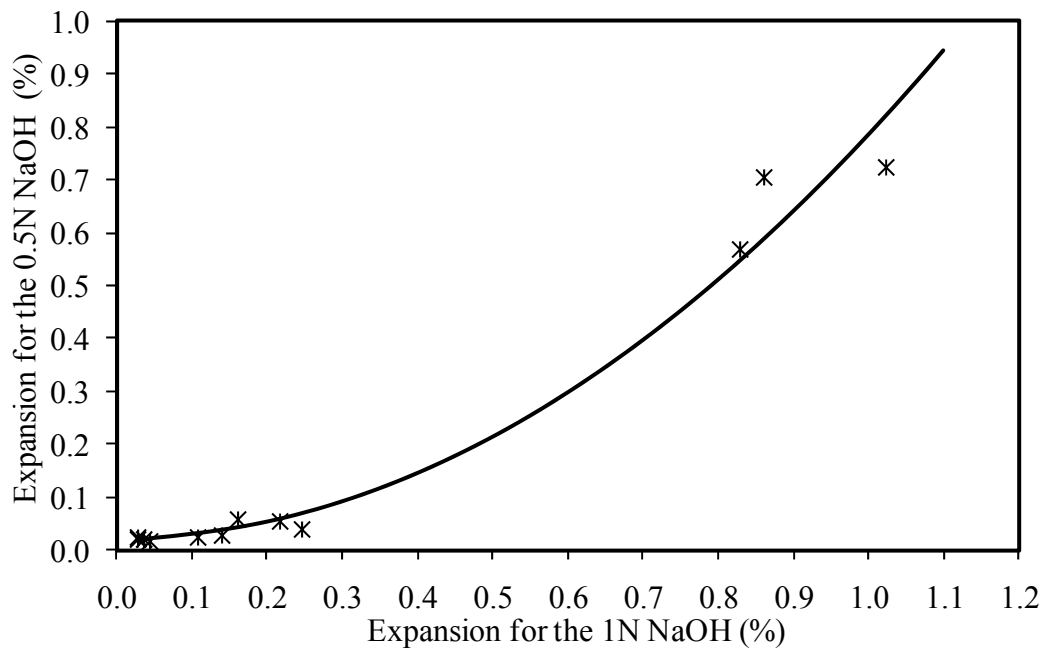


Figure 3.9: 14-day expansion of the mortars for the 0.5 and 1N solutions

$$y = a + bx^2 + \frac{c}{x^2} \quad \text{Eq. 3.2}$$

Where:

x and y are the expansions of mortar bars for the 1 and 0.5N NaOH solutions, respectively; a , b and c are the regression variables

Table 3.2: Statistical data for Equation 3.2, and the failure criteria of ASTM C 1260 for the 0.5N solution at various immersion ages

Parameters		14-Day	28-Day	56-Day	98-Day
Regression Variables	<i>a</i>	0.02334	0.049040	0.122355	0.208086
	<i>b</i>	0.76123	0.532931	0.432405	0.375439
	<i>c</i>	0.00000	-0.00006	-0.00042	-0.00100
Prob(t) of Regression variables	<i>a</i>	0.36091	0.15237	0.00923	0.00046
	<i>b</i>	0.000000	0.00000	0.00000	0.00000
	<i>c</i>	0.90995	0.73121	0.34421	0.12937
Prob(F)		0.00000	0.00000	0.00000	0.00000
R ²		0.973	0.971	0.972	0.972
Failure criteria of ASTM C 1260 for the 1N NaOH		0.10%	0.33%	0.48%	0.57%
Failure criteria of ASTM C 1260 for the 0.5N NaOH		0.030%	0.105%	0.220%	0.325%

The 14-day failure limit of ASTM C 1260 for the 0.5N solution of 0.04% was first proposed by Stark et al. (1993). However, the above mentioned criterion classified some innocuous aggregates as reactive in the research investigations conducted by Touma et al. (2001a and 2001c). The reason might be that the expansion of the mortar bars for the 0.5N NaOH solution at the immersion age of 14 days was diminutive (Shon et al., 2002). The analysis of this study revealed the 14-day expansion limit of 0.030% for the ASTM C 1260 using 0.5N NaOH solution. In order to obtain a more reproducible ASR-related expansion of the mortar bars for the 0.5N solution, Shon et al. (2002) suggested extending the testing period to at least 28 days. However, no failure criteria had been established for the mortar bars submerged in the 0.5N soak solution at the immersion ages of 28 days or more. This study revealed the expansion limit of 0.105% at the test duration of 28 days, which confirmed the findings of the research conducted by Shon et

al. (2002); the expansion of the mortar bars for the 0.5N solution at 28 days was comparable to that obtained for the 1N solution at 14 days (0.10%). Extending the immersion ages to 56 and 98 days, the proposed threshold expansion limits of the mortar bars for the 0.5N solution were 0.220 and 0.325%, respectively. The alkali-silica reactivity of the trial aggregates was evaluated based on the four suggested failure criteria of ASTM C 1260 for the 0.5N solution at 14, 28, 56 and 98 days, and was compared with that of for the 0.5N solution, as described in Section 3.1.5.

The failure criteria of ASTM C 1260 for the 0.25N solution at the immersion ages of 14, 28, 56 and 98 days were also evaluated using a similar approach to those were used for the 0.5N soak solution. The 14-day expansion of ASTM C 1260 for the 0.25 and 1N solutions is shown in Figure 3.10. The correlation between the expansions of the mortar bars for the two concentrations (1 and 0.25N) of NaOH solution is presented by Equation 3.3. The identical equation was also represented the best fit for the test mortar bars at the ages of 28, 56 and 98 days. Table 3.3 shows the statistical data for the regression curve, regression variables a and b , Prob(t) of each regression variable, Prob(F), and coefficient of multiple determination at the ages of 14, 28, 56 and 98 days. The R^2 values shown in Table 3.3 demonstrate that the regression curve fitted more with a longer immersion age.

The 14-day failure limit of ASTM C 1260 for the 0.25N soak solution of 0.020% expansion was first proposed by Stark (1993). The limit was declared too conservative for most aggregates (Touma et al., 2001a, 2001c, 2004). Additionally, Touma et al. stated that the expansion limit of the mortar bars for the 0.25N solution needed to below the expansion limit of 0.02% at 14 days. This study proposes the 14-day failure limit of ASTM C 1260 for the 0.25N solution of 0.013% expansion. Past investigations

(Johnston, 1994; Touma et al., 2001a; and Shon et al., 2002) showed that the expansion of the mortar bars for the 0.25N solution was very small even at the immersion age of 28 days for the aggregates that were reactive under the 1N NaOH solution. Shon et al. (2002) suggested the test duration of ASTM C 1260 for the 0.25N solution should be extended beyond 28 days. However, past studies offered no failure criteria for the 0.25N solution beyond the immersion age of 14 days. In this study, the proposed failure limits of ASTM C 1260 for the 0.25N solution were found to be 0.026, 0.042 and 0.068% at the immersion ages of 28, 56 and 98 days, respectively. The levels of alkali-silica reactivity of the trial aggregates were evaluated based on the expansion limits of ASTM C 1260 for the 1 and 0.25N solutions, as described in Section 3.1.6.

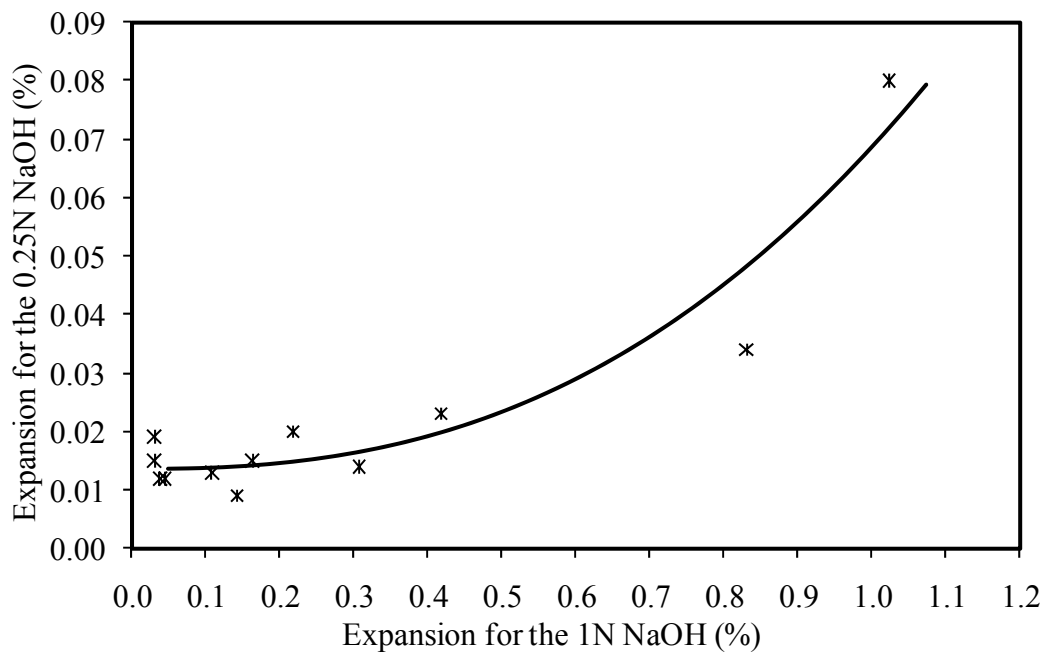


Figure 3.10: The expansion of the mortars for the 0.25 and 1N solutions

$$y = a + bx^{2.5} \quad \text{Eq. 3.3}$$

Where:

x and y are the expansions under 1 and 0.25N solutions, respectively

a and b are the regression variables

Table 3.3: Statistical data for Equation 3.3, and the failure criteria of the mortar bars for the 0.25N soak solution at various immersion ages

Parameters		14-Day	28-Day	56-Day	98-Day
Regression Variables	a	0.01343	0.02425	0.02832	0.03378
	b	0.05529	0.03970	0.08700	0.13742
Prob(t) of Regression variables	a	0.00005	0.00102	0.03603	0.01698
	b	0.00000	0.00000	0.00000	0.00000
Prob(F)		0.00001	0.00000	0.00000	0.00000
R^2		0.910	0.900	0.957	0.992
Failure criteria of the mortars for the 1N NaOH		0.100%	0.330%	0.480%	0.570%
Failure criteria for the mortars for the 0.25N NaOH		0.013%	0.026%	0.042%	0.068%

3.1.5 Aggregate classifications based on the failure criteria of ASTM C 1260 for the 0.5N solution

In this study, the effect of the 0.5N NaOH on the alkali-silica reactivity of the trial aggregates was evaluated, and the results were compared to those found for the companion mortar bars immersed in the 1N NaOH solution. Table 3.4 documents the classifications of the trial aggregates (innocuous or reactive) based on the four suggested failure limits of ASTM C 1260 for the 0.5N and 1N solutions at ages of 14, 28, 56 and 98 days.

Of the fourteen selected aggregates, Table 3.4 demonstrated that the ASR classifications of the twelve aggregates showed identical results based on the 14-day failure limits of ASTM C 1260 for both 1 and 0.5N NaOH soak solutions. Those of the remaining two aggregate groups (SN-B and NN-A) produced conflicting results; they were shown as reactive for the standard test solution, and innocuous for the 0.5N solution, respectively. The reason could be that the expansion of some reactive aggregates for the 0.5N solution was very small at 14 days, and that might have not produced sufficient ASR-related expansion.

Once the test duration of ASTM C 1260 was extended to 28 days, the twelve of the fourteen aggregates resided in the same level of ASR for both the 0.5 and 1N NaOH solutions. The remaining two aggregate groups (SN-F and SN-I) showed different results: the SN-F aggregate was classified reactive for the 1N solution, and innocuous for the 0.5N NaOH, respectively; whereas the SN-I aggregate was innocuous for the 1N solution and became reactive for the 0.5N solution, respectively. The reason for discrepancy may be due to the increase in expansion for some aggregates for the 0.5N solution was slow between the immersion ages of 14 and 28 days.

As soon as the test duration of ASTM C 1260 for the 1 and 0.5N NaOH was extended from 28 to 56 days, an abrupt increase in ASR-induced expansion was observed. The two aggregate groups (SN-C and SN-F) that shown innocuous for the 0.5N solution at 28 days became reactive at the immersion age of 56 days, displaying an identical reactivity based on the 56-day expansion limits of the mortar bars for the 1N NaOH solution. Hence, the aggregate classifications of the fourteen trial sources showed a perfect agreement based on the suggested failure criteria of ASTM C 1260 for both soak solution

concentrations at the immersion age of 56 days. Further prolonging the test duration to 98 days, the ASR classifications of the investigated aggregates replicated the outcome demonstrated at 56 days.

Table 3.4: Comparison of aggregate classifications based on the failure criteria of ASTM C 1260 for the 1 and 0.5N soak solutions at various immersion ages

Agg. ID	14-day		28-day		56-day		98-day	
	1N (0.10%)	0.5N (0.03%)	1N (0.33%)	0.5N (0.105%)	1N (0.48%)	0.5N (0.22%)	1N (0.57%)	0.5N (0.325%)
SN-A	I	I	I	I	I	I	I	I
SN-B	R	I	I	I	I	I	I	I
SN-C	R	R	R	R	R	R	R	R
SN-D	I	I	I	I	I	I	I	I
SN-E	I	I	I	I	I	I	I	I
SN-F	R	R	R	I	R	R	R	R
SN-G	R	R	R	R	R	R	R	R
SN-H	I	I	I	I	I	I	I	I
SN-I	R	R	I	R	I	I	I	I
SN-J	R	R	R	R	R	R	R	R
NN-A	R	I	I	I	I	I	I	I
NN-B	R	R	R	R	R	R	R	R
NN-C	R	R	R	R	R	R	R	R
NN-D	R	R	R	R	R	R	R	R

As can be seen, the alkali-silica reactivity of the trial aggregates for the 0.5N soak solution at 14 days did show a good correlation with that obtained for the 1N soak solution, particularly at the later stage of immersion a perfect match between the results of the two NaOH solutions was found. The levels of ASR of the selected aggregates, based on ASTM C 1260 for the 0.5N soak solution, showed a perfect match with those of the standard test solution at the immersion ages of 56 days, and nearly identical results at the immersion age of 98 days. Therefore, the reliability and compatibility of aggregate

reactivity between the two solution concentrations increased with an increase in the testing duration.

In summary, the failure limits of ASTM C 1260 for both 0.5N and 1N solutions at the immersion ages of 14, 28, 56 and 98 days resulted in four aggregate groups (SN-A, SN-D, SN-E and SN-H) innocuous and six aggregate groups (SN-C, SN-G, SN-J, NN-B, NN-C and NN-D) reactive. However, the alkali-silica reactivity of the remaining four aggregate groups (SN-B, SN-F, SN-I and NN-A) generated contradictory results. By extending the test duration of ASTM C 1260 from 14 to at least 56 days, a good correlation was observed on the ASR of the trial aggregates based on the expansion limits of the mortar bars for 1N and 0.5N solutions.

3.1.6 Aggregate classifications based on the failure criteria of ASTM C 1260 in 0.25N Solution

The impact of the 0.25N storage solution of ASTM C 1260 on the ASR expansion was also evaluated to justify whether the utilization of the 0.25N NaOH could be reliably correlated with the levels of alkali-silica reactivity of the mortar bars experienced for the 1N NaOH soak solution. The observations were accomplished based on the expansion limits of ASTM C 1260 for the 1 and 0.25N soak solutions at the immersion ages of 14, 28, 56 and 98 days. The results are documented in Table 3.5.

At the immersion age of 14 days, Table 3.5 illustrates that the nine of the fourteen aggregates exhibited similar alkali-silica reactivity classifications for the 1 and 0.25N NaOH solutions. Of the remaining five aggregates that generated conflicting results for the 1 and 0.25N solutions, the three aggregate groups (SN-B, SN-C and NN-A) displayed reactive for the 1N, whereas they executed innocuous behavior for the 0.25N solution,

and the remaining two aggregates (SN-A and SN-E) displayed innocuous behavior for the 1N solution, whereas they were shown reactive for the 0.25N soak solution.

Table 3.5: Comparison of aggregate classifications based on the failure criteria of ASTM C 1260 for the 1 and 0.25N soak solutions at various immersion ages

Agg. ID	14-Day		28-Day		56-Day		98-Day	
	1N (0.10%)	0.25N (0.013%)	1N (0.33%)	0.25N (0.026%)	1N (0.48%)	0.25N (0.042)	1N (0.57%)	0.25N (0.068)
SN-A	I	R	I	I	I	I	I	I
SN-B	R	I	I	I	I	I	I	I
SN-C	R	I	R	I	R	I	R	I
SN-D	I	I	I	I	I	I	I	I
SN-E	I	R	I	R	I	R	I	R
SN-F	R	R	R	I	R	I	R	I
SN-G	R	R	R	R	R	R	R	R
SN-H	I	I	I	I	I	I	I	I
SN-I	R	R	I	R	I	I	I	I
SN-J	R	R	R	R	R	R	R	R
NN-A	R	I	I	R	I	R	I	R
NN-B	R	R	R	R	R	R	R	R
NN-C	R	R	R	R	R	R	R	R
NN-D	R	R	R	R	R	R	R	R

Once the test duration was extended to 28 days, the alkali-silica reactivity of the nine aggregate groups for the 0.25N soak solution corresponded well with that obtained for the standard test solution of 1N NaOH. The remaining four aggregates (SN-C, SN-F, SN-J and NN-A) had incompatible outcomes; two aggregates (SN-C and SN-F) were prone to be reactive, and the remaining two (SN-J and NN-A) aggregates were classified innocuous for the 1N soak solution. The results indicated that mortar bars prepared with the SN-J and NN-A aggregates were incapable of producing any considerable expansion for the 0.25N NaOH even at 28 days. At the extended test periods of 56 and 98 days, the level of ASR of the ten aggregate groups immersed in the 0.25N NaOH showed identical

results when immersed in the 1N NaOH solution. The levels of ASR of the trial aggregates for the 0.25 and 1N soak solutions at the immersion age of 98 days replicated the results obtained at the immersion age of 56 days.

The classifications of the trial aggregates for the 0.25N soak solution was not fully consistent as compared to those obtained for the 1N NaOH. Of the fourteen trial aggregates, the five aggregate groups (SN-G, SN-J, NN-B, NN-C and NN-D) were reactive, and the remaining nine aggregate groups showed innocuous behavior for the reduced soak solution concentration at the immersion ages of 28, 56 and 98 days. Extending the testing period of ASTM C 1260 to 6 months or longer for the 0.25N solution may offer a better correlation amongst the two concentrations of NaOH solutions. On the other hand, the extension of the test duration may defeat the purpose of the accelerated mortar bar test.

3.1.7 Role of soak solution concentrations on the expansion of ASTM C 1260

The effect of three soak solution (NaOH) concentrations of ASTM C 1260; namely, 1N (standard), 0.5N and 0.25N; on the expansion of the mortar bars prepared with the three dosages of cement alkalis of 0.42, 0.84 and 1.26% $\text{Na}_2\text{O}_{\text{eq}}$ was evaluated at various immersion ages. For the test duration of 14 days, the expansion of the mortar bars containing the selected aggregate groups as related to the trial soak solution concentrations of ASTM C 1260 is shown in Figure 3.11. As can be seen, the expansion under the three concentrations of NaOH solution varied extensively among the investigated aggregates. The 14-day expansion of the mortar bars made with 0.42% cement alkali varied from 0.030 (SN-A) to 1.023% (NN-B) for the 1N, 0.022 (SN-A) to 0.725% (NN-B) for the 0.5N, and 0.009 (NN-A) to 0.080% (NN-B) for the 0.25N soak

solutions, respectively. For some aggregate groups, the ASR reactivity remained low under the three selected NaOH solutions. For example, the 14-day expansion of the four aggregate groups (SN-A, SN-D, SN-E, and SN-H) for the 1, 0.5 and 0.25N solutions was very small as compared to that of the remaining ten aggregate groups under their respective solutions.

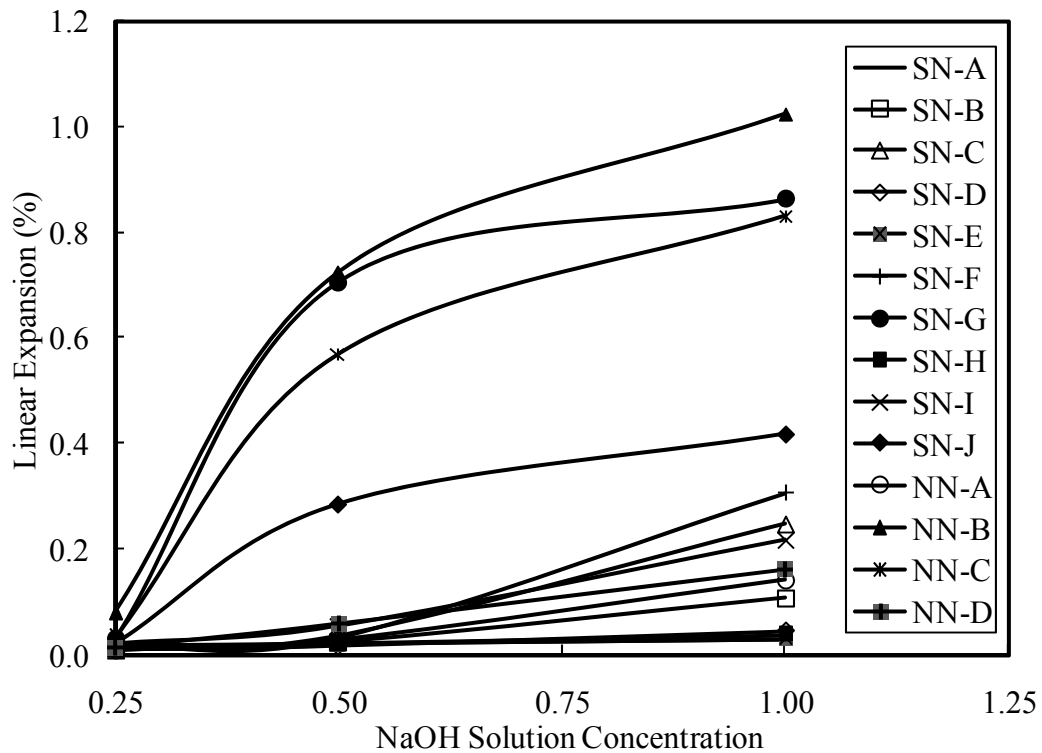


Figure 3.11: Effect of soak solution strength on ASR expansion at 14 days

The overall observation is that the expansion of the trial aggregates increased with an increase in the soak solution strength. Clearly, for the soak solution with high OH⁻ concentration, the initial reaction induces the formation of higher amount of ASR gel, which leads to a larger overall expansion, thus suggesting that the increase in solution concentration not only accelerates expansion, but also increases the ASR gel formation.

3.1.7.1 Expansion ratio as related to solution strength and immersion age

The expansion of the mortar bar containing each trial aggregate for the 0.5 and 0.25N NaOH was expressed in terms of expansion ratio of the mortar bars prepared with the companion aggregate sources for the 1N solution at various immersion ages. The expansion ratio of the test mortar bars for the 0.5 and 1N solutions ($ER_{0.5N/1N}$) over the immersion age is illustrated in Figure 3.12. The data shows that the $ER_{0.5N/1N}$ for the trial aggregates varied extensively at 14 days, and the variation in the $ER_{0.5N/1N}$ decreased with an increase in the test duration. However, the ratio for each investigated aggregate became steady at the immersion age of 56 days except for the SN-B and SN-F aggregate groups, for which the ratio increased gradually and never leveled off at the extended ages. This generated an idea in extending the test duration of ASTM C 1260 for 0.5N solution to at least 56 days. In the case of the three aggregate groups (SN-A, SN-E, and SN-H), the ratio was the highest at the early age of immersion (14 days), and increased gradually with an increase in the test duration. The trend of the $ER_{0.5N/1N}$ over the test duration for Group-A aggregates was quite opposite of the Group-B aggregates; the $ER_{0.5N/1N}$ decreased slowly with an increase in the test duration. On the whole, the maximum increase in the $ER_{0.5N/1N}$ was recorded between the immersion ages of 14 and 28 days. At the immersion age of 56 days or more, the $ER_{0.5N/1N}$ for the most of the aggregate sources became fairly leveled off, indicating the expansion ratio of the mortar bars for the 0.5N solution as compared to that for the 1N solution was the same.

Figure 3.13 presents the expansion ratio of the mortar bars for the 0.25 and 1N soak solutions ($ER_{0.25/1N}$) over the immersion age. As can be seen, the $ER_{0.25/1N}$ for the trial aggregates varied widely throughout the test duration. The behavior of the expansion

ratio at different immersion ages depended upon the value of 14-day expansion of each aggregate group obtained for the 1N solution. For the innocuous aggregates, the ratio was highest at 14 days, and it decreased with an increase in test duration. For the aggregates having the 14-day expansion for the 1N solution of more than 0.4%, the $ER_{0.25/1N}$ was very small at 14 days, and increased rapidly with an increase in test duration. Conversely, the $ER_{0.25/1N}$ was very small throughout the span of the test duration for the aggregates having the 14-day expansions in between 0.1 and 0.4%. At the immersion age of 98 days, the $E_{0.25/1N}$ for the fourteen selected aggregates became stable except for the NN-C and NN-B aggregates.

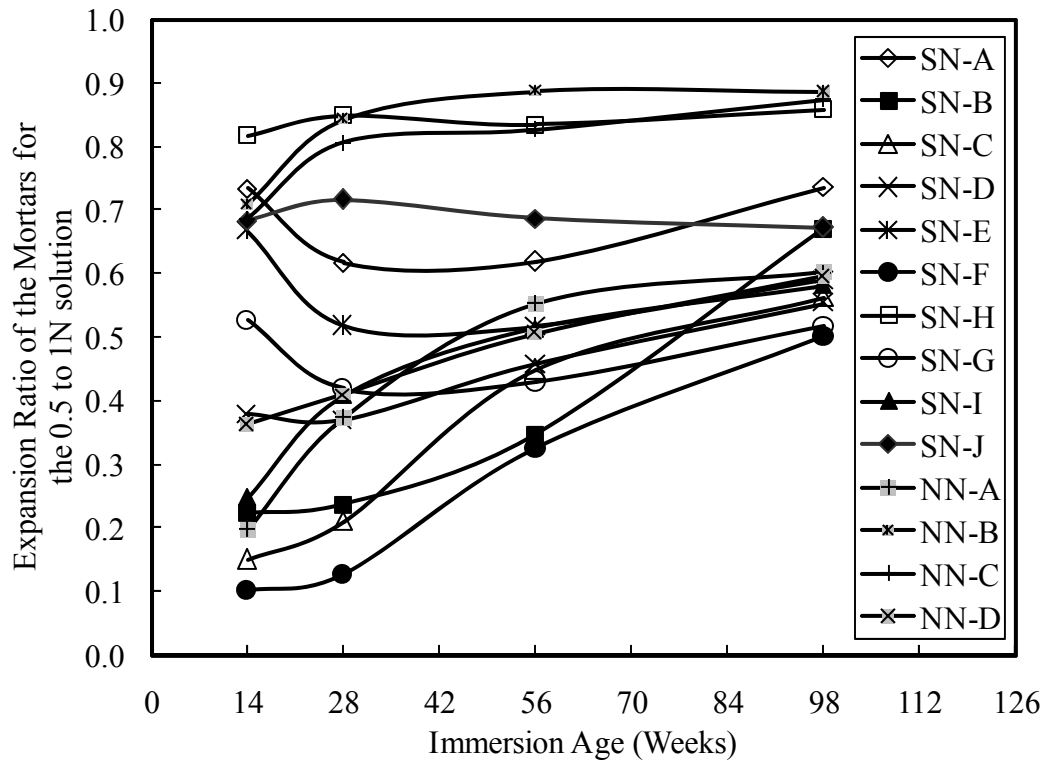


Figure 3.12: Expansion ratio of the mortar bars for the 0.5 and 1N NaOH soak solutions

Overall, the expansion ratio of the mortar bars for the 0.25 to 1N soak solutions over the immersion age increased for the aggregates having the 14-day expansions of more than 0.40%. The ratio decreased for the aggregates producing the 14-day expansions of less than 0.10%, and remained constant for the aggregates generating the 14-day expansions in between 0.10 and 0.40%. At the immersion age of 98 days, the ratio was uniform for all aggregates except for the aggregates showing the expansions under 1N NaOH of more than 1.0%.

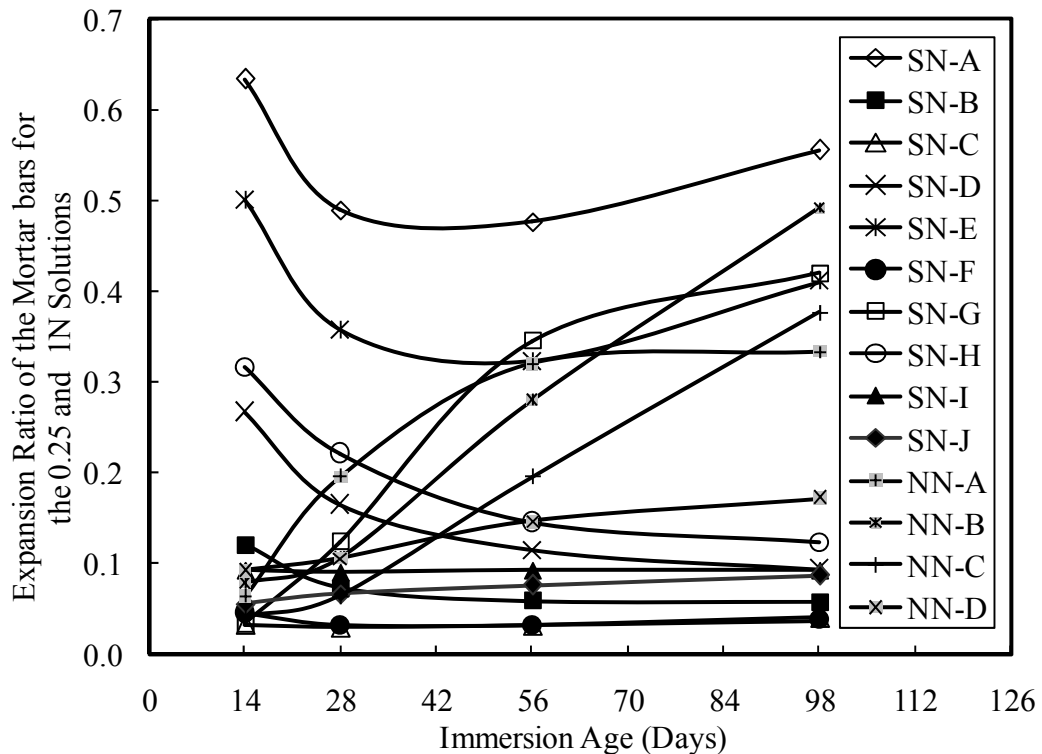


Figure 3.13: Expansion ratio of the mortars for the 0.25 and 1N NaOH

Compared to the expansion for the 1N solution, the expansion development for the 0.5 and 0.25N solutions fluctuated more with the levels of alkali-silica reactivity of the trial aggregates. The ratio of the expansion for the 0.5 and 1N, and 0.25 and 1N varied

with the immersion ages, and it became stabilized at the immersion ages of 56 days or more. Therefore, evaluating the alkali-silica reactivity based the failure criteria of the mortar bars at the early immersion age may prove to be insufficient. It is recommended that the test duration of ASTM C 1260 be extended from 14 to at least 56 days in order to properly evaluate the alkali-silica reactivity of an aggregate.

3.1.7.2 Expansion of ASTM C 1260 for the three solution concentrations as presented in ternary diagram

The influence of three concentrations of alkali soak solution on the ASR expansions of mortar bars was also evaluated with the help of a ternary diagram, where (i) the summation of the expansions of the mortar bars prepared with each trial aggregate for the 1, 0.5 and 0.25N NaOH solutions, so-called Total Expansion (TE), was normalized to 1 (i.e. 100%), and (ii) the expansion of each trial aggregate for the individual solution to the total expansion of the mortar bars for the three soak solutions, termed as Fraction of Total Expansion (FTE), was expressed as a percentage. For instance, if the ASR expansions of the mortar bars containing SN-A aggregate for the 1, 0.5 and 0.25N solutions were 0.030, 0.034 and 0.042%, respectively, then, the total expansion (TE) became 0.07%, and the FTE for the 1, 0.5 and 0.25N solutions became 42.3, 31.1 and 26.8%, respectively.

The 14-day FTEs of each trial aggregate for the 1, 0.5 and 0.25N solutions were presented in a ternary diagram as seen in Figure 3.14. The data shows that the FTEs for the investigated aggregates varied from 42.3 (SN-A) to 87.2% (SN-F) for the 1N, 8.8 (SN-F) to 44.2% (SN-G) for the 0.5N, and finally, 1.8 (SN-G) to 26.8% (SN-A) for the 0.25N NaOH solution, respectively. The scattered data points in Figure 3.14 indicated that the variation in ASR expansion of the mortar bars for the three solutions lacked a

specific pattern, which supported the idea that the alkali-silica reaction of each aggregate acted differently for the different soak solution concentrations of ASTM C 1260. In Figure 3.14, a separation line could be drawn at the FTE value of 10% for the 0.25N solution to distinguish the classifications of the trial aggregates into innocuous and reactive. The aggregates having more than 10% FTE for the 0.25N solution were shown innocuous, and those producing less were prone to be reactive. Based on ideas, Group-A aggregates (SN-A, SN-B, SN-D and SN-H) were innocuous.

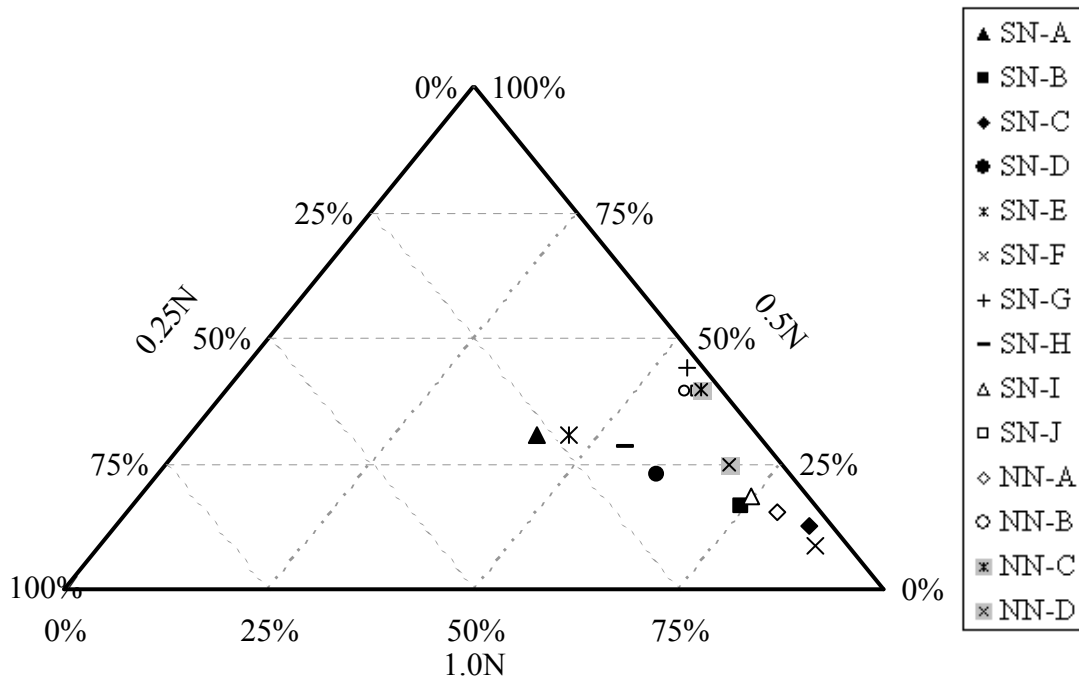


Figure 3.14: Influence of soak solution concentrations of ASTM C 1260 at 14 days

The FTEs of the SN-G, SN-J, NN-B and NN-C aggregate groups (designated by Group-1 aggregates) for the 0.25N soak solution were found 1.8, 3.2, 4.4 and 2.4%, respectively. The data points for these aggregate groups were concentrated in a small region by the 0.5N axis. It was noticed that the influence of Group-1 aggregates for the

0.25N soak solution had a little impact on the ASR-induced expansion as compared to that for the higher concentrations of alkali soak solution. Alternatively, the data point for the remaining ten aggregate groups, designated by Group-2 aggregates, stayed almost in a straight line, as shown in Figure 3.14. It was revealed that, for the Group-2 aggregates, the FTE of mortar bars under the 1N NaOH solution increased with an increase in that of 0.5N and 0.25N NaOH solutions.

At the extended immersion age of 98 days, the FTEs of the fourteen investigated aggregates for the three selected solutions showed are shown in the ternary diagram of Figure 3.15. As can be seen, the data points were diverged largely for the 1N and 0.25N soak solutions of ASTM C 1260, whereas they were compactly located for the 0.5N soak solution. As an example, the FTEs of the fourteen trial aggregates varied from 42.1 to 65% with an average of 54.8% for the 1N, 29.9 to 38.8% with an average of 34.8% for the 0.5N and 2.4 to 24.2% with an average of 10.4% for the 0.25N the soak solution, respectively. The variation in the FTEs for the 0.5N soak solution was very small, whereas that for the 1 and 0.25N soak solutions was very extensive. Therefore, the expansions of the mortar bars for the 0.5N soak solution showed more reliable results with respect to soak solution concentration and immersion age when compared to the results obtained by using 1N and 0.25N NaOH solutions. The finding confirmed that the earlier recommendations suggested by Sims (1992); the influence of the mortar bars for the 0.5N soak solution on the ASR expansion had more consistent results than those found using 0.25 and 1N soak solutions at the extended immersion ages.

The difference in expansion of the mortar bars for the 1 and 0.5N solutions decreased with an increase in the immersion age. At the immersion ages of 28, 56 and 98 days, the

expansion for the 0.5N soak solution was reduced by 68, 54 and 43% of the expansion for the 1N soak solution. However, the reduction in expansion of the mortar bars cured in the 0.25N soak solution as compared to that of for the 1N solution remained unchanged, approximately 90% at the immersion ages of 28, 56 and 98 days. The finding suggests that the trial mortar bars submerged in the 1N soak solution expands most during the early age of immersion, and the expansion rate decreases with an increase in the test duration. In the case of the 0.5N NaOH-cured mortar bars, the expansion caused by ASR is gradual over the immersion age. The ASR-induced expansion for the 0.25N solution is very small over the span of the testing, suggesting that the solution concentration provides an environment less conducive to alkali-silica reactivity.

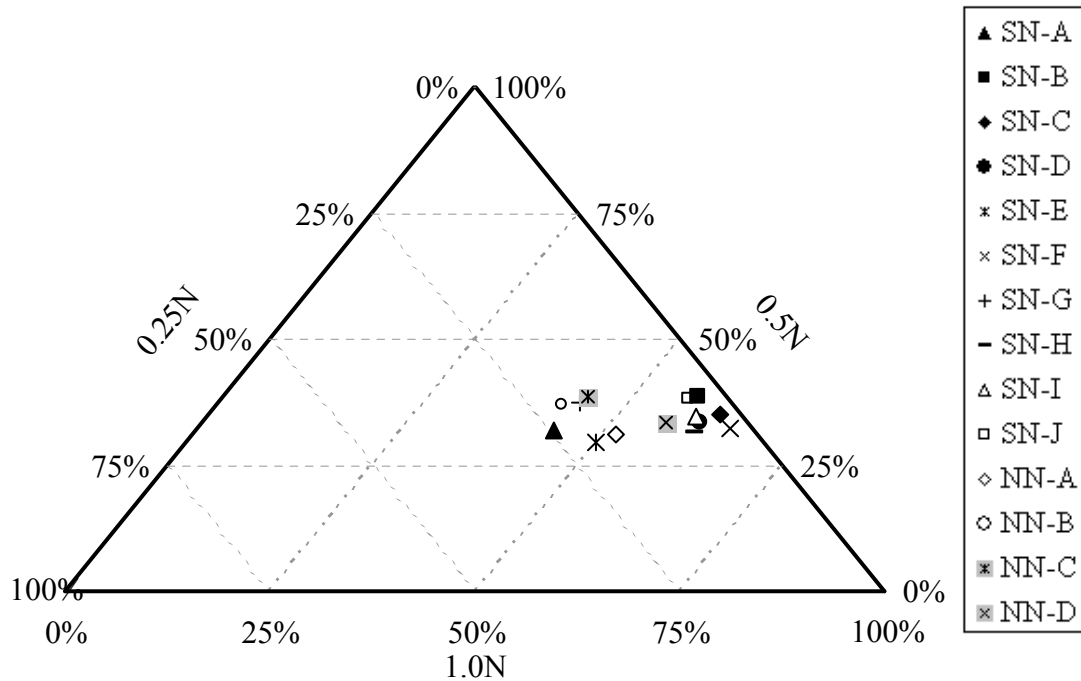


Figure 3.15: Influence of soak solution concentrations on 98-day ASR expansions of 0.42% cement alkali

3.1.7.3 ASR-induced cracks on the mortars as related to soak solution strength

The ASR-related cracks on the surface of the mortar bars submerged in the three soak solution concentrations of ASTM C 1260 were also examined. Figure 3.16 shows the mortar bars made with NN-C aggregate that were submerged in the 1, 0.5 and 0.25N solutions at 80°C for the test duration of 98 days. As can be seen, the specimen cured in the 1N solution was experienced with severe map cracking (Fig. 3.16a), and the frequency and extent of cracks decreased with a decrease in the concentration of alkali solution. Once the soak solution concentration was reduced to 0.5N, the number of cracks were reduced and became isolated, and the widths of ASR-induced cracks were condensed (Fig. 3.16b). The mortar bars submerged in the 0.25N solution were undergone with a limited number of tiny cracks (Fig. 3.16c). It can be stated that the severity of the ASR-induced cracks is also influenced by the concentrations of the NaOH solution.

3.1.8 Role of cement alkali on the expansion of mortar bars

In order to evaluate the impact of cement alkalis on expansion, the specimens made with each selected aggregate were tested for the sodium hydroxide solutions of varying concentrations, such as 1N (standard), 0.5N, and 0.25N, at the immersion ages of 14, 28, 56 and 98 days. A typical ASR-induced expansions of the mortar bars for the 1, 0.5 and 0.25N solutions as related to cement alkali and immersion age are illustrated in Figure 3.17. As can be seen, the 1N NaOH-cured mortar bars expanded slowly with an increase in cement alkalis. The difference in the alkali concentration of the 1N NaOH solution and the mortar bars made with 0.42% cement alkali was insignificant as compared to that of the identical solution and the specimens prepared with 0.84 and 1.26% cement alkalis.



(a) Mortar bar submerged in the 1N NaOH



(b) Mortar bar submerged in the 0.5N NaOH



(c) Mortar bar submerged in the 0.25N NaOH

Figure 3.16: Influence of soak solution concentrations of ASTM C 1260 on ASR-induced cracks for the NN-C aggregate group

The difference between the alkali concentrations of 0.5N NaOH soak solution and that of the test mortar was more noticeable. As such, a moderate increase in expansion was seen for the specimens cured in the 0.5N NaOH solution. In the case of the 0.25N solution, the difference in alkali concentration between the soak solution and test mortar bars was substantial, and the resulting ASR-induced expansion increased rapidly with an increase in cement alkalis.

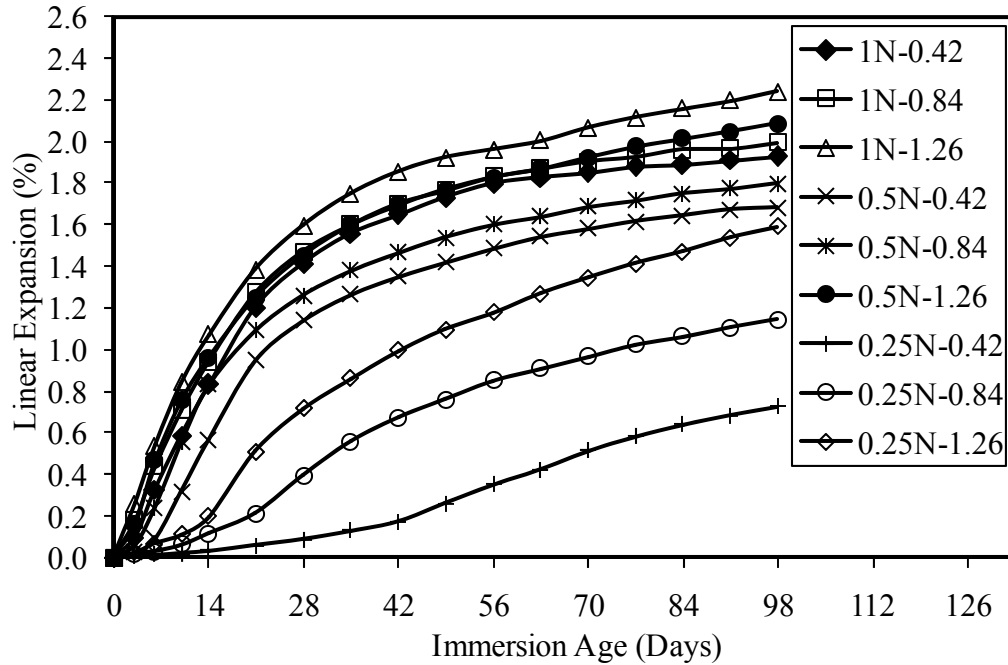


Figure 3.17: Expansion of mortar bars made with SN-G aggregate and three rates of cement alkalis for the 1N solution

The impact of cement alkalis on the ASR-induced expansion of the mortar bars is described in following two approaches:

3.1.8.1 ASR expansion as related to cement alkalis and immersion ages

This section discusses the role of cement alkalis on the expansion of mortar bars for the three soak solution concentrations at the test durations of 14, 28, 56 and 98 days. The 14-day expansion of the test mortar bars containing fourteen trial aggregates and three rates of cement alkalis for the 1N soak solution is plotted in Figure 3.18. As can be seen, a linear correlation, represented by Equation 3.5, existed between the expansions of the mortar bars containing 0.42 and 0.84% cement alkalis with a R^2 value of 0.9978, and those made with 0.42 and 1.26% cement alkalis with a R^2 value of 0.9937, respectively. However, the correlation between the dependent and independent variables was stronger at the extended immersion ages of 28, 56 and 98 days. Additionally, Equation 3.4 was

also most suitable for the dependent (expansion of the mortar bars containing 0.84 and 1.26% cement alkali) and independent parameters (expansion of the mortar bars made with 0.42% cement alkali) for the soak solutions of the 0.5 and 0.25N NaOH at the immersion ages of 14, 28, 56 and 98 days.

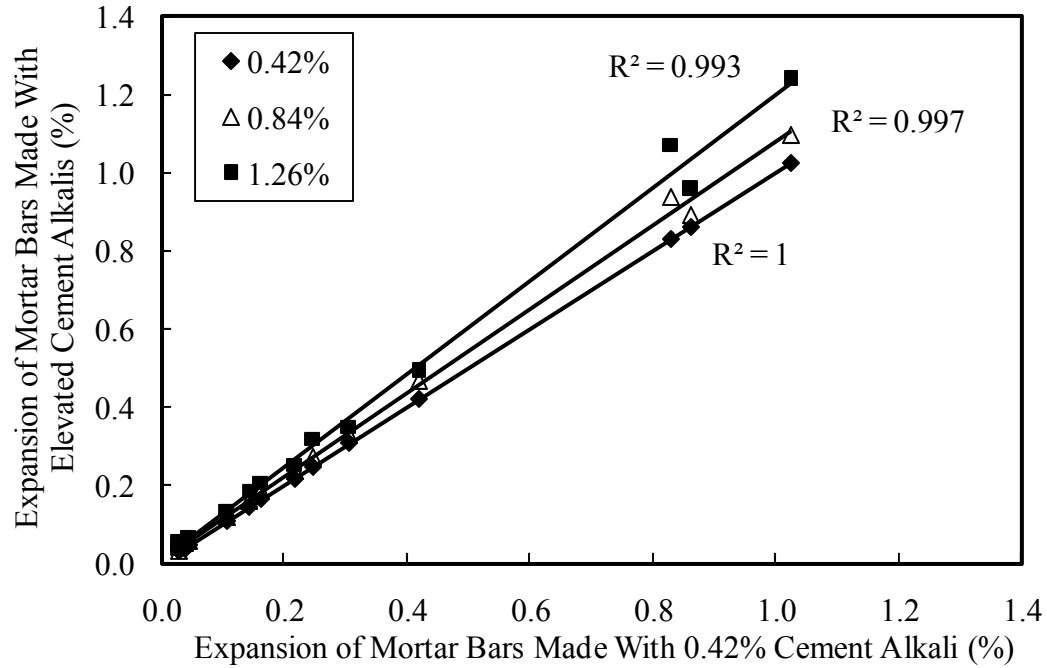


Figure 3.18: 14-day expansion of mortar bars for the 1N solution as related to cement alkalis

$$y = ax + b \quad \text{Eq. 3.4}$$

Where:

x is the expansion of the mortar bars made with 0.42% cement alkali

y is the expansion of the mortars made with elevated cement alkali

a and b are the regression variables, which represent the slope and intercept of the linear line

For the each soak solution concentration, the regression parameters a and b , Prob(t) of each parameter, and the coefficient of multiple determination (R^2) for the regression lines of the expansion of the mortars containing 0.42 vs. 0.84%, and 0.42 vs. 1.26%

cement alkalis are illustrated in Tables 3.7 and 3.8, respectively. The R^2 value of the regression line for each soak solution at four distinct immersion ages showed a good fit. Additionally, the Prob(F) of the regression equation of 0.0 signified a strong correlations between the dependent and independent variables.

As mentioned earlier, ASR-induced expansion varied extensively due to the aggregate mineralogy. To account for this variation, the expansion of the mortar bars containing 0.42% cement alkali for the three soak solution concentrations at which the aggregate shown to be reactive at the immersion ages of 14, 28, 56 and 98 days (i.e. the failure criteria at different immersion ages) was used for the investigation. Using Equation 3.4 and the expansion limits of the mortar bars containing 0.42% cement alkalis for the 1, 0.5 and 0.25N solutions at the four distinct immersion ages, the failure criteria of the mortar bars containing 0.84 and 1.26% cement alkalis for the respective soak solutions at the corresponding immersion ages were evaluated, and the results are presented in Tables 3.6 and 3.7, respectively.

Tables 3.6 and 3.7 documented the percent increase in expansion of the mortar bars (PIIE) made with 0.84 and 1.26% $\text{Na}_2\text{O}_{\text{eq}}$ cement alkalis for the 1, 0.5 and 0.25N solutions as compared to the expansion of the mortar bars containing 0.42% cement alkali for the corresponding soak solutions at the immersion ages of 14, 28, 56 and 98 days. The results are illustrated in Figure 3.19. As can be seen, the percent increase in expansion of the test mortar bars for each soak solution was highest at 14 days, and decreased with an increase in the immersion age. In general, the reduction rate in the PIIE due to the elevated cement alkalis of 0.84 and 1.26% $\text{Na}_2\text{O}_{\text{eq}}$ was insignificant for the higher concentration of soak solution than that of for the lower alkali concentrations.

Table 3.6: Statistical data for Equation 3.4 and the failure criteria of the mortar bars prepared with 0.84% cement alkali

Solution NaOH	Immersion Age (Days)	Regression Variables		Prob(t) of Regression Variables		R ²	Expansion of the mortars for cement alkali		PIIE
		a	b	a	b		0.42% ^a	0.84% ^b	
1N	14	1.0699	0.0076	0	0.2773	0.998	0.100	0.115	15.00
	28	1.0304	0.0126	0	0.0072	0.999	0.330	0.353	6.970
	56	1.0175	0.0198	0	0.0241	0.999	0.480	0.508	5.83
	98	1.0218	0.0240	0	0.0646	0.999	0.570	0.606	6.32
0.5N	14	1.2261	0.0083	0	0.6539	0.976	0.030	0.045	50.00
	28	1.1069	0.0100	0	0.3268	0.997	0.105	0.126	20.00
	56	1.0838	0.0180	0	0.0942	0.998	0.220	0.256	16.36
	98	1.0796	0.0242	0	0.1001	0.997	0.325	0.375	15.38
0.25N	14	1.4679	-0.0008	0	0.7015	0.977	0.013	0.018	38.46
	28	1.9237	-0.0156	0	0.1186	0.944	0.026	0.035	34.62
	56	1.3468	-0.0034	0	0.7737	0.980	0.042	0.054	28.57
	98	1.6000	-0.0192	0	0.0014	0.999	0.068	0.088	29.41

^aFrom Tables 3.2 and 3.3

^bUsing $\text{Exp}_{(0.84\%)} = \text{Exp}_{(0.42\%)} a + b$

Table 3.7: Statistical data for Equation 3.4 and the failure criteria of the mortar bars prepared with 1.26% cement alkali

Normality of NaOH	Immersion Age (Days)	Regression Variables		Prob(t) of Regression Variables		R ²	Expansion of the mortars for cement alkali		PIIE
		a	b	a	b		0.42% ^a	1.26% ^b	
1N	14	1.1906	0.0083	0	0.5176	0.994	0.100	0.127	27.00
	28	1.1195	0.0111	0	0.4441	0.996	0.330	0.381	15.45
	56	1.1023	0.0135	0	0.4399	0.997	0.480	0.543	13.13
	98	1.1207	0.0117	0	0.5246	0.997	0.570	0.651	14.21
0.5N	14	1.4415	0.0117	0	0.6460	0.967	0.030	0.055	83.33
	28	1.2284	0.0204	0	0.3079	0.990	0.105	0.150	42.86
	56	1.1971	0.0282	0	0.0667	0.997	0.220	0.292	32.73
	98	1.2011	0.0424	0	0.0807	0.994	0.325	0.432	32.92
0.25N	14	5.6256	-0.0469	0	0.0054	0.901	0.013	0.026	100.00
	28	3.7714	-0.0514	0	0.0010	0.964	0.026	0.047	80.77
	56	2.1110	-0.0260	0	0.1919	0.980	0.042	0.064	52.38
	98	2.0340	-0.0330	0	0.2027	0.980	0.068	0.104	52.94

^aFrom Tables 3.2 and 3.3

^bUsing $\text{Exp}_{(1.26\%)} = \text{Exp}_{(0.42\%)} a + b$

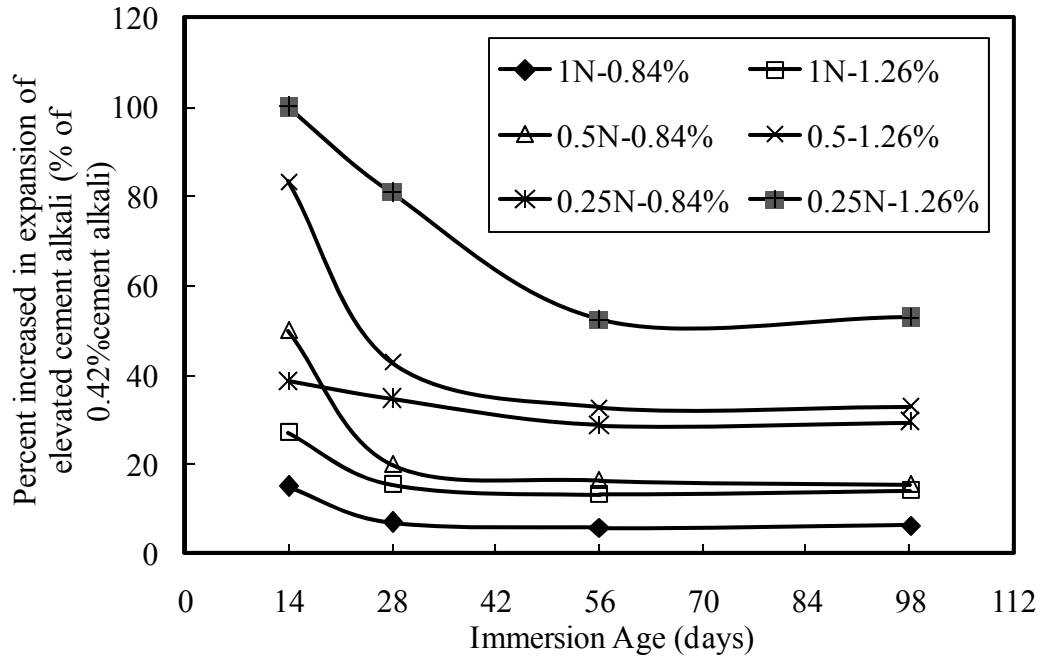


Figure 3.19: Influence of cement alkalis for the three soak solution concentrations

At the immersion age of 14 days, the percent increase in expansion of the mortar bars prepared with 0.84 and 1.26% cement alkalis as compared to the expansion of the mortars having 0.42% cement alkali was increased by 15 and 27% for the 1N, 50 and 83.3% for the 0.5N, and 46.2 and 101.5% for the 0.25N solutions, respectively. The PIIE for the 1 and 0.5N NaOH decreased rapidly between the immersion ages of 14 and 28 days, and the rate was nearly constant thereafter. In the case of the 0.25N solution, the PIIE of the mortar bars containing 0.84% cement alkali as compared to the expansion of the mortar bars made with 0.42% cement alkali decreased slowly, whereas that of the 1.26% cement alkali decreased rapidly up to the immersion age of 56 days. Extending the test duration to 98 days, the expansion of the mortar bars prepared with 0.84 and 1.26% cement alkalis as compared to the expansion of the mortar bars containing 0.42% cement alkali was increased by 6.3 and 14.2% for the 1N solution, 15.4 and 32.9% for the 0.5N solution,

and 26.2 and 54% for the 0.25N solution, respectively. The results confirmed the outcome of the study conducted by Hooton and Rogers (1993) who demonstrated that an increase in cement alkali content from 0.40 to 0.92% only resulted in an average 8.2% increase in expansion under 1N solution. This study confirms that the cement alkali has little to no influence on ASR-induced expansion at the extended immersion ages.

The following concluding remarks can be drawn from this section:

- a. The influence of cement alkalis on the expansion of ASTM C 1260 primarily depended on soak solution concentrations and test duration.
- b. The percent increase in expansion of the mortar bars made with 0.84 and 1.26% cement alkalis as compared to the expansion of the mortar bars containing 0.42% cement alkalis was significant for the reduced soak solution concentration and the severity decreased with an increase in soak solution concentration.
- c. Overall, the influence of cement alkalis on ASR-induced expansion is relatively small and gradual with an increase in cement alkalis for the 1N NaOH soak solution. In the 0.5N NaOH soak solution, the effect is moderate and gradual. In the case of the 0.25N NaOH soak solution, the increase in cement alkalis produces rapid and large increase in the ASR-induced expansions of mortar bars.

3.1.8.2 Expansion of ASTM C 1260 as related to cement alkalis as presented in ternary diagram

The expansion of the mortar bars prepared with the fourteen trial aggregates and three rates of cement alkalis was evaluated for the 1, 0.5 and 0.25N solutions at various immersion ages with the help of a ternary diagram, where (a) the summation of the expansions of the mortar bars containing three rates of cement alkalis for each soak

solution concentration was normalized to 1 (100%) and (b) for each soak solution concentration, the expansion of the mortar bars containing each cement alkali to the total expansion of the mortar bars containing three rates of cement alkalis, expressed as percentage, was termed as Fraction of Total Expansion (FTE). With the help of the FTE, the impact of cement alkalis on ASR expansion was evaluated for the three soak solutions at various immersion ages.

3.1.9.2.1 1N NaOH soak solution

The 14-day FTEs of the mortar bars containing three dosages of cement alkalis for the 1N soak solution are presented in the ternary diagram of Figure 3.20. As can be seen, the variation in the 14-day FTEs of the test mortar bars containing three dosages of cement alkalis was insignificant among the trial aggregates. For instance, the FTEs of the mortar bars varied from 29.5 to 32.7% for the 0.42% cement alkali, 32.1 to 34.3% for the 0.84% cement alkali, and 34 to 37.2% for the 1.26% cement alkali, respectively. Owing to that viewpoint, all data were concentrated in a small region in the ternary diagram (Figure 3.20), suggesting that the ASR expansion of the mortar bars for the 1N soak solution increased quite linearly with an increase in cement alkalis at the early age of 14 days. Since the test mortar bars expanded with an increase in the immersion age, a change in the magnitude of FTEs for the companion mortar bars took place. At the ultimate test duration of 98 days, the FTEs of the mortar bars for the 1N soak solution varied from 26.0 to 31.8% for the 0.42 % cement alkali, 32.1 to 35.5% for the 0.84% cement alkali, and 35.3 to 40.3% for the 1.26% cement alkali, respectively, indicating that the ASR expansion was more linear with an increase in cement alkali at the later immersion age.

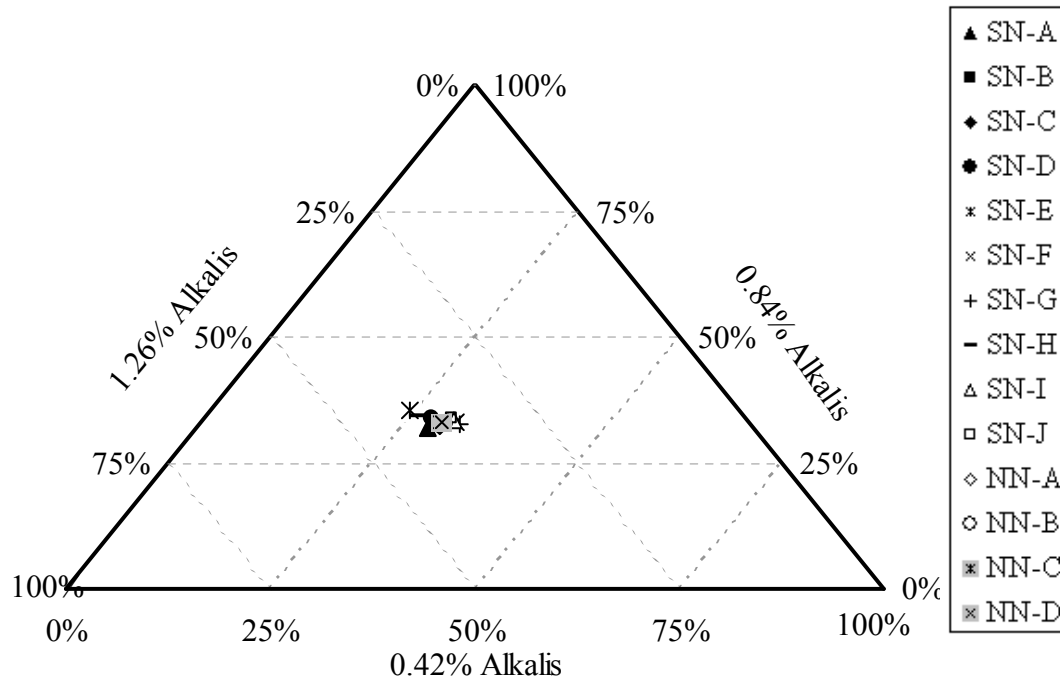


Figure 3.20: Influence of cement alkalis on the expansion of ASTM C 1260 for the 1N solution at the immersion age of 14 days

3.1.8.2.2 0.5N NaOH soak solution

Altering soak solution concentration from 1 to 0.5N NaOH, the 14-day FTEs of the test mortar bars prepared with three rates of cement alkalis are illustrated in Figure 3.21. As can be seen, the data points (markers) were more dispersed than those for the standard test solution (Fig. 3.21). Of the fourteen investigated aggregates, the data points of the three aggregates were away from the others, whereas those of the remaining eleven aggregates (Group-1 aggregates) were concentrated in a small region. Incrementing cement alkali from 0.42 to 1.26%, for the 0.5N solution, the ASR expansion of SN-G aggregate increased unexpectedly, while that of SN-J and NN-D aggregate occurred very slowly, and the Group-1 aggregates had a linear influence on the ASR expansion.

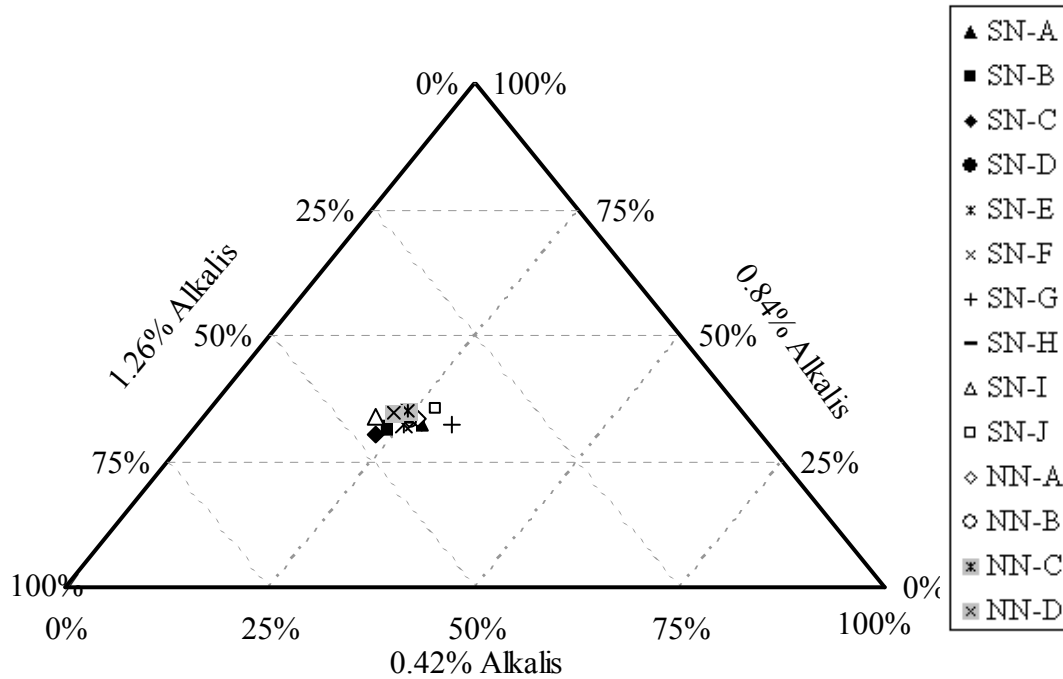


Figure 3.21: Influence of cement alkalis on the expansion of ASTM C 1260 for the 0.5N solution at the immersion age of 14 days

As the expansion of the mortar bars for the 0.5N soak solution increased with an increase in the cement alkali and the immersion age, the FTE of the fourteen aggregates containing three rates of cement alkali also varied. The FTE values became stabilized with an increase in immersion age. The 98-day FTEs of the trial aggregates containing three rates of cement alkali are depicted in Figure 3.22. It was shown that all trial aggregates including the SN-G, SN-J and NN-D aggregate groups were crowded in a small region, indicating that the 98-day expansions of the mortar bars made with 0.84 and 1.26% cement alkalis under the 0.5N soak solution were linearly correlated, and the results were more stable than that obtained for the early immersion of 14 days.

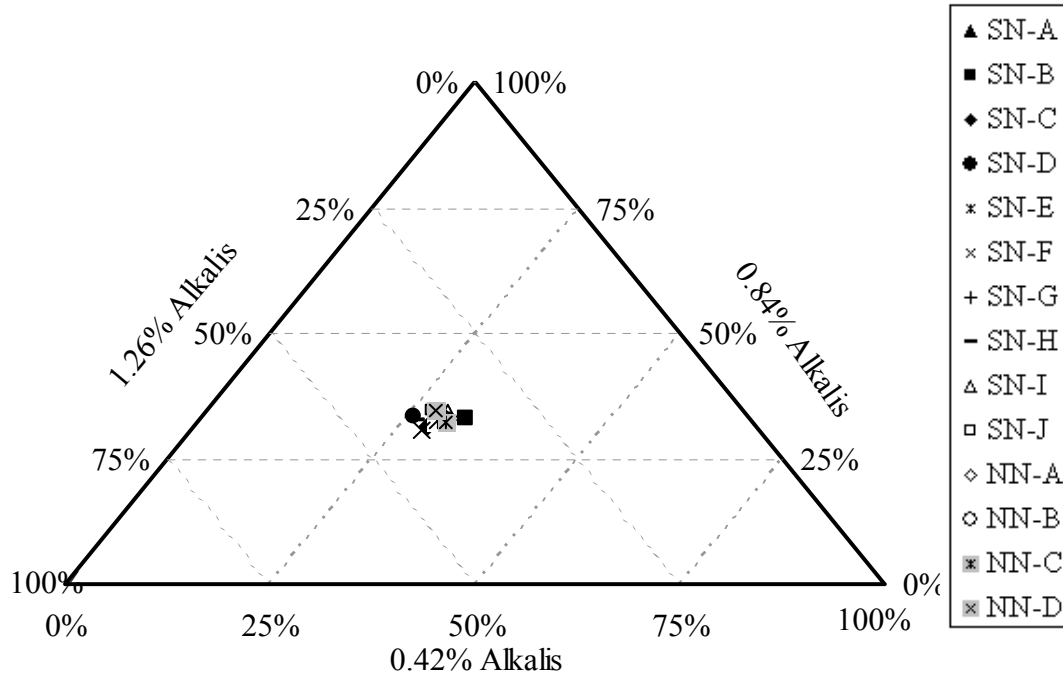


Figure 3.22: Influence of cement alkalis on the expansion of ASTM C 1260 for the 0.5N solution at the immersion age of 98 days

3.1.8.2.3 0.25N NaOH soak solution

Once the solution concentration was reduced to 0.25N, the 14-day FTEs of the test specimens containing three rates of cement alkalis varied in a wide range as shown in Figure 3.23. As can be depicted, the data points were more scattered than those of for the 1 and 0.5N soak solutions. Of the fourteen trial aggregates, the variation in the 14-day FTE was consistent for only the eight aggregates (including five innocuous aggregates) (Group-2 aggregates) due to the variations of cement alkalis. The data points of Group-2 aggregates were located in a compacted region in Figure 3.23. Raising cement alkali had a little effect on the expansion of those aggregates. Conversely, the expansions of the remaining six aggregates, SN-G, NN-B, NN-C, NN-D, SN-C and NN-A (Group-3 aggregates) for the 0.25N soak solution expanded rapidly, and their data points remained isolated away from the Group-2 aggregates. It was observed that the data points of

Group-3 aggregates having the FTE value of less than 25% for the 0.42% cement alkali and more than 45% for 1.26% cement alkali, exhibited an unexpected expansion when cement alkalis were elevated. That suggested that the ASR expansions of Group-3 aggregates were not consistent at the early stage of testing with increased cement alkalis.

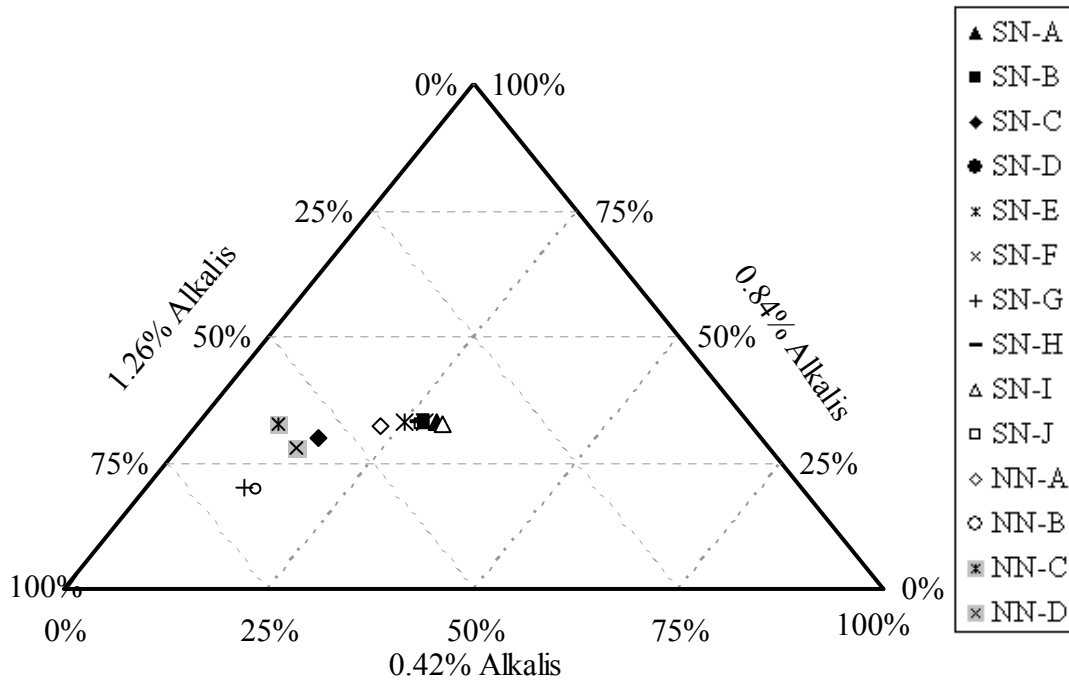


Figure 3.23: Influence of cement alkalis on the expansion of ASTM C 1260 for the 0.25N solution at the immersion age of 14 days

As the storage duration of the mortar bars prolonged, the expansion rate of Group-2 aggregates increased and that of Group-3 aggregates decreased with an increase in the cement alkali. The 98-day FTE of the fourteen aggregates containing three rates of cement alkali for the 0.25N solution is plotted in a ternary diagram of Figure 3.26. The data points in the figure were denser as compared to those at the early immersion age of 14 days (Fig. 3.23). Hence, the impact of cement alkalis on the 98-day expansions of the fourteen trial aggregates for the 0.25N soak solution was fairly uniform.

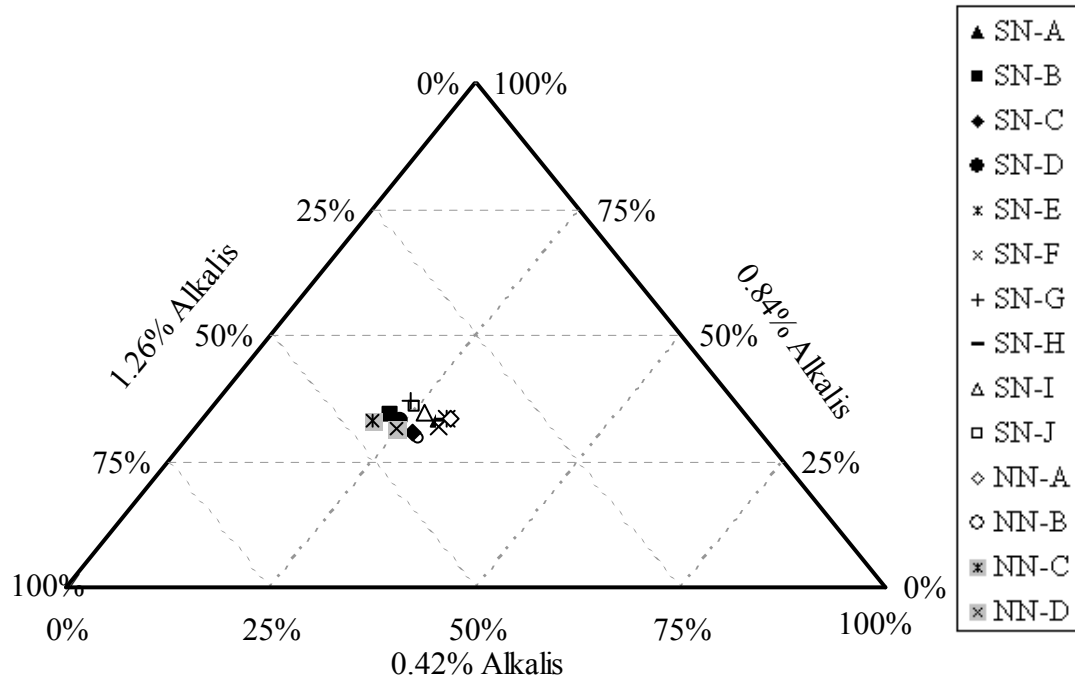


Figure 3.24: Influence of cement alkalis on the expansion of ASTM C 1260 for the 0.25N solution at the immersion age of 98 days

3.1.9 Summary alkali-silica reactivity of mortar bars made with three rates of cement alkali for the 1, 0.5 and 0.25N solutions

The levels of alkali-silica reactivity of the fourteen trial aggregates were evaluated based on the failure criteria of the mortar bars made with three levels of cement alkalis for the 1, 0.5 and 0.25N NaOH at the immersion ages of 14, 28, 56 and 98 days. The results are documented in Table 3.8. As can be seen, the five aggregate groups of SN-G, SN-J, NN-B, NN-C and NN-D were classified reactive, and the another five aggregate groups of SN-A, SN-B, SN-D, SN-E and SN-H were found to be innocuous as per the failure criteria of the mortar bars under the three trial solutions (1, 0.5 and 0.25N NaOH) at the immersion ages of 14, 28, 56 and 98 days. The remaining four aggregate groups (SN-C, SN-F, SN-I, NN-A and NN-D) generated contradictory results on the level of alkali-silica reactivity.

Table 3.8: Levels of alkali-silica reactivity of the selected aggregates

Agg. ID	Cem. Alk.	1N				0.5N				0.25N			
		14	28	56	98	14	28	56	98	14	28	56	98
SN-A	0.42	I	I	I	I	I	I	I	I	I	I	I	I
	0.84	I	I	I	I	I	I	I	I	R	I	I	I
	1.26	I	I	I	I	I	I	I	I	I	I	I	I
SN-B	0.42	R	I	I	I	I	I	I	R	I	I	I	I
	0.84	R	I	I	I	I	I	I	I	I	I	I	I
	1.26	R	I	I	I	I	I	I	I	I	I	I	I
SN-C	0.42	R	R	R	R	R	R	R	R	I	I	I	I
	0.84	R	R	R	R	R	R	R	R	I	I	I	I
	1.26	R	R	R	R	R	R	R	R	I	I	I	I
SN-D	0.42	I	I	I	I	I	I	I	I	I	I	I	I
	0.84	I	I	I	I	I	I	I	I	I	I	I	I
	1.26	I	I	I	I	I	I	I	I	I	I	I	I
SN-E	0.42	I	I	I	I	I	I	I	I	R	I	I	I
	0.84	I	I	I	I	I	I	I	I	I	I	I	I
	1.26	I	I	I	I	I	I	I	I	I	I	I	I
SN-F	0.42	R	R	R	R	R	R	R	R	I	I	I	I
	0.84	R	R	R	R	R	R	R	R	I	I	I	I
	1.26	R	R	R	R	R	R	R	R	I	I	I	I
SN-G	0.42	R	R	R	R	R	R	R	R	R	R	R	R
	0.84	R	R	R	R	R	R	R	R	R	R	R	R
	1.26	R	R	R	R	R	R	R	R	R	R	R	R
SN-H	0.42	I	I	I	I	I	I	I	I	I	I	I	I
	0.84	I	I	I	I	I	I	I	I	I	I	I	I
	1.26	I	I	I	I	I	I	I	I	I	I	I	I
SN-I	0.42	R	I	I	I	R	R	I	I	R	R	I	I
	0.84	R	I	I	I	R	R	I	I	R	I	I	I
	1.26	R	I	I	I	R	R	I	I	I	I	I	I
SN-J	0.42	R	R	R	R	R	R	R	R	R	R	R	R
	0.84	R	R	R	R	R	R	R	R	R	R	R	R
	1.26	R	R	R	R	R	R	R	R	R	R	R	R
NN-A	0.42	R	I	I	I	I	I	I	I	I	R	R	R
	0.84	R	I	I	I	I	I	I	I	I	R	R	R
	1.26	R	I	I	I	I	I	I	I	I	R	R	R
NN-B	0.42	R	R	R	R	R	R	R	R	R	R	R	R
	0.84	R	R	R	R	R	R	R	R	R	R	R	R
	1.26	R	R	R	R	R	R	R	R	R	R	R	R
NN-C	0.42	R	R	R	R	R	R	R	R	R	R	R	R
	0.84	R	R	R	R	R	R	R	R	R	R	R	R
	1.26	R	R	R	R	R	R	R	R	R	R	R	R
NN-D	0.42	R	R	R	R	R	R	R	R	R	R	R	R
	0.84	R	R	R	R	R	R	R	R	R	R	R	R
	1.26	R	R	R	R	R	R	R	R	R	R	R	R

I = Innocuous; R = Reactive

Of the above-mentioned four aggregates, the two aggregate groups (SN-C and SN-F) exhibited excess reactivity under the 1 and 0.5N solutions, whereas they showed innocuous behavior under the 0.25N solution at the four distinct immersion ages. The opposite phenomenon was observed for the NN-A aggregate group. The aggregate was found to be reactive under the 0.25N NaOH, whereas it was categorized as innocuous for both 1 and 0.5N soak solutions with some exceptions. The performance of the SN-I aggregate group under the three soak solutions at the four distinct immersion ages showed contradictory results. For instance, the SN-I aggregate produced excess reactivity at the early age of immersion (14 or 28 days), and it grew to be innocuous at the ages of 56 days or more. Thus, it can be concluded that different reactivities can be expected for the some aggregate groups when solution or test duration is altered.

The number of reactive aggregates (from the fourteen trial sources) identified by the proposed expansion limits of the mortar bars containing three dosages of cement alkalis under the 1, 0.5 and 0.25N NaOH solutions at the immersion ages of 14, 28, 56, and 98 days is shown in Table 3.9. As can be seen, the ten of the fourteen selected aggregates was identified as reactive based on the expansion limits of the mortar bars under the 1N solution at 14 days. For the same solution, the extended failure limits at 28, 56, and 98 days identified three aggregate groups (SN-B, SN-I and NN-A) as innocuous and seven aggregate groups as reactive. Reducing the soak solution concentration from 1 to 0.5N, the above-mentioned seven aggregate groups were susceptible to alkali-silica reactivity at the four distinct immersion ages with minor exceptions. However, the number of reactive aggregates reduced to six when the soak solution strength was reduced from 1 to 0.25N.

Overall, for the most part, raising cement alkalis from 0.42% to 0.84 and 1.26% in the mortar bars, the alkali-silica reactivity of the fourteen trial aggregates showed a perfect correlation for the 1, 0.5 and 0.25N solutions at 14, 28, 56 and 98 days. It is concluded that alkali-silica reactivity of an aggregate for the AMBT test (ASTM C 1260) can broadly be expressed as a function of aggregate mineralogy, soak solution concentration, cement alkalis, and the immersion age.

Table 3.9: Number of reactive aggregates (from the fourteen investigated aggregates) based on the suggested failure criteria

Solution Strength	Immersion Age (Days)	Cement Alkali ($\text{Na}_2\text{O}_{\text{eq}}$)		
		0.42%	0.84%	1.26%
1N	14	10 (<i>u, v, r, s, w</i>)	10 (<i>u, v, r, s, w</i>)	10 (<i>u, v, r, s, w</i>)
	28	7 (<i>u, v</i>)	7 (<i>u, v</i>)	7 (<i>u, v</i>)
	56	7 (<i>u, v</i>)	7 (<i>u, v</i>)	7 (<i>u, v</i>)
	98	7 (<i>u, v</i>)	7 (<i>u, v</i>)	7 (<i>u, v</i>)
0.5N	14	8 (<i>u, v, s</i>)	7 (<i>u, v</i>)	7 (<i>u, v</i>)
	28	7 (<i>u, v</i>)	7 (<i>u, v</i>)	7 (<i>u, v</i>)
	56	7 (<i>u, v</i>)	7 (<i>u, v</i>)	7 (<i>u, v</i>)
	98	8 (<i>u, v, r</i>)	7 (<i>u, v</i>)	7 (<i>u, v</i>)
0.25N	14	8 (<i>u, w, p, q</i>)	7 (<i>u, w, q</i>)	6 (<i>u, w</i>)
	28	7 (<i>u, w, s</i>)	6 (<i>u, w</i>)	6 (<i>u, w</i>)
	56	6 (<i>u, w</i>)	6 (<i>u, w</i>)	6 (<i>u, w</i>)
	98	6 (<i>u, w</i>)	6 (<i>u, w</i>)	6 (<i>u, w</i>)

p = SN-A; *q* = SN-E; *r* = SN-B; *s* = SN-I; *u* = SN-G, SN-J, NN-B, NN-C, NN-D;
v = SN-C, SN-F; *w* = NN-A

Based on Table 3.9, the following conclusions can be summarized:

- Under the alkali soak solution of 1N NaOH, the 14-day failure limit of ASTM C 1260 resulted in higher reactivity for some aggregates. The failure criteria of the mortar bars at the extended immersion ages of 28, 56 and 98 days provided more reliable reactivity as compared to that obtained at 14 days.

- b. For the 0.5N NaOH soak solution, the proposed expansion limits of ASTM C 1260 was capable of identifying the actual levels of ASR.
- c. In the case of the 0.25N solution, the trial aggregates showed underestimated reactivity of the selected aggregates. Aggregates showing reactive under the reduced soak solution concentration at the extended immersion ages were also considered as reactive under the 1 and 0.5N NaOH at any immersion age.
- d. In order to evaluate ASR of an aggregate based on the accelerated mortar bar test, it is highly recommended to utilize the failure limits of the mortar bars under the 1 or 0.5N NaOH. However, the study shows that the 0.5N NaOH soak solution generated more reliable results than those obtained under the 1N NaOH soak solution.

3.2 ASR using Modified ASTM C 1293

The ASTM C 1293 (prism) test is used to monitor the ASR-induced expansion of concrete prisms immersed in water at 38°C for one year. In the prism test, the aggregate showing one-year expansion of less than 0.040% is considered innocuous, more than 0.080% is highly reactive, and in between is declared slowly reactive.

In order to evaluate the ASR of an aggregate in a shorter period of time, the storage environments of ASTM C 1293 were modified to an elevated temperature of 80°C (176°F) and a relative humidity of 100%. Additionally, the prisms were immersed in two distinct soak solutions of 1N NaOH and distilled water. The expansion readings of the individual prism are presented in the Appendix A.

3.2.1 Prisms Submerged in the 1N NaOH at 80°C (ASTM C 1293M1)

Past investigations demonstrated that the expansions of alkali-cured prisms at 80°C (ASTM C 1293M1) depended on the alkali concentration of soak solution, immersion temperature, and test duration (Bérubé & Frenette, 1994; Touma et al., 2001; and Folliard et al., 2005). The ASR-related expansions of alkali-cured prisms made with the fourteen trial aggregates as related to immersion age are illustrated in Figure 3.25. As can be seen, the progression in expansion varied primarily depending on the aggregate mineralogy. For instance, the alkali-cured prisms made with the SN-A, SN-E and NN-A aggregate groups expanded very slowly, and those prepared with the SN-I and SN-H aggregate groups expanded slowly with an increase in immersion age. For the remaining nine aggregates, the ASR-induced expansion increased progressively with an increase in the immersion age. The study revealed that the high alkali solution (1N NaOH) elevated alkali content of the prisms, which ultimately resulted in high expansions for most aggregates during the 6-month testing period.

Figure 3.25 also demonstrates that the expansion deviation among the trial aggregates was low at early age, and became more diverged with the test duration. At the extended immersion age of 26 weeks, the variation in the ASR-induced expansions became substantial among the investigated aggregates.

Past investigations revealed that the prisms cured in the 1N solution at 80°C exceeding the 4-week expansions of 0.080% were considered highly reactive, less than 0.040% were regarded innocuous, and in between two expansion values were treated slowly reactive aggregates (Touma et al., 2001; and Folliard et al., 2005). The suggested 4-week expansion limit of 0.04% had been proved to be unreliable for assessing the

potential alkali-silica reactivity of some aggregates (Bérubé & Frenette, 1994; and Touma et al., 2001). As a result, in addition to the 4-week expansion limit of ASTM C 1293M1, the failure criteria at the extended immersion ages of 8, 13 and 26 weeks were proposed in order to evaluate the extent of alkali-silica reactivity of an aggregate.

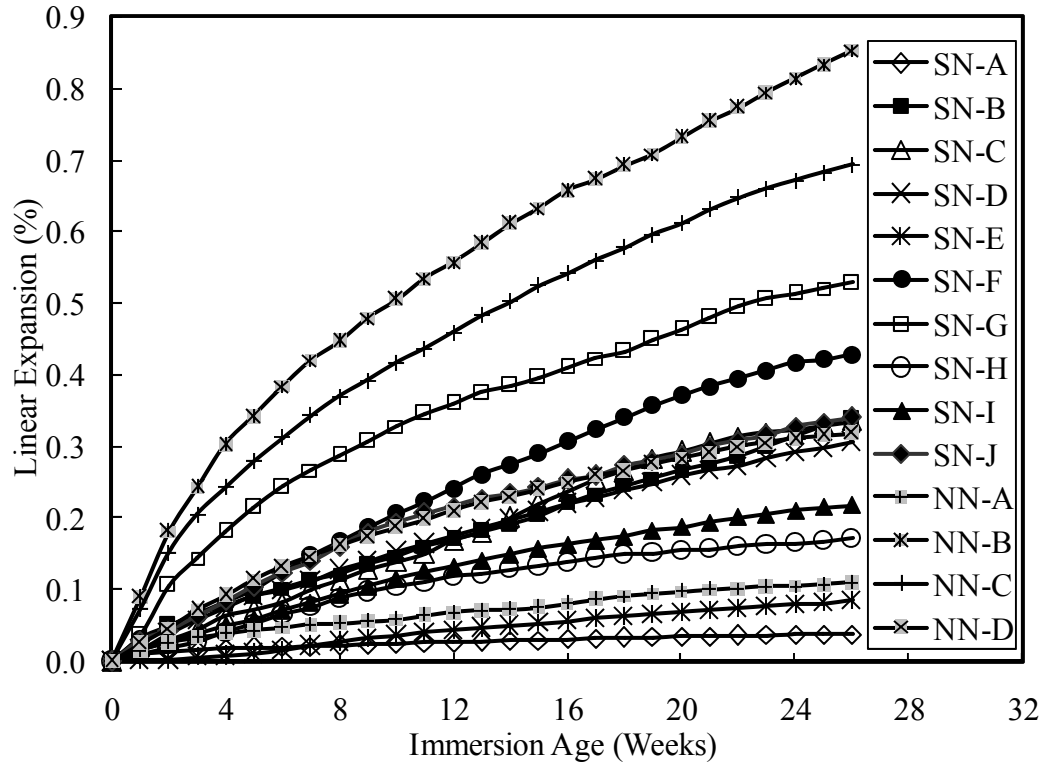


Figure 3.25: Expansion of alkali-cured prisms at 80°C (C 1293M1)

The expansion progression of the alkali-cured prisms at the test durations of 8, 13, and 26 weeks as related to the 4-week expansion of the companion aggregate sources is illustrated in Figure 3.26. As can be seen, a linear correlation existed between the expansions at 4 weeks and those at the immersion ages of 8, 13 and 26 weeks with R^2 values of 0.969, 0.924 and 0.832, respectively. Therefore, the linear correlation of ASR

expansion at early-age immersion (4-week) and later-age immersion found to be insignificant.

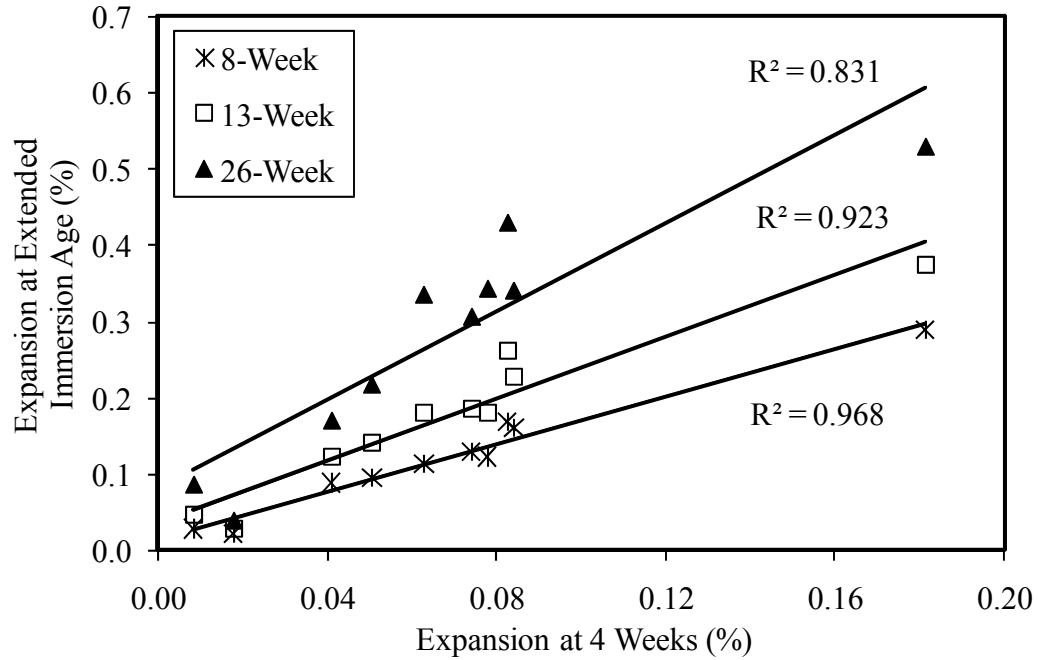


Figure 3.26: ASR expansion of alkaline-cured prisms at the immersion ages of 4, 8, 13 and 26 weeks

3.2.1.1 Determination of the failure criteria of ASTM C 1293M1

The ASR expansion of the alkali-cured prisms at 80°C over the immersion age varied due to the mineralogy, physical characteristics and/or atomic structure of aggregate. Depending on any or combinations of these parameters, some aggregates expanded fast at the early age, while the others grew slowly with an increase in the immersion age. Equation 3.6 represents the average ASR-induced expansion of the alkali-cured prisms containing the fourteen trial aggregates (AAE) over the immersion age of 26 weeks. The F and T tests were performed to confirm the significance of coefficients a , b and c in the regression model. The following results were found: Prob(t) = 0.020016, 0.22863 and

0.01518 for a , b and c , respectively. The value of Prob(F) of 0.0 indicated that both the average expansion of alkali-cured prisms and the immersion age showed a good correlation.

Equation 3.6 demonstrated that the average expansions of the alkali-cured prisms containing the fourteen trial aggregates were 0.096, 0.160, 0.223 and 0.342% at the immersion ages of 4, 8, 13, and 26 weeks, respectively. Since the 4-week suggested failure limit of ASTM C 1293M1 was 0.04%, the above mentioned regression curve was needed to be shifted downward by 0.056 (=0.096-0.040%) units at the ages of 4, 8, 13 and 26 weeks to represent the failure limit curve, which determined the expansion criteria of the alkali-cured prisms of 0.105 (=0.160-0.056), 0.165 (=0.223-0.056) and 0.285% (=0.342- 0.056) at the immersion ages of 8, 13 and 26 weeks, respectively.

$$y = a + bt + \frac{c}{\sqrt{t}} \quad \text{Eq. 3.5}$$

Where:

y is the average expansion of the fourteen aggregates; t is the immersion age in weeks
 a , b and c are the regression variables, and they are -0.254845, 0.007445 and 0.181735, respectively

Table 3.10 documents the levels of ASR of the trial aggregates based on the expansion limits of 1N alkali-cured prisms at 80°C at the immersion ages of 4, 8, 13 and 26 weeks. As can be seen, of the fourteen trial aggregates, the 4-week failure criteria resulted in the three aggregates (SN-A, SN-E and SN-H) innocuous, and the remaining eleven aggregates reactive. It was noted that the levels of ASR of the trial aggregates matched perfectly based on the proposed expansion limits of ASTM C 1293M1 at the ages of 8, 13 and 26 weeks. The study also revealed that the 4-week expansion limit generated conservative results for the two aggregates (SN-I and NN-A). The four

suggested failure limits of ASTM C 1293M1 resulted in identifying five aggregates (SN-A, SN-E, SN-I, SN-H and NN-A) as innocuous, and the remaining nine aggregates as reactive. It can be stated that the expansion limits at the extended immersion ages produced more reliable results than those generated at the early immersion age of 4 weeks. It was concluded that aggregates showing the 4-week expansions of more than 0.08% were shown excessive expansions at all extended immersion ages.

Table 3.10: Aggregate classifications based on the failure criteria of ASTM 1293M1 (prisms submerged in the 1N NaOH at 80°C)

Agg. ID	4-Week (0.04%)	8-Week (0.105%)	13-Week (0.165%)	26-Week (0.285%)	ASR Type
SN-A	I	I	I	I	I
SN-B	R	R	R	R	R
SN-C	R	R	R	R	R
SN-D	R	R	R	R	R
SN-E	I	I	I	I	I
SN-F	R	R	R	R	R
SN-G	R	R	R	R	R
SN-H	I	I	I	I	I
SN-I	R	I	I	I	I
SN-J	R	R	R	R	R
NN-A	R	I	I	I	I
NN-B	R	R	R	R	R
NN-C	R	R	R	R	R
NN-D	R	R	R	R	R

I = Innocuous, R = Reactive

3.2.1.2 ASR-induced cracks on the surface of alkali-cured prisms

The ASR-induced cracks formed on the surface of alkali-cured prisms were also examined. Figures 3.27 and 3.28 illustrate the 6-month alkali-cured prisms made with innocuous and reactive aggregates, as determined by the proposed 4-, 8-, 13- and 26-

week expansion limits of ASTM C 1293M1, respectively. As seen in Figure 3.27, the prisms made with the innocuous aggregate (SN-A) showed no visible cracks even at the immersion age of 6 months. However, severe cracks (map cracks) were noted on the surface of the specimens prepared with the reactive aggregate (NN-B) as depicted in Figure 3.28. It was observed that, at the early age of immersion, micro cracks were formed on the outer surface of the prisms containing reactive aggregates due to the tension exerted by the alkali-silica reactions.

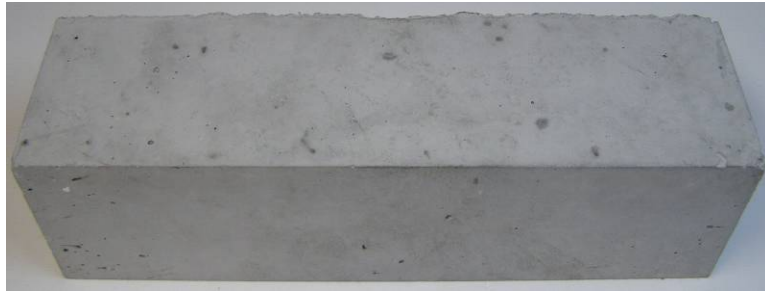


Figure 3.27: Prism containing innocuous aggregate (SN-A)



Figure 3.28: Prism containing highly reactive aggregate (NN-B)

As the test duration prolonged, additional alkali-silica reactions took place in the specimens resulting in an increase in expansion and surface cracking, a common symptom of ASR. The ASR-induced cracks sometime forced the reactive aggregates to

pop out from the specimens due to the tension generated by alkali-silica reactions (Fig. 3.29), which was another common sign of alkali-silica reactivity. It can be stated that the progression in cracks caused by alkali-silica reactivity is directly associated with the increase in the expansion of the test prisms, which in turn is linked with the aggregate reactivity.



Figure 3.29: Aggregates popped-out from the prism of highly reactive aggregate (SN-G)

3.2.2 Prisms submerged in the distilled water at 80°C (ASTM C 1293M2)

In this modification of ASTM C 1293, the prisms were immersed in the distilled water at the temperature of 80°C. The difference in alkali concentration within the prisms and soak solution (as distilled water) was significantly less as compared to that of the specimens immersed in a 1N NaOH solution. Therefore, the leaching effect of alkalis from the water-cured prisms to the soak solution (water), i.e. alkali dilution in the pore solution of the specimens, reduced the amount of alkalis available for alkali-silica reactions (Rogers & Hooton, 1991; and Bérubé & Frenette, 1994). Therefore, the

expansion of the water-cured specimens were expected to be simply less than that of the companion prisms immersed in a 1N NaOH solution at the temperature of 80°C.

The progression of expansion behavior of the prisms made with fourteen trial aggregates immersed in water at the temperature of 80°C as function of the immersion age is illustrated in Figure 3.30. As can be seen, the expansion of the selected aggregates increased slowly with an increase in the test duration, and varied from one aggregate to another. After the immersion age of 4 weeks, the progression in expansion of the SN-A and SN-E aggregate groups was nearly zero, and that of for the SN-H and NN-A aggregate groups was very slow. For the remaining ten aggregates, the ASR-induced expansions increased gradually with an increase in the immersion age.

The expansions of the water-cured specimens among the fourteen trial aggregates varied from 0.003 and 0.016% at 4 weeks, 0.006 and 0.020% at 8 weeks, 0.009 and 0.024% at 13 weeks, and 0.011 and 0.036% at 26 weeks, respectively. Those of alkali-cured prisms were 0.008 and 0.303% at 4 weeks, 0.022 and 0.447% at 8 weeks, 0.028 and 0.584% at 13 weeks and 0.038 and 0.853% at 26 weeks, respectively. It was noted that a substantial reduction in expansion of the test specimens was observed when the soak solution was altered from the 1N NaOH to distilled water.

The expansion progression of the water-cured prisms at the immersion ages of 8, 13 and 26 weeks was compared with the 4-week expansion of the companion aggregate sources, as shown in Figure 3.31. A linear correlation with a R^2 value of 0.93 existed between the expansions at the test durations of 4 and 8 weeks. The relationship between ASR-induced expansions and the selected immersion ages showed less statistical reliability with an increase in the immersion age.

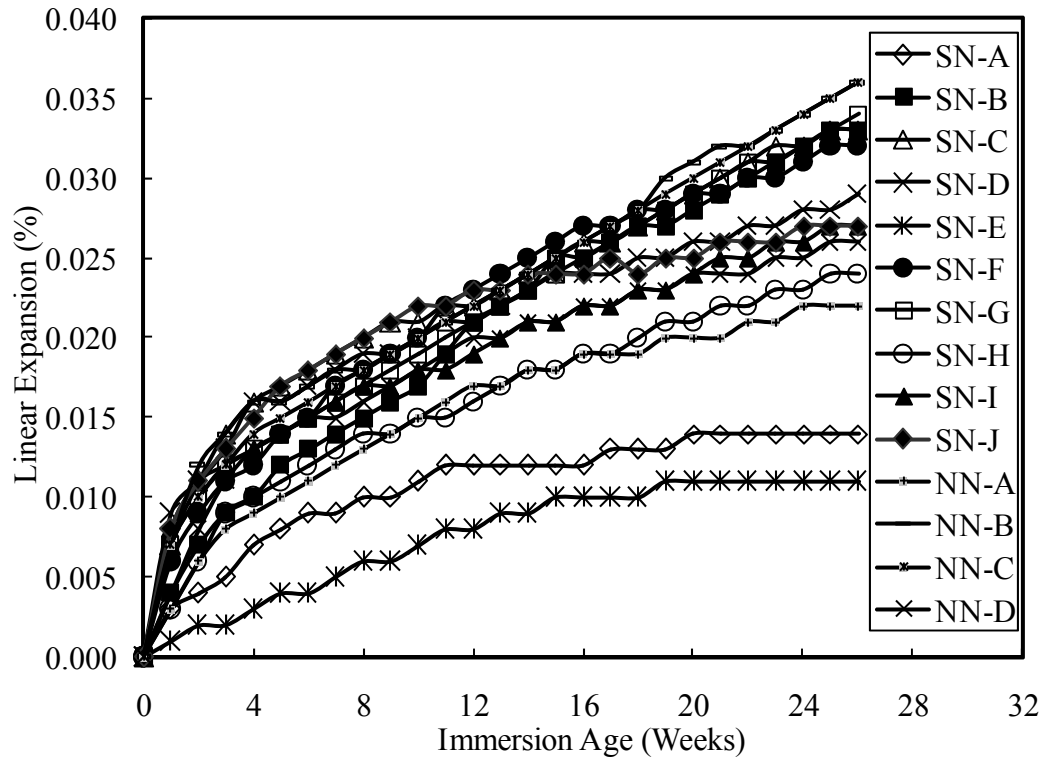


Figure 3.30: Expansion of concrete prisms submerged in water at 80°C

3.2.2.1 Determination of the failure criteria of ASTM C 1293M2

The failure criteria of the water-cured prisms at the temperature of 80°C (ASTM C 1293M2) had not been established by any previous research investigations. In this study, the expansion limits of ASTM C 1293M2 were evaluated at the immersion ages of 4, 8, 13 and 26 weeks by utilizing those of the alkali-cured prisms at the corresponding immersion ages. Due to that perspective, the expansions of water- and alkali-cured prisms prepared with the fourteen selected aggregates was correlated, and presented by Equation 3.6.

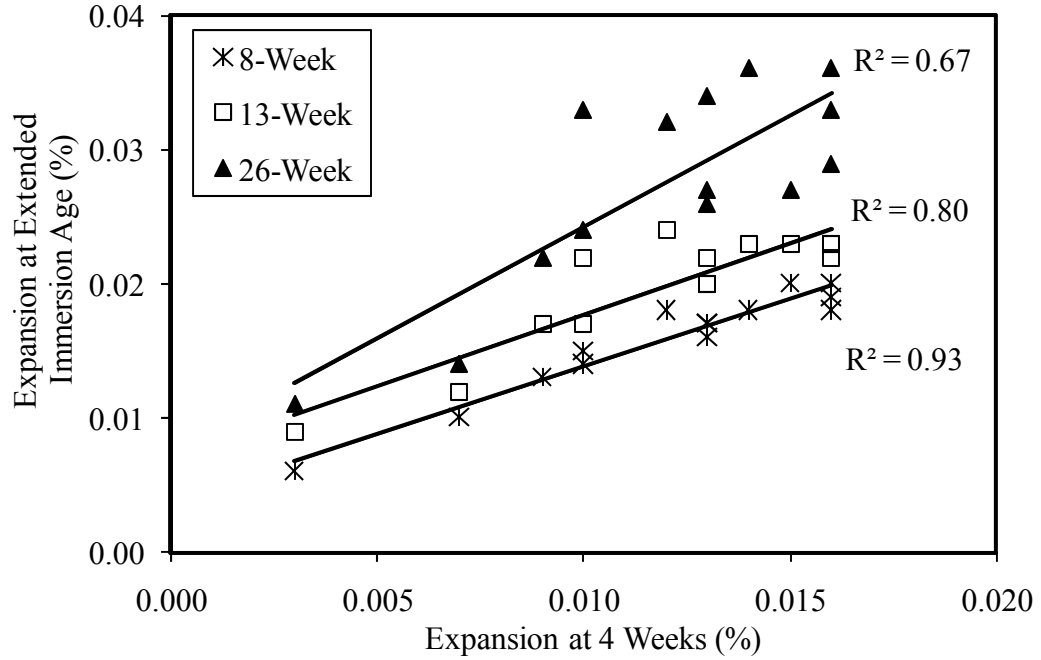


Figure 3.31: ASR expansion of water-cured prisms at the immersion ages of 4, 13 and 26 weeks

Though the development in ASR-related expansions between the alkali- and water-cured specimens was quite different, a marginal correlation was observed between the expansions of the prisms submerged in the 1N NaOH and those immersed in distilled water. Substituting the expansion limits of the alkali-cure prisms at 4, 8, 13 and 26 weeks in Equation 3.6, the failure criteria of the water-cured prisms at the corresponding ages were determined. The statistical data for Equation 3.6 along with the failure criteria of water-cured prisms are tabulated in Table 3.11.

$$y = a + \frac{b}{x} + \frac{c}{x^{1.5}} \quad \text{Eq. 3.6}$$

Where:

x and y are the expansions of alkali- and water-cured prisms at t weeks, respectively
a, b and c are the regression parameters

Table 3.11: Statistical data for Equation 3.7 and the failure criteria of water-cured prisms at various immersion ages

Parameters		4-Week	8-Week	13-Week	26-Week
Regression Variables	<i>a</i>	0.016023	0.020085	0.026636	0.040578
	<i>b</i>	-0.000289	-0.000510	-0.001464	-0.004740
	<i>c</i>	0.000016	0.000036	0.000172	0.000726
Prob(t) of Regression Variables	<i>a</i>	0.0	0.0	0.0	0.0
	<i>b</i>	0.014010	0.19362	0.00285	0.00004
	<i>c</i>	0.076490	0.51041	0.01863	0.00022
Prob(F)		0.00043	0.00016	0.00003	0.00000
R ²		0.860	0.861	0.851	0.902
Failure Criteria of Alkali-cured Prisms at 80°C		0.040%	0.105%	0.165%	0.285%
Failure Criteria of Water-cured Prisms at 80°C		0.011%	0.016%	0.020%	0.028%

Since the ASR-induced expansion did not show a good correlation between the immersion ages of 4 and 26 weeks, the 26-week failure criteria for the water-cured prisms at 80°C would not produce consistent results for the alkali-silica reactivity. It was stated that the prisms submerged in water for the test duration of 6 months showed very little expansion due to more dilution of hydroxyl ions (OH⁻) from the prisms into the distilled water. In this study, three failure limits of the water-cured prisms at 80°C were proposed in differentiating the trial aggregates into reactive and innocuous. They were: 0.011% expansion at 4 weeks, 0.016% at 8 weeks and 0.020% expansion at 13 weeks. The aggregates generating the expansions of less than these failure criteria were considered to be innocuous, and those exceeding the criteria were treated potentially reactive. The levels of alkali-silica reactivity of the fourteen selected aggregates were carried out based on the three suggested failure criteria of the water-cured prisms as

shown in Table 3.12. The final remark on the alkali-silica reactivity of each trial aggregate is also tabulated in Table 3.12.

Table 3.12: Aggregate classifications based on the failure criteria of the water-cured prisms at 80°C (ASTM C 1293M2)

Agg. ID	4-Week (0.011%)	8-Week (0.016%)	13-Week (0.020%)	Recommended ASR
SN-A	I	I	I	I
SN-B	I	I	R	R
SN-C	R	R	R	R
SN-D	R	R	R	R
SN-E	I	I	I	I
SN-F	R	R	R	R
SN-G	R	R	R	R
SN-H	I	I	I	I
SN-I	R	I	I	I
SN-J	R	R	R	R
NN-A	I	I	I	I
NN-B	R	R	R	R
NN-C	R	R	R	R
NN-D	R	R	R	R

I=Innocuous; R=Reactive

Of the fourteen trial aggregates, Table 3.12 demonstrated that the five aggregate groups (SN-A, SN-E, SN-H, SN-I and NN-A) were considered innocuous and the remaining nine aggregates were prone to be reactive. The levels of ASR of the two aggregate groups (SN-B and SN-I) generated inconsistent results based on the three expansion criteria of ASTM C 1293M2. The prisms made with SN-I aggregate expanded rapidly at early age, and slowly thereafter, whereas the progression of ASR expansion of SN-B aggregate was quite opposite to that of SN-I aggregate.

The cracks due to the alkali-silica reactivity on the surface of the water-cured prisms at 80°C were also examined. No ASR-induced symptoms (map cracks, pop-outs etc.) were detected on the surface of the test specimens prepared with highly reactive aggregates even at the immersion age of 6 months. Since the expansion of water-cured prisms was very small throughout the test duration of 26 weeks, a small variation in expansion among each specimen made with same aggregate source might produce a huge difference between the mean and the individual value. Additionally, a tiny variation in the ASR-related expansions of water-cured prisms in the multi-laboratory could lead an erroneous outcome on aggregate classifications. Therefore, assessing the alkali-silica reactivity of an aggregate using ASTM C 1293M2 (prisms submerged in water at the temperature of 80°C) may be harder as compared to that of alkali-immersed prisms.

3.2.3 Comparison of aggregate classifications based on the ASTM C 1293M1 and ASTM C 1293

The fourteen trial aggregates were classified into either innocuous or reactive based on the suggested failure criteria of ASTM C 1293M1 and C 1293M2 at the early and extended immersion ages. The results are illustrated in Table 3.13. As can be seen, of the fourteen investigated aggregates, the 4-week failure criteria of ASTM C 1293M1 and C 1293M2 resulted in a correlation on the levels of ASR of the thirteen aggregates. However, at the extended immersion age, the alkali-silica reactivity classification of all aggregates was exactly identical using the two methods. Using the proposed failure criteria of modified ASTM C 1293 tests, the three of fourteen aggregates exhibited innocuous behavior and the eight aggregates displayed reactive, and the remaining three aggregates produced conflicting results.

As stated earlier, the reason for the same discrepancy between the two modifications of ASTM C 1293 was that the expansion rate of the prisms due to the high strength of alkaline solution (1N NaOH) developed rapidly, whereas in the case of the distilled water as a soak solution, the progress in expansion was very slow. Moreover, water-cured test produced smaller expansions, making it more conducive to potential errors.

Table 3.13: Comparison of aggregate classifications based on the failure criteria of modified ASTM C 1293

Agg. ID	ASTM C 1293M1 (Submerged in 1N NaOH at 80°C)		ASTM C 1293M2 (Submerged in Water at 20°C)	
	Failure Criteria at 4 Weeks	Failure Criteria at 4, 8, 13 and 26 Weeks	Failure Criteria at 4 Weeks	Failure Criteria at 4, 8, 13 and 26 Weeks
SN-A	I	I	I	I
SN-B	R	R	I	R
SN-C	R	R	R	R
SN-D	R	R	R	R
SN-E	I	I	I	I
SN-F	R	R	R	R
SN-G	R	R	R	R
SN-H	I	I	I	I
SN-I	R	I	R	I
SN-J	R	R	R	R
NN-A	R	I	I	I
NN-B	R	R	R	R
NN-C	R	R	R	R
NN-D	R	R	R	R

3.3 Alkali-Carbonate Reactivity Using ASTM C 1105

The standard test method of ASTM C 1105 for the length change of concrete prisms due to alkali-carbonate reaction is conducted in a period of one year to detect the trial aggregates that are susceptible to alkali-carbonate reactivity. The expansion readings of individual samples are tabulated in the Appendix A.

The three failure criteria of ASTM C 1105 of 0.0150, 0.025, and 0.030% at the ages of 3, 6 and 12 months, respectively, were applied to distinguish the alkali-carbonate reactivity of the selected aggregates. The evaluation of each trial aggregate due to ACR is documented in Table 3.14. Of the fourteen aggregates, as can be seen, only four aggregate groups (SN-F, NN-A, NN-B and NN-C) displayed the signs of alkali-carbonate reactivity at the immersion age of 3 months. Lengthening the test duration to 6 months, the two aggregates (SN-F and NN-A) that were shown to be reactive at 3 months became innocuous at 6 months. The behavior of the remaining two aggregates (NN-B and NN-C) was unaffected at the immersion age of 6 months.

Table 3.14: Alkali-carbonate reactivity of the fourteen investigated aggregates

Agg. ID	3-Month (0.015%)	6-Month (0.020%)	12-Month (0.030%)
SN-A	I	I	I
SN-B	I	I	I
SN-C	I	I	I
SN-D	I	I	I
SN-E	I	I	I
SN-F	R	I	I
SN-G	I	I	I
SN-H	I	I	I
SN-I	I	I	I
SN-J	I	I	I
NN-A	R	I	I
NN-B	R	R	R
NN-C	R	R	R
NN-D	I	I	I

I = Innocuous (not reactive); R = Reactive

When the prisms were cured in an extended period of 12 months, the levels of alkali-carbonate reactivity of all investigated aggregates produced similar conclusions to those

obtained at the 6-month testing period; the NN-B and NN-C aggregates were reactive, whereas the remaining twelve aggregates were classified innocuous. It was also observed that the late-age results were more consistent than those obtained at the early stage. It should also be mentioned that the 12-month expansion of NN-B and NN-C was slightly higher than the failure criteria of 0.030% expansion. Consequently, the alkali-carbonate reactivity may not be a great concern for these two aggregate groups.

3.4 Concluding Remarks on the Alkali-Aggregate Reactivity

Table 3.15 documents the classifications of alkali-silica reactivity of the fourteen trial aggregates based on (i) the expansion limits of the mortar bar and prism specimens at the early and extended immersion ages, and (ii) the mineralogy of aggregate (rock type). In addition, the aggregates that were susceptible to alkali-carbonate reactivity (ACR) as per the requirements of ASTM C 1105 are also listed in Table 3.15.

Of the fourteen investigated aggregates, the three aggregate groups SN-A, SN-E and SN-H were considered innocuous, the seven aggregate groups (SN-C, SN-F, SN-G, SN-J, NN-B, NN-C and NN-D) were declared reactive, and the remaining four aggregate groups (SN-B, SN-D, SN-I and NN-A) yielded conflicting results based on the proposed failure criteria as discussed in Table 3.15.

The five aggregate groups (SN-A, SN-E, SN-H, SN-I and NN-A) that showing innocuous behavior based on the failure criteria of ASTM C 1293 at the extended immersion ages exhibited a similar reactivity at the extended failure criteria of mortar bars.

Table 3.15: Levels of alkali-aggregate reactivity of the investigated aggregates

Agg. ID	ASR								ACR
	Rock Type ^a	ASTM C 1260			Modified ASTM C 1293				ASTM C 1105 ^f
		14-Day Failure Criteria (0.10%)	Extended Failure Criteria ^b	Extended Failure Criteria ^c	ASTM C 1293M1		ASTM C 1293M2		
					4-Week Failure Criteria (0.04%)	Extended Failure Criteria ^d	4-Week Failure Criteria (0.011%)	Extended Failure Criteria ^e	
SN-A	I	I	I	I	I	I	I	I	I
SN-B	SR	SR	I	I	R	I	R	I	I
SN-C	R	HR	R	R	R	R	R	R	I
SN-D	I	I	I	I	R	R	R	R	I
SN-E	I	I	I	I	I	I	I	I	I
SN-F	R	HR	R	R	R	R	R	R	I
SN-G	R	HR	R	R	R	R	R	R	I
SN-H	I	I	I	I	I	I	I	I	I
SN-I	R	HR	I	I	R	I	I	R	I
SN-J	R	HR	R	R	R	R	R	R	I
NN-A	R	SR	I	I	I	I	I	I	I
NN-B	R	HR	R	R	R	R	R	R	R
NN-C	R	HR	R	R	R	R	R	R	R
NN-D	R	SR	R	R	R	R	R	R	I

I = Innocuous, R = Reactive

^aBased on the previous research investigations as mentioned in Tables 2.2 and 2.3

^bBased on the expansion limits of mortar bars of 0.10% at 14 days, 0.28% at 28 days and 0.47% at 56 days

^cBased on expansion limits of mortar bars of 0.10% at 14 days, 0.33% at 28 days and 0.48% at 56 days

^d4-, 8-, 13- and 26-week failure limits of alkali-cured prisms of 0.04, 0.105, 0.165 and 0.285%, respectively

^e4-, 8- and 13-week expansion limits of water-cured prisms of 0.011, 0.016 and 0.020%, respectively

^fFailure criteria of 0.015% at 3 months, 0.020% at 6 months, and 0.030% at 12 months

The 14-day failure criteria of the ASTM C 1260 test showed three aggregate groups SN-D, NN-A and SN-I as innocuous, slowly reactive and highly reactive, respectively. However, the proposed failure criteria of the mortar bars and prisms declared the NN-A aggregate innocuous. The alkali- and water-cured prisms made with the SN-D aggregate exceeded the expansion limits at the immersion ages of 4, 8, 13 and 26 weeks. The SN-B aggregate was considered reactive based on the failure criteria of the mortar bars and prisms at the early age, whereas it showed an innocuous behavior at the extended immersion ages. Since the expansion of the SN-I aggregate group was barely above the failure limits for some tests, this aggregate group was declared as innocuous.

In the case of detecting alkali-carbonate reactivity (ACR) of fourteen aggregate quarries, only two aggregate groups (NN-B and NN-C) showed excess reactivity, and the remaining twelve aggregate groups were innocuous at the immersion age of 1 year.

Based on the findings of this study, the following observations can be drawn:

- a. The 14-day failure criteria of ASTM C 1260, the 4-week expansion limits of ASTM C 1293M1 and ASTM C 1293M2, and the aggregate mineralogy resulted in the conservative ASR classifications for some aggregates. In some cases, aggregate groups showing reactive behavior at early age were innocuous at the extended failure criteria, whereas those declared as reactive at early age produced opposite results when evaluated by the extended failure limits.
- b. The extended failure criteria of the alkali-cured prisms produced identical results on the level of ASR of the selected aggregates when compared to those obtained based on the expansion limits of the mortar bars for the standard soak solution (1N NaOH) at the immersion ages of 14, 28, 56 and 98 days.

- c. The results of the ASTM C 1260 at 14, 28 and 56 days coupled with those of the ASTM C 1293M1 at the test durations of 4, 8, 13 and 28 weeks can be used as a reliable indicator to predict the potential for deleterious alkali-silica reactivity. The aggregates generating expansions of more than the prescribed expansion limits of both mortar bars and prisms at the extended immersion ages were classified as reactive or potentially reactive. These aggregates required special attentions to suppress their ASR-induced expansions and cracks below the threshold limits of the mortar bars and prisms at various immersion ages before their use in concrete. Conversely, those showing innocuous behavior at the extended failure criteria of ASTM C 1260, and ASTM C 1293M1, can be safely used in concrete-related activities. Aggregates producing the conflicting results on the alkali-silica reactivity based on the extended failure criteria of two methods may require additional testing to conclude their susceptibility to alkali-silica reactivity. Since the losses in the mechanical properties of concrete (ultimate compressive strength and modulus of elasticity) are also affected by alkali-silica reactions, the ASR of each trial aggregate was also evaluated on the basis of losses in strength and stiffness, as discussed in Chapter 4.

CHAPTER 4

LOSS IN MECHANICAL PROPERTIES DUE TO ASR

This chapter describes the ASR-related losses in ultimate compressive strength and modulus of elasticity of the concrete cylinders containing aggregates obtained from the fourteen different quarries. Twelve 4 in. by 8 in. (102 mm by 204 mm) cylinders containing each selected aggregate with the targeted gradation, as shown in Table 2.3, were cast. Six cylinders were stored in a curing room with a relative humidity (RH) of 100% at a room temperature of 20°C, whereas the remainders were immersed in the 1N NaOH soak solution at an elevated temperature of 80°C. Three water-cured and three alkali-cured cylindrical specimens were subjected to a uni-axial compression test as per requirements of the ASTM C 39 and ASTM C 469 at the immersion ages of 28 and 180 days. The ultimate compressive strength and stiffness for each trial aggregates were obtained from the four groups of specimens. They were: (i) the 28-day ultimate compressive strength and modulus of elasticity of water-cured cylinders at 20°C, (ii) the 28-day ultimate compressive strength and modulus of elasticity of alkaline-cured cylinders at 80°C, (iii) the 6-month ultimate compressive strength and modulus of elasticity of water-cured cylinders at 20°C, and (iv) the 6-month ultimate compressive strength and modulus of elasticity of alkaline-cured cylinders at 80°C. The results are documented in the Appendix B.

The percent loss in compressive strength (LICS) of the cylinders made with each trial aggregate was determined by subtracting the ultimate compressive strength of alkali-cured cylinders at 28 and 180 days from that of the water-cured specimens at the corresponding immersion ages. Additionally, the loss in compressive strength of alkali-

cured cylinders between the ages of 28 and 180 days was also determined. Similarly, the 28-day and 6-month loss in stiffness (LIS) of alkali-cured cylinders, and the loss in stiffness of alkali-cured specimens between the ages of 28 and 180 days were also determined.

4.1 Loss in Ultimate Compressive Strength Due to ASR

The mechanical properties of cement-based materials involve a thermally-activated reaction, called hydration, and the development of hydration is a function of time (Clay, 1989; Swamy, 1992; Jones & Clark, 1997; and Ahmed et al., 2003). The increase in the rate of hydration is prominent at the beginning of concrete casting, and is relatively slow after the immersion age of 28 days. The surrounding environmental factors, such as the temperature and the relative humidity of air, affect the hydration rate as well. The increased temperature accelerates hydration reactions, which enhance the development rate of the solid structure of the binder in the initial periods of hydration. On the other hand, the effect of decreased temperature on cement hydration is quite different. In such circumstances, the hydration reactions in the initial periods are slow, and grow with an increased immersion age. The ultimate compressive strength of concrete cylinders increases with an increase in temperature to a maximum of about 180°F (82.2°C), and then decreases rapidly until a certain temperature is reached, after which it remains nearly constant (Ludwig & Pence, 1956).

Since the rate of hydration increases with an increase in immersion temperature, the ultimate compressive strength of the alkali-cured cylinders at 80°C is expected to be higher than that of the water-cured specimens at 20°C at the ages of 28 and 180 days. However, past investigations demonstrated that the difference in the ultimate

compressive strength of the cylinders cured in water at the temperatures of 80°C and 20°C was no longer noticeable at the extended immersion age (Černý & Rovnaníková, 2002; Savva et al., 2005; and Youssef & Moftah, 2007). That is because the ultimate compressive strength of water-cured specimens having a immersion temperature of up to 200°F (93.3°C) does not appear to have a significant effect on that of the specimens cured at 20°C) (Chang et al., 2006). The ultimate compressive strength of both water- and alkali-cured specimens at 6 months are suspected to be higher than that at 28 days due to the more hydrations take place for the extended period of time.

Table 4.1 shows the 28- and 180-day water-cured and alkali-cured compressive strength and the loss in compressive strength (LICS) of the alkali-cured cylinders at 28 day and 180 days, and that between the ages of 28 days and 180 days. Additionally, the ASR classifications of the fourteen trial aggregates based on the suggested expansion limits of ASTM C 1260 and ASTM C 1293M1 at the extended immersion ages are also documented in Table 4.1. The following observations can be made from Table 4.1.

- a. Extending the immersion age of the water-cured specimens from 28 days to 6 months, the gain in strength due to increased hydration was greater than the potential loss in strength due to ASR. It appears that the curing environment (low temperature and water as soak solution) and the curing age of 6 months are not severe and long enough for alkali-silica reactivity to adversely impact compressive strength. The compressive strength due to an increase in immersion age from 28 days to 180 days resulted in a uniform increase in strength of approximately 19.4%.

- b. For the alkali-cured cylinders, the net gain/loss in strength due to increased hydration with an increase in the immersion age from 28 to 180 days and the loss due to ASR varied depending upon aggregate source and the extent of ASR-based expansion. The loss in strength of the cylinders made with reactive aggregates was more than the gain in strength due to increased hydration. However, the opposite phenomenon observed for the specimens prepared with innocuous aggregates; the gain in strength due to increased hydration was more than the loss in strength due to ASR.
- c. At the test duration of 28 days, the increase in the curing temperature from 20°C to 80°C resulted in about 10.2% gain in the compressive strength of alkali-cured cylinders, except the NN-B aggregate group. In the case of the NN-B aggregate, having the expansions of the mortar bars 1.023% at 14 days and that of the alkali-cured prisms of 0.303% at 4 weeks, an approximately 22% loss in the ultimate compressive strength was observed. Moreover, the results revealed that the 4 weeks immersion age (early immersion age) was not long enough to induce loss in strength of alkali-cured cylinders even when the curing temperature was increased from 20°C to 80°C.
- d. When immersion age increased from 28 days to 180 days, depending on the aggregate source and degree of alkali-silica reactivity, the gain in strength decreased or loss in strength increased with an increase in curing temperature from 20°C to 80°C. As such, the loss or gain in the compressive strength of alkali-cured cylinder at 6 months was more than that of 4 weeks due to increased alkali-silica reactivities.

A typical stress-strain curve of the four groups of the concrete cylinders made with an innocuous aggregate group, evaluated by the extended failure limits of ASTM C 1260 and modified ASTM C 1293 (prisms cured in the 1N NaOH at 80°C), is shown in Figure 4.1. As can be seen, the 6-month alkaline-cured cylinders at 80°C showed the highest ultimate strength, and the 28-day water-cured cylinders at 20°C showed the lowest. The specimens immersed in the 1N NaOH solution at the elevated temperature showed higher compressive strength than those cured in the water at 20°C both at 28 and 180 days. Additionally, the ultimate compressive strength of the 6-month water-cured cylinders at low temperature was more than the 28-day alkaline-cured cylinders at the elevated temperature. An aggregate is innocuous if its compressive strength for the four types of cylinder specimens follows the above-mentioned pattern.

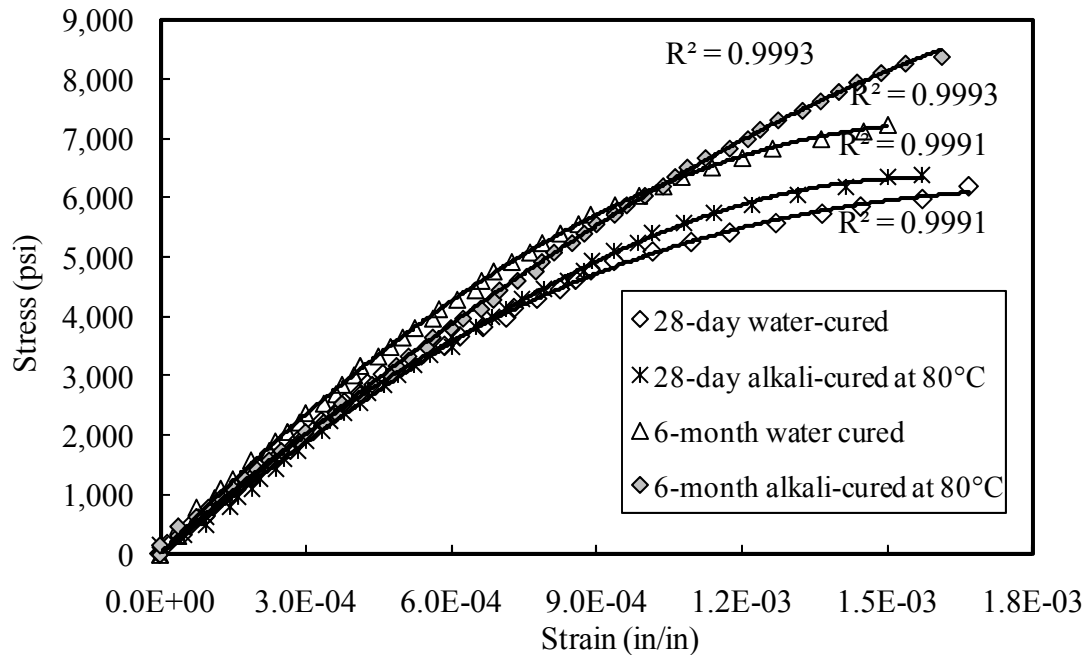


Figure 4.1: Stress-strain curve of the cylinders prepared with innocuous aggregate (SN-A)

Table 4.1: ASR classifications of the trial aggregates and percent loss in compressive strength

Agg. ID	ASR classifications		Water-cured Cylinders at 20°C			Alkali-cured Cylinders at 80°C			PLICS of alkali-cured cylinders at 4 weeks	PLICS of alkali-cured cylinders at 26 weeks
	Based on expansion limits of mortar bars at extended ages	Based on expansion limits of alkali-cured prisms at extended ages	4-Week comp. strength (psi)	26-Week comp. strength (psi)	PLICS of water-cured cylinders between 4 and 26 weeks	4-Week comp. strength (psi)	26-Week comp. strength (psi)	PLICS of alkali-cured cylinders between 4 and 26 weeks		
SN-A	I	I	5952.7	7156.9	-20.2	6379.5	8425.1	-32.1	-7.2	-17.7
SN-B	I	R	5723.7	6829.9	-19.3	5959.8	6030.2	-1.2	-4.1	11.7
SN-C	R	R	4294.6	5329.1	-24.1	4577.2	4072.4	11.0	-6.6	23.6
SN-D	I	I	5619.6	6468.4	-15.1	6226.0	6658.0	-6.9	-10.8	-2.9
SN-E	I	I	5412.8	6417.9	-18.6	5986.6	8431.2	-40.8	-10.6	-31.4
SN-F	R	R	5340.9	6526.4	-22.2	5941.5	5298.0	10.8	-11.2	18.8
SN-G	R	R	4962.6	5898.9	-18.9	5168.6	3239.1	37.3	-4.2	45.1
SN-H	I	I	5470.6	6537.7	-19.5	6625.4	6838.5	-3.2	-21.1	-4.6
SN-I	I	I	4687.9	5552.3	-18.4	5022.5	5653.0	-12.6	-7.1	-1.8
SN-J	R	R	4890.5	5752.9	-17.6	5620.7	5079.1	9.6	-14.9	11.7
NN-A	I	I	6238.2	7545.9	-21.0	6999.7	7763.8	-10.9	-12.2	-2.9
NN-B	R	R	5055.6	6040.9	-19.5	3939.4	3427.0	13.0	22.1	43.3
NN-C	R	R	4806.9	5676.7	-18.1	5025.5	4203.9	16.3	-4.5	25.9
NN-D	R	R	4875.5	5814.2	-19.3	5727.8	5625.9	1.8	-17.5	3.2

Negative sign (-) sign indicates gain in strength

PLICS = Percent loss in compressive strength

I = Innocuous; R = Reactive

Figure 4.2 illustrates the stress-strain curves of the four sets of cylinder made with a reactive aggregate group, evaluated by the ASTM C 1260 and modified ASTM C 1293 at extended test duration. The figure shows that the ultimate compressive strength of alkali-cured cylinders at 80°C decreased with an increase in the immersion age from 28 to 180 days due to the adverse effects of excessive ASR-induced expansion and cracks. A loss in the ultimate compressive strength was also observed between the water- and alkali-cured specimens at the extended immersion age of 6 months. The comparison among the ultimate compressive strength of the four cylinder groups made with reactive aggregates showed an opposite pattern to that seen for innocuous aggregates (Fig. 4.1).

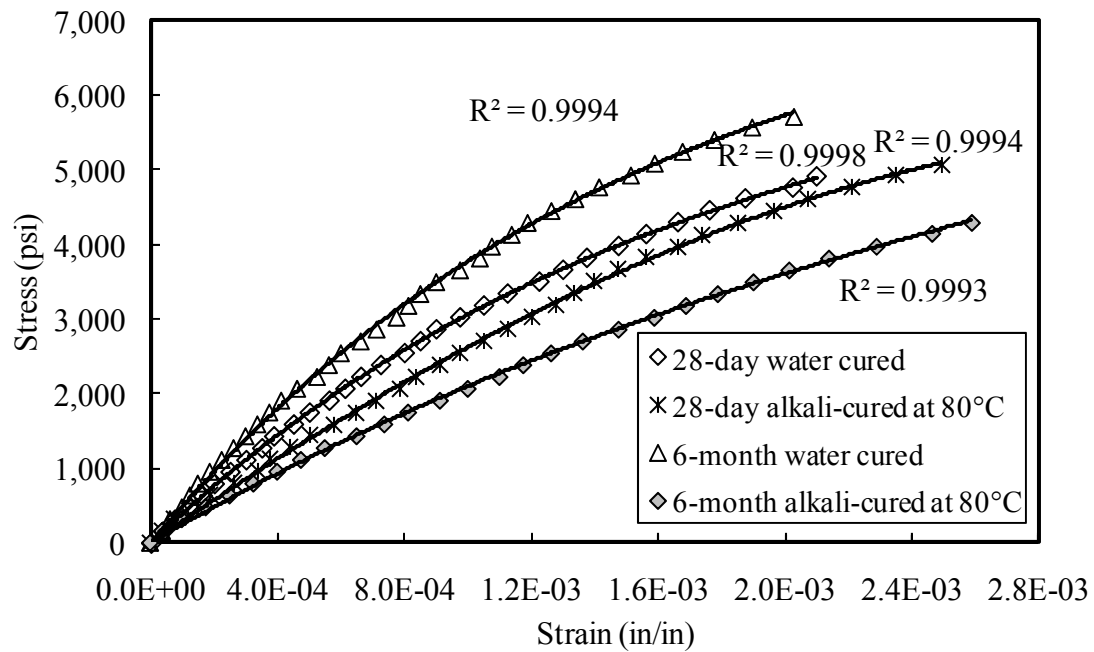


Figure 4.2: Stress-strain curves of the cylinders made with reactive aggregate (NN-C)

4.1.1 Failure criteria due to loss in compressive strength

This section deals with the determination of loss in ultimate compressive strength of concrete cylinder at which an aggregate can be classified as innocuous or reactive. For this purpose, correlations between the 28- and 180-day LICS of alkali-cured cylinders made with each trial aggregate and the expansions of the mortar bars and alkali-cured prisms at different immersion ages were obtained. Afterward, the failure criteria of the loss in compressive strength due to ASR were determined by utilizing the proposed expansion limits of the mortar bars and alkali-cured prisms at different immersion ages.

4.1.1.1 Failure criteria of the 28-day loss in compressive strength of alkali-cured cylinders

The findings of this study proved that the compressive strength was not affected during the early age (28 days). As such, no failure criteria of the 28-day loss in compressive strength of alkali-cured cylinders were proposed.

4.1.1.2 Failure criteria of the 6-month loss in compressive strength of alkali-cured cylinders

When the test duration was extended from 28 to 180 days, the loss in compressive strength of the alkali-cured cylinders made with reactive aggregate due to ASR was more pronounced as compared to the gain in compressive strength due to increased hydration. In the case of the innocuous aggregates, however, the growth in compressive strength due to enhanced hydration exceeded the loss in strength due to slight or no ASR-induced expansions. As such, the net gain or loss in strength due to the dual effects of increased hydration and ASR reactions provided a trend value depending on alkali-silica reactivity.

The relationship between the 6-month loss in compressive strength of alkali-cured cylinders made with each trial aggregate and the expansions of the mortar bars containing the companion aggregate at the ages of 14, 28, and 56 days was established. For the point of discussion, the 6-month loss in compressive strength of alkali-cured cylinder as related to the expansion of mortar bars at 14 days is illustrated in Figure 4.3. The data show that the 6-month LICS of alkali-cured cylinder increased with an increase in the 14-day expansion of the mortar bars. The correlation is presented by Equation 4.1. The same pattern of equation was also found for the 6-month LICS of alkali-cured cylinders and the expansion of the mortar bars at 28 and 56 days.

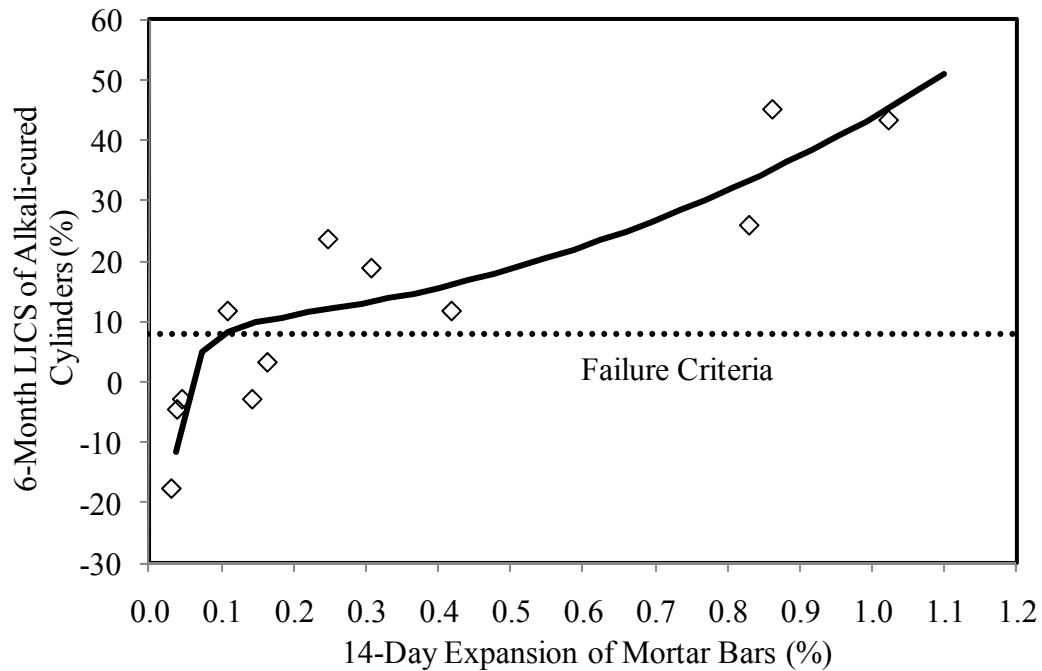


Figure 4.3: The 6-month loss in alkali-cured compressive strength as related to the expansion of the mortar bars at 14 days

$$Y = a + bx^2 + \frac{c}{x^2} \quad \text{Eq. 4.1}$$

The statistical data for Equation 4.1, such as the regression parameters a, b and c, Prob(t) of each regression parameter, co-efficient of multiple determination (R^2), and Prob(F), are documented in Table 4.2. The threshold limits of the 6-month LICS of alkali-cured cylinders were evaluated by substituting the suggested expansion limits of the mortar bars at the immersion ages of 14, 28, and 56 days in Equation 4.1. The findings are presented in Table 4.2. As can be seen, the 14-, 28- and 56-day expansion limits of the mortar bars under the 1N solution resulted in the 6-month loss in compressive strength of alkali-cured cylinder of about 8%, which was adopted to evaluate the level of ASR of the trial aggregates.

Table 4.2: Statistical parameters for Equation 4.1, and the failure criteria of the 6-month loss in compression strength of alkali-cured cylinders

Variables		Immersion Age (Days)		
		14	28	56
Regression Parameters	a	10.44003	7.01019	6.441354
	b	33.43641	15.56001	9.92697
	c	-0.02984	-0.07821	-0.14051
Prob(t) of Regression Parameters	a	0.01750	0.14265	0.27919
	b	0.00117	0.00296	0.01201
	c	0.00073	0.00654	0.03287
Prob(F)		0.00013	0.00002	0.00034
R^2		0.89	0.88	0.75
Expansion limits of the mortar bars (%)		0.10	0.33 ^a (0.28) ^b	0.48 ^a (0.47) ^b
Failure criteria of the 6-month loss in compressive strength of alkali-cured cylinders (%)		7.8	8.0 ^c (7.2) ^d	8.1 ^c (8.0) ^d

^aProposed by Rogers (1991), and Hooton and Rogers (1993); ^bProposed by Islam in this study

^c6-month LICS of alkali-cured cylinder established from the expansion limits suggested by Rogers (1991), and Hooton & Rogers (1993)

^d6-month LICS of alkali-cured cylinder established from the expansion limits suggested by Islam in this study

The 6-month loss in compressive strength of alkali-cured cylinders was also correlated with the expansions of the alkali-cured prisms at the ages of 4, 8, 13, and 26 week. Figure 4.4 illustrates the loss in compressive strength at 6 months as associated with the 4-week expansion of the alkali-cured prisms. The data shows that the LICS decreased with an increased in the expansion of the prisms. The relationship of the dependent and independent variables of Figure 4.4 is shown in Equation 4.2. The 6-month loss in compressive strength of alkali-cured cylinders vs. the expansions of the alkali-cured prisms at the ages of 8, 13, and 26 weeks showed a similar pattern to that of the 6-month LICS of alkali-cured cylinder vs. the 4-week expansion of the prisms (Fig. 4.3).

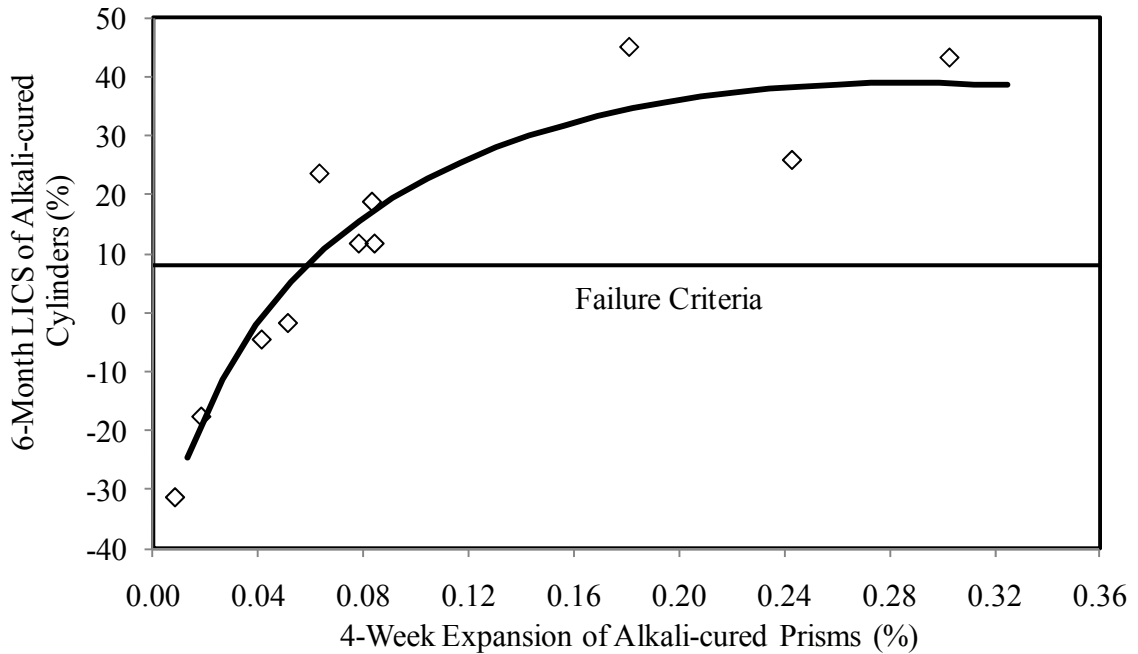


Figure 4.4: The 6-month loss in compressive strength of alkali-cured cylinder as related to the expansion of the alkali-cure prisms at 4 weeks

$$Y = a + bx + cx^{0.5} \quad \text{Eq. 4.2}$$

The statistical data for Equation 4.2 along with the failure criteria for the 6-month loss in compressive strength of alkali-cured cylinders are documented in Table 4.3. As can be seen, the proposed 4-week failure criteria of ASTM C 1293M1 resulted in a low value of the 6-month LICS of alkali-cured cylinder. The threshold limit of the 6-month LICS of alkali-cured cylinder as a function of 4-week expansion limit of the alkali-cured prism was of 1.3%. However, the 6-month LICS of the alkali-cured cylinder of 8% evaluated by the extended failure criteria of ASTM C 1293M1 at 8, 13, and 26 weeks was found to be fairly consistent. That means, for the most part, the reactive aggregates identified by the failure criteria of mortar bars and those of alkali-cured prisms produced the 6-month loss in compressive strength of alkali-cured cylinder in excess of 8%.

Table 4.3: Statistical parameters for Equation 4.2, and the failure criteria due to the 6-month loss in compressive strength

Variables		Immersion Age (Weeks)			
		4	8	13	26
Regression Parameters	a	-63.54455	-45.04291	-57.02533	-51.43838
	b	-356.61172	-48.73734	-79.50510	-19.99951
	c	382.40086	157.41135	190.13714	122.07975
Prob(t) of Regression Parameters	a	0.00129	0.00740	0.02244	0.02347
	b	0.02886	0.57476	0.43492	0.75187
	c	0.00272	0.04997	0.07172	0.11531
Prob(F)		0.00011	0.00008	0.00094	0.00031
R ²		0.90	0.88	0.83	0.83
Expansion limits of ASTM C 1293M1 (%)		0.040 ^a	0.105 ^b	0.165 ^b	0.285 ^b
Loss in compressive strength of alkali-cured cylinders at 6 months (%)		-1.3	8.5	7.1	8.0

^aProposed by Touma et al. (2001); ^bSuggested by Islam in this study

4.1.1.3 Failure criteria due to the loss in compressive strength of the alkali-cured cylinders between 28 days and 180 days

As mentioned earlier, the ultimate compressive strength of alkali-cured cylinders made with each trial aggregate between the ages of 28 and 180 days varied depending on the reactivity of aggregate. Due to the adverse affect of ASR, the ultimate compressive strength of the test specimens made with the reactive aggregates decreased with an increase in the test duration from 28 days to 180 days. On the other hand, a gain in ultimate compressive strength with an increase in immersion age was observed for the specimens made with the innocuous aggregates due to the increased hydrations and lack of ASR reactions.

In order to select a limit of the loss in compressive strength of alkali-cured cylinders at the ages of 28 and 180 days at which an aggregate behaved reactive, a correlation was sought between the loss in compressive strength of alkali-cured cylinders at 180 days and that of between the ages of 28 and 180 days. The results are shown in Figure 4.5. A linear correlation was found between the dependent and independent variables. Using the suggested failure limit of the 6-month LICS of alkali-cured cylinders of 8.0%, the failure limit for the loss in compressive strength of the alkali-cured cylinders between the ages of 28 and 180 days was found to be -0.5%. The idea indicated that the ultimate compressive strength of the alkali-cured cylinders made with the innocuous aggregate at 6 months would gain a minimum of 0.5% of that obtained at 28 days. On the other hand, for the specimens made with reactive aggregates immersed in the 1N NaOH at 80°C, the 6-month gain in strength due to increased hydration would be a maximum of 0.5% of the compressive strength at 28 days.

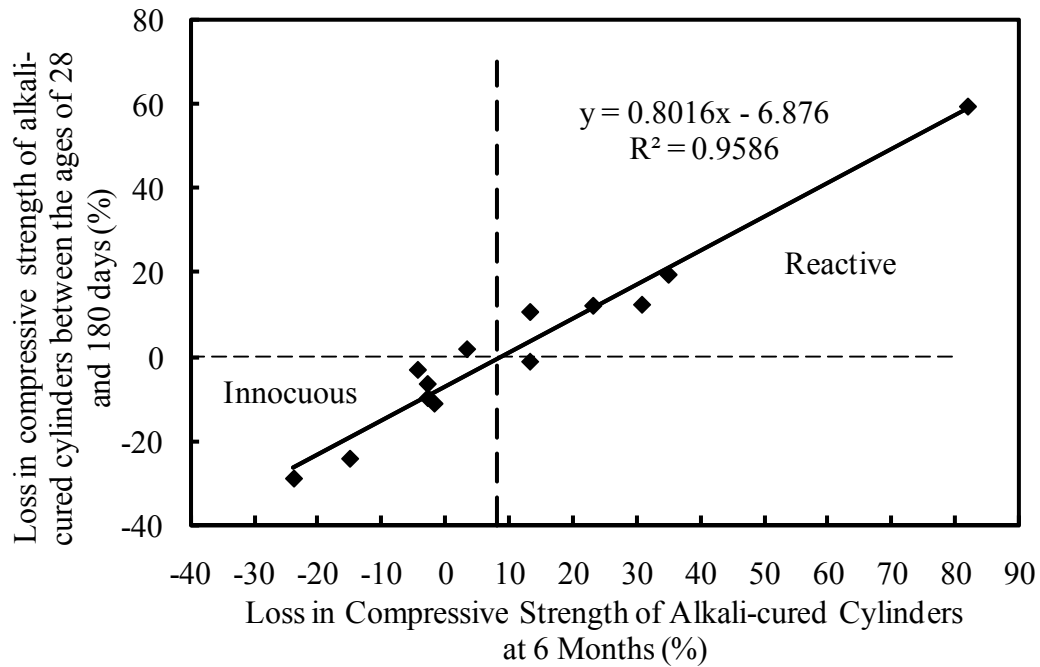


Figure 4.5: Loss in compressive strength of alkali-cured cylinders at 6 months and that of the alkali-cured cylinders between the ages of 28 days and 180 days

4.1.2 Trial aggregate classifications based on the proposed failure criteria of loss in compressive strength

Table 4.4 shows the categorization of the trial aggregates based on the 6-month loss in compressive strength of alkali-cured cylinder and the loss in compressive strength of those specimens between the ages of 28 and 180 days.

As can be seen in Table 4.4, the six aggregate groups (SN-C, SN-F, SN-G, SN-J, NN-B, and NN-C) were shown reactive, and other six aggregate groups (SN-A, SN-D, SN-E, SN-H, SN-I and NN-A) were found to be innocuous, and the remaining two aggregate groups (SN-B and NN-D) produced conflicting results. Since the compressive strength of limestone aggregate (SN-B) decreases with an increase in the immersion temperature

(Savva et al., 2005), the SN-B aggregate might be considered innocuous though its 6-month LICS of the alkali-cured cylinders slightly exceeded the proposed failure limit of 8%. Finally, the level of ASR of the trial aggregates evaluated by the suggested failure limits of the loss in compressive strength of alkali-cured cylinders at 6 months and the loss in compressive strength of alkali-cured cylinder between the ages of 28 and 180 days showed a good correlation.

Table 4.4: Loss in compressive strength (LICS) and aggregate classifications

Agg. ID	Percent LICS of alkali-cured cylinders between 4 and 26 weeks (LICS _{4w-26w})	ASR classifications base on LICS _{4w-26w} of -0.5%	Percent LICS of alkali-cured cylinders at 6 (LICS _{26w})	ASR classifications based on LICS _{26w} of 8%	Recommended ASR
SN-A	-32.1	I	-17.7	I	I
SN-B	-1.2	I	11.7	R	I
SN-C	11.0	R	23.6	R	R
SN-D	-6.9	I	-2.9	I	I
SN-E	-40.8	I	-31.4	I	I
SN-F	10.8	R	18.8	R	R
SN-G	37.3	R	45.1	R	R
SN-H	-3.2	I	-4.6	I	I
SN-I	-12.6	I	-1.8	I	I
SN-J	9.6	R	11.7	R	R
NN-A	-10.9	I	-2.9	I	I
NN-B	13.0	R	43.3	R	R
NN-C	16.3	R	25.9	R	R
NN-D	1.8	R	3.2	I	R

Negative sign (-) indicates gain in strength

In summary the finding suggests that the early-age compressive strength is not a good indicator to predict alkali-silica reactivity. However, at the late immersion age (6 months), the compressive strength became a reliable indicator for alkali-silica reactivity.

4.2 Loss in Modulus of Elasticity Due to ASR

The modulus of elasticity (MOE), also known as Young's Modulus or stiffness, at low temperature increases with an increase in the immersion age (Schneider, 1988). Conversely, at the early immersion age, the stiffness decreases with an increase in immersion temperature. Savva et al. (2005) concluded that a continuous drop in the modulus of elasticity showed with an increase in curing temperature. With an increased in ASR due to an increase in immersion age, the 6-month MOE decreases further with an increase in immersion temperature. The relationship of the normalized elastic modulus (E_{cr}/E_c) in compression with the temperature (T) ranging from 20 to 120°C can be expressed in Equation 4.3 (Chang et al., 2006). Substituting for 80°C in the equation, the expected normalized elastic modulus was to be 0.901. In another word, the MOE of the water-cured cylinders at 80°C is approximately 0.901 times that at 20°C. The ratio decreases more when the soak solution is altered to a 1N NaOH.

$$E_{cr}/E_c = -0.00165 * T + 1.033 \quad \text{For } 20^\circ\text{C} < T < 120^\circ\text{C} \quad \text{Eq. 4.3}$$

Past investigations as well as the part of this study concluded that the ASR ultimately had no influence on the 28-day compressive strength. However, for the same test duration, a tremendous alkali-silica reaction took place between the reactive silica of the aggregates and the OH⁻ of the alkalis present in the concrete. As a result, the strain of the cylinders prepared with reactive aggregates submerged in the 1N NaOH solution at 80°C increased significantly due to the micro-cracking formed on the specimen. Owing to that viewpoint, these specimens experienced a loss in stiffness as early as 28 days of immersion.

Earlier studies and this investigation reported that the ultimate compressive strength decreased due to reactivity of an aggregate at the later ages. As the immersion age prolonged, the micro-cracks due to ASR became more severe and eventually produced map cracking that resulted in a higher strain with a small increase in load. It was expected that the extension of the test duration from 28 days to 180 days could produce excessive loss in stiffness for the cylinders prepared with the reactive aggregates due to multiple effects of the ASR-induced expansion, the reduced compressive strength, and the increased strain.

Table 4.5 illustrates the 28-day and 6-month loss in stiffness of alkali-cured cylinders and the loss in stiffness of alkali-cured cylinders between the ages of 28 and 180 days. In addition, the ASR classifications of the trial aggregates based on the extended expansion limits of ASTM C 1260 and ASTM C 1293M1 are documented in Table 4.5. Based on the findings of Table 4.5, the following observations are made:

- a. Overall, the stiffness of water-cured cylinders at 20°C increased with an increase in immersion age due to the increased hydration and lack of favorable environment for ASR reactions.
- b. At the early immersion age (28 days), increasing the curing temperature from 20°C to 80°C resulted in the loss in stiffness due to the combined effects of increased hydration and alkali-silica reactivity. Since the loss in stiffness due to temperature effect was nearly identical for all aggregates, the loss in stiffness between the alkali- and water-cured cylinders mainly depended on the aggregate reactivity. As such, the cylinders made with reactive aggregates experienced more loss in stiffness than those prepared with innocuous aggregates.

- c. Extending the immersion age from 28 to 180 days, the loss in stiffness in the alkali-cured specimens increased due to the dual effects of extensive ASR-induced expansion and elevated temperature. Since the loss in stiffness due to increased temperature remained the same for all aggregates, the net loss in stiffness varied depending on aggregate reactivity. The loss in stiffness between the alkali- and water-cured cylinders at 180 days exceeded that obtained at 28 days.
- d. For the alkali-cured cylinders at 80°C, the loss in stiffness between the immersion ages of 28 days and 180 days also increased due to the ASR-induced expansion and continued deterioration in MOE with increases in immersion age.

4.2.1 Determination of the failure criteria based on the loss in stiffness

This section deals with the ASR-induced loss in stiffness at which an aggregate considered reactive. The failure criteria of the loss in stiffness of alkali-cured cylinders at 28 and 180 days, and those of the alkali-cured cylinders between the ages of 28 and 180 days were established.

4.2.1.1 Failure criteria of 28-day loss in stiffness of alkali-cured cylinders

The results of this study showed that only a small amount of increase in the 28-day stiffness was observed for aggregate groups of SN-E and NN-A. On the other hand, a wide range of loss in stiffness (7.9 to 49%) was noted for the cylinders made with the remaining twelve aggregate groups.

Table 4.5: ASR classifications of the trial aggregates and percent loss in stiffness

Agg. ID	ASR classifications		Water-cured Cylinders at 20°C			Alkali-cured Cylinders at 80°C			PLIS of alkali-cured cylinders At 4 weeks	PLIS of alkali-cured cylinders at 26 weeks
	Based on expansion limits of mortar bars at extended ages	Based on expansion limits of alkali-cured prisms at extended ages	4-Week stiffness (psi)	26-Week stiffness (psi)	PLIS of water-cured cylinders between 4 and 26 weeks	4-Week stiffness (psi)	26-Week stiffness (psi)	PLIS of alkali-cured cylinders between 4 and 26 weeks		
SN-A	I	I	6.00E+06	6.40E+06	1.8	5.89E+06	5.98E+06	-1.5	1.8	6.6
SN-B	I	R	4.94E+06	5.14E+06	25.5	3.68E+06	3.73E+06	-1.4	25.5	27.4
SN-C	R	R	3.98E+06	4.24E+06	7.0	3.70E+06	2.99E+06	19.2	7.0	29.5
SN-D	I	I	3.20E+06	3.40E+06	19.4	2.58E+06	2.26E+06	12.4	19.4	33.5
SN-E	I	I	6.44E+06	7.04E+06	7.9	5.93E+06	6.41E+06	-8.1	7.9	8.9
SN-F	R	R	5.35E+06	5.81E+06	19.1	4.33E+06	3.69E+06	14.8	19.1	36.5
SN-G	R	R	3.91E+06	4.12E+06	43.0	2.23E+06	1.55E+06	30.5	43.0	62.4
SN-H	I	I	4.11E+06	4.30E+06	28.0	2.96E+06	2.01E+06	32.1	28.0	53.3
SN-I	I	I	2.90E+06	3.63E+06	-12.4	3.26E+06	2.69E+06	17.5	-12.4	25.9
SN-J	R	R	3.49E+06	4.11E+06	-19.5	4.17E+06	2.39E+06	42.7	-19.5	41.8
NN-A	I	I	3.81E+06	4.03E+06	1.6	3.75E+06	3.75E+06	0.0	1.6	6.9
NN-B	R	R	3.84E+06	4.44E+06	49.2	1.95E+06	1.92E+06	1.5	49.2	56.8
NN-C	R	R	3.48E+06	4.18E+06	28.2	2.50E+06	2.00E+06	20.0	28.2	52.2
NN-D	R	R	3.47E+06	4.33E+06	34.6	2.27E+06	1.96E+06	13.7	34.6	54.7

Negative sign (-) indicates gain in stiffness

PLIS = Percent loss in stiffness

I = Innocuous; R = Reactive

At the early age of immersion, the micro cracking was progressive and varied from aggregate to aggregates, which resulted in a large variation in the loss in stiffness among the fourteen selected aggregates. As such, no failure limit of the 28-day loss in stiffness was suggested.

4.2.1.2 Failure criteria of the 6-month loss in stiffness of alkali-cured cylinders

ASR-induced cracks of the cylinders increased in size and frequency with an increase in the immersion age. At the extended immersion age of 6 months, the cracks due to the alkali-silica reactivity became matured. The failure criteria of the 6-month loss in stiffness of alkali-cured cylinders were evaluated by utilizing those of the mortar bars and prisms at various immersion ages. To achieve the above-stated objective, a correlation was made between the 6-month loss in stiffness and the 14-day expansion of the mortar bars containing the companion aggregate sources. The result is shown in Figure 4.6.

As seen in Figure 4.6, the 6-month LIS of alkali-cured cylinder was a function of the expansions at 14 days. The shape of the curve was also traced using Equation 4.4. The 6-month LIS of alkali-cured cylinder vs. the ASR-induced expansions of the mortar bars at the ages of 28 and 56 days also showed a similar pattern to that of the 6-month LIS vs. the 14-day expansion of the mortar bars. The statistical data for Equation 4.4 are given in Table 4.6. The R^2 value of each regression curve showed a good fit between the 6-month LIS and the expansion of mortar bars at 14, 28 and 56 days. Finally, the failure limit of the 6-month loss in stiffness, at which an aggregate classification can be made, was established by utilizing Equation 4.4 and the expansion limits of the mortar bars suggested by ASTM C 1260, Rogers (1991), Hooton and Rogers (1993), and Islam in this study.

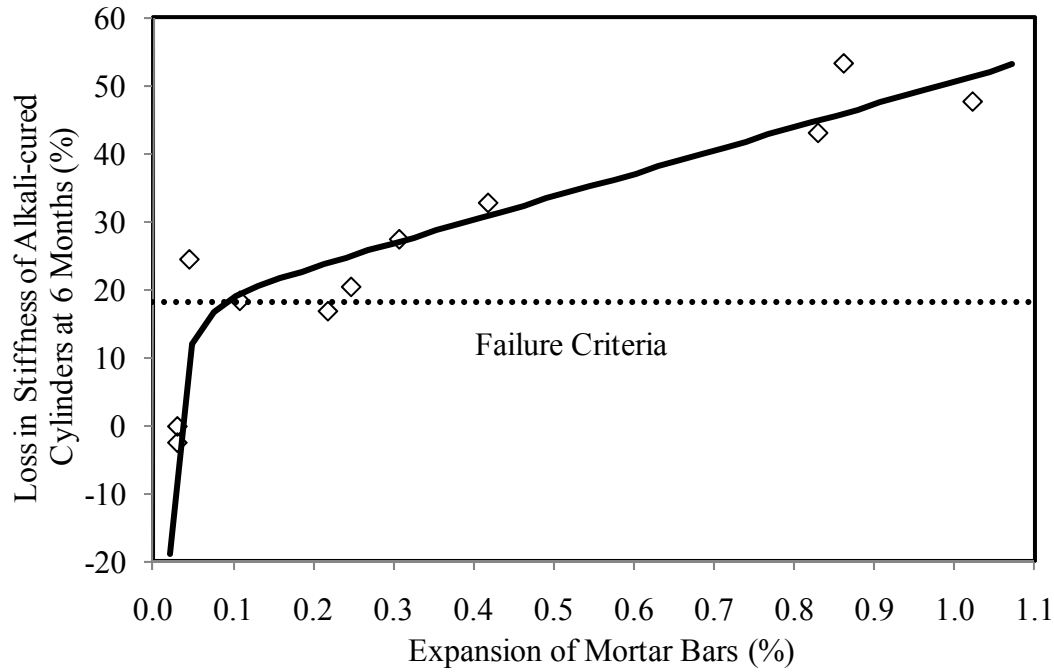


Figure 4.6: The 6-month loss in stiffness (alkali-cured vs. water-cured) as related to the expansion of the mortar bars at 14 days

$$y = a + bx + \frac{c}{x^2} \quad \text{Eq. 4.4}$$

Table 4.6: Statistical parameters for Equation 4.4, and the failure criteria of the 6-month loss in stiffness of alkali-cured cylinder

Variables		Immersion Age (Days)		
		14	28	56
Regression Parameters	a	16.83274	16.54955	14.19432
	b	33.77859	21.92507	18.47465
	c	-0.01461	-0.04541	-0.08012
Prob(t) of Regression Parameters	a	0.00395	0.00469	0.02369
	b	0.00135	0.00174	0.00361
	c	0.03495	0.02616	0.06816
Prob(F)		0.00013	0.00017	0.00063
R ²		0.89	0.86	0.84
Expansion limits of the mortar bars (%)		0.10	0.33 ^a (0.28) ^b	0.48 ^a (0.47) ^b
Failure criteria of the 6-month loss in stiff (%)		18.7	24.0 ^c (22.1) ^d	22.7 ^c (22.5) ^d

^aProposed by Rogers (1991); and Hooton & Rogers (1993); ^bProposed by Islam in this study

^cEvaluated from the expansion limits proposed by Rogers (1991), Hooton & Rogers (1993)

^dEvaluated from the expansion limits suggested by Islam in this study

As can be seen in Table 4.6, the 14-day expansion limit of mortar bars resulted in the 6-month loss in stiffness of 18.7%. The 28- and 56-day expansion limits resulted in a slightly higher the 6-month LIS value than that obtained at 14 days. To remain conservative, it is suggested that the aggregates possessing the 6-month loss in stiffness of more than 18% were considered reactive and those generating the less amount were classified innocuous.

The correlation between the 6-month loss in stiffness of alkali-cured cylinder and the expansions of the alkali-cured prisms at the test durations of 4, 8, 13 and 26 weeks was also evaluated. Figure 4.7 presents the 6-month loss in stiffness of alkali-cured cylinders and the 4-week expansion of the alkali-cured cylinders. As can be seen, the LIS at 6 months increased with an increase in the expansion of the mortar bars at 14 days. The relationship is expressed by Equation 4.5. The equation was also shown a good fit when the expansion of the prisms was altered from 4 weeks to 8, 13 and 26 weeks. The statistical parameters of Equation 4.5 for the 6-month loss in stiffness vs. the expansion of the prisms at 4, 8, 13 and 26 weeks were documented in Table 4.7. Utilizing the expansion limits of the alkali-cured prisms at the above-mentioned four immersion ages, and Equation 4.5, the failure criteria of the 6-month loss in stiffness of alkali-cured cylinder were determined.

The loss in stiffness at 6 months obtained from the 8-, 13- and 26-week failure criteria of the alkali-cured prisms at 80°C showed a good agreement, whereas the 4-week expansion limit resulted in an overestimated outcome.

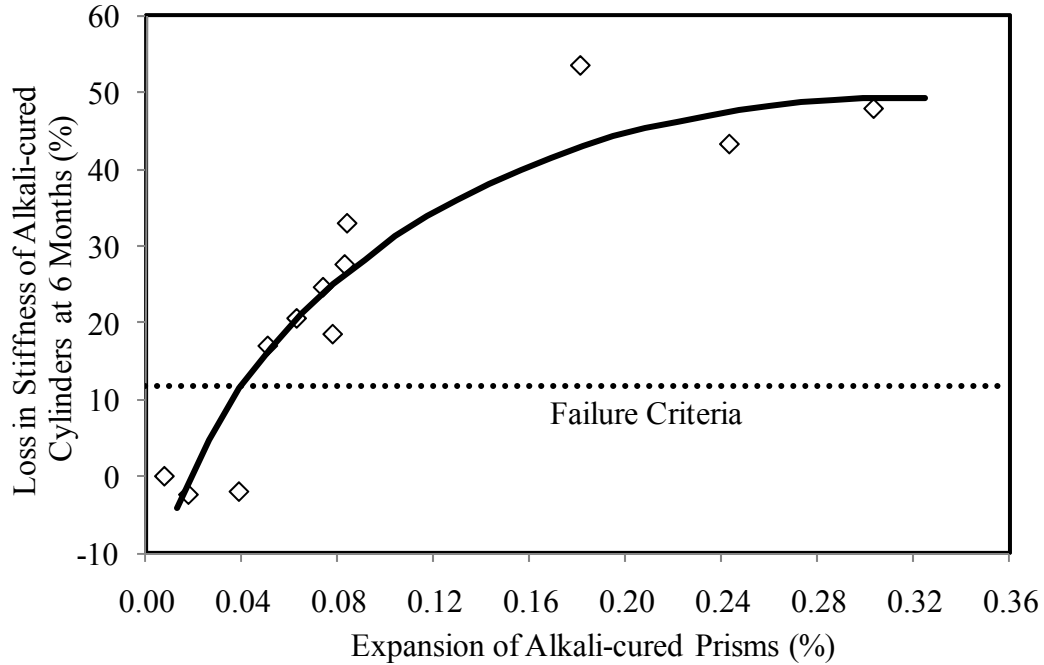


Figure 4.7: The loss in stiffness at 6 months of alkali-cured cylinder as related to the expansion of the alkali-cure prisms at 4 weeks

$$y = a + bx^2 + cx^{0.5} \quad \text{Eq. 4.5}$$

Table 4.7: Statistical parameters for Equation 4.5, and the failure criteria due to the 6-month loss in stiffness of alkali-cured cylinders

Variables		Immersion Age (Weeks)			
		4	8	13	26
Regression Parameters	a	-63.54455	-45.04291	-57.02533	-51.43838
	b	-356.61172	-48.73734	-79.50510	-19.99951
	c	382.40086	157.41135	190.13714	122.07975
Prob(t) of Regression Parameters	a	0.00129	0.00740	0.02244	0.02347
	b	0.02886	0.57476	0.43492	0.75187
	c	0.00272	0.04997	0.07172	0.11531
Prob(F)		0.00011	0.00008	0.00094	0.00031
R ²		0.90	0.88	0.83	0.83
Expansion limits of ASTM C 1293M1 (%)		0.040	0.105	0.165	0.285
Loss in compressive strength at 6 months (%)		11.9	19.7	21	22

4.2.1.3 Failure criteria of the loss in stiffness of the alkali-cured cylinders between the ages of 28 and 180 days

The loss in stiffness of the alkali-cured cylinders made with the fourteen selected aggregates at the immersion ages of 28 and 180 days was correlated with the 6-month loss in stiffness of alkali-cured cylinders. The result is shown in Figure 4.8. As can be seen, a linear correlation existed between the independent and depended variables. Utilizing the 6-month LIS of alkali-cured cylinder of 18%, Figure 4.8 resulted in the failure limit of the LIS of the alkali-cured cylinders between the ages of 28 and 180 days of 9%. The results indicated that the 6-month loss in stiffness of alkali-cured cylinders was roughly doubled the loss in stiffness of alkali-cured cylinders between the ages of 28 and 180 days. The study suggested that the aggregates were declared reactive if their 6-month loss in stiffness of alkali-cured cylinders was more than 18% or their loss in stiffness of alkali-cured cylinders between 28 and 180 days was more than 9%.

4.2.1.4 Alkali-silica reactivity of the trial aggregates based on the proposed failure criteria of loss in stiffness

Table 4.8 documents the ASR classifications of the fourteen trial aggregates based on the 6-month loss in stiffness of alkali-cured cylinders at 6 months, and the loss in stiffness of alkali-cured specimens between the ages of 28 and 180 days. As can be seen, of the fourteen aggregates tested, the four aggregate groups (SN-A, SN-B, SN-E, and NN-A) were shown innocuous, the nine aggregate groups (SN-C, SN-D, SN-F, SN-G, SN-H, SN-J, NN-B, NN-C and NN-D) were declared reactive, and the remaining one aggregate group (SN-I) showed a different result on ASR based on the proposed failure criteria.

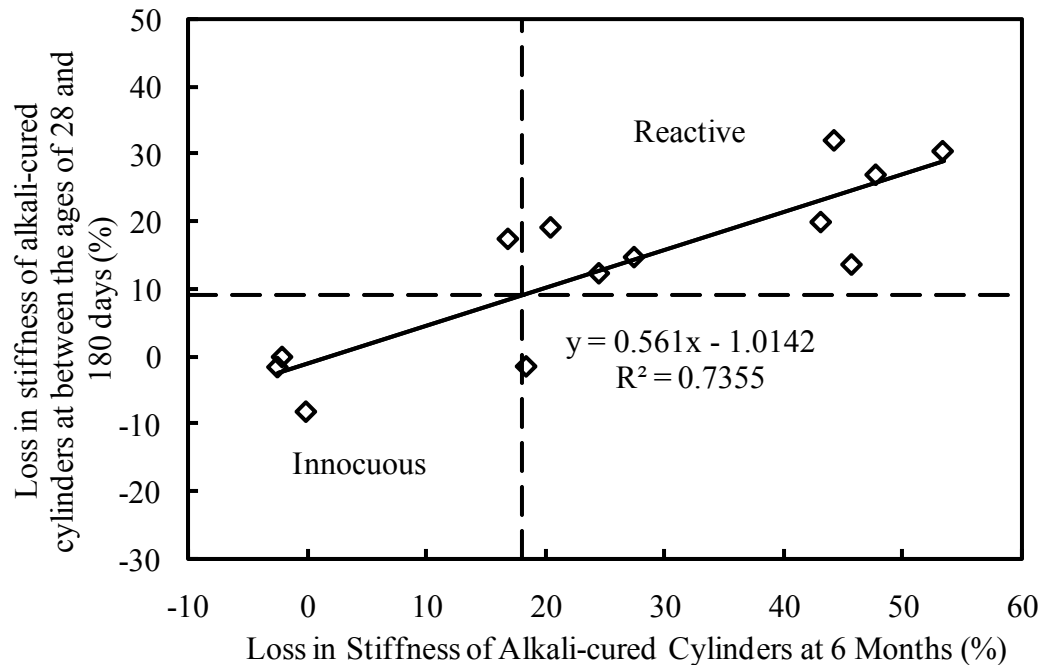


Figure 4.8: The 6-month loss in stiffness of alkali-cured cylinders as related to the loss in stiffness of alkali-cured cylinders between the ages of 28 and 180 days

The study showed that the loss in stiffness due to alkali-silica reactivity occurred in early age of immersion age (28 days). The degree of severity on the loss in stiffness increased with an increase in the test duration. The failure criteria of the 6-month loss in stiffness of alkali-cured cylinder and of the loss in stiffness of the alkali-cured cylinders between the ages of 28 and 180 days resulted in a good agreement on the levels of ASR of the trial aggregates.

The study revealed that alkali-silica reaction in concrete reduced concrete stiffness significantly both at the early and extended immersion age. At the later stages of immersion, the modulus of elasticity became more severe due to the extensive cracking that took place on the specimens of reactive aggregates. The extensive ASR-induced fine cracks also led to a higher ductility.

Table 4.8: Loss in stiffness (LIS) for each aggregate and the classification of ASR of the trial aggregate

Agg. ID	Percent LIS of alkali-cured cylinders between 28 and 180 days (LIS _{4w-26a})	ASR base on LIS _{4w-26a} of 9%	Percent LIS of alkali-cured cylinders 6 months (LIS _{26w})	ASR based on LIS _{26w} of 18%	Recommended ASR
SN-A	-1.5	I	-2.44	I	I
SN-B	-1.4	I	18.43	I ^a	I
SN-C	19.2	R	20.48	R	R
SN-D	12.4	R	24.53	R	R
SN-E	-8.1	I	-0.05	I	I
SN-F	14.8	R	27.49	R	R
SN-G	30.5	R	53.38	R	R
SN-H	32.1	R	44.26	R	R
SN-I	17.5	R	16.90	I	R
SN-J	42.7	R	32.85	R	R
NN-A	0.0	I	-2.05	I	I
NN-B	1.5 ^b	R	47.76	R	R
NN-C	20.0	R	43.15	R	R
NN-D	13.7	R	45.73	R	R

Negative sign (-) indicates gain in strength

^aTreated as innocuous since the value is slightly higher

^bStiffness of the alkali-cured cylinders was severely affected at 28 days

4.3 Comparison of Aggregate Classifications Due to Loss in Strength and Stiffness

The fourteen trial aggregates were classified into innocuous (I) and reactive (R) based on the proposed failure criteria of loss in compressive strength and loss in stiffness. The results are documented in Table 4.9. As can be seen, of the fourteen investigated aggregates, the four aggregate groups (SN-A, SN-B, SN-E, and NN-A) were shown innocuous, the seven aggregates were considered reactive, and the remaining three aggregate groups (SN-D, SN-I and SN-H) produced conflicting results. Unlike failure limits of the loss in compressive strength and the expansion limits of mortar bars and

alkali-cured prisms, the proposed failure criteria of the loss in stiffness resulted in the over-rated activity for three aggregate groups (SN-D, SN-I and SN-H). Since the modulus of elasticity of concrete cylinders prepared with the limestone aggregate (SN-H) decreases rapidly with an increase in the immersion temperature (Savva et al., 2005), the SN-H aggregate can be declared as innocuous because the mortar bars and prisms made with this aggregate produced very low expansions throughout the test durations. As a result, aggregate mineralogy can impact mechanical and expansion properties differently from each other.

Table 4.9: ASR classifications of the trial aggregates based on the loss in mechanical properties (compressive strength and stiffness)

Agg. ID	Aggregate classifications based on loss in compressive strength ^a	Aggregate classifications based on loss in stiffness ^b
SN-A	I	I
SN-B	I	I
SN-C	R	R
SN-D	I	R
SN-E	I	I
SN-F	R	R
SN-G	R	R
SN-H	I	R ^c
SN-I	I	R
SN-J	R	R
NN-A	I	I
NN-B	R	R
NN-C	R	R
NN-D	R ^d	R

^a6-month loss in compressive strength of alkali-cured cylinders, and the loss in alkali-cured cylinders between the ages of 28 days and 180 days of -0.5%

^b6-month loss in stiffness of alkali-cured cylinders of 18%, and the loss in stiffness of alkali-cured cylinders between the ages of 28 days and 180 days of 9%

^cSN-H aggregate classified as limestone (based on its chemical composition) is more susceptible to loss in stiffness

With compared to the loss in ultimate compressive strength of concrete, the static modulus of elasticity was more sensitive to alkali-silica reaction. The ASR reactions in concrete reduced the young's modulus of concrete significantly both at the early and extended immersion ages. Particularly, at the late-age immersion, the effect on modulus of elasticity became more severe due to the extensive cracks developed in the specimens made with the reactive aggregates.

4.4 ASR-induced cracks on the surface of concrete cylinders

The ASR-induced cracks formed on the surface of test cylinders prepared with the trial aggregates were carefully examined. Figure 4.9 shows the 6-month alkali-cured cylinders made with innocuous and highly reactive aggregates, as determined by the 6-month loss in compression strength and stiffness. As seen in Figure 4.9a, the cylinders prepared with innocuous aggregate showed no visible cracks after being submerged in a 1N NaOH solution at 80°C for the test duration of 6 months. On the other hand, the alkali-cured cylinders made with reactive aggregates experienced various patterns of severe cracks on the surface as depicted in Figure 4.9b. The severity of the ASR-induced cracks depended upon the aggregate mineralogy and the extent of its ASR-induced expansion activity.

4.5 Failure Mechanisms of Concrete Cylinders due to ASR

The failure mechanisms of the concrete cylinders in compression were also clearly affected by alkali-silica reactivity. The differences in the crack patterns of the damaged concretes were reflected by the mode of failure and the shape of stress-strain curve. The damaged concretes due to alkali-silica reactivity showed a non-linear increase in the



(a) Cylinders made with the innocuous aggregate (SN-E)



(b) Cylinders made with the reactive aggregate (NN-C)

Figure 4.9: ASR-induced cracks on the surface of the 6-month alkali-cured cylinders made with the (a) innocuous aggregate (SN-E), (b) reactive aggregate (NN-C)

stress-strain curve before the peak compression strength, with a more gradual softening than non-reactive concrete, indicating that extensive meandering and branching of cracks. The strain at any particular stress was the highest for the cylinders cured in alkaline solution at 80°C and the lowest for water-cured cylinders at 20°C at both immersion ages of 28 days and 6 months. The variability in test results increased for the concretes affected by ASR, especially when severe reactions took place.

The failure mode of the undamaged concrete specimens, the cylinders prepared with innocuous aggregates, was conical, as shown in Figure 4.10a, and the specimen failed suddenly with a boisterous sound. Damaged concrete cylinders (incorporated with reactive aggregates) failed in an irregular fashion, which was predominantly by the ASR cracks, as shown in Figure 4.10b, with a crumbling sound. It was observed that the cylinders containing reactive aggregates collapsed with several chunks of concrete through the direction of the loading (Fig. 4.10b).

In addition to inspecting the failure modes of concrete cylinders, discoloration of the specimens was also an indication of alkali-silica reactivity. The ingress of alkaline soak solution to the inside of cylinder specimens through the ASR-induced cracks tended to increase the occurrence of ASR inside of the concrete. Discoloration associated with ASR reactions was probably due to the formation of ASR gels which carbonated with time and exposure to air, became white and hard with desiccation cracks similar to those observed in thin layers of dried mud. Coarse aggregates inside the cylinders of three highly reactive aggregates were also severely affected by ASR at the immersion age of 6 months, for they can easily be crushed by applying pressure with finger tips, suggesting that the strength of the aggregates was deteriorated due to the ASR reaction.



(a) Cylinder made with innocuous agg.



(b) Cylinder made with reactive agg.

Figure 4.10: Failure mode of the 6-month alkali-cured cylinders prepared with the (a) the innocuous aggregate (SN-A), and (b) reactive aggregate (SN-G)

4.6 Aggregate Classifications Based on Eight Evaluation Methods

The ASR classifications of the fourteen trial aggregates were compiled and compared with based on (a) the expansion limits of the mortar bars at early and extended immersion ages, (b) the expansion limits of the alkali-cured prisms at 80°C (ASTM C 1293M1) at early and extended immersion ages, and (c) the loss in ultimate compressive strength and stiffness of concrete cylinders. Additionally, each trial aggregate susceptible to ASR reactivity based on its mineralogy also categorized. Furthermore, the agreement among the evaluation methods for each trial aggregate was explored. The results are documented in Table 4.10.

As can be seen in Table 4.10, the seven aggregate groups (SN-C, SN-F, SN-G, SN-J, NN-B, NN-C and NN-D) were shown reactive, and the two aggregate groups (SN-A and

SN-E) were found innocuous, and the remaining five aggregate groups (SN-B, SN-D, SN-H, SN-I and NN-A) showed conflicting results based on the eight evaluation methods used to identify the extent of alkali-silica reactivity.

Of the eight evaluation methods used, only the three evaluation methods of aggregate mineralogy, and the expansion limits of the ASTM C 1293M1 at early and extended immersion ages declared the SN-B aggregate to be reactive. Since the 4-week failure criteria of ASTM C 1293M1 was found to be unreliable and the aggregate mineralogy (rock type) sometime offered erroneous conclusions on aggregate classifications, the SN-B aggregate was categorized innocuous.

One of the eight evaluation methods, loss in stiffness due to ASR, confirmed SN-H aggregate group (limestone), whereas the remaining seven methods found it to be innocuous. Since the modulus of elasticity of limestone aggregate (SN-H) decreases with an increase in immersion temperature, the SN-H aggregate was classified innocuous.

The aggregate group NN-A were declared reactive based on the two evaluation methods of the mineralogy of aggregate and the 14-day expansion limit of the mortar bars. The above-mentioned two evaluation methods coupled with the loss in stiffness declared the SN-I aggregate group reactive. Since these three evaluation methods declared some innocuous aggregate as reactive, the ASR classifications of SN-I and NN-A aggregates based on the remaining five evaluation methods showed a more consistent reactivity.

Based on the results of the study presented herein, the following conclusions can be made:

- a. Alkali-silica reactivity of trial aggregates evaluated by rock mineralogy showed a strong correlation with the results obtained from ASTM C 1260 at the immersion age of 14 days or those obtained from the alkali-cured prisms at 4 weeks. On the other hand, aggregates showing reactive based on its mineralogy and the expansion limits of mortar bars at 14 days and alkali-cured prisms at 4 weeks occasionally produced conflicting results on the aggregate classification when compared with the remaining five evaluation methods.
- b. The conflicting findings obtained between those of the early-age failure criteria of the ASTM C 1260 and ASTM C 1293M1 were eliminated by extending the test duration to at least 56 days and 3 months, respectively, and by utilizing the expansion limits established for the extended immersion ages.
- c. The ASR classifications of the fourteen trial aggregates based on the proposed failure criteria of the loss in ultimate compressive strength of concrete cylinders made with companion aggregate produced identical conclusions to those determined by the failure criteria of the mortar bars and alkali-cured prisms at the extended immersion ages. However, the failure limit of the loss in stiffness overestimated the level of alkali-silica reactivity for some aggregates. Since the loss in stiffness of concrete cylinders due to alkali-silica reactivity depends on a number of interrelated factors, the aggregate classification made this method may result in a conservative outcome, requiring additional evaluation methods.

Table 4.10: ASR classifications of the trial aggregates based on rock mineralogy, the expansions of mortar bars at early and extended immersion ages and those of alkali-cured prisms at 28 days and extended immersion ages, loss in mechanical properties

Agg. ID	Rock Types ^a	ASTM C 1260			Modified ASTM C 1293M1		Loss of Mechanical Properties		Compatibility among the evaluation methods (out of 8)
		14-Day (0.10%)	Extended Failure Criteria ^b	Extended Failure Criteria ^c	4-Week (0.04%)	Extended Failure Criteria ^d	Loss in compressive strength ^e	Loss in stiffness ^f	
SN-A	I	I	I	I	I	I	I	I	8
SN-B	R	I	I	I	R	R	I	I	5
SN-C	R	R	R	R	R	R	R	R	8
SN-D	R	I	I	I	R	I	I	R	5
SN-E	I	I	I	I	I	I	I	I	8
SN-F	R	R	R	R	R	R	R	R	8
SN-G	R	R	R	R	R	R	R	R	8
SN-H	I	I	I	I	I	I	I	R ^g	7
SN-I	R	R	I	I	I	I	I	R	5
SN-J	R	R	R	R	R	R	R	R	8
NN-A	R	R	I	I	I	I	I	I	6
NN-B	R	R	R	R	R	R	R	R	8
NN-C	R	R	R	R	R	R	R	R	8
NN-D	R	R	R	R	R	R	R	R	8

I = Innocuous; R = Reactive; ^aBased on the previous research findings, as illustrated in Table 2.4

^bExpansion limits of 0.28% at 28 days and 0.47% at 56 days (Islam in this study)

^cExpansion limits of 0.33% at 28 days and 0.48% at 56 days (Roger, 1991; and Hooton & Rogers, 1993)

^dExpansion limits of 0.040, 0.105, 0.165 and 0.285% at 4, 8, 13, and 26 weeks, respectively (Proposed by Islam in this study)

^e6-month loss in compressive strength (alkali-cured vs. water-cured) of 8% and the loss in compressive strength of alkali-cured cylinders between the ages of 28 days and 180 days of -0.50% (Islam in this study)

^f6-month loss in stiffness between alkali- and water-cured of 18% and the loss in stiffness of alkali-cured cylinders between the ages of 28 days and 180 days of 9% (Islam in this study)

^gAggregate classified as limestone, based on its chemical compositions, more sensitive to stiffness (Savva et al., 2005)

- d. It is suggested that an aggregate can be potentially reactive if its expansion of mortar bar exceeds 0.28% at 28 days, or that of the alkali-cured prisms at 80°C exceeds 0.080% at 4 weeks, or the 6-month loss in compressive strength is more than 10%, or the 6-month loss in stiffness exceeds 25%.
- e. The outcomes of this study suggest that no single test is capable of providing a definitive assessment on the alkali-aggregate reactivity of an aggregate. However, the combination of standard test methods, coupled with the historical performance records, can provide a reliable assessment on the potential for alkali-aggregate reactivity.
- f. The seven aggregate groups (SN-C, SN-F, SN-G, NN-J, NN-B, NN-C, and NN-D), determined by the eight evaluation methods were proved to be reactive. The adverse effects of the ASR-related damages (excessive expansion, cracks, and loss in mechanical properties) of these aggregates are alleviated through various mitigation methods which are described in Chapter 5.

CHAPTER 5

CONTROLLING ASR EXPANSION

In this chapter, three mitigation techniques in suppressing the excessive expansion of the reactive aggregates due to alkali-silica reactivity are studied. The first mitigation technique, the most practical and beneficial means of suppressing ASR-induced expansion, is the use of Class F fly ash as a partial replacement of Portland cement by weight. The second mitigation technique employs various amounts of lithium nitrate salt to inhibit severe ASR-induced expansion of the seven selected reactive aggregates. The third mitigation technique deals with the combined use of Class F fly ash and lithium nitrate. The discussion of results for each mitigation technique is presented below.

5.1 Blending Class F Fly Ash as a Partial Replacement of Portland Cement

5.1.1 Introduction

ASTM C 1260 was used to evaluate the effectiveness of Class F fly ash, having CaO content of 7.4%, in controlling ASR-related expansion of seven reactive aggregates for which four aggregates (SN-C, SN-F, SN-G and SN-J) were obtained from the Southern Nevada, and the remaining three (NN-B, NN-C and NN-D) were acquired from the Northern Nevada. The influence of four dosages of Class F fly ash, namely 15, 20, 25 and 30%, as a partial replacement of Portland cement (with alkali content of 0.42% $\text{Na}_2\text{O}_{\text{eq}}$) by weight on the ASR expansion was investigated. The expansion reading of the test mortar bars was taken at the immersion ages of 3, 6, 10 and 14 days, and weekly thereafter up to 98 days. The results of the individual sample are documented in the Appendix C.

The results of the study revealed the strong influence of the trial Class F fly ash dosages in arresting the alkali-silica reactivity of the selected reactive aggregates. A typical ASR expansion of the test mortar bars as related to the investigated fly ash dosages and immersion ages is shown in Figure 5.1. As can be seen, (i) the test mortar bars expanded with an increase in immersion age, and (ii) the expansion of the mortar bars decreased with an increase in fly ash content. The 14-day expansion of the untreated mortar bars made with the SN-F aggregate (0.307%) was reduced to 0.082, 0.057, 0.041 and 0.030% when a portion of Portland cement was replaced by 15, 20, 25 and 30%, respectively, with Class F fly ash. For the same aggregate, the expansion progression for the 15% fly ash at the immersion ages of 28, 56 and 98 days were 2.07, 4.29 and 6.77 times the expansion at 14 days, respectively. The characteristics of the remaining six aggregates followed a similar pattern to that of the SN-F aggregate.

The 14-day expansion of the mortar bars made with each trial reactive aggregate and fly ash dosage is shown in Figure 5.2. Based on the failure criteria of ASTM C 1260 of 0.10%, three of the seven reactive aggregates turned to be innocuous when the 15% Portland cement was substituted by Class F fly ash. For the 20% replacement of Portland cement, the excessive expansion of the SN-J aggregate was entirely suppressed, while the remaining three aggregate (SN-G, NN-B and NN-C) groups were still above the established expansion limit of 0.10%. However, these three aggregates displayed innocuous behavior once fly ash content in the mortar bars was raised to 25% by weight of Portland cement. Finally, blending with the highest fly ash dosage (30%) in the test mortar bars, the 14-day expansion of all selected aggregates was reduced significantly, well below the failure limit of ASTM C 1260.

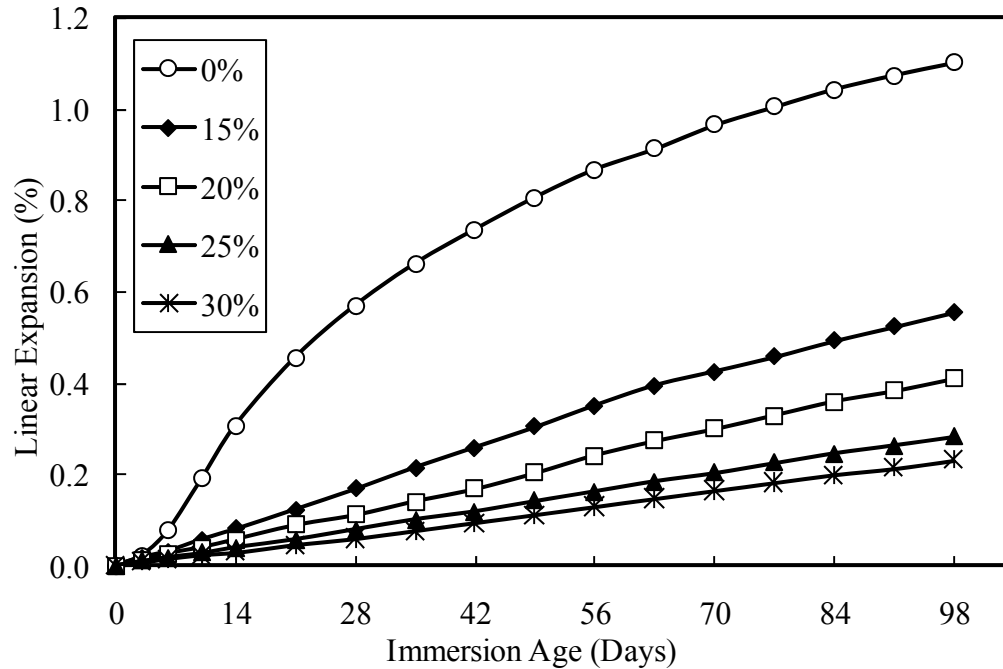


Figure 5.1: Effect of Class F fly ash on the ASR expansion of SN-F aggregate

Figure 5.3 shows the optimum dosages of Class F fly ash in reducing the ASR-induced expansion of the mortar bars made with the trial reactive aggregates at the immersion age of 28 days based on the suggested failure limits of 0.33% (FC1); proposed by Hooton (1991), and Rogers and Hooton (1993); and of 0.28% (FC2), suggested by Islam in this study. As can be noticed, the 15% fly ash was needed to suppress the expansions of the four reactive aggregates below the above mentioned threshold limits. Elevating fly ash content at a dosage of 20% was capable of controlling the expansion of the SN-G aggregate below the threshold limit proposed by Islam in this study. The 28-day expansion criteria of the ASTM C 1260 suggested by Hooton (1991), and Rogers and Hooton (1993) classified the SN-G aggregate as reactive. For the remaining two aggregate groups (NN-B and NN-C), a higher fly ash dosage of 25% was needed in order to produce innocuous behavior under both proposed failure limits.

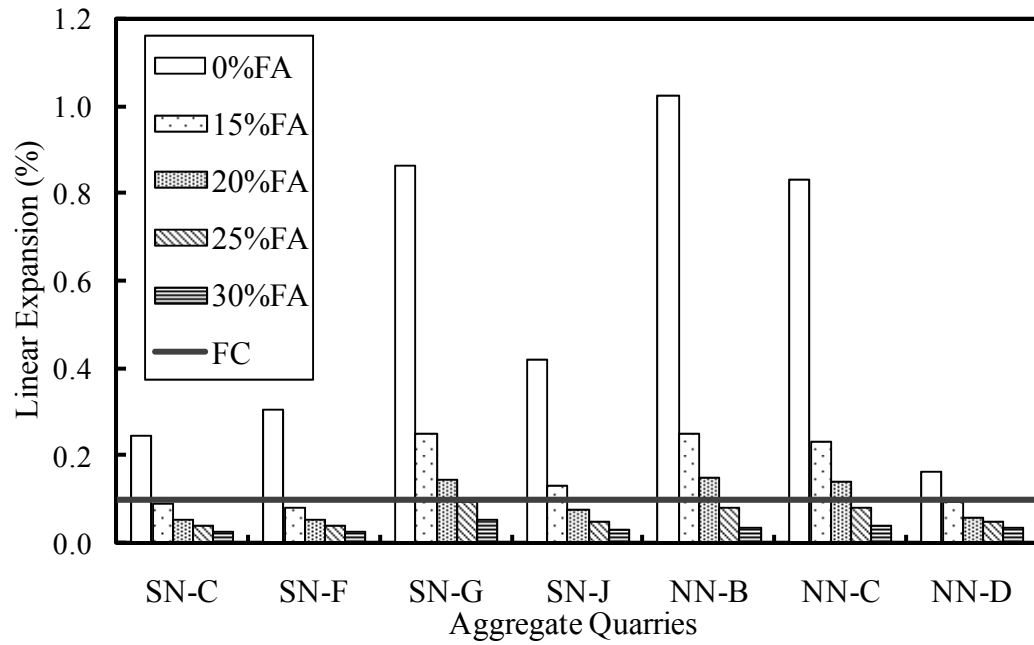


Figure 5.2: The 14-day expansion of mortar bars prepared with trial aggregates and various amounts of Class F fly ash dosages

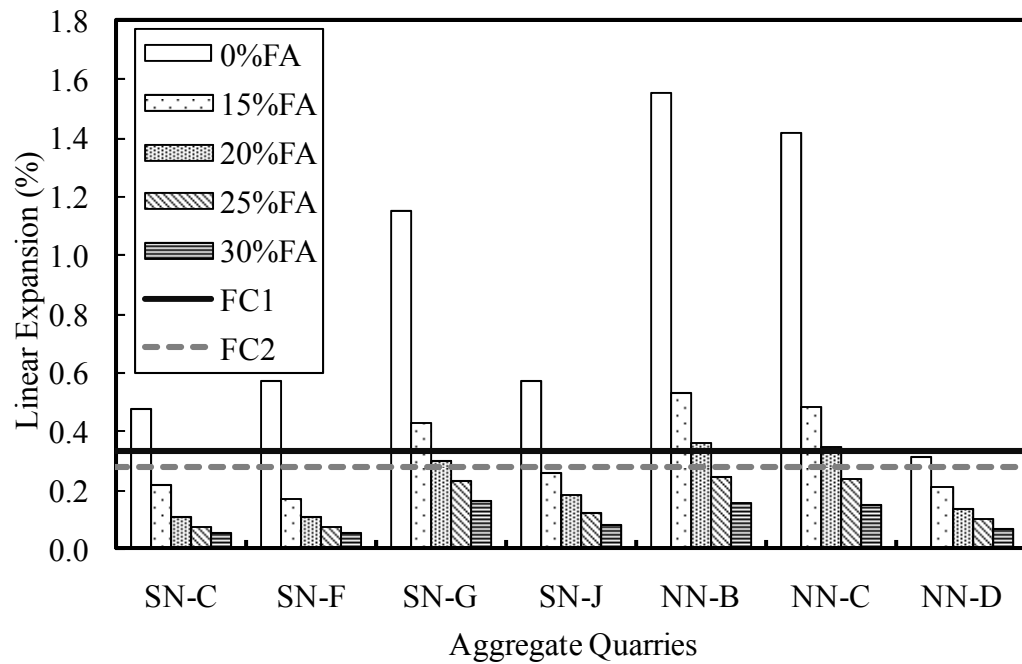


Figure 5.3: The 28-day expansion of mortar bars prepared with trial aggregates and various amounts of Class F fly ash dosages

Figure 5.4 illustrates the 56-day expansion of the mortar bars containing each trial reactive aggregate and Class F fly ash dosage. Utilizing the suggested expansion limits of ASTM C 1260 at the immersion age of 56 days of 0.48% (FC1), proposed by Hooton (1991), and Rogers and Hooton (1993), and that of 0.47% (FC2), suggested by Islam in this study, Figure 5.4 revealed that the use of 15% Class F fly ash was sufficient in suppressing the excessive expansions of the SN-F, SN-J and NN-D aggregates. Elevating cement replacements by Class F fly ash dosages from 15% to 20 and 25%, the ASR-induced expansions of the SN-C and SN-G aggregates were reduced to 0.25 and 0.434%, respectively. Finally, the expansions of the untreated mortar bars containing the remaining two (NN-B and NN-C) aggregates were controlled with the use of 30% Class F fly ash as a partial by weight replacement of Portland cement.

Table 5.1 documents the optimum fly ash dosages required to suppress the excess expansions of the trial reactive aggregates at the immersion ages of 14, 28 and 56 days. As can be seen, the amount of Class F fly ash to inhibit ASR-related expansions of the SN-F and NN-D aggregates at the early age of immersion (14 days) was also shown effective in holding back the adverse effect of ASR at the extended immersion ages of 28 and 56 days. However, for the three aggregates (SN-C, NV-B and NV-C), a higher dosage of Class F fly ash was required to suppress ASR expansions at 28 and 58 days than that required at 14 days. In the case of the SN-J aggregate, the fly-ash-mortar bars generated conflicting results: the use of 15% Class F fly ash was capable of inhibiting ASR-related expansions at 28 and 56 days, whereas this amount was insufficient to reduce the expansion below the expansion limit of 0.10% at 14 days.

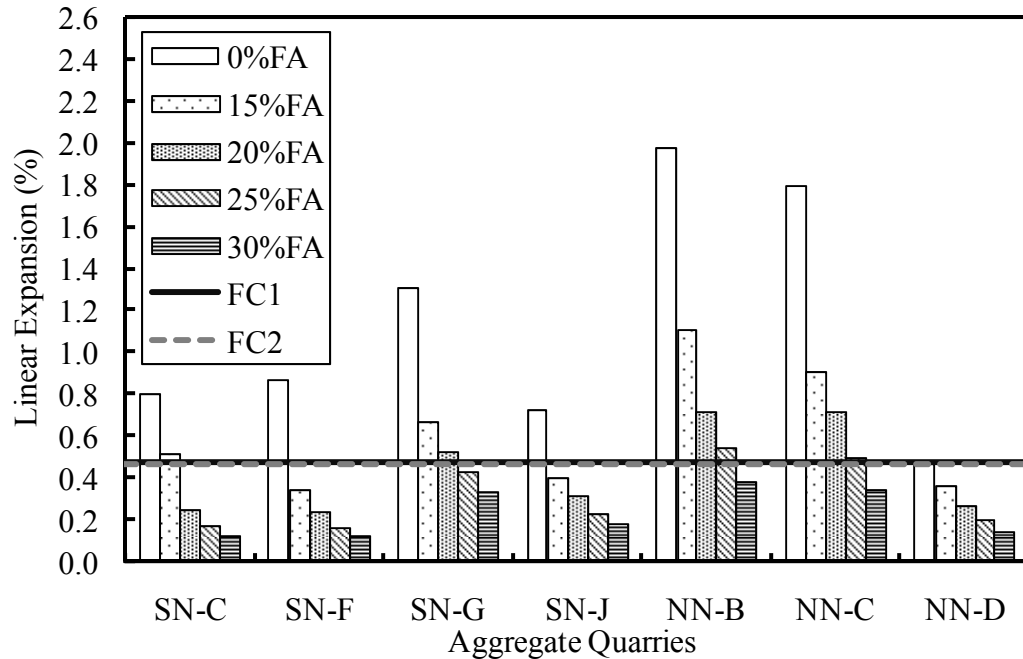


Figure 5.4: The 56-day expansion of the mortar bars prepared with trial aggregates and various amounts of Class F fly ash dosages

It was acknowledged that the 28- and 56-day failure criteria resulted in a good agreement on the classifications of the trial aggregates when treated by various dosages of Class F fly ash with the exception of the SN-G aggregate. For that particular aggregate group, the 20% fly-ash-mortar bars produced 0.30% expansion at the immersion age of 28 days, which resulted in reactive and innocuous based on the expansion limits of 0.33% and 0.28%, respectively. As the alkali-silica reactivity of an aggregate depended on a number of factors, it was recommended to use the minimum amount of Class F fly ash that was sufficient to suppress ASR-related expansions below the 0.10% at 14 days, 0.28% at 28 days and 0.47% at 56 days. To that extent, the recommended optimum Class F fly ash dosages needed to control ASR were: 15% for the SN-F and NN-D aggregates, 20% for the SN-C and SN-J aggregates, 25% for the SN-G aggregate and 30% for the NN-B and NN-C aggregates, respectively. It was concluded that the aggregate that

showed reactive at 14 days and innocuous behavior at the extended immersion ages of 28 and 56 days, described in Chapter 3, required only 15% Class F fly ash with CaO content of 7.4% to restrain the expansions below the prescribed limits of 0.10% at 14 days, 0.28% at 28 days and 0.47% at 56 days.

Table 5.1: Minimum dosage of Class F fly ash to suppress ASR expansion

Agg. ID	14-Day ^a (0.10%)	28-Day		56-Day	
		(0.28%) ^b	(0.33%) ^c	(0.47%) ^b	(0.48%) ^c
SN-C	15	15	20	20	20
SN-F	15	15	15	15	15
SN-G	25	20	25	25	25
SN-J	20	15	15	15	20
NN-B	25	25	30	30	30
NN-C	25	25	30	30	30
NN-D	15	15	0	0	0

^aFailure criteria based on ASTM C 1260

^bFailure criteria proposed by Islam in this study

^cFailure criteria suggested by Hooton (1991); and Rogers & Hooton (1993)

5.1.2 ASR-induced cracks of the mortar bars as related to various fly ash dosages

The cracks on the surface of the test mortar bars due to alkali-silica reactivity were also examined. Figure 5.5 shows the effect of various fly ash contents as related to ASR-induced cracks of the mortar bars containing the NN-B aggregate. As can be seen, the ASR-related cracks of the test mortar bars reduced with an increase in fly ash content. The severe cracks of the untreated specimen (having no fly ash content) (Fig. 5.5a) were significantly reduced when the 15% Portland cement by weight was substituted by Class F fly ash (Fig. 5.5b). The cracks were also eliminated progressively for the mortar bars treated with the 20 and 25% Class F fly ash as shown in Figures 5.5c and 5.5d,

respectively. Lastly, blending 30% Class F fly ash as a partial replacement of Portland cement, the ASR cracks were entirely mitigated (Fig. 5.5e). It can be stated that the diminution of ASR-related cracks of the test mortar bars made with the reactive aggregates is directly linked to the amount of Class F fly ash present in the mortar bar.

5.1.3 Reduction in expansion of the mortar bars made with fly ash dosages

The effectiveness of the four trial Class F fly ash dosages in reducing the ASR-related expansion of the selected reactive aggregates was also expressed in terms of the Reduction in Expansion (RIE) of the untreated mortar bars prepared with the companion test mortar bars at various immersion ages. A typical reduction in expansion of the mortar bars as related to the immersion ages and fly ash contents is illustrated in Figure 5.6. The figure shows that the RIE of the test mortar bars increased with increasing fly ash content, and decreased with an increase in test duration. For each trial fly ash dosage, the RIE at the immersion age of 6 days was the highest, and then gradually decreased with increases in the test duration. After 2 to 3 months of immersion age, the RIE of the test mortar bars became relatively constant; indicating the expansion of the fly ash-specimens was similar to that of the untreated mortar bars. Additionally, the results revealed that the RIE decreased rapidly with an increase in immersion age at lower fly ash content (15%) than that obtained for the higher fly ash-mortar bars. As seen in Figure 5.6 and with an increase in fly ash dosage from 15 to 30% with increments of 5%, the 14-day expansion of the untreated mortar bars made with the SN-J aggregate was reduced by 54.6, 71.6, 78.0 and 82.1%, respectively. The characteristics of the remaining six aggregates demonstrated a similar pattern to that of the SN-J aggregate.



(a) Untreated mortar bars



(b) Treated mortar bars with the 15% Class F fly ash



(c) Treated mortar bars with the 20% Class F fly ash



(d) Treated mortar bars with the 25% Class F fly ash



(e) Treated mortar bars with the 30% Class F fly ash

Figure 5.5: Influence of Class F fly ash dosages on ASR cracks

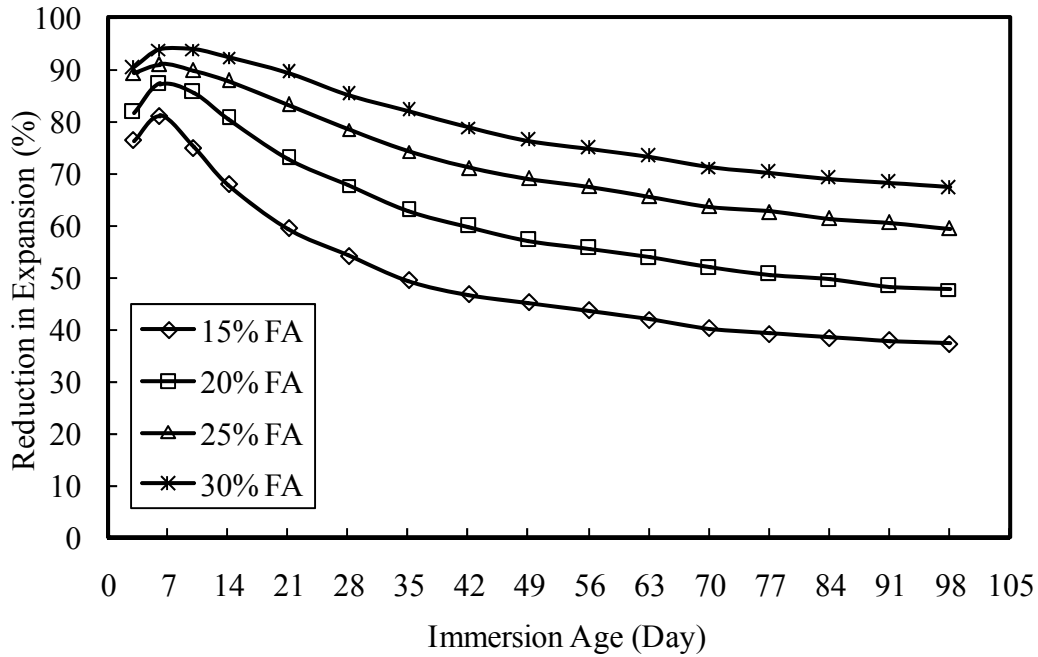


Figure 5.6: Reduction in expansion of the mortar bars made with SN-J aggregate and various rates of fly ash dosage

5.3.1 RIE of the fly-ash-containing mortar bars as a function of immersion age

This section highlights the reduction in expansion of the test mortar bars containing each trial fly ash dosage as related to the immersion ages. Figure 5.7 illustrates the role of 15% Class F fly ash in the mortar bars prepared with the selected reactive aggregates on the reduction in expansion of the untreated specimens at the immersion ages of 14, 28, 56 and 98 days. As can be seen, the RIE of the test specimens decreased rapidly with an increase in immersion age, and that varied extensively from aggregate to aggregate. With compared to the percent reduction in expansion of the test mortar bars at 14, 28, 56 and 98 days, the use of 15% Class F fly ash showed the most effective for the SN-F aggregate, and the least for the NN-D aggregate. For the remaining five aggregates, conversely, the RIE of the 15%-fly-ash-mortar bars over the test duration decreased gradually.

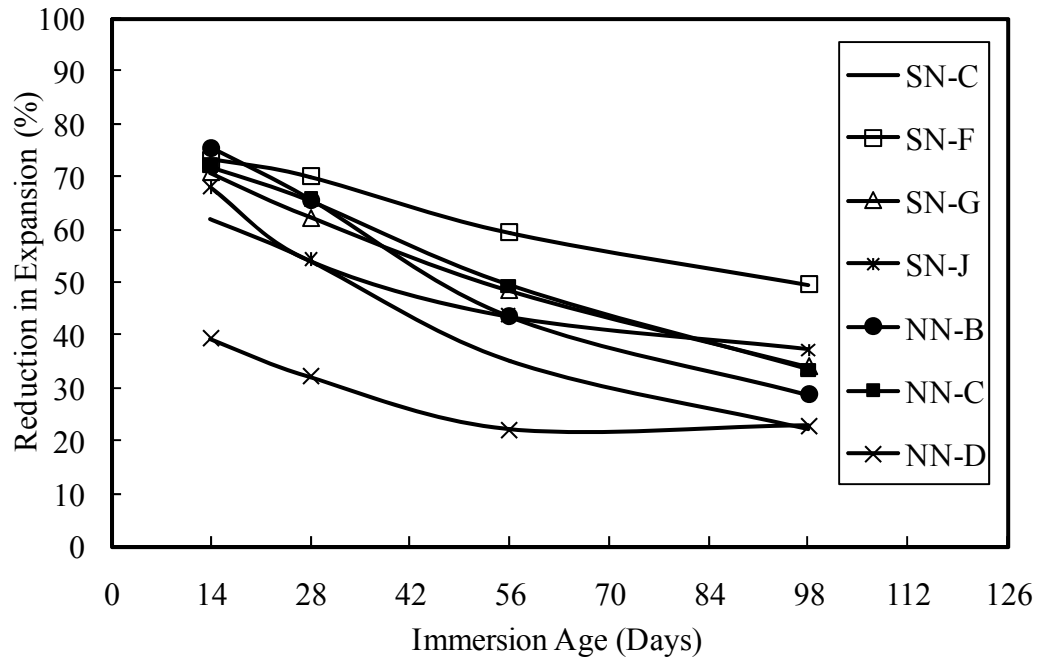


Figure 5.7: RIE of the test mortar bars prepared with the 15% fly ash

The RIE of the test mortar bars increased when the fly ash dosage was elevated from 15 to 20 and 25%, and the variation in the RIE among the trial reactive aggregates decreased. The influence of the 30% Class F fly ash as associated to the reduction in expansion over the test duration of 98 days was evaluated in Figure 5.8. As can be seen, the decrease in the RIE of the mortar bars containing 30% fly ash was fairly moderate for all aggregates at the immersion ages of 14, 28, 56 and 98 days as compared to those made with the 15% fly ash content (Fig. 5.7). As can be seen, a small decrease in the RIE over the immersion age was observed for the SN-C, SN-F and NN-D aggregates, and the trend was slightly steeper for the remaining four aggregates. However, a fairly linear correlation was obtained between the RIE of the 30%-fly ash mortar bars and the test duration.

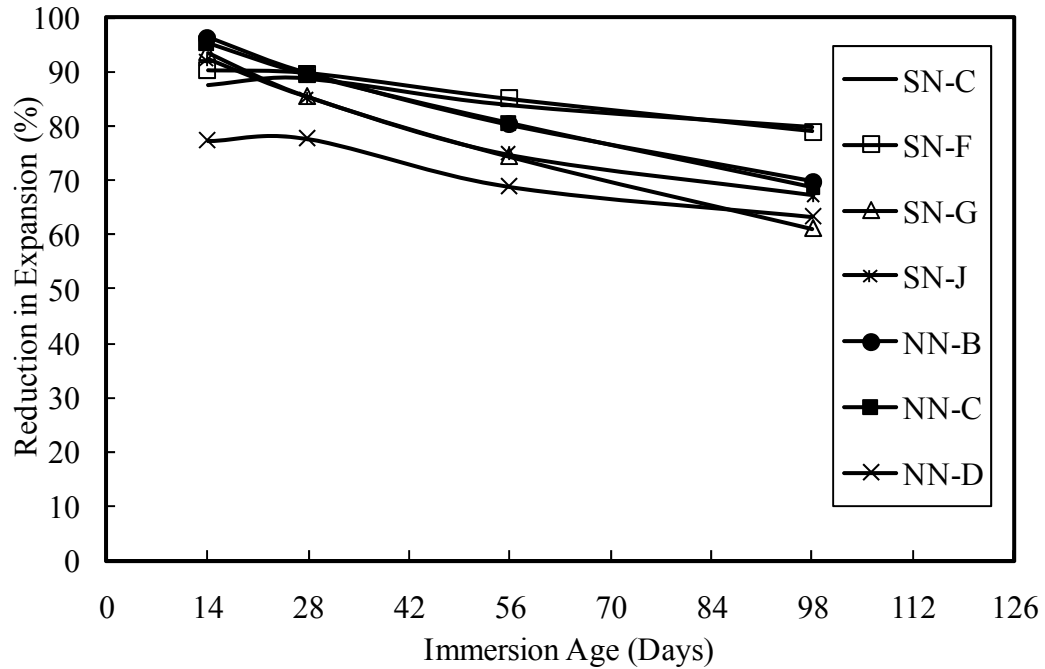


Figure 5.8: RIE of the test mortar bars prepared with the 30% fly ash

5.3.2 RIE of the fly-ash-containing mortar bars as function of fly ash content

The reduction in expansion of the mortar bars as related to the Class F fly ash dosages was evaluated at the immersion ages of 14, 28, 56 and 98 days. The 14-day RIE of the test mortar bars as related to the various fly ash contents is shown in Figure 5.9. As can be seen, the RIE of the mortar bars made with the seven trial reactive aggregates varied from 39.3 to 75.5% with an average of 65.8% for the 15% fly ash, 61.3 to 85.1% with an average of 78.9% for the 20% fly ash, 68.7 to 91.6% with an average of 85.2% for the 25% fly ash, and 77.3 to 96.3% with an average of 90.3% for the 30% fly ash, respectively. The minimum and maximum reduction in expansions due to the four selected fly ash dosages were observed for the mortar bars containing NN-D and NN-B aggregates, which produced the lowest and highest expansions of the untreated mortar bars, respectively. Overall, for all trial aggregates, the increase in the 14-day RIE of the

test mortar bars was fairly gradual with an increase in the fly ash dosages from 15 to 30% as a partial replacement of Portland cement. In general, it can be stated that the 14-day RIE of the test mortar bars is directly related with the ASR-induced expansion of the untreated mortar bars.

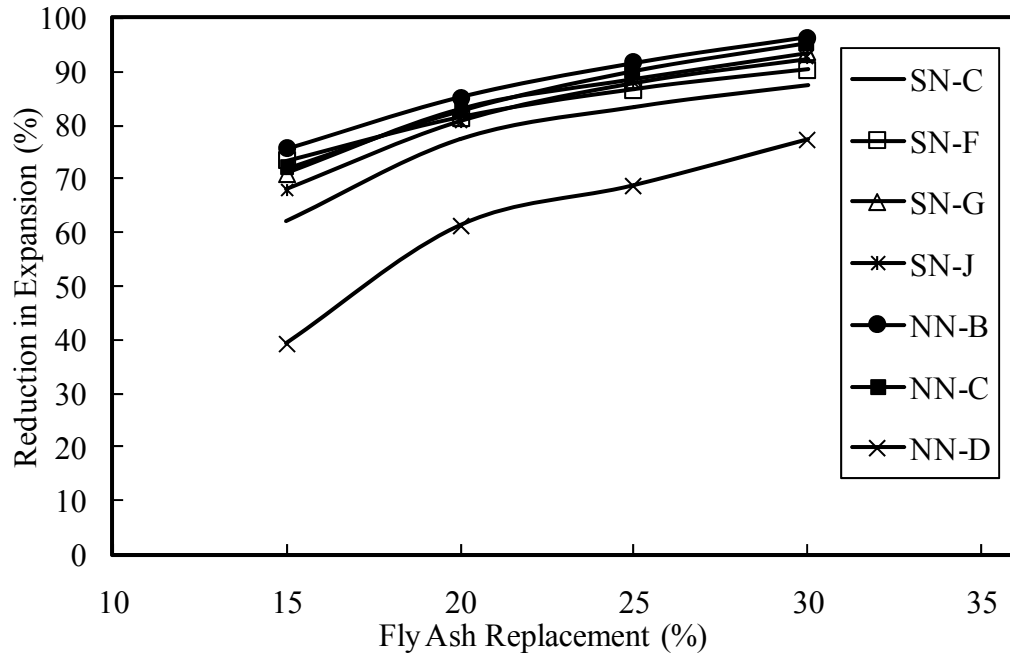


Figure 5.9: RIE of the test mortar bars made with various fly ash dosages at 14 days

As the immersion age prolonged, the variation in the RIE of the fly-ash mortar bars among the selected reactive aggregates increased. Figure 5.10 illustrates the 98-day RIE of the test mortar bars containing four trial Class F fly ash dosages. As can be seen, the 98-day RIE of the trial mortar bars varied from 22.3 to 49.6% for the 15% fly ash, 39.3 to 62.9% for the 20% fly ash, 50.0 to 74.2% for the 25% fly ash, and 61.1 to 79.8% for the 30% fly ash, respectively. At the extended immersion age of 98 days, the maximum and minimum reduction in expansions occurred for the specimens containing SN-F and SN-J

aggregate, respectively. On the whole, the reduction in expansion of all selected aggregates increased gradually with an increase in fly ash dosage except for the SN-C aggregate, for which the RIE increased rapidly between the fly ash dosages of 15 and 20%. For most aggregate groups, the 98-day RIE of the test mortar bars did not follow the expansions of untreated specimens in the descending order.

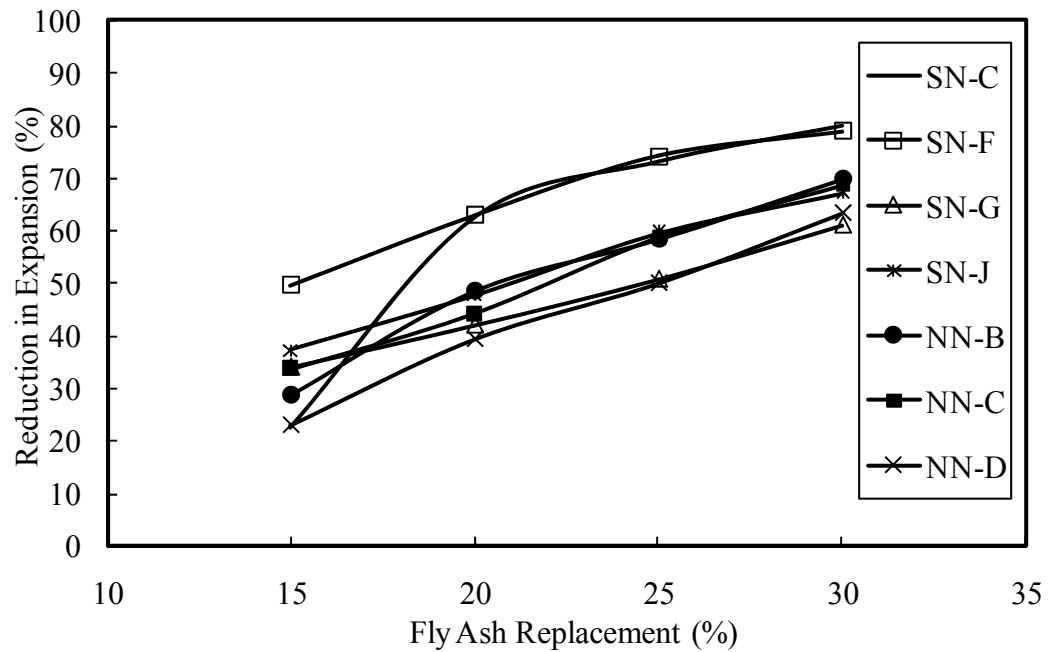


Figure 5.10: RIE of the test mortar bars made with various fly ash dosages at 98 days

At the test durations of 14, 28, 56 and 98 days, the RIE among the trial reactive aggregates differed slightly more for the lower-fly ash mortar bars than that of the higher-fly ash specimens. The variation in the RIE for the higher-fly ash mortar bars increased as compared to that of the lower-fly ash specimens.

5.1.3.3 RIE of the fly-ash-containing mortar bars as related to fly ash dosages and immersion ages

The average reduction in expansion (ARIE) of the test mortar bars prepared with each trial fly ash content and reactive aggregate was also examined at various immersion ages as illustrated in Figure 5.11. As can be seen, a linear correlation existed between the ARIE of the mortar bars containing each trial Class F fly ash dosage and the corresponding immersion ages. Replacing 15, 20, 25 and 30% Portland cement by Class F fly ash, the average reduction in expansions of the untreated mortar bars were reduced by 65.8, 78.8, 85.2 and 90.3% at 14 days, and 32.5, 49.5, 60.6 and 69.8% at 98 days, respectively. The decrease in the ARIE between the immersion ages of 14 and 98 days was 33.2, 29.3, 24.6 and 20.5% for the fly ash dosages of 15, 20, 25 and 30%, respectively. Since the variation in the RIE among the selected aggregates was more for the lower fly ash dosage than that of for higher fly ash content, which demonstrated that the slope of the regression line (ARIE vs. immersion age) became less flattered with increases in fly ash replacements.

5.1.4 Effect of chemical compositions of Class F fly ash on ASR expansion

This section represents the effectiveness of various Class F fly ash dosages in preventing ASR-induced expansion from the viewpoint of the chemical compositions of the secondary cementitious materials of the mixture. The composition of Class F fly ash makes a significant difference in its influence on the ASR-induced expansion (McKeen et al., 1998; Malvar et al., 2002; and Kerenidis, 2007). The chemical evaluations of Class F fly ash have two distinct influences on alkali-silica reaction, such as constituents that take place in pozzolanic reaction reducing expansion and promoting expansion (Malvar et al.

2001, Malvar & Lenke, 2006). The ingredients that reduce expansion, such as SiO_2 , Al_2O_3 , and Fe_2O_3 , can also be replaced by their SiO_2 molar equivalents $[\text{SiO}_{2(\text{eq})}]$ as presented in Equation 5.1. Those that increase expansion, such as CaO , $\text{Na}_2\text{O}_{\text{eq}}$, MgO , and SO_3 , can be substituted by their CaO molar equivalents (CaO_{eq}) as seen in Equation 5.2.

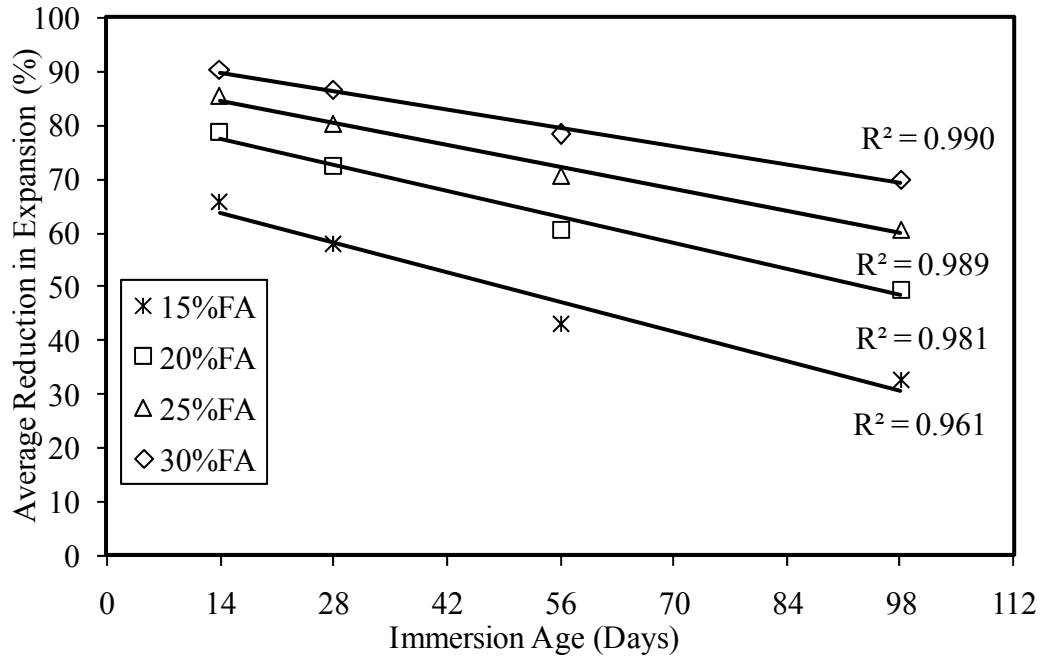


Figure 5.11: The average reduction in expansion (ARIE) of the mortar bars containing eight reactive aggregate and fly ash dosage

$$\text{SiO}_{2\text{eq}} = \text{SiO}_2 + 0.589\text{Al}_2\text{O}_3 + 0.376\text{Fe}_2\text{O}_3 \quad \text{Eq. 5.1}$$

$$\text{CaO}_{\text{eq}} = \text{CaO} + 0.905\text{Na}_2\text{O}_{\text{eq}} + 1.391\text{MgO} + 0.700\text{SO}_3 \quad \text{Eq. 5.2}$$

The efficacy of fly ash compositions in arresting the ASR expansion was also evaluated by analyzing the ratio of equivalent calcium oxide to equivalent silica oxide of the cementitious materials of the mixture. A greater amount of silica in the fly ash (i.e. less amount of CaO) translates a lower Ca/Si ratio at which greater amounts of hydrates

are formed, and thus a greater amount of alkalis are removed from the pore solution (Kerenidis, 2007). Conversely, a higher level of calcium in fly ash elevates the Ca/Si ratio that forms less hydration and thus the decrease in alkalinity will be less pronounced.

The equivalent CaO, SiO₂, and the ratio of equivalent CaO to equivalent SiO₂ contents of the mixtures containing five dosages of Class F fly ash as a partial replacement of Portland cement is shown in Table 5.2. The computations were made on a weight and composition basis of each cementitious material, Portland cement and Class F fly ash, in each trial mixture. The percent fly ash content (FA) vs. CaO_{eq}, SiO_{2(eq)} and the ratio of CaO_{eq} and SiO_{2(eq)} content of the mixture showed a perfect linear correlation with R² values of 1.0, 1.0 and 0.98, as presented in Equations 5.3, 5.4 and 5.5, respectively.

Table 5.2: SiO_{2(eq)}, CaO_{eq} and CaO_{eq}/SiO_{2(eq)} of SCMs in the mortar bars

Fly Ash Replacement (%)	SiO _{2(eq)} ^a (%)	CaO _{eq} ^b (%)	CaO _{eq} /SiO _{2eq}
0	24.40	71.84	2.94
15	31.61	62.27	1.97
20	34.02	59.07	1.74
25	36.42	55.88	1.53
30	38.83	52.69	1.36

^aUsing Equation 5.1; ^bUsing Equation 5.2

$$\text{FA (\%)} = 2.079(\text{SiO}_{2\text{eq}}) - 50.723 \quad \text{Eq. 5.3}$$

$$\text{FA (\%)} = -1.5663(\text{CaO}_{\text{eq}}) + 112.530 \quad \text{Eq. 5.4}$$

$$\text{FA (\%)} = -18.841(\text{CaO}_{\text{eq}}/\text{SiO}_{2\text{eq}}) + 53.597 \quad \text{Eq. 5.5}$$

5.1.4.1 Effect of equivalent SiO₂ of the SCMs on ASR expansion

This section describes the equivalent SiO₂ content of SCMs in the trial mortar bars which was capable to suppress ASR-induced expansion below the adopted failure limits of mortar bars at various immersion ages. A typical expansion of the test mortar bars as related to the equivalent SiO₂ of the SCMs is shown in Figure 5.12. As can be seen, the expansion of the NN-D aggregate decreased with increasing equivalent SiO₂ of the mixture. The equivalent SiO₂ content of the test specimens, which corresponded various fly ash content, and the expansion of these mortar bars revealed a linear correlation with a R^2 value of 0.982. The expansion behavior of the mortar bars containing the remaining six aggregates and the four dosages of Class F fly ash displayed a similar trend to that of the NN-D aggregate. The statistical parameters of the regression line, such as slope (m), intercept (c) and co-efficient of multiple determination (R^2), for each reactive aggregate at the ages of 14, 28 and 56 days are tabulated in Table 5.3. The R^2 values in Table 5.3 indicated a good correlation between the expansions of the mortar bars and the equivalent SiO₂ content of the mixtures containing each trial reactive aggregate at three distinct immersion ages.

The slope and intercept of Equation 5.6 for the trial reactive aggregates were also expressed as a function of untreated expansion of the corresponding mortar bars at the immersion ages of 14, 28 and 56 days. Figure 5.13 shows the relationship between the slopes of the regression line and the expansions of the untreated mortar bars at the immersion age of 14 days. As can be seen, the slope of the regression line increased with an increase in the expansion of the untreated mortar bar, and the correlation was followed by Equation 5.7. The slopes of the regression lines at the test durations of 28 and 56 days

were followed to a similar pattern to that of Equation 5.7, and were presented in Equations 5.8 and 5.9, respectively. Prob(F) of the regression Equations 5.7, 5.8 and 5.9 was shown as 0.0 with a R^2 values of 0.999, 0.998 and 0.994, respectively.

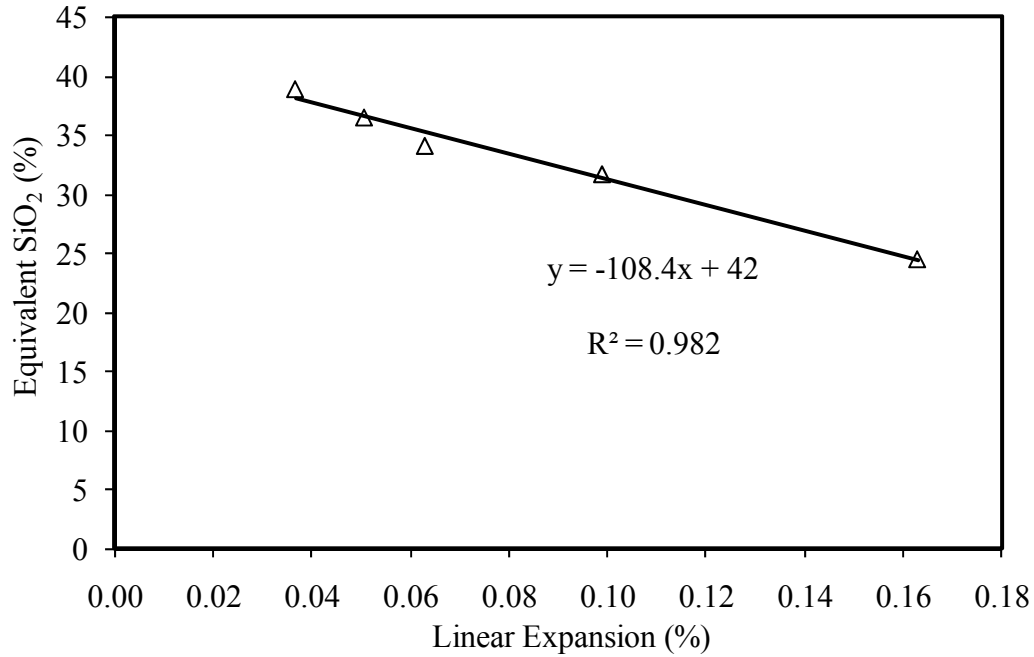


Figure 5.12: The 14-day expansion of the mortar bars made with the NN-D aggregate as related to the SiO_{2(eq)} of the specimen

$$\text{SiO}_{2(\text{eq})} = m E + c \quad \text{Eq. 5.6}$$

where:

E is the expansion of mortar bars containing 0, 15, 20, 25 and 30% Class F fly ash dosages as a partial replacement of Portland cement

m and c are the slope and intercept, respectively

Table 5.3: The statistical data for Equation 5.6 for each trial reactive aggregate at various immersion ages

Agg. ID	14-Day			28-Day			56-Day		
	Slope (m)	Intercept (c)	R ²	Slope (m)	Intercept (c)	R ²	Slope (m)	Intercept (c)	R ²
SN-C	-60.17	38.70	0.93	-31.57	39.00	0.96	-19.31	40.30	0.96
SN-F	-45.18	37.73	0.89	-24.89	37.99	0.90	-17.90	39.34	0.95
SN-G	-15.96	37.57	0.91	-13.36	39.17	0.93	-14.17	42.34	0.97
SN-J	-33.67	37.88	0.93	-28.16	39.94	0.97	-25.77	42.72	0.99
NN-B	-12.96	37.07	0.90	-9.48	38.47	0.93	-8.67	41.29	0.98
NN-C	-16.43	37.43	0.92	-10.48	38.60	0.93	-9.69	41.32	0.98
NN-D	-108.45	42.00	0.98	-56.80	42.53	0.98	-42.12	45.35	0.96

$$m_{14-d} = 8.84 + \frac{(-20.7)}{E_{14-d}^{0.5}} + \frac{(-1.76)}{E_{14-d}^2} \quad \text{Eq. 5.7}$$

$$m_{28-d} = 4.52 + \frac{(-16.1)}{E_{28-d}^{0.5}} + \frac{(-3.2)}{E_{28-d}^2} \quad \text{Eq. 5.8}$$

$$m_{56-d} = -0.33 + \frac{(-10.2)}{E_{56-d}^{0.5}} + \frac{(-6.2)}{E_{56-d}^2} \quad \text{Eq. 5.9}$$

Where:

m_{14-d} , m_{28-d} and m_{56-d} are the slopes of the regression line at 14, 28 and 56 days, respectively

E_{14-d} , E_{28-d} and E_{56-d} are the untreated expansions at 14, 28 and 56 days, respectively

Figure 5.14 shows the intercept of Equation 5.6 for each trial aggregates as related to the untreated expansion of the companion aggregate sources at the immersion age of 14 days. As can be seen, the value of the intercept decreased with an increase in the expansion of the untreated mortar bars. The trend of the curve is represented in Equation 5.10. The expansion of untreated test mortar bars at the extended immersion ages of 28 and 56 days vs. the slope of the regression line showed a similar pattern to that of at 14 days, as documented in Equations 5.11 and 5.12, respectively. The

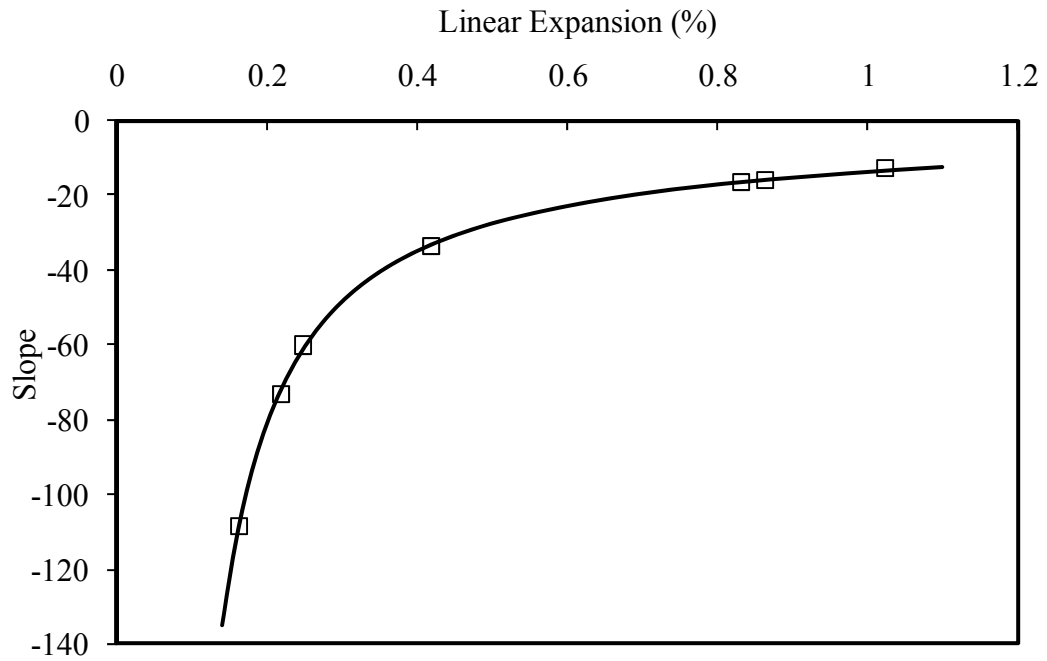


Figure 5.13: The expansion of the untreated mortar bars and the slopes of Equation 5.6 at the immersion age of 14 days

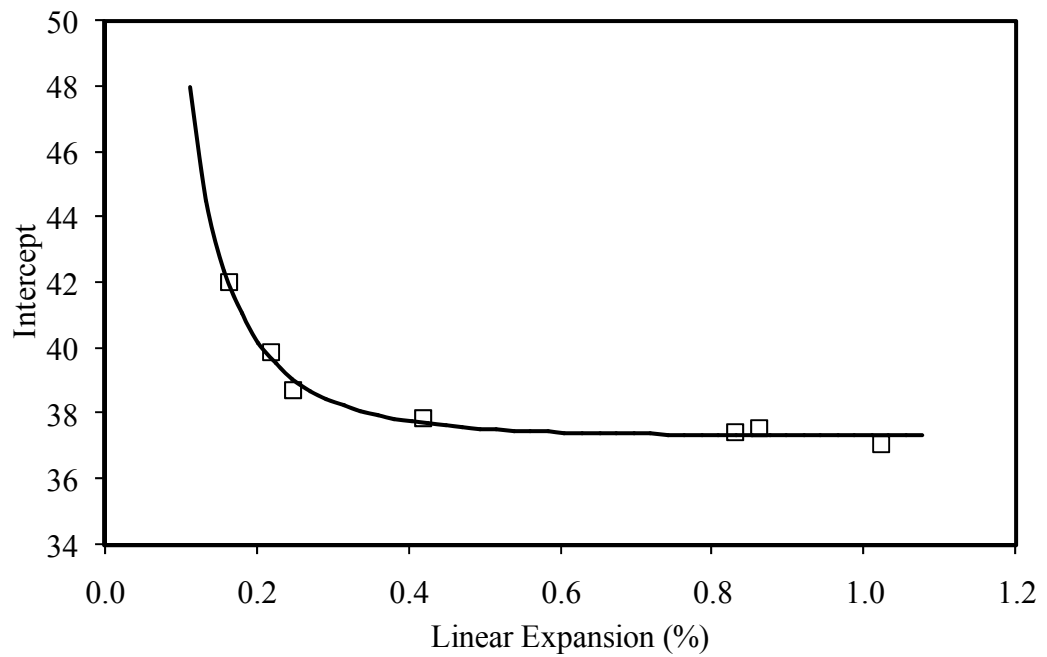


Figure 5.14: The expansion of the untreated mortar bars and the intercept of Equation 5.6 at the immersion age of 14 days

coefficient of multiple determination (R^2) with more than 0.99, and Prob(F) of 0.0 for the Equations 5.10-5.12 indicated a good fit between the expansions of untreated specimens and the equivalent SiO_2 of the trial mixtures.

$$c_{14-d} = 37.81 + \frac{(-0.6)}{E_{14-d}^{0.5}} + \frac{0.15}{E_{14-d}^2} \quad \text{Eq. 5.10}$$

$$c_{28-d} = 40.04 + \frac{(-1.9)}{E_{28-d}^{0.5}} + \frac{(0.6)}{E_{28-d}^2} \quad \text{Eq. 5.11}$$

$$c_{56-d} = 41.4 + \frac{(-0.25)}{E_{56-d}^{0.5}} + \frac{1}{E_{56-d}^2} \quad \text{Eq. 5.12}$$

Where:

c_{14-d} , c_{28-d} and c_{56-d} are the intercepts of the regression line at 14, 28 and 56 days, respectively

E_{14-d} , E_{28-d} and E_{56-d} are the expansions of the untreated mortar bars at 14, 28 and 56 days, respectively

The slope and intercept of Equation 5.6 for each trial aggregate at the immersion age of 14 days were computed by introducing the reserve calculation in substituting the expansion of untreated test mortar bars at the corresponding age in Equations 5.7 and 5.10, respectively. The amount of equivalent SiO_2 of the mortar bar required to suppress the 14-day expansion of each trial reactive aggregate below the failure criteria of 0.10% was also evaluated by substituting the values of m and c for the companion aggregate sources in Equation 5.6. Finally, Equation 5.3 gave the minimum amount of Class F fly ash to control the alkali-silica reactivity of each trial aggregate. The procedures for determining the minimum analytical Class F fly ash for the investigated reactive aggregates are shown in Table 5.4.

Similarly, the required amount of Class F fly ash, evaluated by the analytical method, in inhibiting the excessive expansion of the trial aggregates below the expansion limits of

0.28 and 0.33% at 28 days and 0.47 and 0.48% at 56 days was determined, and the results are shown in Tables 5.5 and 5.6, respectively.

Table 5.4: The optimum fly ash content for the trial aggregates to suppress ASR expansion at the immersion age of 14 days

Agg. ID	Expansion of untreated mortar bar (%)	Statistical parameters		Expansion of treated mortar bars (%)	Analytical fly ash content (%) ^c
		m^a	c^b		
SN-C	0.247	-60.50	38.78	0.099	18.09
SN-F	0.307	-15.80	37.36	0.082	23.71
SN-G	0.862	-46.05	38.03	0.099	20.50
SN-J	0.418	-32.35	37.51	0.080	21.81
NN-B	1.023	-13.49	37.41	0.086	24.65
NN-C	0.830	-16.37	37.35	0.084	24.08
NN-D	0.163	-108.26	41.96	0.099	14.22

^aUsing Equation 5.7; ^bUsing Equation 5.10; ^cUsing Equation 5.5

Table 5.5: The optimum analytical fly ash dosages to suppress ASR expansion at 28 days

Agg. ID	Expansion of untreated mortar bar (%)	Expansion of treated mortar bar (%)		Fly ash dosage to control ASR expansion	
		Below 0.33% ^a	Below 0.28% ^b	Below 0.33% ^a	Below 0.28% ^b
SN-C	0.475	0.218	0.218	17.35	17.35
SN-F	0.569	0.17	0.17	21.73	21.73
SN-G	1.151	0.300	0.280	21.79	22.32
SN-J	0.57	0.261	0.261	16.79	16.79
NN-B	1.549	0.251	0.251	24.72	24.72
NN-C	1.414	0.244	0.244	24.41	24.41
NN-D	0.312	0.312	0.212	0.67	12.45

^aProposed by Hooton (1991); and Rogers & Hooton (1993)

^bSuggested by Islam in this study

Table 5.7 represents the required minimum experimental and analytical fly ash dosages needed to arrest the excessive expansion of the selected reactive aggregates at the immersion ages of 14, 28 and 56 days. As can be seen, there was a good agreement between the experimental and analytical results for the five of seven aggregate sources at the above mentioned three immersion ages. For the remaining two aggregates (SN-C and SN-F), the difference in the optimum fly ash dosages evaluated by the experimental procedure and analytical model was less at the early immersion age of 14 days than that of at the extended immersion ages of 28 and 56 days.

Table 5.6: The optimum analytical fly ash dosages to suppress ASR expansion at 56 days

Agg. ID	Expansion of untreated mortar bars (%)	Expansion of treated mortar bars (%)		Fly ash dosage to suppress ASR expansion (%)	
		Below 0.48% ^a	Below 0.47% ^b	Below 0.48% ^a	Below 0.47% ^b
SN-C	0.799	0.250	0.250	27.17	27.17
SN-F	0.867	0.434	0.434	20.36	20.36
SN-G	1.305	0.424	0.424	24.97	24.97
SN-J	0.725	0.409	0.409	18.64	18.64
NN-B	1.975	0.389	0.389	28.06	28.06
NN-C	1.794	0.352	0.352	28.40	28.40
NN-D	0.471	0.471	0.471	2.05	2.05

^aProposed by Hooton (1991); and Rogers & Hooton (1993)

^bSuggested by Islam in this study

As the amount of Class F fly ash needed to control alkali-silica reactivity of the reactive aggregates depended on the physio-chemical properties of the aggregates and cementitious materials in the mixture, the recommended minimum fly ash dosage that would be capable of holding back the untreated expansions below the threshold limits of 0.1% at 14 days, 0.28% at 28 days and 0.47% at 56 days. The analytical model provides

an idea in selecting Class F fly ash dosages to suppress the alkali-silica reactivity at the immersion ages of 14, 28 and 56 days for the aggregates having known expansion of the untreated mortar bars at the corresponding immersion ages. However, it can be suggested that each reactive aggregate source needs to be tested by using the job cement before it is used in concrete.

Table 5.7: Comparison between the experimental fly ash dosages (EFA) and the analytical fly ash dosages (AFA), evaluated by using the equivalent SiO_2 content of the mortar bar, to inhibit ASR at different immersion ages

Agg. ID	14-Day ^a		28-Day				56-Day			
	EFA (%)	AFA (%)	Proposed by previous studies ^b		Proposed by Islam in this study		Proposed by previous studies ^b		Proposed by Islam in this study	
			EFA (%)	AFA (%)	EFA (%)	AFA (%)	EFA (%)	AFA (%)	EFA (%)	AFA (%)
SN-C	15.0	18.09	15.0	17.35	15.0	17.35	20.0	27.17	20.0	27.17
SN-F	15.0	23.71	15.0	21.73	15.0	21.73	15.0	20.36	15.0	20.36
SN-G	25.0	20.50	20.0	21.79	25.0	22.32	25.0	24.97	25.0	24.97
SN-J	20.0	21.81	15.0	16.79	15.0	16.79	20.0	18.64	20.0	18.64
NN-B	25.0	24.65	25.0	24.72	25.0	24.72	30.0	28.06	30.0	28.06
NN-C	25.0	24.08	25.0	24.41	25.0	24.41	30.0	28.40	30.0	28.40
NN-D	15.0	14.22	0.0	0.67	15.0	12.45	0.0	2.05	0.0	2.05

^aProposed by ASTM C 1260

^bProposed by Hooton (1991); and Rogers & Hooton (1993)

5.1.4.2 Effect of equivalent CaO content of the mortar bars on the ASR expansion

In this section, the equivalent CaO of the mixtures was utilized to evaluate the optimum fly ash dosages to inhibit the alkali-silica reactivity of the investigated reactive aggregates at the ages of 14, 28 and 56 days. The procedures were similar to those for determining Class F fly ash by using the equivalent SiO_2 of the mixture, as described in the previous section.

The ASR-induced expansion of the test mortar bars showed a linear correlation with the amount of equivalent CaO in the mixture; the expansion decreased with an increase in the equivalent CaO in the mortar bars. The slope and intercept of the regression line (expansion of the test mortar bars vs. the equivalent CaO of the SCMs in the mortar bar) were determined for each reactive aggregate at the three immersion ages of 14, 28 and 56 days. The slope and intercept of the regression line were expressed as a function of the expansion of the untreated mortar bars.

At first, the slope (m) and intercept (c) of the regression equation of the expansion of the untreated mortar bars made with each trial reactive aggregate vs. the CaO_{eq} of SCMs were obtained at the ages of 14, 28, and 56 days. Using the values of m and c , the expansion of the untreated mortar bars at which it needed to suppress below the expansion limits of 0.10% at 14, 0.28 and 0.33% at 28, and 0.47 and 0.48% at 56 days provided the optimum amount of Class F fly ash dosages. The effective experimental and analytical fly ash dosages required to control alkali-silica reactivity of the trial reactive aggregates at the three immersion ages are tabulated in Table 5.8. As can be seen, a good agreement existed between the minimum required experimental and analytical fly ash contents. The optimum fly ash dosages evaluated by the experimental program and analytical model showed a better agreement at 14 days than those obtained for the extended immersion ages.

5.1.4.3 Effect of the ratio of equivalent CaO to equivalent SiO_2 of the mortar bars on ASR expansion

The optimum analytical fly ash dosages that were capable of controlling the alkali-silica reactivity of each trial reactive aggregate at the immersion ages of 14, 28 and 56 days were also evaluated using the combined use of equivalent CaO and SiO_2 of the

mixtures and the expansion of the untreated test mortar bars at the corresponding immersion ages. The procedures were identical to those used for the determination of analytical fly ash dosage by using the equivalent SiO_2 of the mortar bars. Table 5.9 documents the minimum required experiment and analytical fly ash dosages at which the expansion of the untreated specimens containing each selected reactive aggregate reduced below the prescribed expansion limits of 0.1% at 14 days, 0.28 and 0.33% at 28 days and 0.47 and 0.48% at 56 days. As can be seen, the estimated amount of Class F fly ash dosage required to mitigate ASR-related expansions of the trial reactive aggregates at three immersion ages correlated well with those of the experiment results.

Table 5.8: Comparison between the experimental fly ash dosage (EFA), and the analytical fly ash dosage (AFA), evaluated by using the equivalent CaO content of the mortar bar, to inhibit ASR at the immersion ages of 14, 28 and 56 days

Agg. ID	14-Day ^a		28-Day				56-Day			
	EFA (%)	AFA (%)	Proposed by previous studies ^b		Proposed by Islam in this study		Proposed by previous studies ^b		Proposed by Islam in this study	
			EFA (%)	AFA (%)	EFA (%)	AFA (%)	EFA (%)	AFA (%)	EFA (%)	AFA (%)
SN-C	15.0	18.06	15.0	17.33	15.0	17.33	20.0	27.15	20.0	27.15
SN-F	15.0	20.47	15.0	21.72	15.0	21.72	15.0	20.35	15.0	20.35
SN-G	25.0	23.69	20.0	21.77	25.0	22.31	25.0	24.96	25.0	24.96
SN-J	20.0	21.79	15.0	16.78	15.0	16.78	20.0	18.63	20.0	18.63
NN-B	25.0	24.64	25.0	24.71	25.0	24.71	30.0	28.04	30.0	28.04
NN-C	25.0	24.07	25.0	24.40	25.0	24.40	30.0	28.39	30.0	28.39
NN-D	15.0	14.18	0.0	0.66	15.0	12.43	0.0	2.04	0.0	2.04

^aProposed by ASTM C 1260

^bBased on the failure criteria suggested by Hooton (1991); and Rogers & Hooton (1993)

Table 5.10 shows the required analytical Class F fly ash dosage to encounter the alkali-silica reactivity of each trial reactive aggregate at the immersion ages of 14, 28 and 56 days based on the equivalent SiO_2 and CaO of the SCMs, and the ratio of equivalent CaO and equivalent SiO_2 of the SCMs. The optimum analytical and experiment Class F fly ash dosages for each trial reactive aggregate are also illustrated in Table 5.10. The minimum analytical Class F fly ash dosages, evaluated by the chemical compositions (the $\text{SiO}_{2(\text{eq})}$, CaO_{eq} , and $\text{CaO}_{\text{eq}}/\text{SiO}_{2(\text{eq})}$ of the mixture for each trial reactive aggregate showed a good agreement. Additionally, the experimental fly ash dosage that was sufficient to inhibit the alkali-silica reactivity showed a good correlation with the analytical fly ash dosage for all reactive aggregates except for the SN-C and SN-F aggregates. The reasons might be due to the aggregate mineralogy, the interactions of the physio-chemical compositions of cementitious materials, and the companion aggregate sources, which may acted differently from one aggregate to another.

Table 5.9: Comparison between the optimum analytical fly ash dosage (AFA), evaluated by using the ratio of CaO_{eq} to $\text{SiO}_{2(\text{eq})}$ of the mortar bars, and the experimental fly ash dosage (EFA) to inhibit ASR at the ages of 14, 28 and 56 days

Agg. ID	14-Day ^a		28-Day				56-Day			
	EFA (%)	AFA (%)	Proposed by previous studies ^b		Proposed by Islam in this study		Proposed by previous studies ^b		Proposed by Islam in this study	
			EFA (%)	AFA (%)	EFA (%)	AFA (%)	EFA (%)	AFA (%)	EFA (%)	AFA (%)
SN-C	15.0	18.12	15.0	17.38	15	17.38	20.0	27.23	20	27.23
SN-F	15.0	23.85	15.0	21.76	15	21.76	15.0	20.44	15	20.44
SN-G	25.0	20.56	20.0	21.84	25	22.39	25.0	24.97	25	24.97
SN-J	20.0	21.91	15.0	16.78	15	16.78	15.0	18.79	15	18.79
NN-B	25.0	24.81	25.0	24.89	25	24.89	30.0	28.04	30	28.04
NN-C	25.0	24.23	25.0	24.55	25	24.55	30.0	28.38	30	28.38
NN-D	15.0	14.27	0.0	1.25	15	12.70	0.0	2.78	15	2.78

^aProposed by ASTM C 1260; ^bHooton (1991); and Rogers & Hooton (1993)

Table 5.10: Optimum analytical Class F fly ash dosage to suppress ASR expansion based on the equivalent SiO_2 , CaO and CaO/SiO_2 of the mixture at the extended failure criteria

Agg. ID	Analytical fly ash dosage (%)			Experimental fly ash dosage (%)
	Based on			
	SiO _{2(eq)}	CaO _{eq}	CaO _{eq} /SiO _{2(eq)}	
SN-C	27.17	27.15	27.23	20
SN-F	20.36	20.35	20.44	15
SN-G	24.97	24.96	24.97	25
SN-J	18.64	18.63	18.79	20
NN-B	28.06	28.04	28.04	30
NN-C	28.40	28.39	28.38	30
NN-D	14.22	14.18	14.27	15

5.2 Adding Lithium Nitrate to the Mixing Water

In this study, the four to six dosages of lithium nitrate, resulting in the lithium-to-alkali molar ratios $[\text{Li}/(\text{Na}+\text{K})]$ of 0.59, 0.74, 0.89, 1.04, 1.18 and 1.33, were added to the mixing water to alleviate the ASR-induced damages of the seven reactive aggregates by using ASTM C 1260. A general agreement in the past research studies existed that about half of the lithium added to suppress ASR-induced expansion was absorbed by the hydrating cement and the uptake of lithium by C–S–H, and the remaining half was available for the suppressive purpose (Stark, 1993; and McKeen et al., 1998). In order to eliminate this concern, the ASTM C 1260 test was modified by adding lithium salt into the alkali soak solution to maintain the same lithium-to-alkali molar ratio in the mortar bars and the soak solution. The expansion readings of the individual mortar bar containing each trial lithium dosage were taken at the immersion ages of 3, 6, 10, 14

days, and weekly thereafter up to 98 days. The results for the trial mortar bars are documented in the Appendix C.

The results of the study clearly revealed that the selected lithium nitrate dosages were effective in reducing the adverse effect of alkali-silica reactivity for each selected reactive aggregates. A typical ASR expansion as a function of the immersion age and various lithium-to-alkali molar ratios is shown in Figure 5.15. As can be seen, the expansion of the test mortar bars increased with an increase in the lithium salt and the test duration. The figure also demonstrated that the untreated mortar bars expanded rapidly at the early age of immersion, and the expansion rate decreased with an increase in immersion age when compared to the untreated mortar bars. The expansion rate of the lithium bearing specimens was fairly small throughout the test duration. Moreover, these treated specimens showed a little tendency to expand after the immersion ages of 2 months.

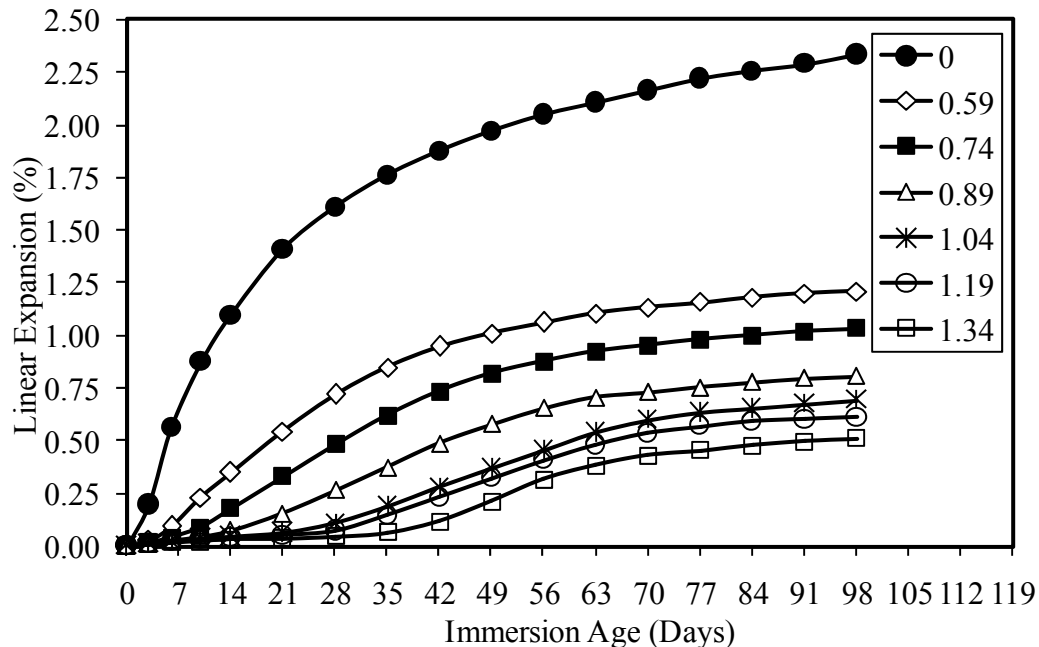


Figure 5.15: Linear expansion of the mortar bars made with NN-B aggregate and various lithium dosages

The ASR-induced expansion of the mortar bars treated with various lithium dosages at the immersion age of 14 days is illustrated in Figure 5.16. As can be seen, the expansion of the test specimens reduced with increasing lithium content. When lithium-to-alkali molar ratio of 0.59 was used, the ASR-induced expansion of the untreated mortar bars was reduced by more than 50% for all reactive aggregates except for the SN-C aggregate. Thus, it is concluded that the use of lithium salt in suppressing alkali-silica reactivity was more effective for the aggregate groups producing a relatively high level of expansion when compared to that of the other trial aggregate groups.

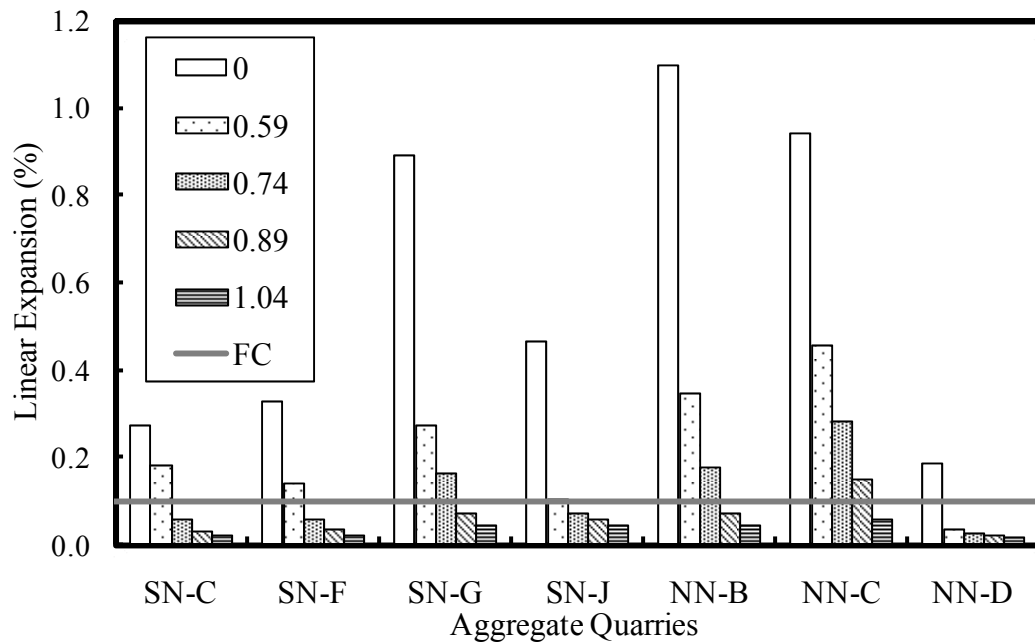


Figure 5.16: The expansions of the mortar bars made with various lithium dosages at 14 days

The optimum lithium dosage in arresting the excessive expansion of the seven reactive aggregates was evaluated based on the 0.10% 14-day expansion limit of ASTM C 1260. The required minimum lithium-to-alkali molar ratios in suppressing the

excessive alkali-silica reactions varied among the trial reactive aggregates. The optimum lithium dosages in controlling the expansion of the untreated mortar bars to the safe limit of 0.10% at 14 days were: 0.59 for the NN-D aggregate, 0.74 for the SN-C, SN-F and SN-J aggregates, 0.89 for the SN-G and NN-B aggregates, and 1.04 for the NN-C aggregate.

The ASR-induced expansions of the lithium bearing mortar bars at the immersion age of 28 days are shown in Figure 5.17. As can be noted, the 28-day expansion limits of the mortar bars of 0.33% (FC1), proposed by Rogers (1991), and Hooton and Rogers (1993), and that of 0.28% (FC2), suggested by Islam in this study, resulted in the optimum lithium-to-alkali molar ratios of 0.59 for the SN-J and NN-D aggregates, 0.74 for the SN-F and SN-G aggregates, and 1.04 for the NN-B and NN-C aggregates, respectively, to limit their ASR expansions below the threshold of 0.28%.

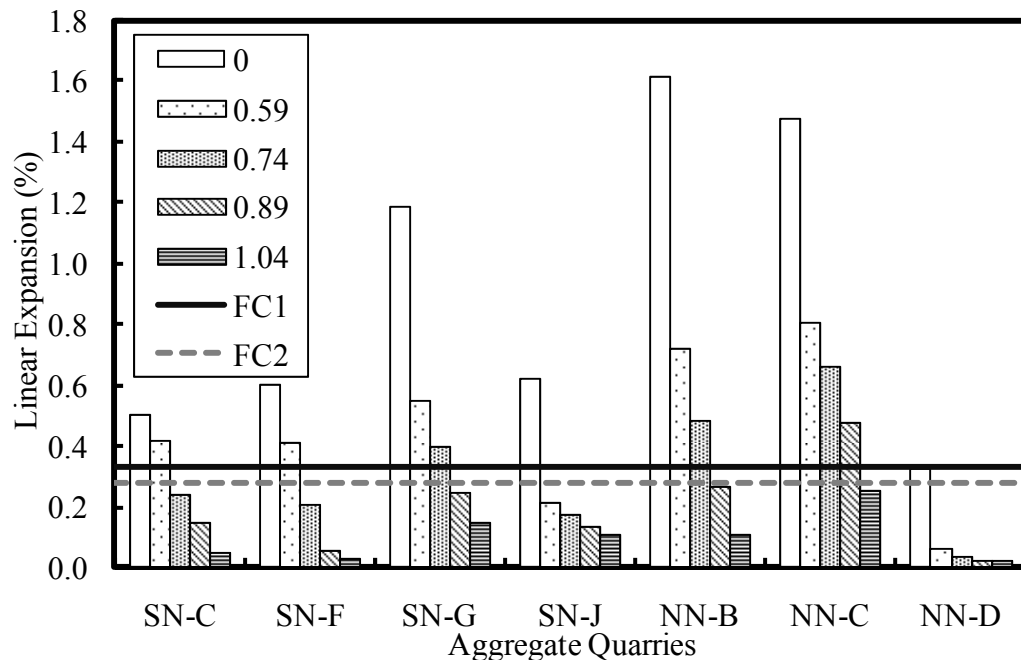


Figure 5.17: The expansions of the mortar bars containing various lithium nitrate dosages at 28 days

Figure 5.18 shows the ASR-related expansions of the test mortar bars prepared with each trial reactive aggregate and lithium-to-alkali molar ratio at the immersion age of 56 days. Using the expansion limits of the mortar bars of 0.48% (FC1), proposed by Roger (1991) and Hooton and Rogers (1993), and of 0.47%, suggested by Islam in this study, the minimum effective lithium-to-alkali molar ratios were 0.59 for the SN-J and NN-D aggregates, 0.74 for the SN-C and SN-F aggregates, 1.04 for the SN-G and NN-B aggregates, and 1.19 for the NN-C aggregate.

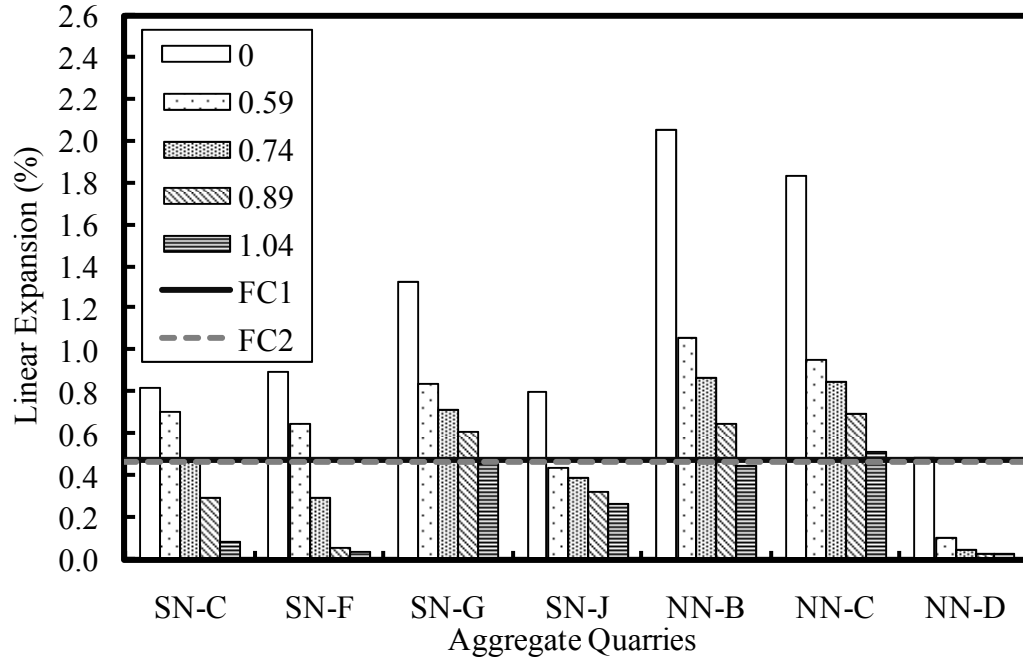


Figure 5.18: The expansions of the mortar bars prepared with various lithium nitrate dosage at 56 days

Table 5.11 documents the optimum amount of lithium nitrate to restrain the excessive expansions caused by alkali-silica reactivity below the failure limits of 0.10% at 14 days, 0.33 and 0.28% at 28 days, and 0.48 and 0.47% at 56 days. As can be seen, for the SN-F, SN-J and NN-D aggregates, the amount of lithium-to-alkali molar ratio to suppress ASR

expansion at the early age of immersion (14 days) was also shown effective in holding back the adverse effect of ASR at the extended immersion ages of 28 and 56 days. In the case of the SN-G, NN-B and NN-C aggregates, a higher lithium dose was required to arrest the excessive expansions due to the alkali-silica reactivity at the immersion age of 56 days as compared to that at 14 and 28 days. The opposite phenomenon was observed for the mortar bars prepared with the SN-J aggregate and lithium-to-alkali molar ratio of 0.59. These specimens produced ASR expansions of more than 0.10% at 14 days (reactive) and less than 0.28% at 28 days and 0.47% at 56 days (innocuous). It was also noticed that the aggregate group NN-D which had been declared reactive at 14 days, and nearly reactive at 28 and 56 days, as described in Chapter 3, required the lithium-to-alkali molar ratio of 0.59 to limit the 14-day expansion below 0.10%.

Table 5.11: Optimum experimental lithium dosage to suppress ASR expansion at 14, 28 and 56 days

Agg. ID	14-Day ^a (0.10%)	28-Day		56-Day		Recommended dosage
		(0.28%) ^b	(0.33%) ^c	(0.47%) ^b	(0.48%) ^c	
SN-C	0.74	0.89	0.74	0.89	0.89	0.89
SN-F	0.74	0.74	0.74	0.74	0.74	0.74
SN-G	0.89	0.89	0.89	1.04	1.04	1.04
SN-J	0.74	0.59	0.59	0.59	0.59	0.74
NN-B	0.89	0.89	0.89	1.04	1.04	1.04
NN-C	1.04	1.04	1.04	1.19	1.19	1.19
NN-D	0.59	0.59	0.59	0.59	0.59	0.59

^aBased on ASTM C 1260; ^bProposed by Islam in this study

^cSuggested by Hooton (1991); and Rogers & Hooton (1993)

Based on the above mentioned results, it is recommended to use the minimum amount of lithium nitrate that is efficient in holding back the ASR expansion below all prescribed

limits at 14, 28 and 56 days. As such, the optimum amount of lithium-to-alkali molar ratio to control the alkali-silica reactivity at the above mentioned three test durations were: 0.59 for the NN-D aggregate, 0.74 for the SN-F and SN-J aggregates, 0.89 for the SN-C aggregate, 1.04 for the SN-G and NN-B aggregates, and 1.19 for the NN-C aggregate. It should be also noted that the results obtained by the Islam's suggested failure criteria confirmed with those obtained from the suggested failure limits proposed by past studies.

5.2.1 ASR-related cracks as function of lithium dosage

The effectiveness of lithium nitrate salt in the mortar bars was also evaluated in terms of the ASR-related cracks on the surface of the test mortar bars, and the results are shown in Figure 5.19. As can be seen, the ASR-induced cracks of the untreated mortar bars reduced with an increase in the lithium content. The severe cracks of the control mortar bars (Fig. 5.19a) were reduced to a limited number of random cracks (Fig. 5.19b) when lithium-to-alkali molar ratio of 0.59 was used. Elevating lithium dosage to 0.74, 0.89 and 1.04, the width and the number of ASR-induced cracks were cut down significantly as shown in Figs. 5.19c, 5.19b and 5.19e, respectively. Finally, the use of the lithium-to-alkali molar ratio of 1.19 nearly eliminated the formation of ASR-related cracks as shown Figure 5.19f.

5.2.1 Reduction in expansion of the lithium-bearing mortar bars

The influence of the four to six dosages of lithium nitrate on the ASR expansion of the test mortar bars made with each selected reactive aggregate was also evaluated in the viewpoint of reduction in expansion (RIE) of the untreated specimens (having no lithium content) at the immersion ages of 14, 28, 56 and 98 days. A general characteristic of the



(a) Untreated mortar bars



(b) Treated mortar bars with the lithium-to-alkali molar ratio of 0.59



(c) Treated mortar bars with the lithium-to-alkali molar ratio of 0.74



(d) Treated mortar bars with the lithium-to-alkali molar ratio of 0.89



(e) Treated mortar bars with the lithium-to-alkali molar ratio of 1.04



(f) Treated mortar bars with lithium-to-alkali molar ratio of 1.19

Figure 5.19: ASR-related cracks on the lithium-bearing mortar bars made with the SN-G aggregate

RIE of the mortar bars as correlated to the lithium dosages and immersion ages is illustrated in Figure 5.20. As can be seen, the RIE increased with an increase in the amount of lithium content in the mortar bars. For each trial lithium dosage, the RIE at the early immersion age of 3 days was highest and then gradually decreased with increases in the test duration. A higher decrease rate of expansion in the early phase of immersion was because the lithium salt was easily available and incorporated in cement during the more active phase of hydration. The decrease in the RIE of the mortar bars over the immersion age was insignificant for the higher lithium-to-alkali molar ratio than that of the specimens made with a lower dosage of lithium salt. The characteristics of the lithium-containing mortar bars prepared with the remaining reactive aggregates showed a similar pattern to that of the NN-C aggregate.

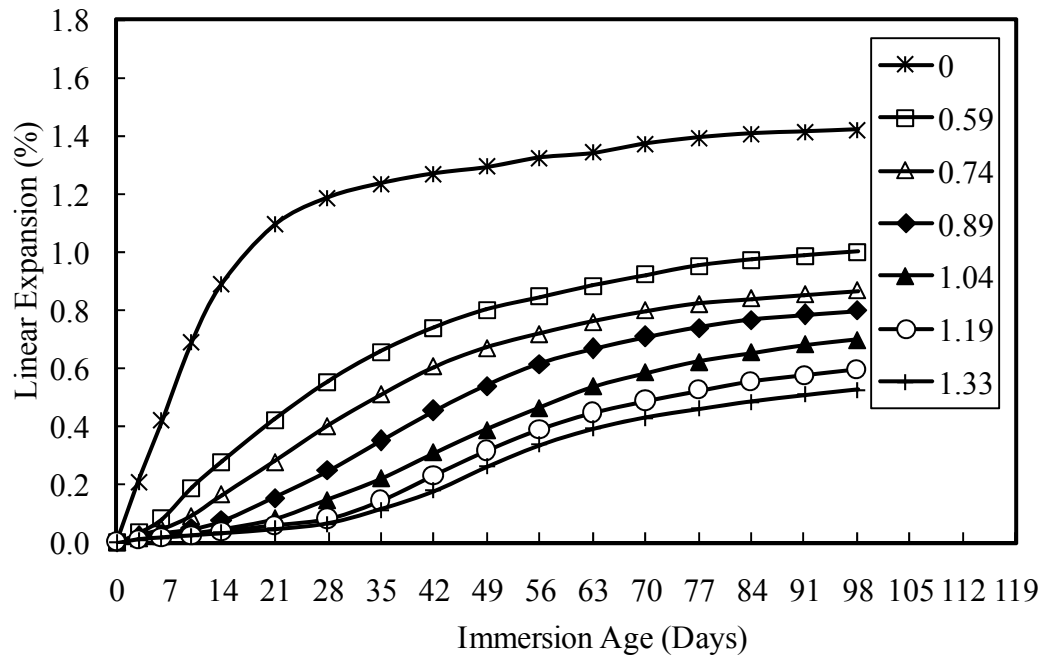


Figure 5.20: The reduction in expansion of the mortar bars made with the NN-C aggregate and various lithium dosages

5.2.1.1 RIE of the lithium-bearing mortar bars as a function of immersion ages

The section describes the influence of the trial lithium dosages at the test durations of 14, 28, 56 and 98 days. The role of lithium-to-alkali molar ratio of 0.59 on the ASR-induced expansion as related to the RIE of the control mortar bars at various immersion ages is illustrated in Figure 5.21. As can be seen, the RIE for the trial aggregates differed at the above mentioned four test durations. For most aggregate groups, the RIE of the mortar bars containing lithium-to-alkali molar ratio of 0.59 was highest at 14 days, and it decreased with an increase in immersion age. In the case of the SN-C, SN-F, NN-B, NN-C and NN-D aggregates, the RIE was nearly constant between the immersion ages of 28 and 98 days. The reduction in expansion for the SN-G and SN-J aggregates was very high at the early stage of immersion and it decreased rapidly with an increase in immersion age. At the extended age of 98 days and the use of lithium-to-alkali molar ratio of 0.59, all curves became stabled and flattened, which demonstrated that increase in expansion of the treated and untreated mortar bars reached a constant value.

The variation in the RIE among the trial reactive aggregates decreased with an increase in lithium dosage. However, the decrease in the RIE was less at the early age of immersion than that of at the extended immersion age. The characteristic of the RIE of the test specimens containing lithium-to-alkali molar ratio of 1.04 over the immersion age of 98 days is depicted in Figure 3.22. The data show that the RIE remained the highest (more than 85%) for the three aggregates (SN-C, SN-F and NN-D) generating the 14-day expansions of untreated mortar bars below 0.35%, and decreased for the remaining four aggregates (SN-G, SN-J, NN-B and NN-C) producing the 14-day expansions exceeding of 0.35%. At the immersion age of 98 days, the RIE dropped to

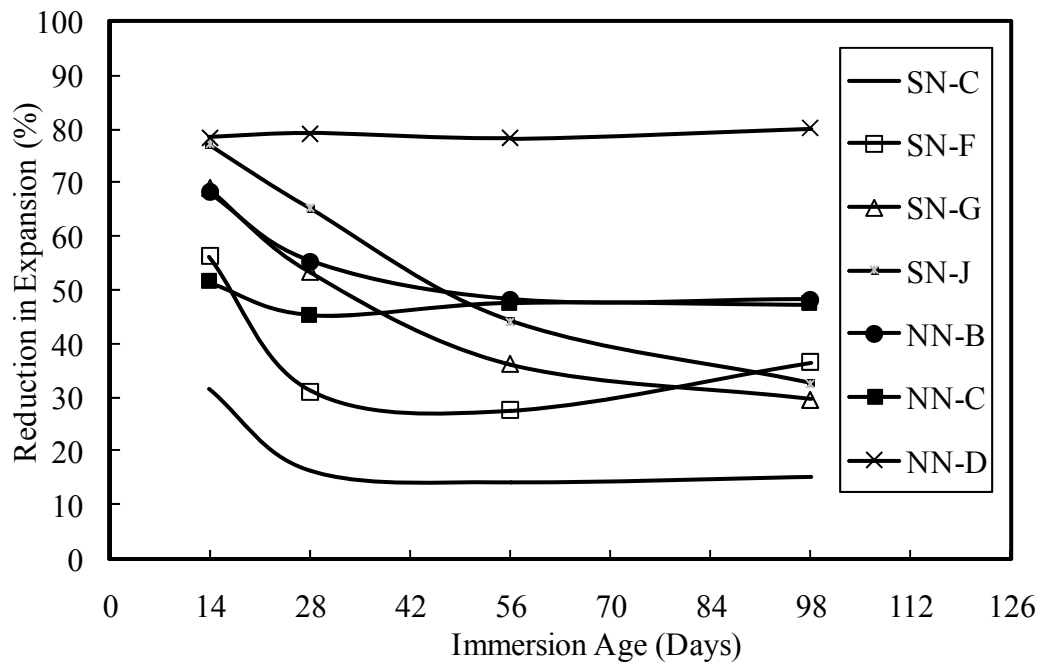


Figure 5.21: The reduction in expansion of the mortar bars treated with the lithium-to-alkali molar ratio of 0.59

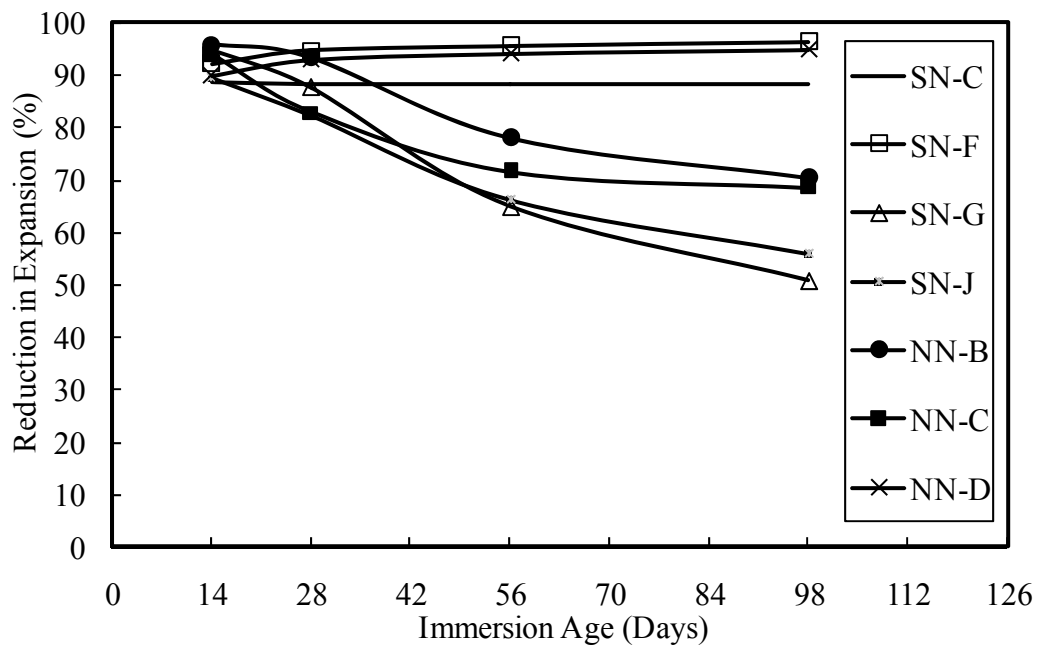


Figure 5.22: The reduction in expansion of the mortar bars treated with the lithium-to-alkali molar ratio of 1.04

50.8, 55.9, 70.3 and 68.5% for the SN-G, SN-J, NN-B and NN-C aggregates, respectively. The results revealed that a higher dosage of lithium salt was more effective to suppress ASR of all trial aggregates both at the early and extended immersion ages.

It was observed that the test duration to achieve a steady RIE depended on the mineralogy, atomic structure of the aggregate and the amount of lithium present in the mixture. However, for all aggregates, the decrease in the RIE over the test duration was less for the higher lithium dosage than that of the lower lithium content. Additionally, when compared to the lower lithium dosages, the variation in the RIE was less pronounced for the higher lithium dosages at the early immersion age than that of the extended test duration.

5.2.1.2 RIE of the lithium-bearing mortar bars as a function of lithium dosages

The trial lithium dosages in the mortar bars as associated to the reduction in expansion of the control mortars at the early age of immersion (14 days) is illustrated in Figure 5.23. As can be observed, the 14-day RIE of the mortar bars containing lithium-to-alkali molar ratio of 0.59 varied among the trial aggregates, and the variation decreased with an increase in lithium content. The 14-day RIE of the test mortar bars containing SN-J and NN-D aggregates was the highest for the lithium-to-alkali molar ratio of 0.59. For these aggregate groups, the increase in the RIE became fairly insignificant with an increase in the lithium dosage. On the other hand, the reduction in expansion of the remaining aggregate groups was low at the lithium dosage of 0.59, and increased rapidly with increasing the lithium-alkali molar ratio up to 0.89, and slowly thereafter. Overall, at the immersion age of 14 days, the required minimum lithium dosage was 0.89 at the level where the RIE for all aggregate groups reached nearly a constant value.

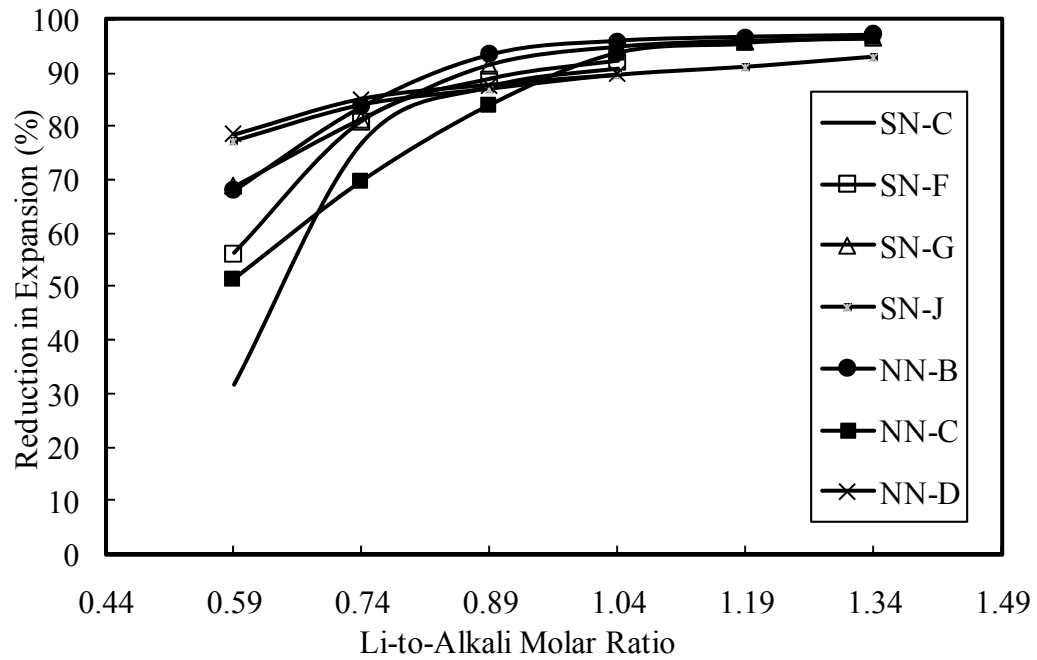


Figure 5.23: The reduction in expansion of the mortar bars made with various lithium dosages at 14 days

Figure 5.24 demonstrates the RIE of the test mortar bars containing the trial lithium dosages at the immersion age of 98 days. As can be seen, the trend of the RIE of the mortar bars vs. lithium dosage was fairly gradual for all aggregate groups except for the SN-C and SN-F aggregates. The 98-day RIE increased rapidly with an increase in lithium dosage up the lithium-to-alkali molar ratios of 1.04 for the SN-C and 0.89 for the SN-F aggregates, respectively. At the extended immersion age of 98 days, the maximum and minimum RIE took place for the mortar bars containing the NN-B and NN-D aggregates, respectively. It was also observed that the variation in the RIE among the trial aggregates incorporated with each lithium-to-alkali molar ratio was more at 98 days than that of at 14 days.

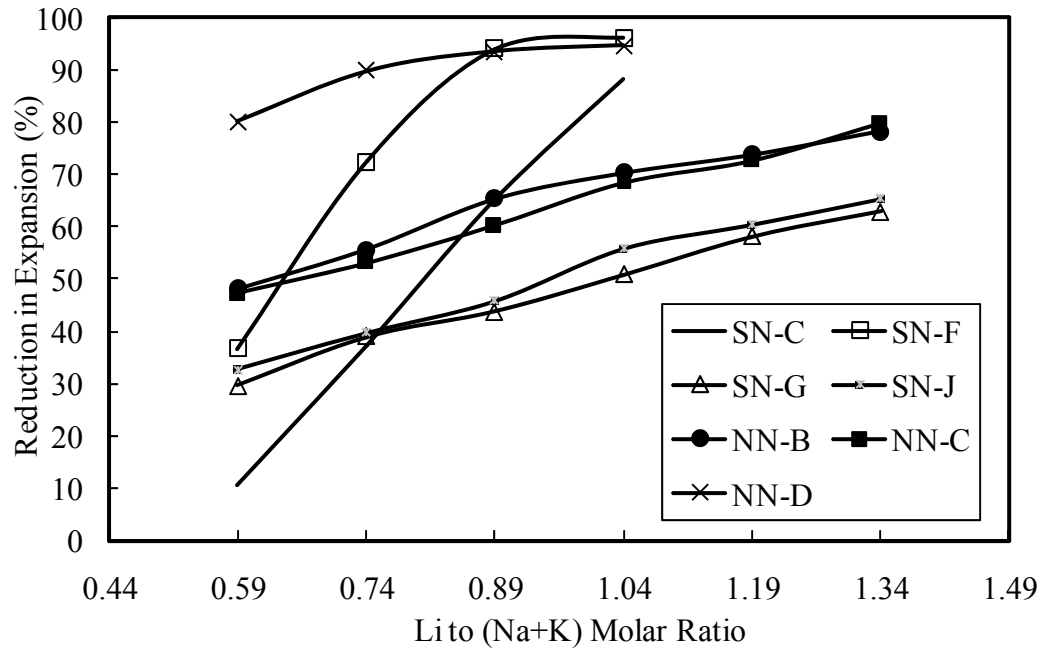


Figure 5.24: The reduction in expansion of the mortar bars containing various lithium dosages at 98 days

5.2.1.3 RIE of the lithium-bearing mortar bars as related to both lithium dosages and immersion ages

The average reduction in expansion (ARIE) of the seven reactive aggregates containing each investigated lithium dosage as related to the immersion age was also evaluated as shown in Figure 5.25. As can be seen, a linear correlation existed between the average reduction in expansion (ARIE) of the specimens made with the four dosages of lithium nitrate incorporated with the seven reactive aggregate groups at the immersion age of 14, 28, 56, 98 days. A minimum increase in the ARIE was noted when the lithium content was elevated from 0.59 to 0.74 (standard dose); whereas a lesser increase in the ARIE was observed between the lithium-to-alkali molar ratios of 0.89 to 1.04. In addition, as the immersion age of the specimens increased, the reduction in expansion decreased. The decrease in the ARIE between the immersion ages of 14 and 98 days was

more for the lower lithium dosages than that of the higher lithium dosages. Since the variation in the RIE among the trial aggregates decreased with an increase in the lithium dosage, the linear regression line improved substantially for the mortar bars having the higher lithium contents.

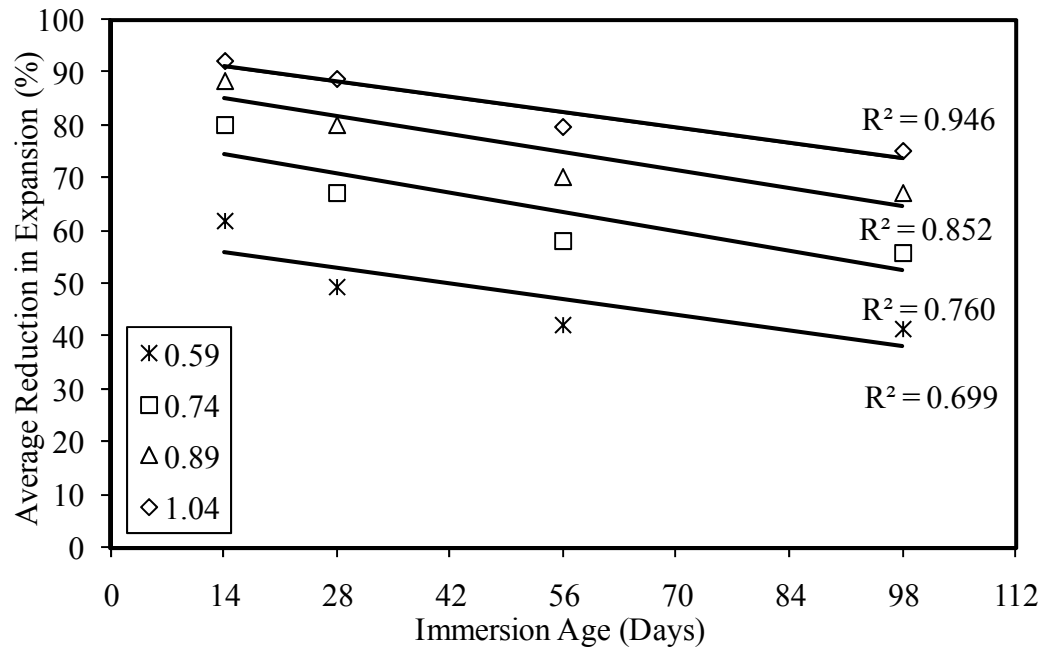


Figure 5.25: Average reduction in expansion of the seven reactive aggregates and various lithium dosages

5.2.3 Analytical model to determine the optimum lithium dosages to control ASR

This section describes the required minimum lithium dosage to counteract the excessive expansion of each selected reactive aggregate due to alkali-silica reactivity. It has been illustrated that the reduction in ASR expansion of each selected reactive aggregate was a function of lithium ions present in the mixture. Moreover, the interaction of lithium salt on each aggregate was quite different. Keeping those in mind, a unique

technique was implemented where the impact of lithium dosage on each aggregate was uniformly determined regardless of aggregate type, mineralogy and its structures etc.

A typical ASR-related expansion of the test mortar bars containing various lithium dosages is illustrated in Figure 5.26. The relationship between the 14-day expansion and the lithium dosage is presented in Equation 5.13. The characteristic of the remaining aggregates showed a similar trend to that of the SN-F aggregate. Additionally, the same regression curve, Equation 5.13, was also shown to be a good fit for the expansions at the ages of 28 and 56 days.

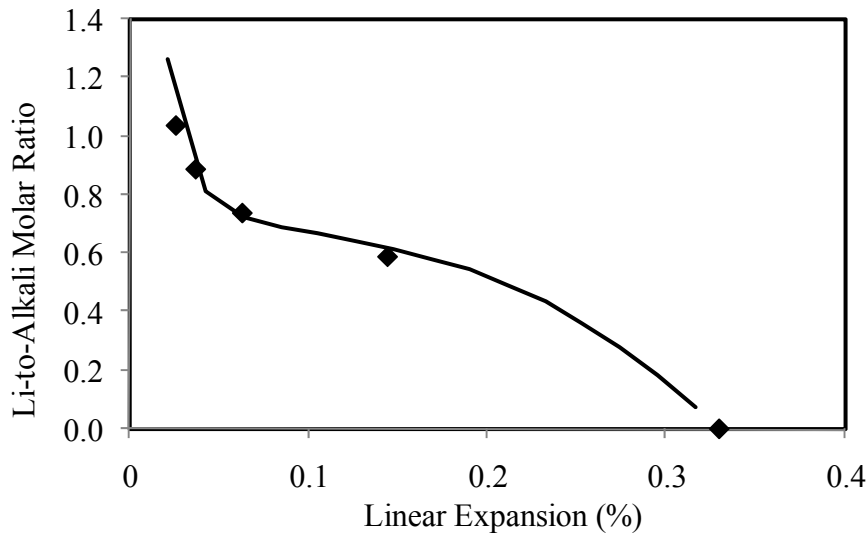


Figure 5.26: The 14-day expansion of the mortar bars containing SN-F aggregate and various lithium dosages

$$Li = a + b * x^3 + \frac{c}{x^2} \quad \text{Eq. 5.13}$$

Where:

Li is the lithium-to-alkali molar ratio in the mortar bars

x is the expansion of the mortar bar made with various lithium dosages

a, b and c are the regression parameters

The statistical parameters of the regression curve, the values of regression parameters a , b and c , Prob(t) of each regression parameter, Prob(F) and coefficient of multiple determination, for each reactive aggregate at the immersion ages of 14, 28 and 56 days are presented in Tables 5.12, 5.13 and 5.14, respectively.

The regression parameters a , b and c of Equation 5.13 for each trial mortar bars at the immersion ages of 14, 28 and 56 days were correlated with the expansion of the untreated mortar bars containing the companion aggregate at the corresponding immersion ages. At the above mentioned three test durations, the best models that represented the parameters a , b and c vs. the untreated expansion are illustrated in Equations 5.14, 5.15 and 5.16, respectively. The statistical data for Equations 5.14-5.16, the regression parameters a' , b' and c' , Prob(t) of each regression parameter, Prob(F) and the coefficient of multiple determination (R^2), at the ages of 14, 28 and 56 days are documented in Tables 5.14, 5.15 and 5.16, respectively.

Table 5.12: Statistical data for Equation 5.13 at the immersion age of 14 days

Agg. ID	Regression Parameters			Prob(t) of each regression variable			Prob(F)	R^2
	a	b	c	a	b	c		
SN-C	0.7524	-20.058	0.0003	0.0056	0.0144	0.0933	0.0117	0.988
SN-F	0.6643	-18.792	0.0003	0.0018	0.0048	0.0151	0.0039	0.996
SN-G	0.7003	-0.998	0.0007	0.0001	0.0008	0.0009	0.0002	0.986
SN-J	0.6112	-6.129	0.0009	0.0006	0.0044	0.0023	0.0006	0.975
NN-B	0.7149	-0.543	0.0006	0.0001	0.0013	0.0016	0.0004	0.980
NN-C	0.8038	-0.987	0.0006	0.0001	0.0020	0.0063	0.0010	0.969
NN-D	0.4736	-74.543	0.0002	0.0022	0.0037	0.0034	0.0011	0.999

Table 5.13: Statistical data for Equation 5.13 at the immersion age of 28 days

Agg. ID	Regression Parameters			Prob(t) of each regression variable			Prob(F)	R ²
	a	b	c	a	b	c		
SN-C	0.8019	-3.675	0.0003	0.0015	0.0047	0.0472	0.0049	0.995
SN-F	0.8019	-3.675	0.0003	0.0015	0.0047	0.0472	0.0049	0.995
SN-G	0.8008	-0.491	0.0025	0.0002	0.0025	0.0078	0.0013	0.965
SN-J	0.6476	-2.776	0.0038	0.0006	0.0044	0.0035	0.0008	0.972
NN-B	0.8201	-0.200	0.0013	0.0003	0.0045	0.0161	0.0028	0.947
NN-C	0.9208	-0.301	0.0013	0.0003	0.0049	0.0564	0.0052	0.928
NN-D	0.5293	-15.930	0.0003	0.0003	0.0005	0.0007	0.0002	1.000

Table 5.14: Statistical data for Equation 5.13 at the immersion age of 56 days

Agg. ID	Regression Parameters			Prob(t) of variables			Prob(F)	R ²
	a	b	c	a	b	c		
SN-C	0.9500	-1.162	0.0009	0.0181	0.0546	0.7096	0.0701	0.930
SN-F	0.8125	-1.093	0.0004	0.0042	0.0126	0.1263	0.0133	0.987
SN-G	0.7411	-0.341	0.0698	0.0000	0.0001	0.0003	0.0000	0.997
SN-J	0.6501	-1.375	0.0279	0.0005	0.0018	0.0021	0.0002	0.986
NN-B	0.7147	-0.086	0.0671	0.0001	0.0011	0.0018	0.0002	0.985
NN-C	0.9152	-0.156	0.0137	0.0005	0.0078	0.0821	0.0078	0.920
NN-D	0.5791	-4.999	0.0004	0.0010	0.0024	0.0041	0.0014	0.999

$$a = a' + b'x + \frac{c'}{x^2} + \frac{d'}{x^3} \quad \text{Eq. 5.14}$$

$$b = a' + b'x + \frac{c'}{x^2} + \frac{d'}{x^3} \quad \text{Eq. 5.15}$$

$$c = a' + b'x^2 + \frac{c'}{x^{1.5}} \quad \text{Eq. 5.16}$$

For each selected reactive aggregate having known expansion of untreated mortar bars at the ages of 14, 28 and 56 days, the regression parameters a, b and c for Equation 5.12 can be determined from Equations 5.13, 5.14 and 5.15, respectively (a', b', c' and d' for Equations 5.13-5.15 can be found from Tables 5.14-5.16). Substituting the values of

a, b and c, and the expansion of the mortar bars below the proposed limits of 0.10% at 14 days, 0.28 and 0.33% at 28 days, and 0.47 and 0.48% at 56 days in Equation 5.13, the effective amount of lithium dose for each trial aggregate at the abovementioned ages was determined. Tables 5.18, 5.19 and 5.20 documents the optimum amount of lithium dosages for each selected reactive aggregate, determined by the proposed analytical model, which were capable of restraining the ASR-related damages at 14, 28 and 56 days, respectively.

Table 5.15: Statistical data for Equation 5.14 at various immersion ages

Variables		14-Day	28-Day	56-Day
Regression Parameters	a'	0.7027	0.6453	0.8300
	b'	0.0515	0.1374	0.0315
	c'	-0.0186	0.0168	-0.1178
	d'	0.0017	-0.0105	0.0233
Prob(t) of each regression parameter	a'	0.0000	0.0842	0.0162
	b'	0.0687	0.4780	0.7831
	c'	0.0011	0.8688	0.3098
	d'	0.0063	0.6662	0.4680
Prob(F)		0.0000	0.0155	0.0106
R ²		0.999	0.910	0.923

Table 5.16: Statistical data for Equation 5.15 at various immersion ages

Variables		14-Day	28-Day	56-Day
Regression Paramers	a'	9.2963	7.1158	11.5366
	b'	-7.9078	-3.8801	-4.7926
	c'	-2.3785	-3.9305	-10.9192
	d'	-0.0773	0.5340	2.5354
Prob(t) of each regression parameter	a'	0.0000	0.0053	0.0373
	b'	0.0001	0.0091	0.0690
	c'	0.0000	0.0007	0.0040
	d'	0.0012	0.0082	0.0085
Prob(F)		0.0000	0.0000	0.0002
R ²		0.999	0.999	0.990

Table 5.17: Statistical data for Equation 5.16 at various immersion ages

Variables		14-Day	28-Day	56-Day
Regression Paramers	a'	0.0002	-0.0003	-0.0150
	b'	0.0023	0.0006	0.1185
	c'	-0.0018	0.0002	-0.0687
Prob(t) of each regression parameter	a'	0.0373	0.5202	0.0000
	b'	0.0827	0.0316	0.0001
	c'	0.1194	0.0960	0.0001
Prob(F)		0.0120	0.0709	0.0003
R ²		0.950	0.870	0.940

Table 5.18: Analytical lithium dosage to suppress ASR expansion below 0.10% at the immersion age of 14 days

Agg. ID	Expansion of untreated mortar bars (%)	Expansion of treated mortar bars ^a (%)	LiNO ₃ dosage [Li/(Na+K)]
SN-C	0.332	0.077	0.83
SN-F	0.329	0.063	0.87
SN-G	0.890	0.076	1.05
SN-J	0.465	0.075	0.93
NN-B	1.098	0.073	1.09
NN-C	0.940	0.059	1.09
NN-D	0.186	0.040	0.81

Table 5.19: Analytical lithium nitrate dosage to suppress ASR expansion at the immersion age of 28 days

Agg. ID	Expansion of untreated mortar bars (%)	Expansion of treated mortar bars (%)		LiNO ₃ dosage [Li/(Na+K)]	
		Below 0.33% ^a	Below 0.28% ^b	Below 0.33% ^a	Below 0.28% ^b
SN-C	0.599	0.289	0.289	0.65	0.75
SN-F	0.599	0.211	0.211	0.72	0.72
SN-G	1.185	0.248	0.248	0.85	0.85
SN-J	0.620	0.216	0.216	0.73	0.73
NN-B	1.610	0.265	0.265	0.88	0.88
NN-C	1.472	0.254	0.254	0.87	0.87
NN-D	0.322	0.322	0.322	0.01	0.71

^aProposed by Hooton (1991); and Rogers & Hooton (1993)

^bSuggested by Islam in this study

Table 5.20: Analytical lithium nitrate dosages to suppress ASR expansion at the immersion age of 56 days

Agg. ID	Expansion of untreated mortar bars (%)	Expansion of treated mortar bars (%)		LiNO ₃ Dose [Li/(Na+K)]	
		Below 0.48% ^a	Below 0.47% ^b	Below 0.48% ^a	Below 0.47% ^b
SN-C	0.901	0.330	0.330	0.90	0.90
SN-F	0.896	0.303	0.303	0.97	0.97
SN-G	1.323	0.464	0.464	1.18	1.18
SN-J	0.800	0.447	0.447	0.43	0.43
NN-B	2.050	0.453	0.453	1.24	1.24
NN-C	1.828	0.411	0.411	1.27	1.27
NN-D	0.488	0.106	0.106	0.69	0.69

^aProposed by Hooton (1991); and Rogers & Hooton (1993)

^bSuggested by Islam in this study

The required amount of lithium dosages for each trial reactive aggregate at the immersion ages of 14, 28 and 56 days, determined by the proposed analytical model as

illustrated in Tables 5.18, 5.19 and 5.20, respectively, were compared with those obtained from the experimental procedures at the corresponding immersion ages. The results are tabulated in Table 5.21. Table 5.21 shows that the 14-, 28- and 56-day failure criteria of the mortar bars resulted in the experimental optimum lithium-to-alkali molar ratios of 0.89, 0.74, 1.04, 0.74, 1.04, 1.19 and 0.59 for the SN-C, SN-F, SN-G, SN-J, NN-B, NN-C and NN-D aggregates, respectively. The analytical model demonstrated the ratios were 0.84, 0.88, 1.05, 0.93, 1.16, 1.14 and 0.81, respectively. The following conclusions can be summarized based on the results obtained:

- a) The proposed analytical model was very efficient in determining the required minimum lithium dosage for the three reactive aggregate groups SN-G, NN-B and NN-C having the 14-day expansions of untreated mortar bars of more than 0.80%.
- b) The method also showed a good correlation between the minimum experimental and analytical lithium dosages for the three aggregate groups SN-C, SN-F and SN-J with the expansions of untreated mortar bars more than 0.10% at 14 days, 0.33% at 28 days and 0.48% at 56 days.
- c) For the last aggregate group (NN-D) showing reactive at 14 days, and nearly reactive at the ages of 28 and 56 days, the amount of lithium nitrate to suppress ASR expansion, determined by the proposed analytical model, was more conservative than that obtained by the experimental program.

The results also revealed that lithium nitrate was found to be more effective for some extremely reactive aggregates, but relatively less effective for some other less reactive ones. Furthermore, the efficacy of lithium in reducing ASR expansion was a function of both the mineral characteristics and the reactivity of the aggregates. For instance, it was

possible that the required amount of lithium in suppressing ASR expansion of highly reactive aggregates was less than that of the slowly reactive aggregates. The proposed analytical model described herein can be used in selecting the initial lithium dosage for suppressing alkali-silica reactivity for any reactive aggregates. It is strongly recommended that each reactive aggregate source should be tested with various dosages of lithium salt before use in concrete.

Table 5.21: Optimum experimental and analytical lithium nitrate dosages to control ASR expansion at the immersion ages of 14, 28 and 56-days

Agg. ID	14-Day ^a		28-Day				56-Day			
	ELD (%)	ALD (%)	Proposed by previous studies ^b		Suggested by Islam in this study		Proposed by previous studies ^b		Suggested by Islam in this study	
			ELD (%)	ALD (%)	ELD (%)	ALD (%)	ELD (%)	ALD (%)	ELD (%)	ALD (%)
SN-C	0.74	0.83	0.74	0.65	0.89	0.75	0.89	0.84	0.89	0.84
SN-F	0.74	0.87	0.74	0.72	0.72	0.72	0.74	0.88	0.74	0.88
SN-G	0.89	1.05	0.89	0.85	0.85	0.85	1.04	0.92	1.04	0.92
SN-J	0.74	0.93	0.74	0.73	0.73	0.73	0.59	0.57	0.59	0.57
NN-B	0.89	1.09	0.89	0.88	0.88	0.88	1.04	1.16	1.04	1.16
NN-C	1.04	1.09	1.04	0.87	0.87	0.87	1.19	1.14	1.19	1.14
NN-D	0.59	0.81	0.00	0.01	0.59	0.71	0.59	0.69	0.59	0.69

ELD = Experimental lithium dosage; ALD = Analytical lithium dosage

^aProposed by ASTM C 1260

^bBased on the failure criteria proposed by Hooton (1991); and Rogers & Hooton (1993)

5.3 The Combined Use of Class F Fly Ash and Lithium Nitrate Salt

For the third mitigation technique in alleviating ASR-related expansion of the four highly reactive aggregates; namely SN-G, SN-J, NN-B and NN-C, a constant amount of lithium nitrate having the Li/(Na+K) of 0.74 combined with two dosages of Class F fly ash (15 and 20%), as a partial replacement of Portland cement by weight, was used. The

expansion readings of the test mortar bars were taken at the immersion ages of 3, 6, 10, 14 days, and weekly thereafter up to 98 days. The results are presented in the Appendix C.

5.3.1 ASR expansion of the fly-ash and lithium-bearing mortar bars as related to the immersion ages

The results obtained from the combined use of Class F fly ash and lithium salt revealed a strong influence in arresting the ASR expansion of the trial aggregates. The progression in expansion of the test mortar bars over the immersion age as related to the individual and combined use of Class F fly ash and lithium dosage is illustrated in Figure 5.27. As can be seen, the 14-day expansion of the untreated mortar bars made with the SN-G aggregate (0.89%) was reduced to 0.251, 0.146 and 0.166% with the use of 15% and 20% Class F fly ash as a partial replacement of Portland cement, and 100% lithium dosage, respectively. When the same aggregate was treated with the combined use of 15% fly ash and 100% lithium salt, denoted by 15%FA+100%Li, the untreated expansion was reduced to 0.042%. Having a constant Li:(Na+K) of 0.74 and elevating Class F fly ash content to 20% by Portland cement replacement, the expansion of the SN-G aggregate group was further decreased to 0.030%. The progression in expansion of the test mortar bars at 28, 56 and 98 days as compared to the 14-day expansion was 1.33, 1.49 and 1.60 times for the untreated mortar bars, 1.73, 2.70 and 3.64 times for the 15%FA, 2.05, 3.60 and 5.49 for the 20%FA, 2.42, 4.35 and 5.23 for the 100%Li, 2.79, 6.90 and 13.02 for the 15%FA+100%Li, and 2.84, 7.40 and 13.56 for the 20%FA+100%Li, respectively. The results also revealed that the most reduction in expansion occurred in the aggregate groups producing a relatively high level of

expansion of the untreated mortar bar at 14 day. A similar funding was also observed for the remaining three aggregate groups.

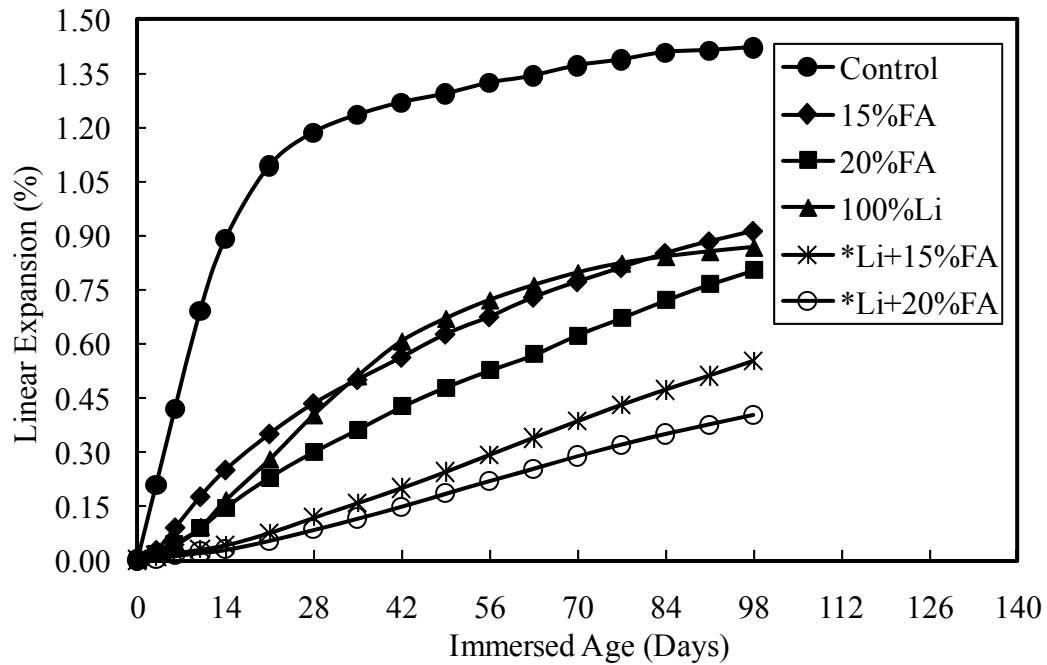


Figure 5.27: Linear expansion of the SN-G aggregate containing fly ash and lithium nitrate individually and jointly

Of the four trial reactive aggregates, the mortar bars made with the SN-G, NN-B and NN-C aggregates and 20% Class F fly ash, as a partial replacement of Portland cement, displayed reactivity at the immersion age of 14 days. The reactivity of these aggregate groups incorporating with the lithium-to-alkali molar ratio of 0.74 reflected the same reactivity to that of the mortar bars containing 20% fly ash. Thus, blending 20% Class F fly ash or adding lithium nitrate at a molar ratio of 0.74, when used individually, were not effective to suppress the 14-day expansions below the expansion limit of 0.10%. The combined effect of 20% fly ash and lithium nitrate at a molar ratio of 0.74 slowed down the 14-day expansions of the SN-G, NN-B and NN-C aggregate groups to 0.030%,

0.029% and 0.027%, respectively. For the remaining aggregate (SN-J), the use of 20% Class F fly ash or 100%Li was found effective in reducing the excessive expansions at the immersion ages of 14, 28 and 56 days. However, the combined use Class F fly ash and lithium salt resulted in a more conservative outcome.

Figure 5.28 shows a typical relationship of the 14-day ASR-induced expansions of the untreated mortar bars and the specimens treated with the 15%FA, 20%FA, 100%Li, 15%FA+100%Li, and 20%FA+100%Li for the aggregate group SN-G. As can be seen, the expansion of the mortar bars due to the dual influence of fly ash and lithium was very small even for the aggregate producing the 14-day control expansion of 1.10%. The results of the study showed that blending 15% fly ash as a partial replacement of Portland cement, the 14-day expansion of control mortar bars prepared with the SN-G (0.862%), NN-B (1.023%) and NN-C (0.830%) was reduced to 0.251, 0.251 and 0.233%, respectively, exceeding the expansion limits of 0.10%. When lithium-to-alkali molar ratio of 0.74 was used, the expansion of these aggregate groups still remained above the failure limit of 0.10%. On the other hand, the combination of 15% Class F fly ash and Li:(Na+K) molar ratio of 0.74 resulted in the 14-day expansion for the aggregate groups of SN-G, NN-B and NN-C of 0.042%, 0.052% and 0.057%, respectively.

The ASR-related expansion of fly-ash or lithium-bearing mortar bars increased rapidly at the early age of immersion, and the expansion decreased with an increase in immersion age. In the case of the lithium bearing specimens, the ASR expansion remained steady after the immersion ages of 2 months. However, the specimens containing both fly ash and lithium salt expanded slowly for the entire test duration of 98 days.

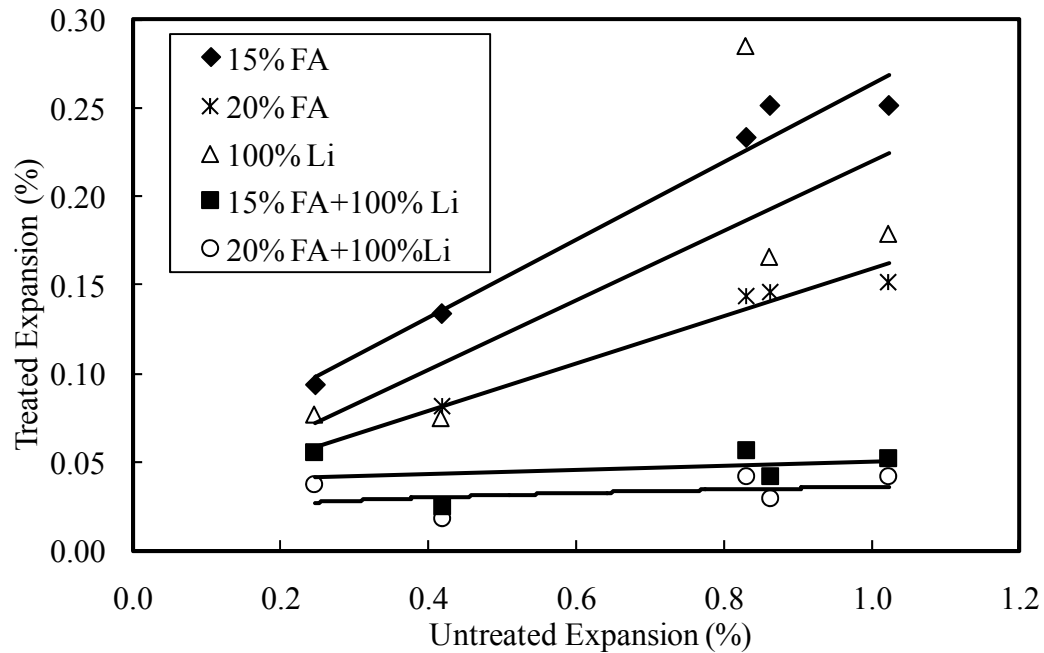


Figure 5.28: The expansion of the treated and untreated mortar bars made with the SN-G aggregate

It was shown that the 15%FA+100%Li was able to suppress the ASR expansion not below only the 0.10% at 14 days, but also 0.33% at 28 days and 0.48% at 56 days for the mortar bars prepared with trial reactive aggregates. To this extent, blending 20% Class F fly ash as a partial replacement of cement conjunction with Li:(Na+K) molar ratio of 0.74 was even more effective in improving ASR mitigation than those of 15% fly ash and 100%Li.

5.3.2 The reduction in expansion of the mortars containing fly ash, lithium, and the combined fly ash and lithium as related to the test durations

The influence of the trial mitigation technique in reducing the ASR-related expansion of the reactive selected aggregates was also expressed in terms of the Reduction in Expansion (RIE) of the untreated mortar bars (having no fly ash or lithium content) at various immersion ages. For each of the ASR mitigation techniques, the RIE at the

immersion age of 3 or 6 days was highest and then gradually decreased with an increase in the test duration. For the immersion age of 14 days, the RIE of the treated mortar bars as compared to that of the untreated/control specimen of the companion aggregate is shown in Figure 5.29. As can be seen, the 14-day RIE of the treated mortar bars made with the selected aggregates varied from 71.2 to 77.2% with an average of 73.9% for the 15% fly ash, 82.6 to 86.2% with an average of 84.3% for the 20% fly ash, 69.7 to 83.8% with an average of 79.6% for the 100%Li, 93.9 to 95.2% with an average of 94.7% for the 15%FA+100%Li, and 95.6 to 96.7% with an average of 96.1% for the 20%FA+100%Li. The results showed that, in general, the difference in the 14-day RIE among the trial aggregates for each mitigation technique was fairly insignificant.

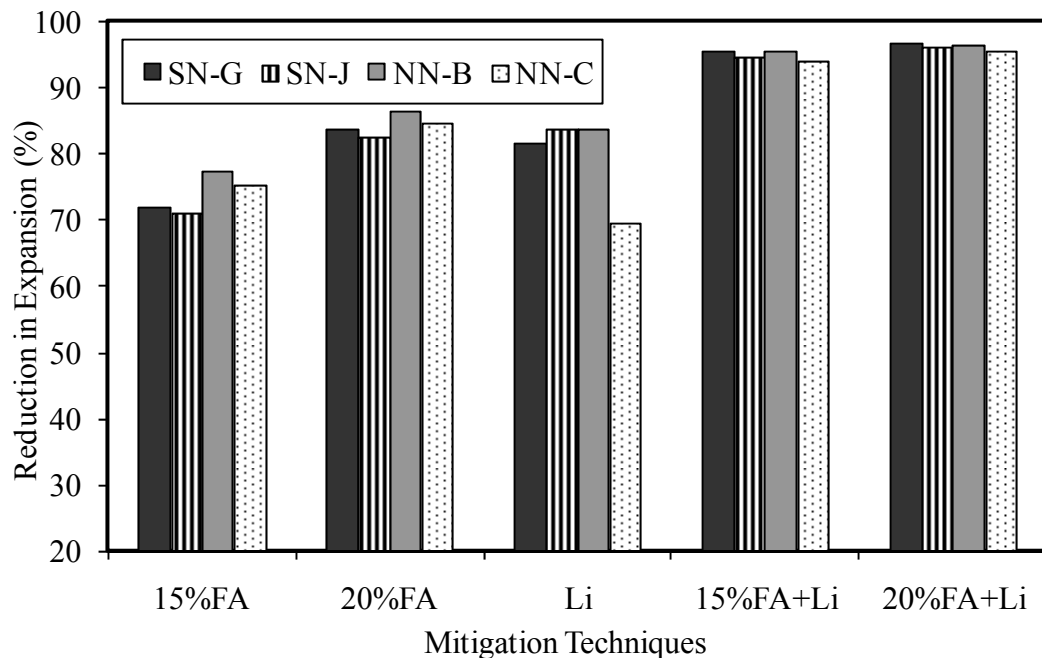


Figure 5.29: Reduction in expansion of the mortar bars containing various mitigation techniques of suppressing ASR (14 days)

The reduction in expansion of the test mortar bars as related to various immersion ages is illustrated in Figure 5.30. As can be seen, the RIE decreased with an increase in test duration. However, the decrease in the RIE over the immersion age varied depending on the ASR mitigation technique. The RIE over the immersion age decreased most for the 15%FA, and decreased most for the combined use of Class F fly ash and lithium dosage. The characteristics of the remaining three aggregates also followed a similar pattern to that of the NN-B aggregate.

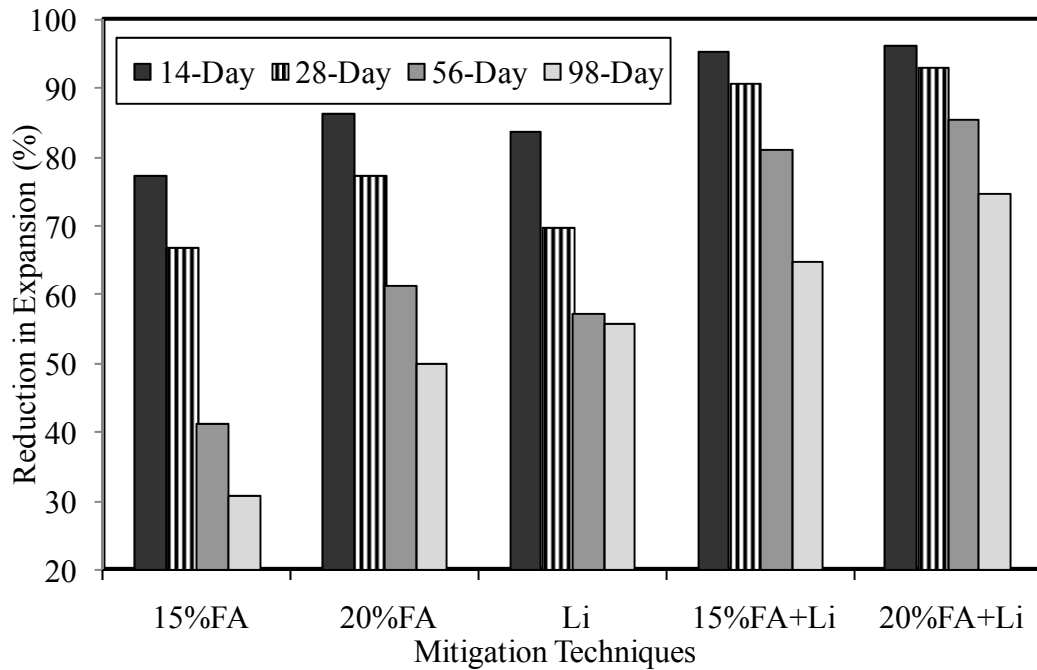


Figure 5.30: Reduction in expansion of the mortar bar containing NN-B aggregate treated with 15 and 20% fly ash, 100% Li, 15%FA+100%Li and 20%FA+100%Li at various ages

The performance of the test mortar bars was also evaluated with respect to the reduction in control expansion at the ultimate test duration of 98 days. The results are shown in Figure 5.33. As can be seen, the 98-day RIE of the mortar bars varied from 30.7

to 44.7% with an average of 36.8% for the 15% fly ash, 43.5 to 53.8% with an average of 48.3% for the 20% fly ash, 39.1 to 55.7% with an average of 47.0% for the 100%Li, 58.5 to 75% with an average of 64.9% for the 15%FA+100%Li, and 71.7 to 80.2% with an average of 74.7% for the 20%FA+100%Li. At the extended immersion age of 98 days, it can be noted that, in general, 100%Li was more effective than the 15%FA, and less effective than the 20%FA. A similar trend was observed at the early immersion age of 14 days (Fig. 5.31). For all selected reactive aggregate groups, the combined use of fly ash and lithium showed most effective in suppressing the excessive expansion of the trial reactive aggregates as compared to the individual effect of fly ash or lithium at 98 days (Fig. 5.31) as compared to that at 14 days (Fig. 5.30).

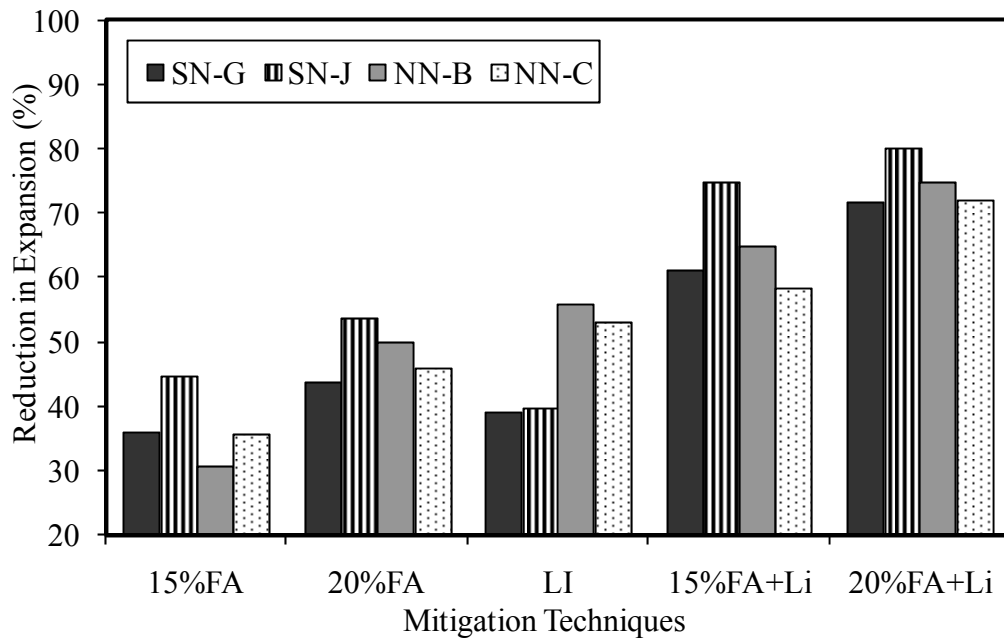


Figure 5.31: Reduction in expansion of the treated mortar bars at 98 days

In summary, for all trial reactive aggregates, the combined use of fly ash and lithium was most influential in arresting ASR expansion at any given immersion age. The RIE

decreased rapidly with an increase in immersion age for the mortar bars made with Class F fly ash or lithium salt than that obtained for the test samples containing both fly ash and lithium nitrate. The reduction in the RIE for each trial aggregate between the immersion ages of 14 and 98 days varied most when fly ash or lithium salt was used. Overall, this mitigation technique (combined fly ash and lithium salt) resulted in less variation in RIE among the selected reactive sources in the extended immersion age (i.e. 98 days) as compared to that obtained in the early age (i.e. 14 days).

5.3.3 ASR-induced cracks of the mortar bars as related to individual and combined effect of fly ash and lithium salt

The ASR-related cracks on the surface of the test mortar bars were also examined and a typical result is shown in Figure 5.32. Using the 15% fly ash as a partial replacement of Portland cement, the width of ASR-induced cracks of the untreated specimens was reduced when compared to the cracks seen in the untreated mortar bars (Fig. 5.32b). Elevating fly ash content to 20%, the specimens were experienced with a limited number of random cracks as seen in Fig. 5.32c. When the lithium-to-alkali molar ratio of 0.74 was used in the test mortar bars, only a few numbers of horizontal cracks were noticed as illustrated in Fig. 5.32d. The combined use of 15% fly ash and 100% lithium dosage reduced the severe cracks of the control specimen significantly as shown in Fig. 5.32e. Cracks were completely mitigated once fly ash content of the these specimens was increased to 20% even after 98 days of immersion age as depicted in Figure 5.32f.



(a) Untreated mortar bars ($E_{14\text{-day}} = 1.10\%$; $E_{98\text{-day}} = 2.34\%$)



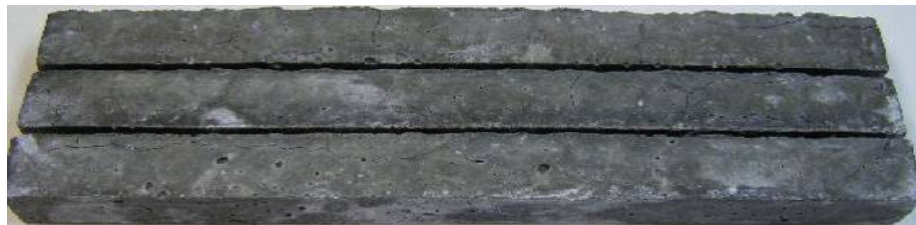
(b) Treated mortar bars with the 15%FA ($E_{14\text{-day}} = 0.25\%$; $E_{98\text{-day}} = 1.62\%$)



(c) Treated mortar bars with the 20%FA ($E_{14\text{-day}} = 0.152\%$; $E_{98\text{-day}} = 1.17\%$)



(d) Treated bars with the 100%Li ($E_{14\text{-day}} = 0.18\%$; $E_{98\text{-day}} = 1.04\%$)



(e) Treated bars with the 15%FA+100%Li ($E_{14\text{-day}} = 0.052\%$; $E_{98\text{-day}} = 0.82\%$)



(f) Treated bars with the 20%FA+100%Li ($E_{14\text{-day}} = 0.042\%$; $E_{98\text{-day}} = 0.59\%$)

Figure 5.32: The 98-day mortar bars made with NN-B aggregate, fly ash, lithium, and the combination of fly ash and lithium

As such, it can be concluded that a combination of lithium nitrate at the manufacturer recommended dosage (lithium-to-alkali molar ratio of 0.74 or 100% lithium) and Class F fly (minimum of 15 percent by weight of Portland cement) is effective in eliminating the ASR-induced cracks of the mortar bars made with investigated reactive aggregates at both early and extended immersion ages.

4.5 Analytical approach to determine the expansion of the mortar bars containing both Class F fly ash and lithium nitrate

A correlation was sought and found among the expansion of the mortar bars prepared with Class F fly ash, lithium nitrate, and the combined fly ash and lithium salt at various immersion ages. The result is shown in Equation 5.17. The regression parameters (a, b and c), and the coefficient of multiple determination (R^2) of Equation 5.17 at three immersion ages are documented in Table 5.22. The R^2 values shown in Table 5.22 indicated a good fit between the expansion of the mortar bars made with Class F fly ash, lithium nitrate, and that containing both fly ash and lithium.

$$Y = a + bX_1 + cX_2 \quad \text{Eq. 5.17}$$

Where:

X_1 , X_2 and Y are the expansions of the mortar bars prepared with Class F fly ash, lithium nitrate, and the combination of both, respectively
a, b and c are the regression variables

Table 5.22: Regression parameters for Equation 5.17 at various immersion ages

Regression Parameters	For 15%FA, 100%Li and 15%FA+100%Li			For 20%FA, 100%Li and 20%FA+100%Li		
	14-Day	28-Day	56-Day	14-Day	28-Day	56-Day
a	0.004	-0.008	-0.016	-0.003	-0.016	-0.014
b	0.099	0.113	-0.022	0.192	0.206	0.183
c	0.107	0.194	0.508	0.060	0.104	0.207
R^2	0.940	0.999	0.980	0.960	0.998	0.980

The analytical expansion of the mortar bars containing both fly ash and lithium nitrate at the immersion ages of 14, 28 and 56 days was evaluated by using Equation 5.17, and the values of a, b and c as shown in Table 5.22, and the expansion of the mortar bars made with fly ash or lithium nitrate at the respective immersion age. The test results were then compared with the experimental expansion of the specimens containing both fly ash and lithium nitrate. A linear correlation with R^2 values of 0.980 and 0.992 were observed between the analytical and experimental results for the mortar bars containing 15%FA+100%Li and 20%FA+100%Li, respectively, at the test durations of 14, 28 and 56 days. Figure 5.33 presents the comparison of the analytical and experimental expansions of the test mortar bars containing the 15%FA+100%Li and 20%FA+100%Li at three immersion ages. As can be seen, a good agreement (with a R^2 value of 0.984) existed between the results obtained from experimental and analytical models.

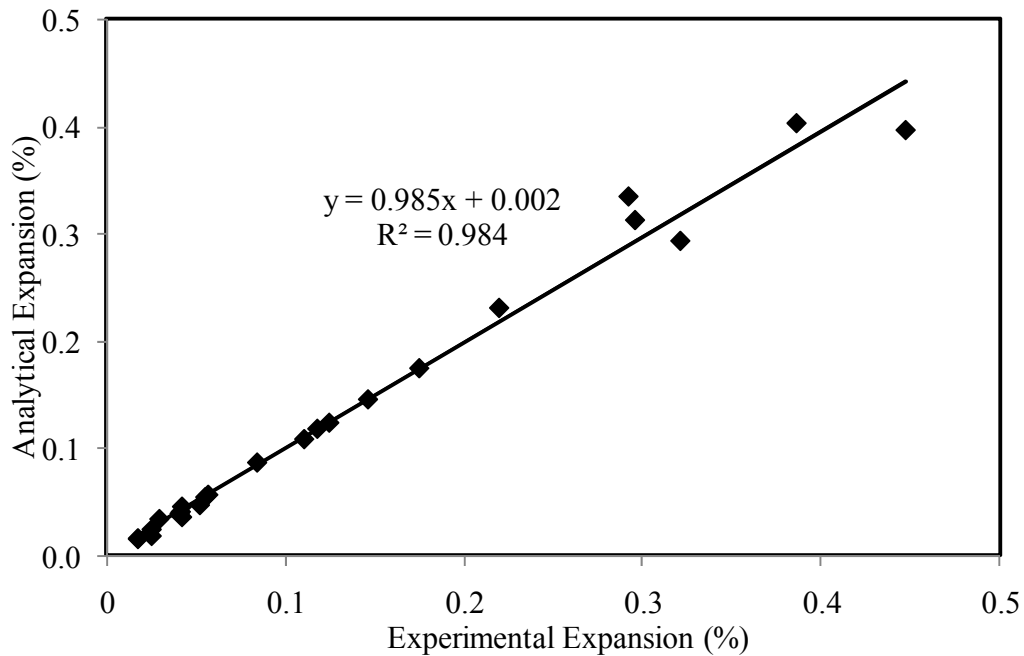


Figure 5.33: Comparison of the results obtained from the experimental and analytical method for the mortar bars containing combined fly ash and lithium salt

5.4 Comparison of the Three Mitigation Techniques in Suppressing ASR

This section describes the efficiency of the three mitigation techniques in suppressing alkali-silica reactivity of the trial reactive aggregates at the immersion ages of 14, 28 and 56 days. The comparison involved a maximum of twelve mixture constituents and proportions for each trial reactive aggregate source; four mixtures for the Class F fly ash, four to six mixtures for the lithium salt, and the two mixtures for the combination of Class F fly ash and lithium nitrate.

Figure 5.34 illustrates the average reduction in expansion, in reference to the expansion of untreated mortar bars, of the test specimens containing ten trial mixtures at the immersion ages of 14, 28, 56 and 98 days. As can be seen, a linear relationship existed between the average RIE of each trial mixture and the immersion age. In general, it can be stated that, the 20% Class F fly ash was more effective than the lithium-to-alkali molar ratio of 0.59, but less effective when lithium-to-alkali molar ratio of 0.74 (standard lithium dosage) was used. The effectiveness of the lithium-to-alkali molar ratio of 0.89 was nearly identical to that of the 25% Class F fly ash at the immersion ages of 14, 28, 56 and 98 days. The combined use of Class F fly ash (15% or 20%) and lithium salt (at a rate of lithium-to-alkali molar ratio of 0.74) showed more effective than the individual use of 30% fly ash or 140% lithium salt at the early age of immersion (14 days). The use of 20%FA+100%Li was found more effective over the 15%FA+100%Li at an extended immersion ages than that obtained at the early immersion age (14 days).

Table 5.23 documents the required optimum dosages of Class F fly ash, lithium nitrate and the combination of Class F fly ash and lithium nitrate salt in restraining the ASR expansion of the mortar bars made with each trial reactive aggregate below the

0.10% at 14 days, 0.28% at 28 days, and 0.47% at 56 days. As seen in Table 5.23, the minimum amount of Class F fly ash or lithium nitrate was needed to counteract the alkali-silica reactivity at the above mentioned three immersion ages varied depending upon the aggregate source used. For instance, blending 15% Class F fly ash as a partial replacement of Portland cement was sufficient to suppress the excessive expansions of the SN-F aggregate group, whereas the effective dosages for the reactive aggregate groups NN-B and NN-C was 30% by weight of cement replacement. In the case of the lithium-bearing mortar bars incorporated with the NN-B and NN-C, the lithium-to-alkali molar ratios of 1.04 and 1.19 were capable of arresting the ASR-induced expansions at the ages of 14, 28 and 56 days. The use of combined standard lithium dose (lithium-to-alkali molar ratio of 0.74) and a moderate amount (15%) of Class F fly ash (with a CaO content of 7.4% or less) as a partial replacement of Portland cement by weight was found to be sufficiently effective in arresting the ASR-related damages for the investigated reactive aggregates at the immersion ages of 14, 28, 56 and 98 days.

The findings demonstrate that different aggregates required different mitigation techniques in controlling alkali-silica reactions. It should also be noted that the final selection of an effective mitigation technique also depends on its effect on early-age and late-age ASR-induced expansions, and the potential economical benefits.

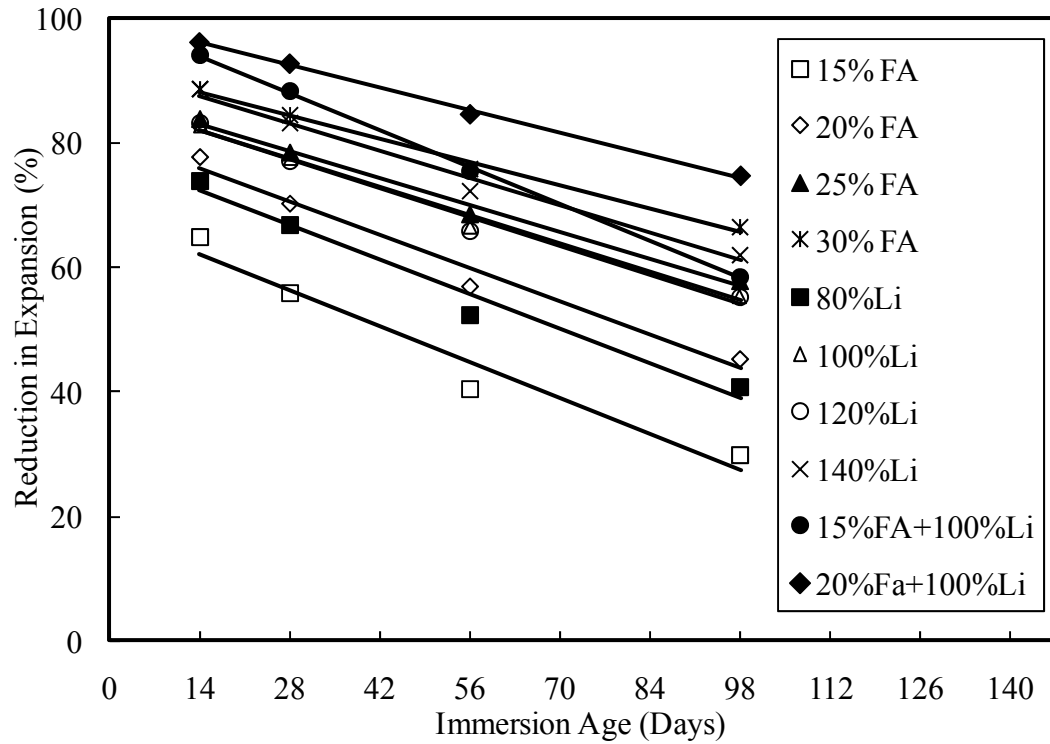


Figure 5.34: The reduction in expansion of the treated mixtures at various immersion ages

Table 5.23: Minimum dosage of Class F fly ash, lithium nitrate, and the combination of fly ash and lithium nitrate at 14, 28 and 56 days

Agg. ID	Fly ash dosage (%)	Lithium dosage [Li:(Na+K)]	Combined fly ash and lithium dosage
SN-C	20	0.89	-
SN-F	15	0.74	-
SN-G	30	1.04	Li*+15%FA
SN-J	20	0.59	Li*+15%FA
NN-B	30	1.04	Li*+15%FA
NN-C	30	1.19	Li*+15%FA
NN-D	20	0.59	-

*Lithium-to-alkali molar ratio of 0.74

CHAPTER 6

CONCLUSION AND RECOMMENDATION

This chapter deals with the conclusions and recommendations generated by this research study, which is solely based on the testing performed on the fourteen selected aggregate quarries. It is strongly recommended that each aggregate suspected of alkali-aggregate reactivity be tested, analyzed, and assessed before it is used in Portland cement concrete. The findings of the study are drawn into the following major categories.

6.1 Identification of Reactive Aggregates

The alkali-silica reactivity of the fourteen trial aggregates was determined by the ASTM C 1260 test for the 1, 0.5 and 0.25N solutions at the immersion ages of 14, 28, 56 and 98 days. Additionally, the influence of cement alkalis on the ASR expansion of the test mortar bars was also evaluated under the three soak solutions at the above-mentioned four immersion ages. In assessing ASR of the trial aggregates, two modifications of ASTM C 1293 test were conducted at the immersion ages of 4, 8, 13 and 26 weeks. They were: the prisms submerged in the 1N NaOH at 80°C (ASTM C 1293M1) and the specimens cured in the distilled water at 80°C (ASTM C 1293M2).

6.1.1 ASR-induced expansions under ASTM C 1260 for the 1N solution

- a. The mortar bars prepared with the fine and crushed coarse aggregates of the companion quarry produce nearly similar ASR-induced expansions. As a result, the use of fine aggregates, instead of graded crushed aggregates, in the ASTM C 1260 minimizes the effort needed for material preparation and reduces the overall cost of the experiment.

- b. Since the 14-day failure limit of ASTM C 1260 of 0.10% is not capable of predicting the actual alkali-silica reactivity of some aggregates, this study proposes the failure criteria of the mortar bars for the 1N solution at the extended immersion ages of 28, 56 and 98 days. The results reveal that aggregates producing the 14-, 28-, 56- and 98-day ASR expansions of 0.10, 0.28, 0.47 and 0.59%, respectively, are considered potentially reactive. The aggregates producing the expansions of less than the four prescribed expansion limits are innocuous. The classifications of the fourteen trial aggregates on the basis of alkali-silica reactivity are perfectly aligned with the expansion criteria proposed by Hooton (1991) and Rogers and Hooton (1993).

6.1.2 Influence of soak solution (NaOH) concentration on ASR-induced expansion

- a. The expansion of the mortar bars for the 1, 0.5 and 0.25N NaOH solutions as related to the immersion age varies depending on the mineralogy of aggregates. For instance, some aggregates expand rapidly at the early age of immersion, but the expansion rate decreases thereafter. On the other hand, several aggregates expand slowly throughout the test, while the others expand less initially, but the rate of expansion increases rapidly at late immersion age.
- b. The trial mortar bars submerged in the 1N soak solution expand mostly during the early state of immersion, and the expansion rate decreases with an increase in test duration. In the case of the 0.5N NaOH-cured mortar bars, the expansion caused by ASR is gradual with an increase in immersion age. The ASR-induced expansion for the 0.25N solution is very small over the span of the testing,

suggesting that the solution concentration provides an environment less conducive to alkali-silica reactivity.

- c. The expansion of the mortar bars immersed in the 0.5 and 0.25N solutions fluctuates more with the immersion age than that of the specimens in the 1N NaOH soak solution. In addition, the expansion ratios of the mortar bars for the 0.5 and 1N NaOH solutions, and 0.25 and 1N NaOH solutions vary with the immersion age, and they become stabilized at the immersion ages of 56 days or more.
- d. Early-age failure criteria (14 days) may result in the overestimation of alkali-silica reactivity of some aggregates. Based on the findings of the study, it is recommended to extend the test duration of ASTM C 1260 from 14 days to at least 56 days in order to properly evaluate aggregates for their alkali-silica reactivities.
- e. The analyses of this study lead to the 14-, 28-, 56- and 98-day expansion limits of ASTM C 1260 for the 0.5N solution of 0.030, 0.105, 0.220, and 0.325%, respectively. With some exceptions, the alkali-silica reactivity of the trial aggregates for the 0.5N soak solution at 14 and 28 days correlates well with that obtained for the 1N soak solution at the same immersion age. The slight discrepancy may be due to the limited increase in expansion for some aggregates immersed in the 0.5N NaOH solution between the immersion age of 14 and 28 days. When the test duration of ASTM C 1260 is extended from 14 to at least 56 days, a perfect correlation of the expansion limit exists between the two soak solutions.

- f. In this study, the proposed failure limits of ASTM C 1260 for the 0.25N NaOH solution are found to be 0.013, 0.026, 0.042 and 0.068% at the immersion ages of 14, 28, 56, and 98 days, respectively. The classifications of the trial aggregates based on the failure criteria of the mortar bars for the 1N and 0.25N NaOH solutions at 14 days do not show a good correlation mainly due to the lower solution concentration and a relatively short immersion age. In addition, the classifications of the trial aggregates for the 0.25N soak solution are not fully consistent with those obtained for the 1N NaOH at the immersion ages of 14, 28, 56 and 98 days. Extending the testing period of ASTM C 1260 to 6 months or longer for the 0.25N soak solution may offer a better correlation amongst the two concentrations of NaOH solutions. On the other hand, the extension of the test duration may defeat the purpose of the accelerated mortar bar test.
- g. The expansions of the mortar bars for the 0.5N soak solution show more reliable results with respect to soak solution concentration and immersion age when compared to the results obtained by using 1N and 0.25N NaOH solutions.
- h. ASR-induced cracks are significantly affected by the aggregate type, severity of soak solution, and the immersion age. The reactivity of an aggregate may be evaluated by examining the cracks formed on the surface of the prisms for the 1N solution. Reactive aggregates experience severe ASR-induced symptoms (map cracks, pop-outs etc.), whereas no ASR-related cracks are seen on the specimens made with innocuous aggregates. Additionally, as the soak solution concentration reduces, the ASR-induced cracks decrease significantly.

6.1.3 Influence of immersion age on the expansion of mortar bars under various soak solutions

The finding suggests that the trial mortar bars submerged in the 1N soak solution expands most during the early age of immersion, and the expansion rate decreases with an increase in the test duration. In the case of the 0.5N NaOH-cured mortar bars, the expansion caused by ASR is gradual over the immersion age. The ASR-induced expansion for the 0.25N solution is very small over the span of the testing, suggesting that the solution concentration provides an environment less conducive to alkali-silica reactivity.

6.1.4 Influence of cement alkalis on ASR-induced expansion

- d. Aside from aggregate mineralogy, the influence of cement alkalis on the ASR-induced expansion of mortar bars depends on soak solution concentration and test duration.
- e. The percent increase in expansion of the mortar bars made with 0.84 and 1.26% cement alkalis, as compared to the expansion of the mortar bars containing 0.42% cement alkalis, is significant for the reduced soak solution concentration. The influence of cement alkalis on ASR-related expansion decreases with an increase in soak solution concentration.
- f. Overall, the influence of cement alkalis on ASR-induced expansion is relatively small and gradual with an increase in cement alkalis for the 1N soak solution. In the 0.5N NaOH soak solution, the effect is moderate and gradual. In the case of the 0.25N NaOH soak solution, the increase in cement alkalis produces rapid and large increase in the ASR-induced expansions of mortar bars.

6.1.5 ASR-induced expansions under modified ASTM C 1293

- a. The study reveals that the high alkali soak solution (1N NaOH) elevates the alkali content of the prisms which ultimately result in higher expansions for most aggregates during the 6-month testing period. The failure limit of ASTM C 1293M1 of 0.04% expansion at 4 weeks results in the overestimated reactivity of some aggregates. Utilizing the proposed expansion limits of ASTM C 1293M1 of 0.105% at 8 weeks, 0.165% at 13 weeks, and 0.285% at 26 weeks produces more reliable results than those generated at the early immersion age of 4 weeks. The results also indicate that the aggregates showing the 4-week expansions of more than 0.08% are potentially reactive at the extended immersion ages.
- b. ASR-induced cracks are formed on the surface of the alkali-cured prisms made with reactive aggregate as early as 4 weeks. Conversely, no cracks are observed on the specimens made with innocuous aggregates even at the immersion age of 6 months.
- c. The soak solution type has a significant impact on the ASR-induced expansion. For the ASTM C 1293M2, the performance of the prisms in the distilled water soak solution is significantly different from the specimens immersed in a 1N NaOH solution. The leaching effect of alkalis from the water-cured prisms to the soak solution (water) reduces the amount of alkalis available for alkali-silica reactions. As such, the ASR-induced expansion of water-cured specimen is sharply below than that of the companion prism immersed in a 1N NaOH solution.

- d. Since the expansion of water-cured prisms under the ASTM C 1293M2 is very small throughout the test duration of 26 weeks, a small variation in expansion among the specimens made with an aggregate source may produce a huge difference between the mean and the individual value. A tiny variation in the ASR-related expansions of water-cured prisms may also lead to an erroneous outcome on aggregate classifications. Therefore, assessing the alkali-silica reactivity of an aggregate using ASTM C 1293M2 (prisms submerged in water at the temperature of 80°C) may be harder as compared to that of alkali-immersed ASTM C 1293. Additionally, no ASR-induced cracks on the surface of water-cured prisms are observed even for the highly reactive aggregate at the age of 6 months.

6.1.6 Influence of aggregate mineralogies on ASR

The results show that the aggregate mineralogies overestimate the reactivity of some aggregates. Considering rock type as a sole criterion for the aggregate's potential for ASR may lead to an erroneous result. Additionally, the mineralogy of aggregate is unable to offer the extent of the reactivity of an aggregate.

6.2 Loss in Mechanical Properties due to ASR

The ASR-induced losses in the 28-day and 180-day moist cured ultimate compressive strength and modulus of elasticity of the concrete cylinders containing aggregates from the fourteen different quarries were evaluated. Additionally, the impact of ASR on the compressive strength and stiffness losses of the alkali-cured cylinders between the immersion ages of 28 and 180 days under the temperature of 80°C was studied. The following conclusions are drawn:

- a. The compressive strength is not generally affected by alkali-silica reactivity during the early stage of curing (28 days). However, aggregates susceptible to the high level of alkali-silica reactivity may experience loss in strength at the early age. At the late stage of curing (6 months), loss in ultimate compressive strength shows an indication of ASR, particular when the cracking of the specimens becomes matured.
- b. The proposed analytical results show that the aggregates experiencing the 6-month loss in compressive strength of more than 8% can be considered as reactive. The loss in compressive strength of the alkali-cured cylinders at 80°C between the ages of 28 and 180 days depends on the reactivity of aggregate. If the compressive strength of alkali-cured cylinders at 180 days is less than that obtained at 28 days by 0.5% or more, the aggregate is considered reactive, and innocuous if otherwise.
- c. A good agreement on the level of ASR of the trial aggregates is obtained based on the above-mentioned failure criteria of the 6-month loss in alkali-cured compressive strength and the loss in alkali-cured cylinders between the ages of 28 days and 6 months.
- d. The reduction in stiffness is more influenced by the ASR when compared to the loss in strength. Alkali-silica reaction in concrete reduces concrete stiffness significantly both at the early and extended immersion ages. As a result, the failure criteria of the 28-day loss in stiffness by a certain value may not produce consistent results on the alkali-aggregate reactivity.

- e. In order to consider an aggregate reactive, the analytical models reveal that the 6-month loss in alkali-cured stiffness (LIS) of more than 18%, and the LIS of the alkali-cured cylinders between the ages of 28 and 180 days of more than 9%. Both failure limits on the loss in stiffness provide an indicator on the degree of alkali-aggregate reactivity.
- f. Both the 28- and 180-day loss in stiffness may overestimate the level of alkali-silica reactivity of some aggregates. As such, other evaluation methods should be used to assess the extent of alkali-silica reactivity.
- g. The failure mechanisms of the concrete cylinders in compression are also affected by alkali-silica reactivity. The undamaged alkali-cured cylinders (specimens prepared with innocuous aggregates) fail in a conical shaped with a boisterous sound. On the other hand, damaged concrete cylinders (the specimens incorporated with reactive aggregates) fail in an irregular fashion, accompanied by the ASR cracks with a crumbling sound.
- h. The alkali-silica reactivity of the trial aggregates shows a good correlation based on the extended expansion limits of ASTM C 1260 and ASTM C 1293M1, and the failure limits of loss in compressive strength. However, limits of ASTM C 1293M1 at 4 weeks, and ASTM C 1260 at 14 days, loss in stiffness, and aggregate mineralogy by themselves may not be a good indicator in predicting the potential for deleterious alkali-silica reactivity.

6.3 Mitigating Techniques to Suppress ASR

The excessive expansions of the mortar bars prepared with the seven selected aggregates were suppressed by utilizing three mitigation techniques. They were: (i)

blending four dosages of Class F fly ash; namely, 15, 20, 25, and 30%; as a partial replacement of Portland cement, (ii) adding four to six dosages of lithium nitrates; namely, lithium-to-alkali molar ratios of 0.59, 0.74, 0.89, 1.04, 1.19, and 1.33; with the mixture water, and (iii) the combined use of Class F fly ash (15 or 20%) and a lithium-to-alkali molar ratio of 0.74. The findings of each ASR mitigation technique can be described below:

6.3.1 Role of Class F fly ash on ASR expansions

- a. The ASR expansion of the test mortar bars decreases with an increase in the fly ash content. The reduction in expansion (RIE) is highest at the early immersion age (usually at 3 or 6 days), and then gradually decreases with an increase in test duration. Additionally, the results reveal that the RIE decreases rapidly, with increased immersion age, at lower fly ash content (15%) than that obtained for the mortar bars made with a higher fly ash dosage (30%).
- b. For some aggregates, the amount of minimum experimental Class F fly ash dosage to inhibit excess ASR-induced expansions at the early age of immersion (14 days) is shown effective in holding back the adverse effect of ASR at the extended immersion ages of 28 and 56 days. However, for most aggregates, a higher dosage of Class F fly ash is required to suppress ASR expansions at 28 and 56 days. As the alkali-silica reactivity of an aggregate depends on a number of factors, it is recommended to use the minimum amount of Class F fly ash that is sufficient to control ASR-induced expansions below the limits of 0.10% at 14 days, 0.28% at 28 days and 0.47% at 56 days. An aggregate not exceeding the three-failure limits is anticipated to perform in an innocuous behavior in the field.

c. The ASR-induced expansions of the trial reactive aggregates decreases linearly with an increase in the equivalent SiO_2 content, and increases proportionally with an increase in the equivalent CaO content of the mortar bars. Additionally, the ratio of the equivalent CaO to equivalent SiO_2 of the mixture shows a linear correlation with the expansion of the fly ash-treated mortar bars.

d. A good agreement exists between the minimum required experimental fly ash dosage and that suggested by the proposed analytical models. The proposed analytical methods may be used to select the minimum amount of Class F fly ash that is capable of limiting the ASR expansion of the selected reactive aggregates below the prescribed failure criteria given at different immersion ages. However, since alkali-silica reactivity involves complex mechanisms based on numerous factors, each aggregate needs to be tested with the job cement and fly ash with known physio-chemical characteristics before it is used in Portland cement concrete.

6.3.2 Role of lithium salt in suppressing ASR

- a. The reduction in expansion (RIE) of the mortar bars made with various lithium dosages is maximum at the early immersion age of 3 days, and then gradually decreases with an increase in the test duration. The study also reveals that the RIE decreases rapidly, with an increase in immersion age, for the mortar bars containing lower lithium dosage than that prepared with a higher lithium content.
- b. A good agreement exists between the required minimum experimental and analytical lithium dosages to control the excessive expansion of the trial reactive aggregates at the immersion ages of 14, 28 and 56 days. The proposed analytical

model can be used in selecting the initial lithium dosage for suppressing alkali-silica reactivity for any reactive aggregates below the suggested failure criteria. However, since aggregates can vary extensively in their mineralogies, it is highly recommended that each reactive aggregate be tested with various lithium dosages before it is used in Portland cement concrete.

- c. The required minimum experimental lithium dosage to suppress excessive ASR-induced expansion of most reactive aggregates below 0.1% at 14 days is less than that required to reduce the expansion below 0.28% at 28 days, and 0.47% at 56 days. As such, it is suggested to use the minimum amount of lithium nitrate to arrest the ASR-related damages based on the 56-day expansion criteria.
- d. The results also reveal that lithium nitrate is found to be more effective for some extremely reactive aggregates, but comparatively less effective for less reactive aggregates. Additionally, lithium-bearing specimens show no tendency to expand after 2 to 3 months of immersion.

6.3.3 Role of combined fly ash and lithium nitrate to suppress ASR

- a. In general, the lithium-to-alkali molar ratio of 0.74 (100% lithium) is slightly more effective than 15% Class F fly ash with CaO contents of 7.4%, and less effective than 20% fly ash. The use of standard lithium dose (lithium-to-alkali molar ratio of 0.74) and a moderate amount (15%) of Class F fly ash (with a CaO content of 7.4%) as a partial replacement of Portland cement by weight is successful in arresting excessive ASR-induced expansions of the investigated reactive aggregates at the immersion ages of 14, 28, and 56 days.

- b. At the immersion age of 14 days, the difference in the reduction in expansion (RIE) for the trial reactive aggregate groups is insignificant among the 15%FA, 20%FA, 100%Li, 15%FA+100%Li, and 20%FA+100%Li. The RIE decreases rapidly, with an increase in immersion age, for the mortar bars made with both fly ash and lithium salt than that of fly ash or lithium bearing specimens. Therefore, at the extended immersion age, the use of combined fly ash and lithium nitrate is very effective in arresting ASR-produced expansions. This mitigation technique is shown to be more effective in inhibiting the excessive expansions of highly reactive aggregates, more so than moderately or slowly reactive aggregates.
- c. A good agreement exists between the experimental and analytical expansions of the mortar bars containing both fly ash and lithium nitrate at the immersion ages of 14, 28 and 56 days. The proposed analytical method may be used in selecting an optimum combined fly ash and lithium salt that is capable to limit the excess expansion of reactive aggregates below the three prescribed expansion criteria for different immersion ages.
- d. The findings of this study suggest that different aggregates may require different mitigation techniques to limit alkali-silica reactions. The final selection of an effective mitigation technique depends on its effect on early-age and late-age ASR-induced expansions, and the potential economical benefits.

6.3.4 ASR-related cracks of the fly ash and lithium bearing mortar bars

The ASR-related cracks on the surface of the test mortar bars are reduced with an increase in fly ash or lithium or both. The optimum minimum dosages of fly ash or lithium salt in suppressing ASR at 14, 28 and 56 days result in a significant reduction in

ASR-related cracks of the test specimens. The ASR-related cracks of the mortar bars prepared with the highly reactive aggregates can be completely mitigated with the proper amount of fly ash, lithium salt, or combination of both.

6.5 Recommendations for Future Studies

Future studies on the alkali-silica reactivity may include the following topics:

- a. A research study is needed to assess the role of different lithium salts, in standalone or in combination with fly ash, in alleviating the excess ASR-induced expansions of reactive aggregates.
- b. A research study is needed to examine the influence of nano-silica; which contains 99.9% SiO_2 and its particle size is less than fly ash, silica fume and slag; in suppressing ASR-induced expansions.
- c. A research study is needed to evaluate the influence of chemical compositions of fly ash (i.e. varying SiO_2 , CaO etc.) on ASR-induced expansions at early and extended immersion ages.

APPENDIX A
CHAPTER 3 DATA

Table A.1: Percent expansion of SN-A aggregate (ASTM C 1260 and its modifications)

Curing age (Day)	Alkali Content of Cement								
	0.42%			0.84%			1.26%		
	NaOH Solution Strength			NaOH Solution Strength			NaOH Solution Strength		
	1.0N	0.50N	0.25N	1.0N	0.50N	0.25N	1.0N	0.50N	0.25N
3	0.008	0.005	0.003	0.012	0.009	0.007	0.017	0.014	0.011
6	0.017	0.013	0.011	0.021	0.018	0.015	0.027	0.023	0.018
10	0.024	0.019	0.016	0.028	0.024	0.019	0.036	0.028	0.023
14	0.030	0.022	0.019	0.034	0.027	0.022	0.042	0.033	0.025
21	0.039	0.026	0.021	0.043	0.031	0.025	0.050	0.039	0.029
28	0.047	0.029	0.023	0.050	0.034	0.028	0.057	0.043	0.032
35	0.053	0.031	0.025	0.055	0.038	0.030	0.062	0.047	0.035
42	0.057	0.034	0.026	0.059	0.041	0.032	0.066	0.051	0.038
49	0.060	0.037	0.028	0.063	0.044	0.035	0.070	0.054	0.040
56	0.063	0.039	0.030	0.066	0.047	0.037	0.073	0.057	0.042
63	0.065	0.041	0.032	0.068	0.050	0.038	0.076	0.060	0.044
70	0.067	0.044	0.033	0.069	0.052	0.040	0.078	0.063	0.046
77	0.068	0.047	0.035	0.071	0.053	0.042	0.081	0.065	0.048
84	0.070	0.049	0.037	0.072	0.056	0.044	0.083	0.067	0.049
91	0.072	0.051	0.038	0.073	0.057	0.046	0.086	0.069	0.051
98	0.072	0.053	0.040	0.075	0.059	0.047	0.087	0.070	0.053

Table A.2: Percent expansion of SN-B aggregate (ASTM C 1260 and its modifications)

Curing age (Day)	Alkali Content of Cement								
	0.42%			0.84%			1.26%		
	NaOH Solution Strength			NaOH Solution Strength			NaOH Solution Strength		
	1.0N	0.50N	0.25N	1.0N	0.50N	0.25N	1.0N	0.50N	0.25N
3	0.017	0.006	0.007	0.022	0.009	0.008	0.027	0.014	0.010
6	0.041	0.010	0.009	0.052	0.016	0.012	0.058	0.024	0.014
10	0.075	0.016	0.011	0.084	0.025	0.014	0.104	0.035	0.017
14	0.108	0.024	0.013	0.118	0.032	0.016	0.135	0.045	0.019
21	0.164	0.036	0.014	0.178	0.048	0.018	0.194	0.061	0.023
28	0.219	0.052	0.016	0.233	0.062	0.020	0.256	0.076	0.027
35	0.270	0.065	0.018	0.286	0.076	0.023	0.314	0.095	0.030
42	0.306	0.080	0.019	0.328	0.093	0.026	0.361	0.112	0.033
49	0.343	0.101	0.021	0.369	0.113	0.028	0.402	0.135	0.036
56	0.375	0.130	0.022	0.408	0.143	0.031	0.437	0.160	0.039
63	0.404	0.158	0.023	0.445	0.170	0.034	0.473	0.189	0.042
70	0.433	0.192	0.025	0.483	0.205	0.037	0.507	0.227	0.046
77	0.460	0.230	0.026	0.516	0.246	0.039	0.545	0.270	0.050
84	0.487	0.271	0.028	0.542	0.282	0.042	0.580	0.309	0.054
91	0.512	0.318	0.030	0.568	0.326	0.046	0.603	0.345	0.058
98	0.535	0.359	0.031	0.593	0.366	0.048	0.625	0.383	0.060

Table A.3: Percent expansion of SN-C aggregate (ASTM C 1260 and its modifications)

Immersed Age (Day)	Alkali Content of Cement								
	0.42%			0.84%			1.26%		
	NaOH Solution Strength			NaOH Solution Strength			NaOH Solution Strength		
	1.0N	0.50N	0.25N	1.0N	0.50N	0.25N	1.0N	0.50N	0.25N
3	0.038	0.005	0.002	0.057	0.014	0.005	0.085	0.024	0.013
6	0.094	0.010	0.003	0.124	0.022	0.008	0.153	0.037	0.018
10	0.170	0.023	0.006	0.201	0.035	0.012	0.243	0.056	0.023
14	0.247	0.037	0.008	0.272	0.049	0.015	0.320	0.076	0.027
21	0.370	0.065	0.012	0.395	0.083	0.019	0.448	0.124	0.031
28	0.475	0.100	0.014	0.502	0.135	0.023	0.563	0.193	0.035
35	0.573	0.159	0.017	0.597	0.198	0.026	0.680	0.275	0.039
42	0.656	0.229	0.019	0.680	0.272	0.028	0.776	0.353	0.043
49	0.729	0.296	0.022	0.755	0.340	0.031	0.859	0.431	0.047
56	0.799	0.359	0.025	0.823	0.410	0.033	0.936	0.507	0.050
63	0.863	0.417	0.029	0.888	0.473	0.036	1.008	0.574	0.053
70	0.924	0.471	0.032	0.953	0.532	0.039	1.075	0.644	0.057
77	0.982	0.520	0.036	1.007	0.576	0.043	1.134	0.713	0.060
84	1.035	0.567	0.039	1.059	0.624	0.046	1.195	0.775	0.064
91	1.086	0.604	0.042	1.109	0.663	0.050	1.250	0.838	0.068
98	1.130	0.636	0.046	1.152	0.700	0.053	1.300	0.886	0.072

Table A.4: Percent expansion of SN-D aggregate (ASTM C 1260 and its modifications)

Curing age (Week)	Alkali Content of Cement								
	0.42%			0.84%			1.26%		
	NaOH Solution Strength			NaOH Solution Strength			NaOH Solution Strength		
	1.0N	0.50N	0.25N	1.0N	0.50N	0.25N	1.0N	0.50N	0.25N
3	0.008	0.006	0.004	0.011	0.007	0.006	0.014	0.011	0.007
6	0.016	0.009	0.006	0.021	0.013	0.009	0.025	0.017	0.011
10	0.029	0.013	0.009	0.038	0.017	0.012	0.044	0.024	0.016
14	0.045	0.017	0.012	0.055	0.023	0.015	0.062	0.031	0.019
21	0.074	0.025	0.015	0.083	0.032	0.018	0.096	0.044	0.023
28	0.103	0.038	0.017	0.117	0.046	0.021	0.136	0.064	0.028
35	0.129	0.049	0.019	0.149	0.059	0.024	0.168	0.081	0.031
42	0.154	0.065	0.021	0.179	0.075	0.026	0.197	0.102	0.035
49	0.178	0.078	0.022	0.204	0.092	0.028	0.226	0.124	0.037
56	0.201	0.092	0.023	0.230	0.110	0.030	0.253	0.145	0.040
63	0.222	0.105	0.024	0.254	0.127	0.032	0.279	0.164	0.042
70	0.240	0.116	0.025	0.273	0.143	0.034	0.303	0.185	0.043
77	0.259	0.131	0.026	0.296	0.161	0.035	0.323	0.208	0.045
84	0.278	0.145	0.027	0.316	0.180	0.036	0.344	0.228	0.047
91	0.294	0.160	0.028	0.342	0.202	0.038	0.363	0.250	0.049
98	0.309	0.171	0.029	0.359	0.223	0.040	0.380	0.269	0.051

Table A.5: Percent expansion of SN-E aggregate (ASTM C 1260 and its modifications)

Curing age (Week)	Alkali Content of Cement								
	0.42%			0.84%			1.26%		
	NaOH Solution Strength			NaOH Solution Strength			NaOH Solution Strength		
	1.0N	0.50N	0.25N	1.0N	0.50N	0.25N	1.0N	0.50N	0.25N
3	0.009	0.008	0.006	0.015	0.012	0.009	0.019	0.014	0.011
6	0.015	0.013	0.009	0.025	0.017	0.014	0.031	0.023	0.017
10	0.023	0.017	0.012	0.035	0.022	0.017	0.041	0.030	0.022
14	0.030	0.020	0.015	0.044	0.026	0.020	0.050	0.034	0.025
21	0.042	0.025	0.018	0.056	0.031	0.023	0.062	0.041	0.028
28	0.056	0.029	0.020	0.067	0.036	0.025	0.074	0.047	0.030
35	0.068	0.034	0.023	0.078	0.041	0.028	0.084	0.053	0.033
42	0.079	0.039	0.026	0.086	0.046	0.031	0.093	0.059	0.035
49	0.086	0.044	0.027	0.094	0.051	0.033	0.102	0.065	0.038
56	0.093	0.048	0.030	0.100	0.055	0.036	0.109	0.071	0.040
63	0.099	0.052	0.032	0.105	0.059	0.038	0.113	0.075	0.043
70	0.103	0.055	0.034	0.108	0.064	0.042	0.117	0.078	0.047
77	0.106	0.058	0.037	0.110	0.068	0.045	0.118	0.080	0.048
84	0.108	0.061	0.039	0.112	0.070	0.047	0.120	0.083	0.051
91	0.110	0.063	0.043	0.113	0.072	0.050	0.121	0.085	0.054
98	0.112	0.066	0.046	0.114	0.075	0.052	0.122	0.087	0.057

Table A.6: Percent expansion of SN-F aggregate (ASTM C 1260 and its modifications)

Curing age (Week)	Alkali Content of Cement								
	0.42%			0.84%			1.26%		
	NaOH Solution Strength			NaOH Solution Strength			NaOH Solution Strength		
	1.0N	0.50N	0.25N	1.0N	0.50N	0.25N	1.0N	0.50N	0.25N
3	0.023	0.010	0.005	0.029	0.016	0.009	0.045	0.017	0.011
6	0.077	0.015	0.010	0.094	0.022	0.013	0.126	0.028	0.015
10	0.192	0.022	0.012	0.221	0.031	0.015	0.239	0.037	0.018
14	0.307	0.031	0.014	0.329	0.039	0.017	0.351	0.049	0.020
21	0.456	0.047	0.016	0.481	0.059	0.019	0.521	0.079	0.023
28	0.569	0.072	0.018	0.599	0.085	0.022	0.643	0.128	0.025
35	0.661	0.108	0.021	0.694	0.128	0.024	0.742	0.189	0.028
42	0.737	0.161	0.022	0.770	0.185	0.026	0.819	0.251	0.031
49	0.807	0.225	0.025	0.838	0.255	0.028	0.895	0.325	0.033
56	0.867	0.282	0.027	0.896	0.325	0.030	0.966	0.401	0.036
63	0.914	0.340	0.029	0.952	0.384	0.033	1.033	0.484	0.040
70	0.965	0.394	0.031	0.996	0.438	0.035	1.094	0.563	0.043
77	1.006	0.439	0.034	1.042	0.487	0.037	1.148	0.635	0.046
84	1.042	0.480	0.036	1.083	0.532	0.040	1.196	0.700	0.049
91	1.073	0.519	0.039	1.120	0.573	0.043	1.239	0.761	0.052
98	1.101	0.552	0.041	1.155	0.612	0.045	1.268	0.811	0.054

Table A.7: Percent expansion of SN-G aggregate (ASTM C 1260 and its modifications)

Curing age (Week)	Alkali Content of Cement								
	0.42%			0.84%			1.26%		
	NaOH Solution Strength			NaOH Solution Strength			NaOH Solution Strength		
	1.0N	0.50N	0.25N	1.0N	0.50N	0.25N	1.0N	0.50N	0.25N
3	0.118	0.042	0.009	0.209	0.066	0.013	0.305	0.149	0.016
6	0.360	0.202	0.013	0.420	0.296	0.021	0.563	0.460	0.031
10	0.632	0.505	0.021	0.691	0.566	0.033	0.806	0.695	0.071
14	0.862	0.705	0.029	0.890	0.737	0.050	0.956	0.831	0.167
21	1.061	0.902	0.077	1.092	0.929	0.158	1.130	0.987	0.379
28	1.151	0.977	0.143	1.185	1.016	0.320	1.205	1.057	0.509
35	1.206	1.015	0.244	1.234	1.054	0.432	1.252	1.108	0.604
42	1.256	1.050	0.335	1.268	1.084	0.527	1.292	1.153	0.690
49	1.280	1.073	0.392	1.292	1.119	0.612	1.327	1.192	0.745
56	1.305	1.089	0.451	1.323	1.150	0.694	1.351	1.226	0.796
63	1.320	1.116	0.489	1.343	1.184	0.759	1.383	1.266	0.840
70	1.350	1.131	0.510	1.371	1.213	0.802	1.419	1.302	0.875
77	1.364	1.148	0.535	1.392	1.243	0.846	1.443	1.336	0.905
84	1.375	1.161	0.553	1.407	1.268	0.878	1.462	1.370	0.932
91	1.379	1.177	0.573	1.413	1.289	0.896	1.480	1.396	0.950
98	1.381	1.185	0.580	1.421	1.310	0.912	1.492	1.421	0.968

Table A.8: Percent expansion of SN-H aggregate (ASTM C 1260 and its modifications)

Curing age (Week)	Alkali Content of Cement								
	0.42%			0.84%			1.26%		
	NaOH Solution Strength			NaOH Solution Strength			NaOH Solution Strength		
	1.0N	0.50N	0.25N	1.0N	0.50N	0.25N	1.0N	0.50N	0.25N
3	0.008	0.007	0.004	0.012	0.009	0.006	0.015	0.012	0.008
6	0.016	0.011	0.007	0.020	0.013	0.009	0.025	0.017	0.012
10	0.025	0.016	0.010	0.033	0.020	0.012	0.041	0.023	0.015
14	0.038	0.020	0.012	0.050	0.025	0.015	0.058	0.031	0.018
21	0.063	0.029	0.016	0.081	0.036	0.018	0.088	0.043	0.022
28	0.086	0.036	0.019	0.109	0.046	0.021	0.119	0.059	0.025
35	0.113	0.046	0.021	0.137	0.060	0.024	0.150	0.078	0.028
42	0.140	0.057	0.023	0.162	0.074	0.026	0.177	0.098	0.030
49	0.164	0.069	0.025	0.190	0.091	0.028	0.202	0.115	0.033
56	0.186	0.080	0.027	0.213	0.106	0.030	0.225	0.133	0.035
63	0.205	0.091	0.029	0.235	0.123	0.032	0.248	0.156	0.037
70	0.226	0.105	0.031	0.256	0.139	0.034	0.270	0.177	0.039
77	0.247	0.119	0.032	0.276	0.155	0.036	0.291	0.195	0.041
84	0.266	0.131	0.034	0.295	0.170	0.038	0.311	0.212	0.043
91	0.284	0.142	0.035	0.311	0.182	0.040	0.329	0.227	0.045
98	0.302	0.156	0.037	0.325	0.193	0.042	0.345	0.240	0.047

Table A.9: Percent expansion of SN-I aggregate (ASTM C 1260 and its modifications)

Curing age (Week)	Alkali Content of Cement								
	0.42%			0.84%			1.26%		
	NaOH Solution Strength			NaOH Solution Strength			NaOH Solution Strength		
	1.0N	0.50N	0.25N	1.0N	0.50N	0.25N	1.0N	0.50N	0.25N
3	0.032	0.012	0.007	0.047	0.017	0.010	0.060	0.024	0.013
6	0.105	0.020	0.012	0.134	0.032	0.014	0.160	0.053	0.018
10	0.181	0.037	0.016	0.199	0.062	0.019	0.215	0.090	0.022
14	0.218	0.054	0.020	0.237	0.087	0.022	0.254	0.116	0.025
21	0.270	0.095	0.025	0.287	0.132	0.028	0.310	0.156	0.031
28	0.311	0.127	0.028	0.332	0.166	0.031	0.353	0.187	0.036
35	0.343	0.154	0.032	0.371	0.191	0.035	0.389	0.214	0.040
42	0.374	0.177	0.035	0.403	0.214	0.038	0.422	0.237	0.044
49	0.401	0.203	0.037	0.430	0.238	0.041	0.453	0.258	0.048
56	0.424	0.218	0.039	0.460	0.257	0.044	0.480	0.275	0.052
63	0.445	0.237	0.041	0.480	0.274	0.047	0.501	0.293	0.056
70	0.464	0.252	0.042	0.501	0.292	0.051	0.522	0.312	0.059
77	0.481	0.268	0.043	0.522	0.310	0.054	0.543	0.327	0.063
84	0.493	0.284	0.045	0.535	0.323	0.057	0.561	0.342	0.066
91	0.506	0.293	0.047	0.546	0.339	0.060	0.579	0.357	0.069
98	0.519	0.302	0.048	0.557	0.355	0.063	0.591	0.370	0.071

Table A.10: Percent expansion of SN-J Aggregate (ASTM C 1260 and its modifications)

Curing age (Week)	Alkali Content of Cement								
	0.42%			0.84%			1.26%		
	NaOH Solution Strength			NaOH Solution Strength			NaOH Solution Strength		
	1.0N	0.50N	0.25N	1.0N	0.50N	0.25N	1.0N	0.50N	0.25N
3	0.093	0.020	0.009	0.127	0.023	0.012	0.170	0.034	0.016
6	0.243	0.060	0.014	0.291	0.103	0.018	0.321	0.134	0.022
10	0.355	0.191	0.018	0.398	0.268	0.024	0.415	0.296	0.028
14	0.418	0.286	0.023	0.465	0.370	0.028	0.493	0.388	0.034
21	0.504	0.359	0.031	0.563	0.442	0.037	0.590	0.462	0.042
28	0.570	0.408	0.038	0.620	0.491	0.047	0.650	0.508	0.052
35	0.614	0.436	0.044	0.675	0.529	0.054	0.697	0.543	0.060
42	0.657	0.456	0.049	0.722	0.561	0.062	0.741	0.579	0.068
49	0.689	0.477	0.052	0.768	0.593	0.068	0.787	0.607	0.075
56	0.725	0.498	0.055	0.800	0.615	0.075	0.821	0.640	0.083
63	0.750	0.517	0.059	0.830	0.637	0.082	0.864	0.670	0.090
70	0.768	0.525	0.062	0.864	0.664	0.087	0.892	0.699	0.096
77	0.795	0.542	0.065	0.894	0.682	0.094	0.929	0.726	0.103
84	0.818	0.556	0.069	0.927	0.701	0.099	0.970	0.756	0.110
91	0.843	0.571	0.072	0.956	0.723	0.105	1.003	0.787	0.115
98	0.866	0.582	0.075	0.981	0.739	0.110	1.034	0.811	0.120

Table A.11: Percent Expansion of NN-A Aggregate (ASTM C 1260 and its modifications)

Curing age (Week)	Alkali Content of Cement								
	0.42%			0.84%			1.26%		
	NaOH Solution Strength			NaOH Solution Strength			NaOH Solution Strength		
	1.0N	0.50N	0.25N	1.0N	0.50N	0.25N	1.0N	0.50N	0.25N
3	0.024	0.005	0.002	0.027	0.007	0.003	0.031	0.009	0.004
6	0.057	0.011	0.004	0.064	0.015	0.007	0.076	0.019	0.009
10	0.108	0.018	0.007	0.122	0.023	0.010	0.139	0.032	0.014
14	0.142	0.028	0.009	0.161	0.036	0.013	0.187	0.043	0.018
21	0.200	0.051	0.019	0.229	0.059	0.024	0.257	0.087	0.033
28	0.241	0.090	0.047	0.277	0.103	0.054	0.314	0.137	0.070
35	0.269	0.128	0.077	0.304	0.145	0.087	0.336	0.168	0.096
42	0.285	0.147	0.088	0.321	0.166	0.099	0.352	0.183	0.107
49	0.293	0.157	0.093	0.330	0.178	0.105	0.359	0.198	0.112
56	0.300	0.166	0.096	0.338	0.187	0.108	0.364	0.209	0.116
63	0.308	0.172	0.098	0.347	0.193	0.111	0.370	0.215	0.120
70	0.310	0.176	0.100	0.349	0.199	0.113	0.375	0.222	0.122
77	0.315	0.183	0.102	0.354	0.206	0.115	0.377	0.226	0.125
84	0.320	0.188	0.105	0.358	0.210	0.117	0.377	0.231	0.126
91	0.324	0.192	0.107	0.362	0.214	0.119	0.379	0.238	0.129
98	0.327	0.197	0.109	0.364	0.219	0.121	0.382	0.243	0.132

Table A.12: Percent Expansion of NN-B Aggregate (ASTM C 1260 and its modifications)

Curing age (Week)	Alkali Content of Cement								
	0.42%			0.84%			1.26%		
	NaOH Solution Strength			NaOH Solution Strength			NaOH Solution Strength		
	1.0N	0.50N	0.25N	1.0N	0.50N	0.25N	1.0N	0.50N	0.25N
3	0.115	0.043	0.008	0.197	0.095	0.025	0.331	0.197	0.053
6	0.405	0.186	0.024	0.561	0.353	0.047	0.661	0.541	0.145
10	0.787	0.453	0.055	0.874	0.664	0.092	0.972	0.924	0.270
14	1.023	0.725	0.080	1.098	0.925	0.116	1.240	1.160	0.391
21	1.348	1.102	0.111	1.407	1.268	0.165	1.563	1.476	0.559
28	1.549	1.306	0.165	1.610	1.510	0.257	1.810	1.719	0.742
35	1.701	1.465	0.225	1.760	1.683	0.390	1.970	1.883	0.893
42	1.804	1.586	0.333	1.876	1.808	0.500	2.100	1.994	1.026
49	1.899	1.666	0.450	1.968	1.887	0.580	2.198	2.087	1.151
56	1.975	1.752	0.552	2.050	1.948	0.670	2.267	2.155	1.252
63	2.044	1.814	0.652	2.105	1.999	0.764	2.332	2.219	1.347
70	2.106	1.869	0.789	2.162	2.045	0.873	2.378	2.265	1.430
77	2.153	1.917	0.883	2.220	2.084	0.964	2.437	2.323	1.518
84	2.202	1.953	0.992	2.254	2.130	1.047	2.467	2.354	1.575
91	2.240	1.987	1.070	2.290	2.170	1.110	2.499	2.387	1.642
98	2.270	2.011	1.115	2.335	2.210	1.164	2.510	2.413	1.672

Table A.13: Percent Expansion of NN-C Aggregate (ASTM C 1260 and its modifications)

Curing age (Week)	Alkali Content of Cement								
	0.42%			0.84%			1.26%		
	NaOH Solution Strength			NaOH Solution Strength			NaOH Solution Strength		
	1.0N	0.50N	0.25N	1.0N	0.50N	0.25N	1.0N	0.50N	0.25N
3	0.098	0.023	0.009	0.177	0.059	0.021	0.262	0.160	0.027
6	0.330	0.093	0.015	0.440	0.242	0.032	0.539	0.468	0.067
10	0.587	0.316	0.021	0.708	0.553	0.062	0.843	0.753	0.110
14	0.830	0.570	0.034	0.940	0.834	0.115	1.072	0.961	0.200
21	1.203	0.947	0.060	1.271	1.092	0.214	1.384	1.247	0.511
28	1.414	1.140	0.090	1.472	1.261	0.397	1.596	1.451	0.715
35	1.556	1.265	0.130	1.601	1.380	0.559	1.749	1.599	0.861
42	1.647	1.350	0.173	1.694	1.467	0.674	1.854	1.698	0.996
49	1.731	1.419	0.262	1.766	1.536	0.761	1.920	1.762	1.098
56	1.794	1.483	0.351	1.828	1.601	0.852	1.960	1.824	1.176
63	1.825	1.541	0.422	1.870	1.640	0.907	2.002	1.867	1.270
70	1.847	1.579	0.515	1.903	1.684	0.967	2.065	1.920	1.343
77	1.877	1.615	0.583	1.923	1.717	1.025	2.114	1.976	1.413
84	1.886	1.644	0.640	1.958	1.748	1.061	2.158	2.011	1.469
91	1.909	1.670	0.685	1.965	1.772	1.104	2.194	2.045	1.536
98	1.926	1.682	0.726	1.993	1.796	1.145	2.240	2.085	1.590

Table A.14: Percent Expansion of NN-D Aggregate (ASTM C 1260 and its modifications)

Curing age (Week)	Alkali Content of Cement								
	0.42%			0.84%			1.26%		
	NaOH Solution Strength			NaOH Solution Strength			NaOH Solution Strength		
	1.0N	0.50N	0.25N	1.0N	0.50N	0.25N	1.0N	0.50N	0.25N
3	0.025	0.019	0.006	0.045	0.024	0.012	0.088	0.060	0.033
6	0.058	0.031	0.009	0.083	0.044	0.019	0.134	0.089	0.048
10	0.114	0.047	0.012	0.138	0.069	0.026	0.184	0.126	0.061
14	0.163	0.059	0.015	0.186	0.091	0.029	0.229	0.161	0.072
21	0.251	0.098	0.023	0.262	0.131	0.037	0.288	0.207	0.086
28	0.312	0.128	0.033	0.322	0.166	0.046	0.340	0.267	0.097
35	0.360	0.148	0.042	0.368	0.197	0.057	0.388	0.320	0.114
42	0.405	0.179	0.049	0.413	0.237	0.066	0.436	0.368	0.131
49	0.444	0.208	0.058	0.455	0.277	0.075	0.479	0.407	0.144
56	0.471	0.238	0.069	0.488	0.315	0.085	0.517	0.447	0.157
63	0.505	0.262	0.078	0.521	0.347	0.095	0.555	0.482	0.170
70	0.534	0.287	0.086	0.547	0.378	0.104	0.592	0.515	0.186
77	0.561	0.311	0.094	0.579	0.407	0.114	0.622	0.545	0.197
84	0.599	0.339	0.101	0.613	0.440	0.124	0.654	0.575	0.210
91	0.628	0.363	0.109	0.641	0.469	0.136	0.684	0.605	0.217
98	0.664	0.395	0.114	0.677	0.494	0.148	0.718	0.630	0.227

Table A.15: Percent expansion of mortar bars made with natural fine aggregate (ASTM C 1260)

Agg. ID	3-day	6-day	10-day	14-day
SN-A	0.006	0.012	0.024	0.037
SN-B	0.016	0.050	0.089	0.120
SN-C	0.030	0.119	0.232	0.277
SN-D	0.006	0.022	0.042	0.066
SN-E	0.011	0.022	0.046	0.073
SN-F	0.027	0.089	0.226	0.347
SN-G	0.177	0.422	0.561	0.748
SN-H	0.012	0.021	0.036	0.054
SN-I	0.024	0.085	0.167	0.211
SN-J	0.066	0.250	0.383	0.475
NN-A	0.026	0.052	0.087	0.106
NN-B	0.186	0.477	0.792	1.032
NN-C	0.156	0.451	0.747	0.943
NN-D	0.021	0.046	0.075	0.105

Table A.16: Percent expansion of aggregates quarried from the Southern Nevada based on ASTM C 1293M1 (Prisms immersed in the 1N NaOH solution at 80°C)

Curing age (Week)	SN-A	SN-B	SN-C	SN-D	SN-E	SN-F	SN-G	SN-H	SN-I	SN-J
1	0.010	0.030	0.020	0.017	0.001	0.032	0.037	0.010	0.016	0.030
2	0.014	0.051	0.031	0.039	0.003	0.048	0.106	0.019	0.027	0.044
3	0.016	0.067	0.045	0.057	0.006	0.066	0.144	0.028	0.039	0.063
4	0.018	0.078	0.063	0.074	0.008	0.083	0.181	0.039	0.051	0.084
5	0.019	0.090	0.072	0.090	0.011	0.100	0.214	0.052	0.059	0.104
6	0.020	0.102	0.082	0.099	0.015	0.125	0.244	0.065	0.072	0.124
7	0.022	0.113	0.101	0.112	0.022	0.148	0.267	0.076	0.082	0.140
8	0.022	0.122	0.112	0.128	0.027	0.168	0.288	0.088	0.094	0.160
9	0.023	0.135	0.128	0.140	0.032	0.187	0.307	0.098	0.105	0.180
10	0.024	0.146	0.139	0.153	0.036	0.207	0.328	0.105	0.115	0.194
11	0.026	0.161	0.150	0.164	0.040	0.223	0.346	0.110	0.125	0.206
12	0.027	0.170	0.169	0.175	0.044	0.242	0.360	0.119	0.132	0.217
13	0.028	0.181	0.180	0.185	0.047	0.261	0.375	0.123	0.141	0.227
14	0.029	0.192	0.201	0.198	0.050	0.275	0.386	0.129	0.150	0.235
15	0.030	0.204	0.220	0.209	0.053	0.291	0.396	0.134	0.157	0.243
16	0.031	0.220	0.237	0.220	0.056	0.307	0.410	0.138	0.163	0.253
17	0.032	0.233	0.254	0.229	0.059	0.324	0.423	0.144	0.169	0.260
18	0.033	0.245	0.266	0.238	0.062	0.340	0.433	0.149	0.175	0.274
19	0.034	0.256	0.284	0.249	0.066	0.357	0.449	0.151	0.182	0.280
20	0.035	0.266	0.293	0.259	0.069	0.371	0.463	0.154	0.187	0.289
21	0.036	0.276	0.304	0.266	0.071	0.383	0.480	0.157	0.194	0.300
22	0.036	0.286	0.314	0.272	0.073	0.395	0.495	0.160	0.200	0.308
23	0.037	0.299	0.320	0.283	0.076	0.407	0.506	0.163	0.205	0.315
24	0.037	0.314	0.324	0.291	0.079	0.417	0.514	0.165	0.210	0.328
25	0.038	0.328	0.330	0.297	0.081	0.421	0.521	0.168	0.214	0.334
26	0.038	0.342	0.336	0.307	0.085	0.429	0.528	0.171	0.217	0.340

Table A.17: Percent expansion of the aggregates quarried from the Northern Nevada based on ASTM C 1293M1 (Prisms immersed in the 1N NaOH solution at 80°C)

Curing age (Week)	NN-A	NN-B	NN-C	NN-D
1	0.015	0.090	0.074	0.025
2	0.026	0.181	0.153	0.047
3	0.034	0.243	0.205	0.072
4	0.039	0.303	0.243	0.092
5	0.043	0.342	0.279	0.114
6	0.047	0.384	0.312	0.132
7	0.051	0.421	0.343	0.147
8	0.053	0.447	0.370	0.162
9	0.056	0.479	0.392	0.174
10	0.058	0.505	0.417	0.188
11	0.064	0.535	0.437	0.199
12	0.068	0.557	0.459	0.211
13	0.071	0.584	0.482	0.222
14	0.073	0.612	0.502	0.230
15	0.076	0.633	0.525	0.241
16	0.080	0.657	0.542	0.250
17	0.086	0.673	0.560	0.259
18	0.091	0.692	0.578	0.267
19	0.094	0.708	0.596	0.276
20	0.097	0.731	0.611	0.284
21	0.100	0.754	0.631	0.291
22	0.102	0.773	0.647	0.300
23	0.104	0.794	0.660	0.306
24	0.105	0.814	0.672	0.311
25	0.107	0.833	0.682	0.316
26	0.110	0.853	0.693	0.319

Table A.18: Percent expansion of the aggregates quarried from the Southern Nevada based on ASTM C 1293M2 (Prisms immersed in the distilled water at 80°C)

Curing age (Week)	SN-A	SN-B	SN-C	SN-D	SN-E	SN-F	SN-G	SN-H	SN-I	SN-J
1	0.003	0.004	0.007	0.009	0.001	0.006	0.007	0.003	0.006	0.008
2	0.004	0.007	0.011	0.011	0.002	0.009	0.010	0.006	0.008	0.011
3	0.005	0.009	0.014	0.013	0.002	0.011	0.012	0.009	0.009	0.013
4	0.007	0.010	0.016	0.016	0.003	0.012	0.013	0.010	0.010	0.015
5	0.008	0.012	0.017	0.016	0.004	0.014	0.014	0.011	0.011	0.017
6	0.009	0.013	0.018	0.017	0.004	0.015	0.015	0.012	0.011	0.018
7	0.009	0.014	0.019	0.018	0.005	0.017	0.016	0.013	0.012	0.019
8	0.010	0.015	0.020	0.019	0.006	0.018	0.017	0.014	0.013	0.020
9	0.010	0.016	0.021	0.019	0.006	0.019	0.018	0.014	0.014	0.021
10	0.011	0.017	0.021	0.020	0.007	0.020	0.019	0.015	0.015	0.022
11	0.012	0.019	0.022	0.021	0.008	0.022	0.020	0.015	0.015	0.022
12	0.012	0.021	0.022	0.021	0.008	0.023	0.021	0.016	0.016	0.023
13	0.012	0.022	0.023	0.022	0.009	0.024	0.022	0.017	0.016	0.023
14	0.012	0.023	0.024	0.023	0.009	0.025	0.023	0.018	0.017	0.024
15	0.012	0.025	0.025	0.024	0.010	0.026	0.024	0.018	0.017	0.024
16	0.012	0.025	0.026	0.024	0.010	0.027	0.025	0.019	0.018	0.024
17	0.013	0.026	0.026	0.024	0.010	0.027	0.026	0.019	0.019	0.025
18	0.013	0.027	0.027	0.025	0.010	0.028	0.027	0.020	0.020	0.024
19	0.013	0.027	0.028	0.025	0.011	0.028	0.028	0.021	0.020	0.025
20	0.014	0.028	0.029	0.026	0.011	0.029	0.029	0.021	0.021	0.025
21	0.014	0.029	0.030	0.026	0.011	0.029	0.030	0.022	0.021	0.026
22	0.014	0.030	0.031	0.027	0.011	0.030	0.031	0.022	0.022	0.026
23	0.014	0.031	0.032	0.027	0.011	0.030	0.031	0.023	0.022	0.026
24	0.014	0.032	0.032	0.028	0.011	0.031	0.032	0.023	0.023	0.027
25	0.014	0.033	0.033	0.028	0.011	0.032	0.033	0.023	0.023	0.027
26	0.014	0.033	0.033	0.029	0.011	0.032	0.034	0.023	0.023	0.027

Table A.19: Percent expansion of the aggregates quarried from the Northern Nevada based on ASTM C 1293M1 (Prisms immersed in the 1N NaOH solution at 80°C)

Curing age (Week)	NN-A	NN-B	NN-C	NN-D
1	0.003	0.007	0.007	0.004
2	0.006	0.012	0.010	0.008
3	0.008	0.014	0.012	0.011
4	0.009	0.016	0.014	0.013
5	0.010	0.016	0.015	0.014
6	0.011	0.017	0.016	0.015
7	0.012	0.018	0.017	0.015
8	0.013	0.018	0.018	0.016
9	0.014	0.019	0.019	0.017
10	0.015	0.020	0.020	0.018
11	0.016	0.021	0.021	0.019
12	0.017	0.022	0.022	0.020
13	0.017	0.023	0.023	0.020
14	0.018	0.024	0.024	0.021
15	0.018	0.025	0.025	0.021
16	0.019	0.026	0.026	0.022
17	0.019	0.027	0.027	0.022
18	0.019	0.028	0.028	0.023
19	0.020	0.030	0.029	0.023
20	0.020	0.031	0.030	0.024
21	0.020	0.032	0.031	0.024
22	0.021	0.032	0.032	0.024
23	0.021	0.033	0.033	0.025
24	0.022	0.034	0.034	0.025
25	0.022	0.035	0.035	0.026
26	0.022	0.036	0.036	0.026

Table A.20: Percent expansion of the aggregates quarried from the Southern Nevada based on ASTM C 1105 (Prisms cured in water at 20°C)

Curing age (Week)	SN-A	SN-B	SN-C	SN-D	SN-E	SN-F	SN-G	SN-H	SN-I	SN-J
1	0.001	0.004	0.004	0.002	0.000	0.005	0.003	0.003	0.005	0.003
2	0.002	0.005	0.004	0.003	0.001	0.008	0.004	0.005	0.006	0.004
3	0.002	0.006	0.005	0.005	0.001	0.010	0.005	0.007	0.007	0.005
4	0.003	0.006	0.007	0.005	0.002	0.011	0.006	0.008	0.008	0.006
5	0.003	0.007	0.008	0.005	0.002	0.012	0.007	0.008	0.009	0.007
6	0.003	0.008	0.009	0.006	0.003	0.012	0.007	0.008	0.009	0.008
7	0.003	0.008	0.009	0.007	0.004	0.013	0.007	0.009	0.009	0.008
8	0.003	0.009	0.009	0.008	0.005	0.013	0.008	0.009	0.009	0.008
9	0.003	0.009	0.010	0.008	0.005	0.014	0.008	0.010	0.010	0.009
10	0.004	0.010	0.010	0.009	0.005	0.014	0.008	0.010	0.010	0.010
11	0.004	0.011	0.011	0.009	0.006	0.015	0.008	0.010	0.010	0.010
12	0.005	0.011	0.011	0.009	0.006	0.015	0.009	0.011	0.011	0.011
13	0.005	0.011	0.012	0.010	0.007	0.015	0.010	0.011	0.011	0.011
14	0.005	0.012	0.012	0.010	0.007	0.016	0.010	0.012	0.012	0.012
16	0.006	0.012	0.013	0.011	0.007	0.016	0.011	0.013	0.013	0.013
18	0.006	0.012	0.013	0.012	0.008	0.016	0.012	0.014	0.014	0.013
20	0.007	0.013	0.014	0.013	0.008	0.017	0.013	0.015	0.015	0.014
22	0.008	0.014	0.014	0.014	0.008	0.017	0.014	0.015	0.015	0.015
24	0.009	0.014	0.015	0.015	0.009	0.018	0.015	0.016	0.015	0.015
26	0.010	0.015	0.015	0.015	0.009	0.018	0.015	0.016	0.016	0.016
30	0.010	0.017	0.016	0.016	0.010	0.018	0.016	0.017	0.016	0.017
34	0.011	0.017	0.016	0.016	0.010	0.018	0.017	0.017	0.017	0.017
38	0.011	0.018	0.017	0.017	0.010	0.019	0.017	0.018	0.018	0.018
42	0.011	0.018	0.017	0.017	0.011	0.020	0.018	0.018	0.018	0.018
47	0.012	0.019	0.018	0.018	0.011	0.020	0.018	0.019	0.018	0.018
52	0.013	0.019	0.018	0.019	0.011	0.021	0.019	0.019	0.019	0.019

Table A.21: Percent expansion of the aggregates quarried from the Northern Nevada based on ASTM C 1105 (Prisms cured in water at 20°C)

Curing age (Week)	NN-A	NN-B	NN-C	NN-D
1	0.003	0.004	0.010	0.001
2	0.005	0.007	0.012	0.004
3	0.007	0.008	0.014	0.007
4	0.008	0.010	0.016	0.008
5	0.009	0.011	0.016	0.009
6	0.011	0.012	0.017	0.009
7	0.012	0.012	0.018	0.010
8	0.013	0.013	0.018	0.010
9	0.013	0.013	0.019	0.011
10	0.013	0.014	0.020	0.011
11	0.014	0.015	0.021	0.012
12	0.014	0.016	0.020	0.013
13	0.015	0.017	0.021	0.014
14	0.016	0.018	0.021	0.015
16	0.017	0.019	0.023	0.015
18	0.018	0.020	0.023	0.016
20	0.018	0.021	0.024	0.016
22	0.019	0.022	0.024	0.017
24	0.019	0.023	0.025	0.018
26	0.020	0.024	0.025	0.018
30	0.020	0.026	0.026	0.019
34	0.021	0.027	0.026	0.020
38	0.021	0.028	0.027	0.020
42	0.021	0.029	0.028	0.021
47	0.022	0.030	0.029	0.021
52	0.022	0.031	0.031	0.022

APPENDIX B
CHAPTER 4 DATA

Table B.1: Ultimate compressive strength (psi) of 4 in x 8 in cylinders at 28 days

Agg. ID	Water-cured			Alkali-cured		
	#1	#2	#3	#1	#2	#3
SN-A	5902.3	5767.0	6188.6	6379.5	6172.7	6347.7
SN-B	5718.5	5354.2	5405.9	6082.0	5961.9	5835.5
SN-C	4303.9	4294.3	4285.5	4402.0	4312.2	4443.4
SN-D	5845.8	5468.8	5544.3	5985.8	6196.6	6226.0
SN-E	5615.9	5237.3	5385.2	5771.0	5632.6	5986.6
SN-F	5308.9	5384.4	5329.5	5860.1	5919.0	6045.5
SN-G	5059.1	4931.8	4896.8	5299.3	5090.9	5115.6
SN-H	5429.0	5483.9	5499.0	6397.4	6375.5	7103.4
SN-I	4653.4	4740.9	4669.3	4985.1	5015.3	5067.0
SN-J	4561.9	4753.6	4890.5	5850.6	5248.4	5763.1
NN-A	6307.2	6029.5	6378.0	6999.2	7134.4	7104.2
NN-B	5024.9	5130.7	5011.4	3797.5	3983.6	4036.9
NN-C	4787.8	4725.0	4908.0	4947.7	5073.8	5055.1
NN-D	4901.3	4901.7	4823.6	5364.5	5392.1	5674.0

Table B.2: Ultimate compressive strength (psi) of 4 in x 8 in cylinders at 6 months

Agg. ID	Water-cured			Alkali-cured		
	#1	#2	#3	#1	#2	#3
SN-A	7239.7	7111.4	7119.7	8431.8	8603.2	8411.5
SN-B	7070.1	7081.9	7159.1	5998.9	6012.0	6079.6
SN-C	6044.6	6061.7	6016.5	4241.4	4072.4	4082.3
SN-D	6498.9	6459.1	6447.2	6658.0	6467.0	6475.8
SN-E	6352.5	6340.6	6560.5	8431.0	8519.7	8522.5
SN-F	6507.8	6449.2	6622.2	5211.0	5218.2	5464.8
SN-G	5744.5	5843.4	6108.9	3278.5	3226.8	3212.0
SN-H	6483.0	6634.9	6495.3	6647.5	6838.5	7103.4
SN-I	5499.8	5552.3	5413.1	5711.4	5496.6	5751.1
SN-J	5768.4	5787.1	5752.9	5055.2	5081.3	5100.9
NN-A	7449.9	7562.1	7625.7	7478.1	7723.6	7803.9
NN-B	6044.6	6061.7	6016.5	3498.0	3349.5	3433.4
NN-C	5740.7	5592.8	5696.6	4155.2	4297.4	4159.2
NN-D	5784.0	5934.1	5724.5	5568.2	5409.1	5484.0

Table B.3: Modulus of elasticity (psi) of 4 in x 8 in concrete cylinders at 28 days

Agg. ID	Water-cured			Alkali-cured		
	#1	#2	#3	#1	#2	#3
SN-A	5.77E+06	6.15E+06	6.00E+06	5.77E+06	5.92E+06	5.98E+06
SN-B	5.19E+06	4.54E+06	4.94E+06	3.63E+06	3.64E+06	3.77E+06
SN-C	3.95E+06	3.92E+06	3.98E+06	3.53E+06	3.84E+06	3.73E+06
SN-D	3.19E+06	3.20E+06	3.20E+06	2.42E+06	2.75E+06	2.57E+06
SN-E	6.38E+06	6.53E+06	6.44E+06	5.97E+06	5.80E+06	6.02E+06
SN-F	5.27E+06	5.18E+06	5.35E+06	4.42E+06	4.16E+06	4.41E+06
SN-G	3.94E+06	3.96E+06	3.91E+06	2.35E+06	1.96E+06	2.39E+06
SN-H	4.17E+06	4.00E+06	4.11E+06	2.90E+06	2.90E+06	3.07E+06
SN-I	2.91E+06	2.78E+06	2.90E+06	3.16E+06	3.42E+06	3.20E+06
SN-J	3.39E+06	3.67E+06	3.49E+06	4.18E+06	4.12E+06	4.22E+06
NN-A	3.86E+06	3.86E+06	3.81E+06	3.81E+06	3.67E+06	3.77E+06
NN-B	3.90E+06	3.91E+06	3.84E+06	2.03E+06	1.91E+06	1.91E+06
NN-C	3.28E+06	3.59E+06	3.48E+06	2.55E+06	2.42E+06	2.53E+06
NN-D	3.46E+06	3.58E+06	3.47E+06	2.32E+06	2.23E+06	2.26E+06

Table B.4: Modulus of elasticity (psi) of 4 in x 8 in concrete cylinders at 6 months

Agg. ID	Water-cured			Alkali-cured		
	#1	#2	#3	#1	#2	#3
SN-A	6.37E+06	6.41E+06	6.42E+06	6.00E+06	5.94E+06	6.00E+06
SN-B	5.11E+06	5.12E+06	5.19E+06	3.73E+06	3.73E+06	3.73E+06
SN-C	4.04E+06	4.34E+06	4.34E+06	3.24E+06	2.87E+06	2.86E+06
SN-D	3.38E+06	3.43E+06	3.39E+06	2.30E+06	2.24E+06	2.24E+06
SN-E	6.66E+06	7.49E+06	6.97E+06	6.28E+06	6.70E+06	6.24E+06
SN-F	5.61E+06	5.74E+06	6.08E+06	3.66E+06	3.67E+06	3.74E+06
SN-G	4.26E+06	4.11E+06	3.99E+06	1.47E+06	1.59E+06	1.59E+06
SN-H	4.48E+06	4.21E+06	4.21E+06	1.98E+06	1.97E+06	2.08E+06
SN-I	3.86E+06	3.55E+06	3.48E+06	2.55E+06	2.67E+06	2.85E+06
SN-J	4.10E+06	3.88E+06	4.35E+06	2.48E+06	2.40E+06	2.30E+06
NN-A	3.90E+06	4.09E+06	4.09E+06	3.69E+06	3.86E+06	3.70E+06
NN-B	4.18E+06	4.66E+06	4.48E+06	1.98E+06	1.87E+06	1.91E+06
NN-C	4.24E+06	4.02E+06	4.28E+06	1.96E+06	2.00E+06	2.03E+06
NN-D	4.17E+06	4.50E+06	4.33E+06	2.02E+06	1.92E+06	1.94E+06

APPENDIX C

CHAPTER 5 DATA

Table C.1: Percent expansions of fly-ash mortar bars made with SN-C and SN-F aggregates

Curing age (Day)	Aggregate ID									
	SN-C					SN-F				
	Class F Fly Ash (%)					% Class F Fly Ash (%)				
	0	15	20	25	30	0	15	20	25	30
3	0.038	0.024	0.015	0.011	0.010	0.023	0.018	0.015	0.011	0.008
6	0.094	0.043	0.026	0.021	0.016	0.077	0.032	0.026	0.019	0.015
10	0.170	0.064	0.040	0.030	0.022	0.192	0.057	0.040	0.030	0.023
14	0.247	0.094	0.056	0.041	0.031	0.307	0.082	0.057	0.041	0.030
21	0.370	0.152	0.082	0.056	0.041	0.456	0.123	0.091	0.058	0.044
28	0.475	0.218	0.115	0.079	0.054	0.569	0.170	0.113	0.080	0.059
35	0.573	0.302	0.151	0.106	0.074	0.661	0.215	0.141	0.101	0.075
42	0.656	0.379	0.181	0.132	0.094	0.737	0.260	0.169	0.120	0.094
49	0.729	0.449	0.216	0.155	0.112	0.807	0.305	0.204	0.143	0.111
56	0.799	0.518	0.250	0.178	0.130	0.867	0.352	0.242	0.164	0.130
63	0.863	0.584	0.278	0.197	0.146	0.914	0.395	0.274	0.186	0.148
70	0.924	0.643	0.309	0.219	0.159	0.965	0.425	0.300	0.205	0.164
77	0.982	0.706	0.340	0.240	0.176	1.006	0.458	0.329	0.226	0.182
84	1.035	0.763	0.368	0.260	0.194	1.042	0.493	0.359	0.246	0.199
91	1.086	0.823	0.396	0.282	0.210	1.073	0.525	0.384	0.264	0.214
98	1.130	0.878	0.425	0.305	0.228	1.101	0.555	0.409	0.284	0.231

Table C.2: Percent expansions of fly-ash mortar bars containing SN-G and SN-J aggregates

Curing age (Day)	Aggregate ID									
	SN-G					SN-J				
	Class F Fly Ash (%)					% Class F Fly Ash (%)				
	0	15	20	25	30	0	15	20	25	30
3	0.118	0.028	0.017	0.012	0.009	0.032	0.017	0.011	0.010	0.008
6	0.360	0.091	0.042	0.030	0.020	0.105	0.035	0.022	0.019	0.017
10	0.632	0.177	0.089	0.052	0.033	0.177	0.066	0.041	0.036	0.029
14	0.862	0.251	0.146	0.099	0.056	0.218	0.099	0.062	0.048	0.039
21	1.061	0.350	0.230	0.170	0.111	0.270	0.158	0.102	0.076	0.058
28	1.151	0.434	0.300	0.236	0.167	0.311	0.198	0.136	0.099	0.077
35	1.206	0.500	0.362	0.288	0.211	0.343	0.236	0.165	0.123	0.099
42	1.256	0.562	0.425	0.341	0.256	0.374	0.268	0.191	0.146	0.120
49	1.280	0.626	0.479	0.390	0.297	0.401	0.297	0.219	0.167	0.137
56	1.305	0.674	0.526	0.434	0.336	0.424	0.321	0.240	0.190	0.157
63	1.320	0.728	0.569	0.475	0.373	0.445	0.341	0.258	0.209	0.175
70	1.350	0.771	0.624	0.517	0.409	0.464	0.367	0.282	0.227	0.194
77	1.364	0.810	0.671	0.558	0.442	0.481	0.385	0.301	0.245	0.211
84	1.375	0.850	0.720	0.602	0.477	0.493	0.403	0.316	0.260	0.225
91	1.379	0.882	0.764	0.642	0.508	0.506	0.417	0.336	0.278	0.241
98	1.381	0.911	0.803	0.679	0.537	0.519	0.430	0.352	0.294	0.254

Table C.3: Percent expansions of fly-ash mortar bars made with NN-B and NN-C aggregates

Curing age (Day)	Aggregate ID									
	NN-B					NN-C				
	Class F Fly Ash (%)					Class F Fly Ash (%)				
	0	15	20	25	30	0	15	20	25	30
3	0.115	0.025	0.017	0.012	0.005	0.098	0.025	0.019	0.014	0.011
6	0.405	0.068	0.035	0.021	0.012	0.330	0.071	0.039	0.022	0.016
10	0.787	0.153	0.081	0.043	0.024	0.587	0.158	0.082	0.042	0.029
14	1.023	0.251	0.152	0.086	0.038	0.830	0.233	0.144	0.084	0.041
21	1.348	0.394	0.260	0.168	0.097	1.203	0.367	0.253	0.169	0.093
28	1.549	0.532	0.363	0.251	0.161	1.414	0.488	0.349	0.244	0.150
35	1.701	0.679	0.457	0.326	0.222	1.556	0.594	0.449	0.311	0.202
42	1.804	0.851	0.555	0.403	0.283	1.647	0.712	0.543	0.377	0.255
49	1.899	1.000	0.646	0.481	0.339	1.731	0.817	0.636	0.437	0.306
56	1.975	1.116	0.721	0.549	0.389	1.794	0.907	0.718	0.496	0.352
63	2.044	1.239	0.812	0.617	0.437	1.825	0.985	0.793	0.558	0.397
70	2.106	1.335	0.887	0.673	0.485	1.847	1.061	0.862	0.608	0.439
77	2.153	1.409	0.963	0.734	0.537	1.877	1.132	0.924	0.663	0.480
84	2.202	1.484	1.031	0.806	0.592	1.886	1.184	0.983	0.706	0.520
91	2.240	1.555	1.108	0.882	0.642	1.909	1.232	1.033	0.752	0.558
98	2.270	1.618	1.170	0.946	0.686	1.926	1.279	1.079	0.800	0.602

Table C.4: Percent expansions of fly-ash mortars made with NN-D aggregate

Curing age (Day)	Class F Fly Ash (%)				
	0	15	20	25	30
3	0.025	0.014	0.011	0.010	0.004
6	0.058	0.036	0.025	0.023	0.017
10	0.114	0.067	0.046	0.037	0.027
14	0.163	0.099	0.063	0.051	0.037
21	0.251	0.158	0.101	0.078	0.054
28	0.312	0.212	0.137	0.104	0.070
35	0.360	0.252	0.169	0.129	0.087
42	0.405	0.293	0.203	0.156	0.108
49	0.444	0.331	0.237	0.183	0.128
56	0.471	0.367	0.268	0.206	0.147
63	0.505	0.396	0.292	0.226	0.165
70	0.534	0.427	0.320	0.251	0.187
77	0.561	0.452	0.344	0.274	0.203
84	0.599	0.474	0.365	0.295	0.218
91	0.628	0.495	0.385	0.314	0.232
98	0.664	0.512	0.403	0.332	0.244

Table C.5: percent expansions of lithium-mortar bars made with SN-C and SN-F aggregates

Curing age (Day))	Aggregate ID									
	SN-C					SN-F				
	Lithium Dosage (%)					Lithium Dosage (%)				
	0	80	100	120	140	0	80	100	120	140
3	0.057	0.016	0.011	0.010	0.009	0.029	0.011	0.010	0.008	0.007
6	0.124	0.037	0.022	0.019	0.017	0.094	0.029	0.018	0.017	0.013
10	0.221	0.104	0.036	0.027	0.022	0.221	0.084	0.040	0.032	0.024
14	0.332	0.227	0.077	0.042	0.031	0.329	0.144	0.063	0.037	0.026
21	0.493	0.383	0.195	0.114	0.050	0.481	0.294	0.139	0.050	0.033
28	0.599	0.502	0.289	0.176	0.059	0.599	0.412	0.211	0.055	0.033
35	0.682	0.583	0.354	0.239	0.072	0.694	0.498	0.255	0.059	0.034
42	0.759	0.649	0.413	0.282	0.080	0.770	0.567	0.282	0.062	0.038
49	0.829	0.715	0.467	0.305	0.089	0.838	0.616	0.294	0.064	0.039
56	0.901	0.774	0.517	0.330	0.098	0.896	0.649	0.303	0.066	0.040
63	0.973	0.829	0.563	0.350	0.104	0.952	0.673	0.308	0.066	0.040
70	1.031	0.880	0.603	0.362	0.113	0.996	0.691	0.311	0.067	0.041
77	1.086	0.924	0.640	0.372	0.122	1.042	0.704	0.314	0.068	0.041
84	1.136	0.963	0.670	0.381	0.128	1.083	0.717	0.317	0.069	0.043
91	1.181	0.999	0.697	0.390	0.132	1.120	0.726	0.318	0.069	0.043
98	1.220	1.032	0.720	0.400	0.134	1.155	0.732	0.318	0.069	0.043

Table C.6: Percent expansions of lithium-mortar bars made with SN-G aggregate

Curing age (Day)	Lithium Dosage (%)						
	0	80	100	120	140	160	180
3	0.209	0.033	0.023	0.019	0.014	0.011	0.009
6	0.420	0.082	0.047	0.031	0.022	0.016	0.015
10	0.691	0.188	0.091	0.048	0.030	0.024	0.023
14	0.890	0.277	0.166	0.076	0.046	0.036	0.032
21	1.092	0.421	0.279	0.155	0.082	0.056	0.046
28	1.185	0.554	0.401	0.248	0.148	0.082	0.066
35	1.234	0.655	0.509	0.349	0.220	0.143	0.114
42	1.268	0.740	0.606	0.453	0.308	0.229	0.177
49	1.292	0.801	0.669	0.541	0.388	0.316	0.260
56	1.323	0.845	0.720	0.615	0.464	0.388	0.337
63	1.343	0.883	0.761	0.666	0.535	0.447	0.392
70	1.371	0.923	0.796	0.707	0.583	0.487	0.430
77	1.392	0.953	0.822	0.740	0.623	0.523	0.460
84	1.407	0.973	0.840	0.765	0.654	0.553	0.486
91	1.413	0.988	0.854	0.784	0.679	0.574	0.508
98	1.421	1.000	0.866	0.799	0.699	0.594	0.526

Table C.7: Percent expansions of lithium-mortar bars made with SN-J aggregate

Curing age (Day)	Lithium Dosage (%)						
	0	80	100	120	140	160	180
3	0.127	0.021	0.017	0.016	0.015	0.013	0.010
6	0.291	0.040	0.027	0.026	0.024	0.021	0.019
10	0.398	0.072	0.050	0.041	0.035	0.031	0.026
14	0.465	0.106	0.075	0.061	0.049	0.042	0.033
21	0.563	0.162	0.127	0.103	0.082	0.061	0.049
28	0.620	0.216	0.175	0.137	0.111	0.090	0.071
35	0.675	0.283	0.239	0.186	0.148	0.122	0.095
42	0.722	0.343	0.293	0.234	0.183	0.162	0.123
49	0.768	0.397	0.351	0.281	0.222	0.202	0.157
56	0.800	0.447	0.392	0.325	0.271	0.240	0.193
63	0.830	0.496	0.440	0.373	0.311	0.275	0.227
70	0.864	0.535	0.480	0.411	0.341	0.308	0.256
77	0.894	0.576	0.511	0.448	0.371	0.334	0.279
84	0.927	0.610	0.548	0.482	0.397	0.356	0.301
91	0.956	0.638	0.569	0.509	0.418	0.373	0.321
98	0.981	0.661	0.590	0.531	0.433	0.388	0.340

Table C.8: Percent expansions of lithium-mortar bars made with NN-B aggregate

Curing age (Day)	Lithium Dosage (%)						
	0	80	100	120	140	160	180
3	0.197	0.030	0.019	0.015	0.013	0.012	0.010
6	0.561	0.093	0.041	0.029	0.024	0.021	0.017
10	0.874	0.231	0.090	0.048	0.035	0.029	0.025
14	1.098	0.350	0.179	0.073	0.046	0.038	0.030
21	1.407	0.546	0.331	0.154	0.064	0.052	0.038
28	1.610	0.719	0.485	0.265	0.108	0.073	0.048
35	1.760	0.850	0.622	0.376	0.191	0.148	0.064
42	1.876	0.948	0.736	0.488	0.277	0.232	0.119
49	1.968	1.011	0.818	0.577	0.370	0.323	0.213
56	2.050	1.062	0.877	0.653	0.453	0.409	0.316
63	2.105	1.107	0.923	0.706	0.540	0.482	0.384
70	2.162	1.135	0.954	0.731	0.599	0.537	0.432
77	2.220	1.159	0.980	0.753	0.635	0.570	0.457
84	2.254	1.182	1.002	0.780	0.655	0.592	0.478
91	2.290	1.198	1.020	0.795	0.675	0.604	0.497
98	2.335	1.210	1.035	0.808	0.693	0.611	0.510

Table C.9: Percent expansions of lithium-mortars made with NN-C aggregate

Curing age (Day)	Lithium Dosage (%)						
	0	80	100	120	140	160	180
3	0.177	0.037	0.025	0.020	0.017	0.014	0.010
6	0.440	0.152	0.057	0.039	0.027	0.023	0.017
10	0.708	0.317	0.179	0.070	0.039	0.033	0.024
14	0.940	0.457	0.285	0.152	0.059	0.043	0.031
21	1.271	0.686	0.505	0.325	0.135	0.066	0.044
28	1.472	0.806	0.660	0.478	0.254	0.118	0.054
35	1.601	0.865	0.742	0.574	0.365	0.206	0.062
42	1.694	0.906	0.795	0.637	0.439	0.285	0.078
49	1.766	0.935	0.827	0.674	0.485	0.358	0.115
56	1.828	0.959	0.852	0.703	0.522	0.411	0.174
63	1.870	0.979	0.872	0.725	0.550	0.456	0.234
70	1.903	0.998	0.890	0.745	0.571	0.491	0.279
77	1.923	1.017	0.906	0.763	0.590	0.512	0.319
84	1.958	1.037	0.920	0.776	0.601	0.527	0.352
91	1.965	1.044	0.925	0.785	0.615	0.537	0.381
98	1.993	1.051	0.932	0.794	0.627	0.543	0.405

Table C.10: Percent expansions of lithium-mortars made with NN-D aggregate

Curing age (Day)	Lithium Dosage (%)				
	0	80	100	120	140
3	0.045	0.014	0.012	0.010	0.008
6	0.083	0.023	0.018	0.015	0.013
10	0.138	0.033	0.024	0.020	0.017
14	0.186	0.040	0.028	0.023	0.019
21	0.262	0.055	0.032	0.025	0.021
28	0.322	0.067	0.035	0.027	0.023
35	0.368	0.077	0.040	0.030	0.025
42	0.413	0.089	0.045	0.032	0.027
49	0.455	0.098	0.048	0.035	0.028
56	0.488	0.106	0.053	0.036	0.029
63	0.521	0.111	0.056	0.037	0.030
70	0.547	0.117	0.058	0.038	0.032
77	0.579	0.122	0.062	0.040	0.034
84	0.613	0.127	0.065	0.042	0.035
91	0.641	0.131	0.067	0.043	0.036
98	0.677	0.135	0.069	0.044	0.036

Table C.11: Percent expansions of SN-G and SN-J aggregates treated with the combination of fly ash and lithium nitrate

Curing age (Day)	Aggregate ID			
	SN-G		SN-J	
	100%Li + 15%FA	100%Li + 20% FA	100%Li + 15%FA	100%Li + 20% FA
3	0.011	0.005	0.006	0.002
6	0.020	0.013	0.012	0.006
10	0.031	0.022	0.019	0.011
14	0.042	0.030	0.025	0.018
21	0.076	0.055	0.042	0.031
28	0.118	0.084	0.055	0.041
35	0.159	0.116	0.069	0.053
42	0.200	0.148	0.084	0.066
49	0.245	0.185	0.107	0.085
56	0.292	0.220	0.128	0.104
63	0.339	0.253	0.150	0.123
70	0.385	0.289	0.174	0.144
77	0.430	0.320	0.195	0.159
84	0.472	0.349	0.213	0.172
91	0.511	0.376	0.230	0.184
98	0.551	0.402	0.245	0.194

Table C.12: Percent expansions of the NN-B and NN-C aggregates treated with the combination of fly ash and lithium nitrate

Curing age (Day)	Aggregate ID			
	NN-B		NN-C	
	100%Li + 15%FA	100%Li + 20% FA	100%Li + 15%FA	100%Li + 20% FA
3	0.015	0.010	0.013	0.007
6	0.023	0.018	0.025	0.016
10	0.037	0.029	0.039	0.027
14	0.052	0.042	0.057	0.042
21	0.095	0.070	0.108	0.074
28	0.146	0.111	0.175	0.125
35	0.205	0.158	0.244	0.174
42	0.266	0.199	0.308	0.223
49	0.327	0.248	0.376	0.271
56	0.386	0.296	0.447	0.321
63	0.466	0.344	0.514	0.369
70	0.540	0.392	0.582	0.417
77	0.621	0.448	0.651	0.456
84	0.692	0.498	0.713	0.491
91	0.015	0.010	0.013	0.007
98	0.023	0.018	0.025	0.016

APPENDIX D

FIGURES

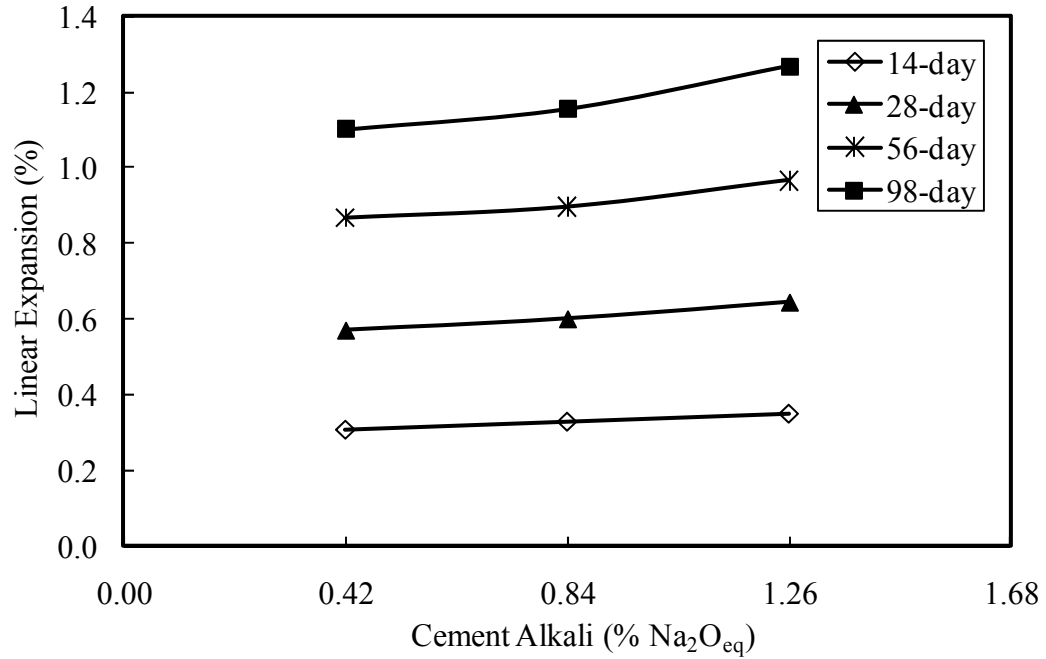


Figure D.1: Influence of cement alkalis on expansion of SN-F aggregate at various immersion ages for the 1N NaOH solution

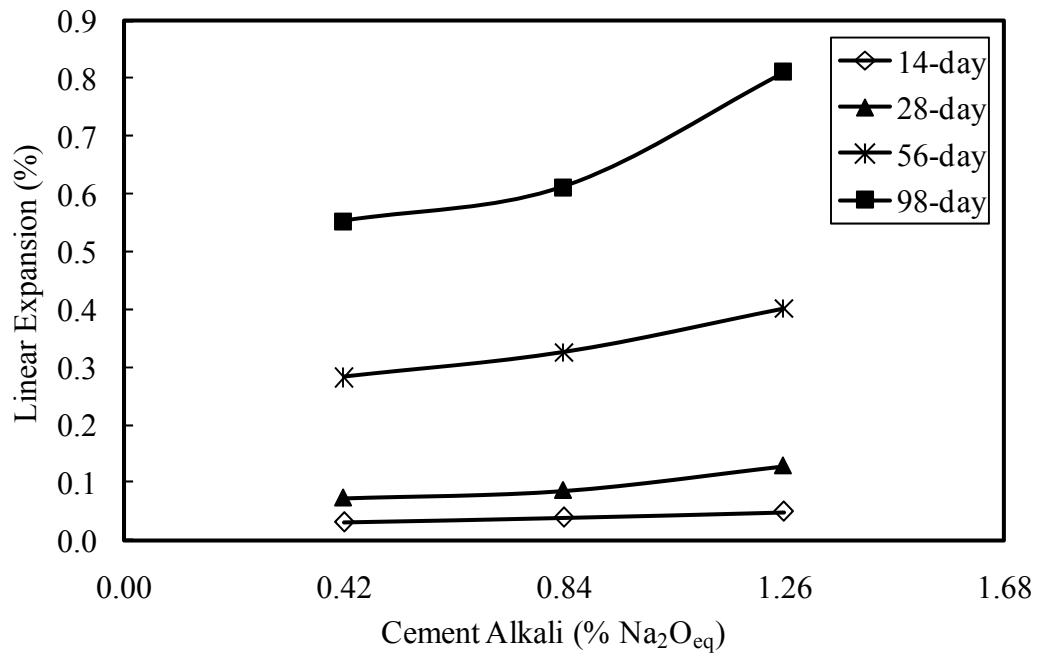


Figure D.2: Influence of cement alkalis on expansion of SN-F aggregate at various immersion ages for the 0.5N NaOH solution

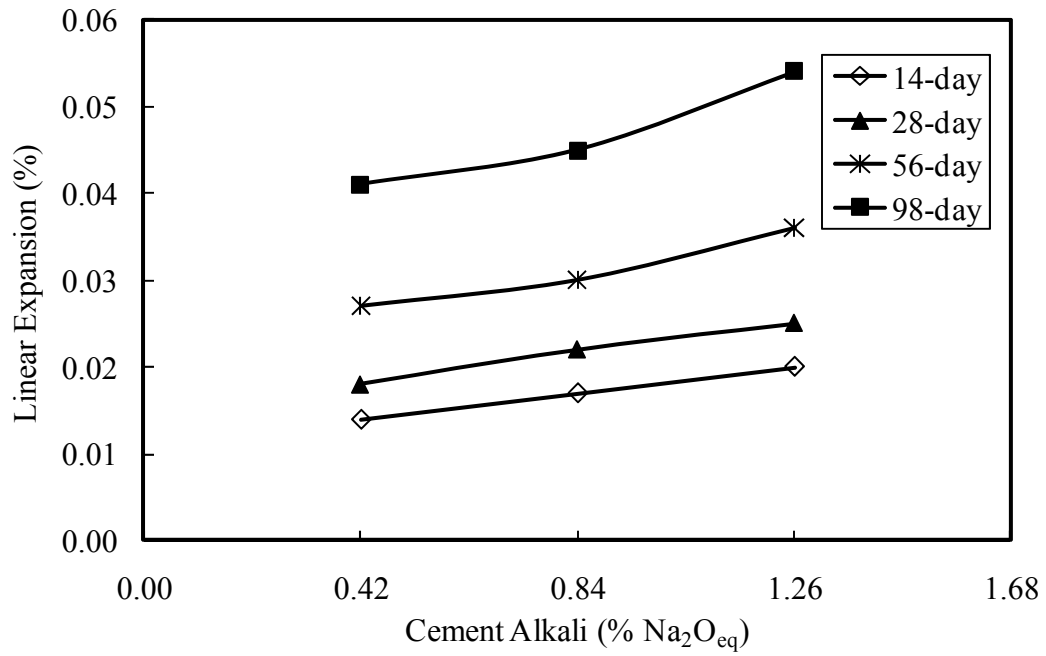


Figure D.3: Influence of cement alkalis on expansion of SN-F aggregate at various immersion ages for the 0.25N NaOH solution

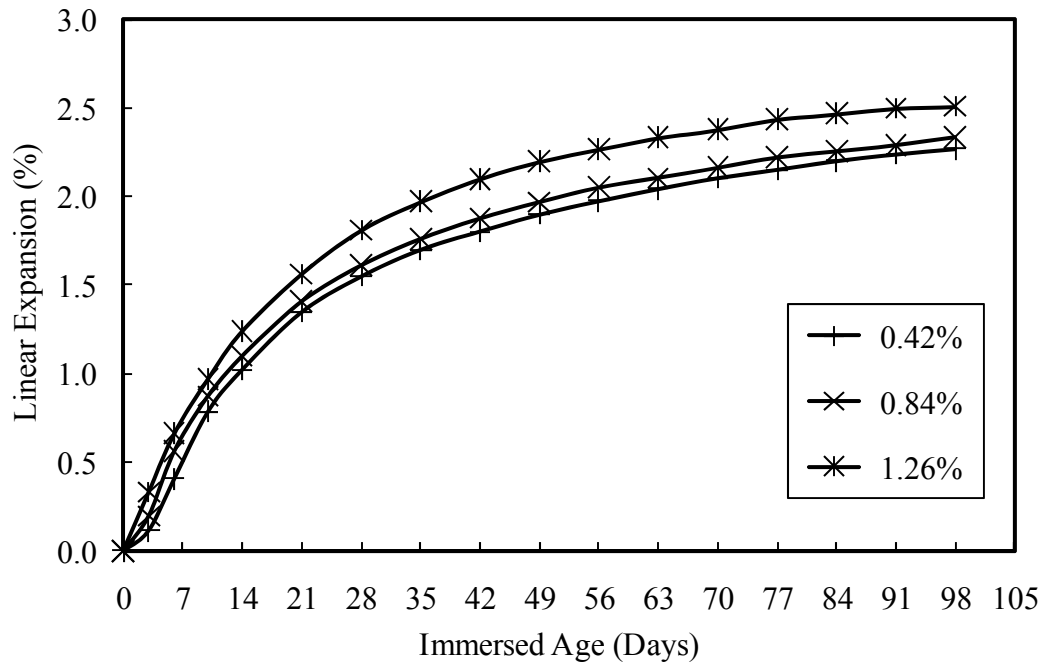


Figure D.4: Influence of cement alkalis on ASR expansion of NN-B aggregate for the 1N NaOH solution

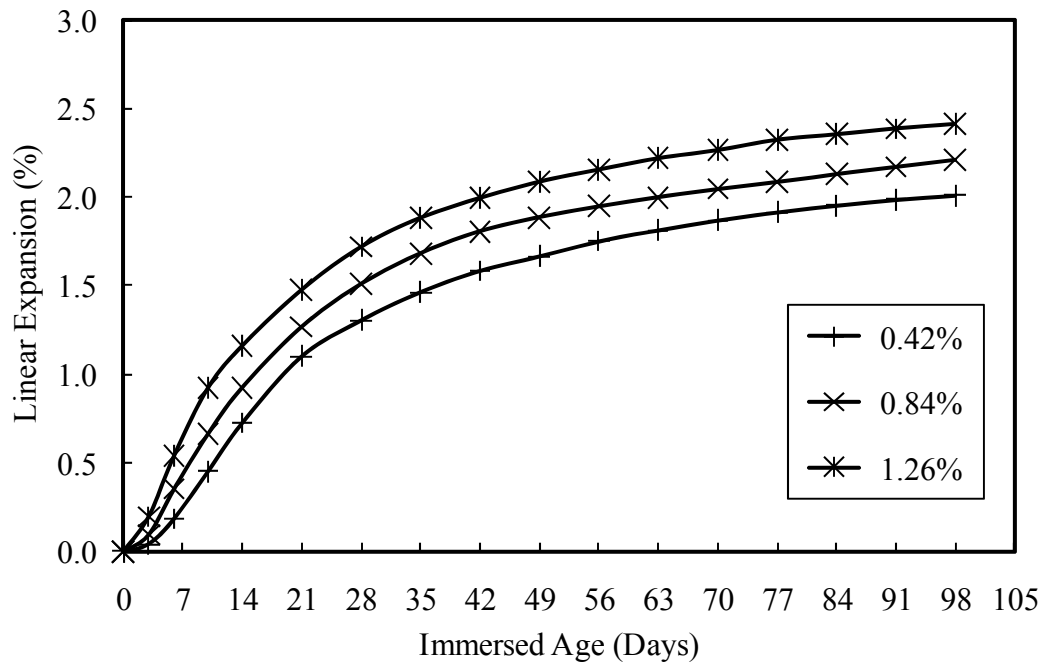


Figure D.5: Influence of cement alkalis on ASR expansion of NN-B aggregate for the 0.5N NaOH solution

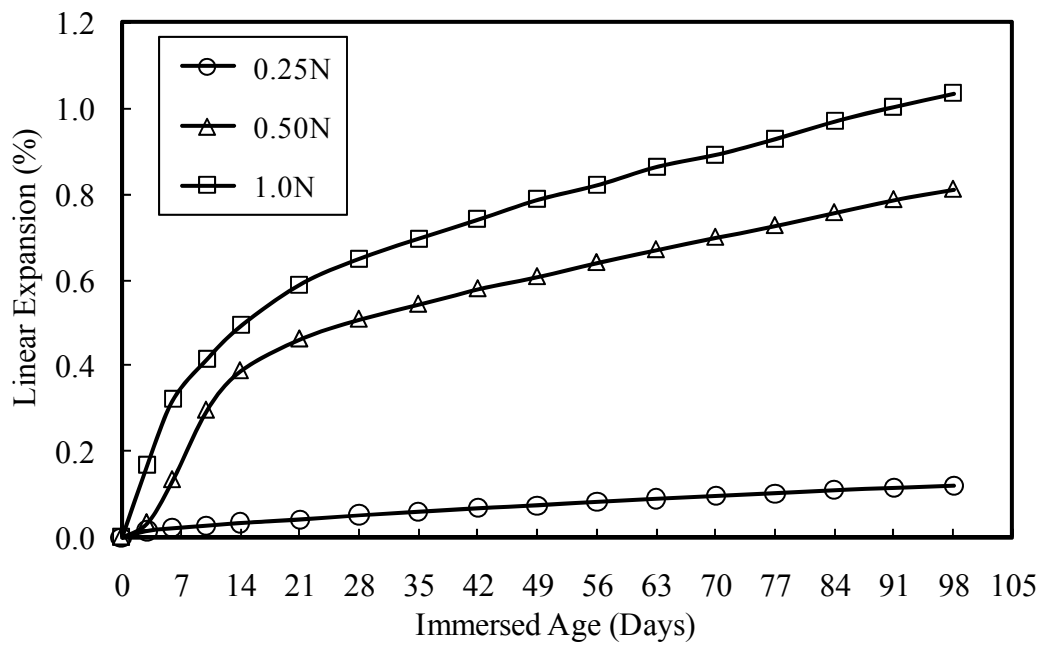


Figure D.6: Influence of soak solution concentration on ASR expansion of SN-J aggregate prepared with 0.42% cement alkalis

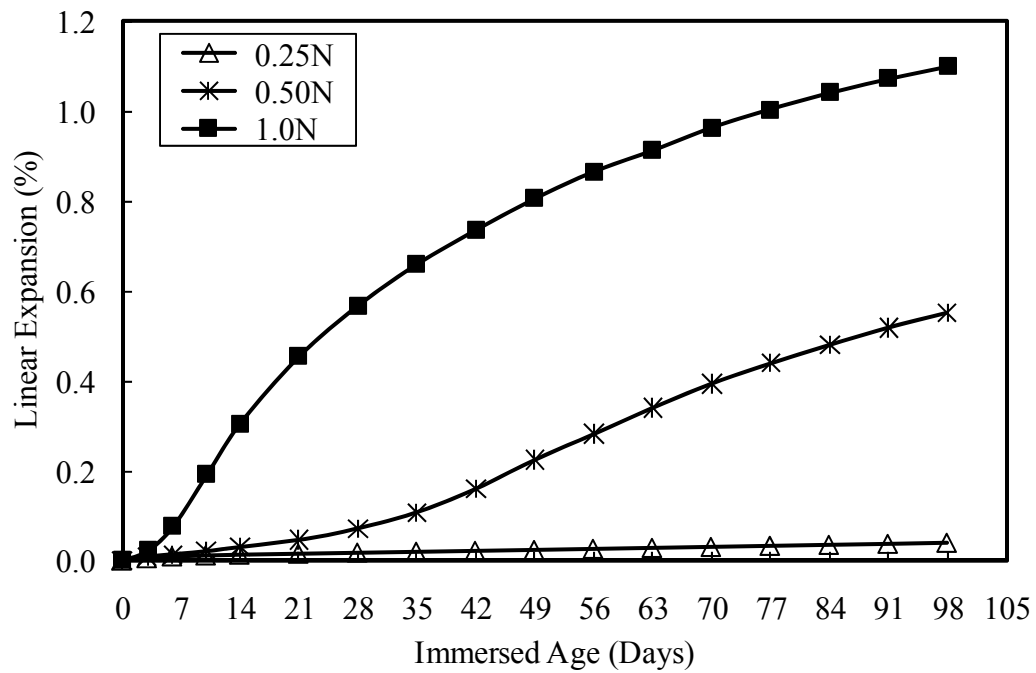


Figure D.7: Influence of soak solution concentration on ASR expansion of SN-F aggregate prepared with 0.42% cement alkalis

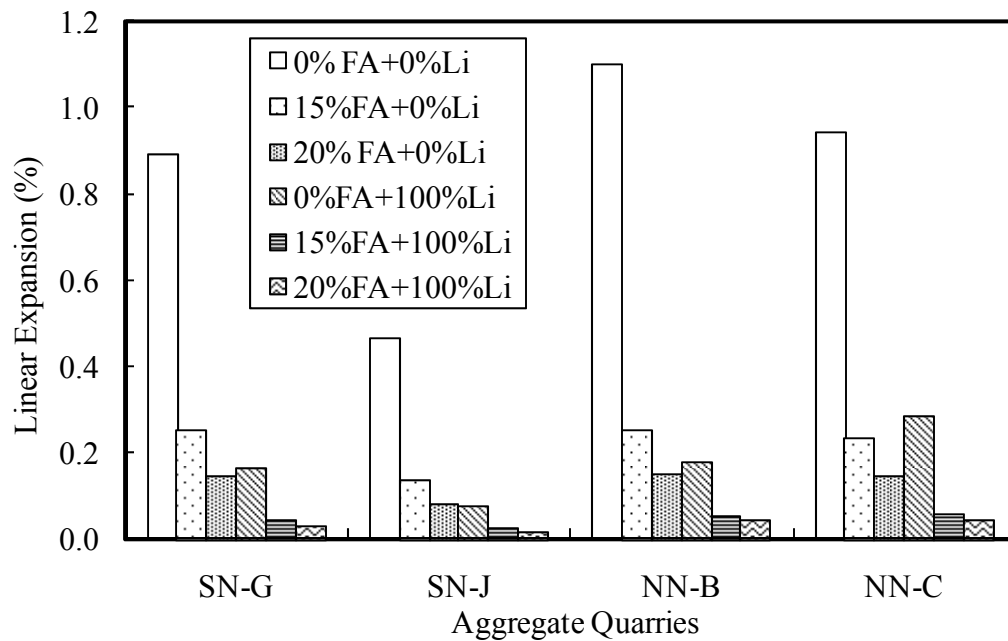


Figure D.7: 14-day expansions of the test mortar bars prepared with 15%FA, 20%FA, 100%Li, 15%FA+100%Li, and 20%FA+100%Li

BIBLIOGRAPHY

- Adam, J.T., "Potential concrete aggregate reactivity in northern Nevada," Master's thesis paper, UMI Microform Number: 1420180, University of Nevada Reno, 2004
- Adams, N., and Stokes, D.B., "Using advanced lithium technology to combat ASR in concrete," Special Products & Practice Spotlight, Concrete International, Aug. 2002
http://www.euclidchemical.com/elit/ci_artical.pdf#search=%22lithium%20ASR%20mitigation%20%22
- Ahmed, T., Burley, E., Rigden, S., and Abu-Tair, A., "The effect of alkali reactivity on the mechanical properties of concrete," Construction and Building Materials, Vol. 17, pp. 123-144, 2003
- Advisory Circular, FAA, AC 150/5380-8, "Handbook of identification of alkali-silica reactivity of airfield pavements," February, 2004
- American Concrete Institute Committee 221, "State-of-the-Art Report on alkali-aggregate reactivity," ACI Manual of Concrete Practice -Part 1. ACI 221.1R-98. American Concrete Institute, Farmington Hills, MI, 1998
- American Concrete Institute (ACI), "Ground granulated blast-furnance as a cementitious constituent in concrete," ACI 233R-95, American Concrete Institute, Farmington Hills, MI, 1995
- Alkali-silica reactions in concrete, <http://www.concrete-experts.com/pages/asr.htm> (accessed on august 28, 2006)
- American Society for Testing and Materials, ASTM C 157/C 157 M, "Test method for length change of hardened hydraulic-cement mortar and concrete," Annual book of ASTM Standards
- American Society for Testing and Materials, ASTM C 277, "Standard test method for potential alkali reactivity of cement aggregates combinations (mortar-bar method)," Annual book of ASTM Standard, 1997
- American Society for Testing and Materials, ASTM C 289, "Standard test method for potential alkali reactivity of aggregates (chemical method)," Annual book of ASTM Standards, 1997
- American Society for Testing and Materials, ASTM C 295, "Standard guide for petrographic examination of aggregates for concrete," Annual book of ASTM Standards, 1997

- American Society for Testing and Materials, ASTM C 490, "Practice for use of apparatus for the determination of length change of hardened cement paste, mortar, and concrete," Annual book of ASTM Standards
- American Society for Testing and Materials, ASTM C 511, "Specification for mixing rooms, moist cabinets, moist rooms, and water storage tanks used in the testing of hydraulic cements and concretes," Annual book of ASTM Standards
- American Society for Testing and Materials, ASTM C 1105-05, "Standard test method for length change of concrete due to alkali-carbonate rock reaction," Annual book of ASTM Standards
- American Society for Testing and Materials, ASTM C 1260, "Standard test method for potential alkali reactivity of aggregates (mortar-bar method)," Annual book of ASTM Standards, 1994
- American Society for Testing and Materials, ASTM C 1293, "Standard test method for concrete aggregates by determination of length change of concrete due to alkali-silica reaction," Annual book of ASTM Standards, 1995
- Back, F., Thorsen, T.S. and Nielsen, M.P., "Load-carrying capacity of structural members subjected to alkali-silica reactions," Construction and Building Materials, Vol. 7, No. 2, pp. 109-115, 1993
- Banahene, N.K., "Inhibiting alkali-silica reaction in concrete with lithium salts," MS Thesis, Dept. of Geology and Geological Eng., University of Windsor, Canada, AAT MM65173, 139 pp., 1991
- Baronio, B., Montanaro, K., and Delmastro, B., "Couplage d'action de certains parametres physiques sur le developpement de la reaction alkali-silice," Material Science to Construction Materials Engineering, 1st Int. Conf Versailles Vol. 3, 1987
- Bektas, F., Turanli, L., and Ostertag, C.P., "New approach in mitigating damage caused by alkali-silica reaction," Journals of Materials Science, Vol. 41, pp.760-763, 2006
- Bektas, F., Wang, K., and Ceylan, H., "Effect of Portland cement fineness on ASTM C 1260 expansion," SN 2963, Portland Cement Association, Skokie, Illinois, USA, 30 pp., 2008
- Berra, M., Mangialardi, T., and Paolini A.E., "Testing natural sands for the alkali reactivity with the ASTM C 1260 mortar bar expansion method," Journal of the Ceramic Society of Japan, Vol. 106, pp. 237 - 241, 1998.

- Berra, M., Mangialardi, T., and Paolini, A.E., "Use of lithium compounds to prevent expansive alkali-silica reactivity in concrete," *Advances in Cement Research*, Vol. 15(4), pp. 145-154, 2003
- Bérubé, M.-A., Duchesne, J., Dorion, J.F., and Rivest, M., "Laboratory assessment of alkali contribution by aggregates to concrete and application to concrete structures affected by alkali-silica reactivity," *Cement and Concrete Research*, Vol. 32, pp. 1215-1227, 2002
- Bérubé, M.A., and Fournier, B., "Canadian experience with testing for alkali-aggregate reactivity in Concrete," *Cement and Concrete Composites*, Vol. 15, pp. 27-47, 1993
- Bérubé, M. A., and Fournier, B. "Testing for alkali-aggregate reactivity in concrete," *Proceedings, Durabilidad Del Concreto*, Monterrey, N.L. Mexico, 1993
- Bérubé, M.-A., and Frenette, J., "Testing concrete for AAR in NaOH and NaCl solutions at 38⁰C and 80⁰C," *Cement and Concrete Composites*, Vol. 16, Is. 3, pp. 189-198, 1994
- Berubé, M.A., and Trambly, C., Fournier, B., Thomas, M.D., and Stokes, D.B. "Influence of lithium-based products proposed for counteraction ASR on the chemistry of pore solution and cement hydrates", *Cement and Concrete Research*, V. 34, pp. 1645, 2004
- Blanks, R., and Kennedy, H., "The technology of cement and concrete," John Wiley & Sons Publication, USA, pp. 299-342, 1955
- Bleszynski, R.F., "Study of the effects of fly ash on alkali-silica reaction in concrete," UMI Dissertation Services, UMI Number: 0-612-51606-7, Graduate department of civil engineering, University of Toronto, 1997
- Bleszynski, R., Hooton, R.D., Thomas, M.D.A., and Rogers, C.A., "Durability of ternary blend concrete with silica fume and blast-furnace slag: Laboratory and Outdoor exposure site studies," *ACI Materials Journals*, pp. 499-508, 2002
- Bleszynski, R.F., and Thomas, M.D.A., "Microstructural studies of alkali-silica reaction in fly ash concrete immersed in alkaline solutions," *Advanced Cement Based Materials*, Vol. 7, pp. 66-78, 1998
- Boddy, A.M., Hooton, R.D., and Thomas, M.D.A., "The effect of product form of silica fume on its ability to control alkali-silica reaction," *Cement and Concrete Research*, Vol. 30, pp. 1139-1150, 2000
- Broekmans, M.A.T.M., "Classification of the alkali-silica reaction in geochemical terms of silica dissolution," *Proceedings of the 7th Euroseminar on Microscopy Applied to*

- Building Materials, Hans S. Pietersen, Joe A. Larbi and Hans H.A. Janssen Editors, Nederland, pp. 155-170, 1999
- Canadian Standards Association (CSA) A23.2-25A, "Test method for detection of alkali-silica reactive aggregate by accelerated expansion of mortar bars." CSA International, Toronto, Ontario, Canada, 2000
- Carlos, C., Mancio, M., Shomglin, K., and Harvey, J., Monteiro, P., and Ali, A., "Accelerated Laboratory Testing for Alkali-Silica Reaction Using ASTM 1293 and Comparison with ASTM 1260," Draft Report prepared for the California Department of Transportation, Pavement Research Center, Institute of Transportation Studies, 2004
- Černý, R., and Rovnaníková, P., "Transport processes in concrete," ISBN 978-0415-24264-6, Taylor & Francis Publisher, 560 pp., 2002
- Chang, Y.F., Chen, Y.H., Sheu, M.S., and Yao, G.C., "Residual stress-strain relationship for concrete after exposure to high temperatures," Cement and Concrete Research, Vol. 36, No. 10, pp. 1999-2005, 2006
- Clayton, N., "Structural performance of ASR affected concrete," Proceedings of the 8th International Conference on Alkali-Aggregate Reaction, Kyoto, Japan, pp. 671-676, 1989.
- Collins, C.L., Ideker, J.H., Willis, G.S., and Kurtis, K.E., "Examination of the effects of LiOH, LiCl, and LiNO₃ on alkali-silica reaction," Cement and Concrete Research, Vol. 34, pp. 1403-1415, 2004
- Concrete technology, Alkali aggregate reaction,
http://www.cement.org/tech/cct_dur_AAR.asp (accessed on August 29, 2006) e
- CSA International, Standard practice to identify degree of alkali-reactivity of aggregates and to identify measures to avoid deleterious expansion in concrete, A23.2-27A, pp. 251-261, 2000
- Deng, M., Han, S.F., Lu, Y.N., Lan, X.H., Hu, Y.L., and Tang, M.S., "Deterioration of concrete structures due to alkali-dolomite reaction in China," Cement and Concrete Research, Vol. 23, pp. 1040-1046, 1993
- Detwiler, R.J., Bhatti, J.I., and Bhattacharja, S., "Supplementary cementing materials for use in blended cements," Research and Development Bulletin RD112T, Portland Cement Association, PCA R&D Serial No. 2038, Skokie, Illinois, USA, 96 pp., 1996
- Diamond, S., "Alkali aggregate reactions in concrete: an annotated bibliography 1931-1991," Strategic Highway Research Program, National Research Council Washington, DC, 1992

- Diamond, S., "Unique response of LiNO₃ as an alkali silica reaction preventive admixture," *Cement and Concrete Research*, Vol. 29, pp. 1271-1275, 1999
- Diamond, S., and Thaulow, N., "A study of expansion due to alkali-silica reaction as conditioned by the grain size of the reactive aggregate," *Cement and Concrete Research*, Vol. 4, No. 4, pp. 591-607, 1974
- Durand, B. "More Results About the Use of Lithium Salts and Mineral Admixtures to Inhibit ASR in Concrete," *Proceedings of the 11th International Conference on Alkali-Aggregate Reaction*, Centre de Recherche Interuniversitaire sur le Beton, Quebec, Canada, p. 623, 2000.
- Ekolu, S.O., "Role of heat curing in concrete durability; effects of lithium salts and chloride ingress on delayed ettringite formation," PhD Dissertation, Department of civil engineering, University of Toronto, 2004
- Ekolu, S.O., Thomas, M.D.A., and Hooton, R.D., "Dual effectiveness of lithium salt in controlling both delayed ettringite formation and ASR in concretes," *Cement and Concrete Research*, Vol. 37, Iss. 6, pp. 942-947, 2007
- Engineering and Design Manual, Standard Practice for Concrete for Civil Works Structures, EM No. 1110-2-2000, Department of the Army, US Army Corps of Engineers, Washington, DC, USA, 1994
- Etcheverry, L., "Lithium nitrate mitigation of alkali-silica reaction (ASR)," Structural Preservative Systems Inc., A structural group company, 2005 accessed on sep. 23, 2006 at <http://www.structural.net/asr/index.html>
- Farage, M.C.R., Alves, J.L.D., and Fairbairn, E.M.R., "Macroscopic model of concrete subjected to alkali-aggregate reaction," *Cement and Concrete Research*, Vol. 34, pp. 495-505, 2004
- Farny, J.A., and Kosmatka, S.H., "Diagnosis and control of alkali-aggregate reactions in concrete," Concrete Information Series, No. IS413.01T, Portland Cement Association. Skokie, IL, USA, ISBN 0 89312 146 0, 24 pp., 1997
- Federal Highway Administration, "Guidelines for detection, analysis, and treatment of materials-related distress in concrete pavements," FHWA-RD-01-163, Vol. 1: final report, March 2002
- Federal Highway Administration, "Guidelines for the use of lithium to mitigate or prevent alkali-silica reaction (ASR)," Publication No. FHWA-RD-03-047, 2003

- Fernandes, I., Noronha, F., and Teles, M., "Microscopic analysis of alkali-aggregate reaction products in 50-year-old concrete," *Material Characterization*, Vol. 53, pp. 295-306, 2004
- Feng, X., Thomas, M.D.A., Bremner, T.W., Balcom, B.J., and Folliard, K.J., "Studies on lithium salts to mitigate ASR-induced expansion in new concrete: a critical review," *Cement and Concrete Research*, Vol. 35, pp. 1789-1796, 2005
- Folliard, K., Barborak, R., Drimalas, T., Du, L., Garber, S., Ideker, J., and Ley, T., Williams, S., Juenger, M., Thomas, M.D.A. and Fournier, B., "Preventing alkali-silica reaction and delayed ettringite formation in new concrete," Project Summary report 0-4085, Center for Transportation Research, University of Texas, Austin, March 2006
- Folliard, K.J., Ideker, J., Thomas, M.D.A., and Fournier, B., "Assessing aggregate reactivity using the accelerated concrete prism test," Draft Report-Prepared for ICAR, 2005
- Folliard, K.J., Thomas, M.D.A., Fournier, T., Kurtis, K.E. and Ideker, J.H., "Interim recommendations for the alkali-silica reaction (ASR)," Office of Infrastructure Research and Development, Federal Highway Administrator, McLean, VA 22101, Report No. FHWA-ART-06-073, pp. 54, 2006
- Folliard, K.J., Thomas, M.D.A., and Kurtis, K.E., "Guidelines for the use of lithium to mitigate or prevent ASR," Publication no. FHWA-RD-03-047, Turner-Fairbank Highway Research Center, VA, USA, 86 pp. July 2003
- Folliard, K.J., Ideker, J., Thomas, M.D.A., and Fournier, B., "Assessing aggregate reactivity using the accelerated concrete prism test," 2004, assessed on 10 July, 2008 at www.mrr.dot.state.mn.us/materials/MEO/2004Spring/MiscPapers/D1Folliard.pdf
- Fournier, B., and Bérubé, M.-A., "Alkali-aggregate reaction in concrete: a review of basic concepts and engineering implications," *Canadian Journals of Civil Engineering*, Vol. 27, pp. 167-191, 2000
- Fournier, B., and Bérubé, M.A., "Application of the NBRI Accelerated Mortar Bar Test to Siliceous Carbonate Aggregates Produced in the St. Lawrence Lowlands (Quebec, Canada). Part 1: Influence of Various Parameters on the Test Results," *Cement and Concrete Research*, Vol. 21, pp. 853-862, 1991
- Fournier, B., Bérubé, M.A., and Rogers, C.A., "Proposed guidelines for the prevention of alkali-aggregate reactivity in new concrete structures," *Transportation Research Record*, No. 1668, Paper No. 99-1176, pp. 48-53, 1999
- Fournier, B.; Nkinamubanzi, P.-C.; and Chevrier, R., "Comparative Field and Laboratory Investigations on the Use of Supplementary Cementing Materials to Control Alkali-Silica Reaction in Concrete," *Proceedings of the Twelfth International Conference*

- Alkali-Aggregate Reaction in Concrete, V. 1, T. Mingshu and D. Min, eds., International Academic Publishers/World Publishing Corp., Beijing, China, pp. 528-537, 1994
- Fuwa, H., and Kawamura, M., "Effects of lithium salts on ASR gel composition and expansion of mortars," *Cement and Concrete Research*, Vol. 33, pp. 913-919, 2003
- Gajda, John, "Development of a lithium bearing cement to inhibit alkali silica reactivity in hardened concrete," *World Cement and Research Development*, pp. 58-62, August, 1996
- Giaccio, G., Zerbino, R., Ponce, J.M. and Batic, O.R., "Mechanical behavior of concretes damaged by alkali-silica reaction," *Cement and Concrete Research*, Vol. 38, pp. 993-1004, 2008
- Gibergues-Carles, A., Cyr, M., Moisson, M., and Ringot, E., "A simple way to mitigate alkali-silica reaction," *Materials and Structures*, Vol. 41, pp. 73-83, 2007
- Grosbois, D.M. and Fontaine, E., "Evaluation of the potential alkali-reactivity of concrete aggregates: performance of testing methods and a producer's point of view, Proceedings, 11th International Conference of Alkali-Aggregate Reactivity in Concrete, Quebec City, QC, Canada, pp. 267-276, 2000
- Grosbois, D.M., and Fontaine, E., "Performance of the 60°C - accelerated concrete prism test for the evaluation of potential alkali-silica reactivity of concrete aggregates, Proceedings, 11th International Conference of Alkali-Aggregate Reactivity in Concrete, Quebec City, QC, Canada, pp. 277-286, 2000
- Gudmundsson, G., and Olafsson, H., "Alkali-silica reactions and silica fume 20 years of experience in Iceland," *Cement and Concrete Research*, Vol. 29, pp. 1289-1297, 1999
- Haddad, R.H. and Qudah, A. "Alkali-silica reaction expansions in high-performance and normal-strength cement grouts reinforced with steel and synthetic fibers," *Mechanics of Composite Materials*, Vol. 41, No. 1, pp. 87-94, 2005
- Hadley, D.W., "Alkali reactivity of carbonate rocks - expansion and dedolomitization," *Proceeding of the Highway Research Board*, Vol. 40, pp. 462-474, 1961
- Haha, M.B., "Mechanical effects of alkali-silica reaction in concrete studied by sem-image analysis," PhD Dissertation, Swiss Institute of Technology Lausanne, 2006
- Hanson, K.F., Van Dam, T.J., Peterson, K.R., and Sutter, L.L., "Effect of sample preparation on chemical composition and morphology of Alkali-silica reaction products," *Transportation Research Record*, Vol. 1834, Paper no. 03-2803, pp. 1-7, 2003

- Helmuth, R.A., and Stark, D., "Alkali-silica reactivity mechanisms," *Materials Science of Concrete III*, J. Skalny, Editor, American Ceramic Society, Waterville, OH, pp. 131-208, 1992
- Melmuth, R., "Alkali-silica reactivity: An overview of Research," Strategic Highway Research Program, SHRP-C-342, National Research Council, Washington, DC, USA, ISBN 0-309-05602-0, 105 pp., 1994
- Hester, D., McNally, C., and Richardson, M., "A study of the influence of slag alkali-silica reactivity of slag concrete," *Construction and Building Materials*, Vol. 19, Issue 9, pp. 661-665, 2005
- Hobbs, W.D., "Alkali-silica reaction in concrete," Thomas Telford, London, 1988
- Holland, T.C., "Silica fume's user manual," U.S. Department of Transportation, Federal Highway Administration, FHWA-IF-05-016, 193 pp., 2005
- Hooton, R.D., "New aggregates alkali-reactivity test methods. Ministry of Transportation, Ontario, Research Report MAT-91-14, 54 pp., 1991
- Hooton, R.D., "Recent developments in testing for ASR in North America," *Proceedings of the 10th International Conference on Alkali-Aggregate Reaction in Concrete*, Australia, pp. 280-287, 1996
- Hudec, P., and Banahene, Nana, "Chemical treatment and additives for controlling alkali reactivity," *Cement and Concrete Composites*, Vol. 15, pp. 21-26, 1993
- Idom G.M., Johansen V., and Thaulow N., "Assessment of causes of cracking in concrete," *Materials Science in Concrete III*, Amer. Ceramic Soc., New York, 1992
- Ikeda, T., Kawabata, Y., Hamada, H., and Sagawa, "Proceedings of the International Conference on Durability of Concrete Structures," Vol.1, pp. 563-569, 2008
- IStructE, "Structural Effects of Alkali-Silica Reaction, Technical Guidance on the Appraisal of Existing Structures," The Institution of Structural Engineers, London, England, 1992
- Jensen, D., Chatterji, S., Christensen, P., and Thallow, P., "Studies of alkali-silica reaction. Part II - effect of air entrainment on expansion," *Cement and Concrete Research*, Vol. 14, pp. 311-315, 1984
- Jensen, V., "Alkali-aggregate reaction in Southern Norway," PhD Dissertation, Division of Geology and Mineral Resources Engineering, The Norwegian, Institute of Technology, University of Trondheim, 1993

- Johnston, D., Stokes, D., Fournier, B., and Surdahl, R., "Kinetic characteristics of ASTM C 1260 testing and ASR-induced concrete damage", International Conference on Alkali-aggregate Reaction in Concrete (12th; 2004; Beijing, China), pp. 338-346, 2004
- Johnston, D., Stokes, D., and Surdahl, R., "A kinetic-based method for interpreting ASTM C 1260," Cement, Concrete and Aggregates, Vol. 22, No. 2, pp. 142-149, 2000
- Johnston, D., Stokes, D., and Surdahl, R., "Construction of lithium/fly ash concrete pavement test sections in interstate 90 in SD," Annual Meeting CD-ROM, Transportation Research Board, 2003
- Jones, A.E.K., and Clark, L.A., "The effects of ASR on the properties of concrete and the implications for assessment," Engineering Structures, Vol. 20, No. 9, pp. 785-791, 1997
- Kapitan, J.G., "Structural assessment of bridge piers with damage similar to alkali-silica reaction and/or delayed ettringite formation," Masters Thesis, University of Texas at Austin, 2006
- Kobayashi, K., Mori, Y., and Nomura, K., "Method of diagnosing alkali-silica reaction by compressive loading test," Journal of Hydraulic, Coastal and Environmental Engineering, No. 460, Vol. 5-18, pp. 151-154, 1993
- Kodera, T., and Kawamura, M., "Effects of externally supplied lithium on the suppression of ASR expansion in mortars," Cement and Concrete Research, Vol. 35, pp. 494-498, 2005
- Korkanç, M., and Tuğrul, A., "Evaluation of selected basalts from the point of alkali-silica reactivity," Cement and Concrete Research, Vol. 35, No. 3, pp. 505-512, 2005
- Kosmatka, S.H., Kerkhoff, B., and Panareses, W.C., "Design and control of concrete mixtures," 14th edition, Engineering bulletin 001, Portland Cement Association, 2002
- Kosmatka, S.H., Kerkhoff, B., and Panarese, W.C., "Design and control of concrete mixtures," Engineering Bulletin 001, 14th edition, Portland Cement Association, Skokie, Illinois, USA, 372 pp., 2002
- Kurtis, K.E., "Transmission soft X-ray microscopy of the alkali-silica reaction," PhD Dissertation, Department of Civil Engineering, University of California at Berkeley, 1998
- Lane, D. S., "Alkali-Silica Reactivity in Virginia," Virginia Transportation Research Council, Final Report No. VTRC 94-R17, 1994

- Lane, D. S., "Laboratory investigation of lithium-bearing compounds for use in concrete," Virginia Transportation Research Council, Charlottesville, VA, USA, Report No. VTRC 02-R16, 2002
- Lane, D. S., and Ozyildirim, C., "Preventive measures for alkali-silica reactions (binary and ternary systems)," *Cement and Concrete Research*, Vol. 29, pp. 1281-1288, 1999
- Lawrence, M., and Vivian, H.F., "The reactions of various alkalies with silica," *Australian Journal of Applied Science*, Vol. 12, No. 1, pp. 96-103, 1961
- Lea, F.M., "The chemistry of cement and concrete," 3rd edition, Chemical Publishing Company Inc., New York, 1970
- Lee, C., "Active alkalis in cement-fly ash paste." *Proceedings: Eighth International Conference on Alkali-Aggregate Reactions*. Kyoto, Japan. pp. 223-228, 1989
- Leger, P., Cote, P., and Tinawi, R., "Finite element analysis of concrete swelling due to alkali-aggregate reactions in dams," *Computers and Structures*, Vol. 60, No. 4, pp. 601-611, 1996
- Leming, M.L., Mitchell, J.F., Johnson, J.K., and Ahmad, S.H. "Investigation of alkali-silica reactivity in North Carolina Highway Structures," Department of Civil Engineering, North Carolina State University, 1996
- Li, X., "Mitigating alkali silica reaction in recycled concrete," PhD Dissertation, Department of civil engineering, University of New Hampshire, USA, 2005
- Lu, D., Mei, L., Xu, X., Tang, M., Mo, X., and Fournier, B., "Alteration of alkali reactive aggregate to alkali-aggregate reaction in concrete (II) expansion and microstructure of concrete microbar," *Cement and Concrete Research*, Vol. 36, pp. 1191-1200, 2006
- Lu, Y.N., Lian, X.H., and Tang, M.S., "Study of the components and microstructure of alkali carbonate rock," *Proceedings, 5th Symposium on Cement Chemistry and Analysis Techniques*, Nanjing (China), Oct. 1992
- Ludwig, N.C., and Pence, S.A., "Properties of Portland cement pastes cured at elevated temperatures and pressures," *Journal of the American Concrete Institute*, Vol. 27, No. 6, pp. 673- 687, 1956
- Lumley, J.S., "ASR suppression by lithium compounds," *Cement and Concrete Research*, Vol. 27, No. 2, pp. 235-244, 1997
- Malvar, L., Cline, G., Burke, D., Rollings, R., Sherman, T., and Greene, J., "Alkali-silica reaction mitigation: State-of-the-Art and recommendations," *ACI Material Journals*, Vol. 99, No. 5, 2002

- Malvar, L.J., and Lenke, L.R., "Minimum fly ash cement replacement to mitigate alkali silica reaction," *Cement and Concrete 1: Alkali & silica reaction 2005* Accessed from <http://www.flyash.info/2005/170mal.pdf>
- Malvar, J., and Lenke, L.R., "Efficiency of fly ash in mitigating alkali-silica reaction based on chemical composition," *ACI Materials Journal*, Vol. 103, No. 5, pp. 319-326, 2006
- Marzouk, H., and Langdon, S., "The effect of alkali-aggregate reactivity on the mechanical properties of high and normal strength concrete," *Cement and Concrete Composites*, Vol. 25, pp. 549-556, 2003
- Mather, B., "How to make concrete that will not suffer deleterious alkali-silica reactions," *Cement and Concrete Research*, Vol. 29, pp. 1277-1280, 1999
- McCoy, W.J., and Caldwell, A.G., "A new approach to inhibiting alkali-aggregate expansion," *Journal of the American Concrete Institute*, Vol. 47, pp. 693-706, 1951
- McKeen, R.G., Lenke, L.R., and Pallachulla, K.K., "Mitigation of alkali-silica reactivity in New Mexico," Work performed for New Mexico State Highway and Transportation Department, Materials Research Center, ATR Institute, University of New Mexico, 1998
- Millard, M.J., and Kurtis, K.E. "Effects of Lithium Nitrate Admixture on Early-Age Cement Hydration," *Cement and Concrete Research*, Vol. 38, No. 4, pp. 500-510, 2008
- Mingshu, T., Min, D., Xianghu, L., and Sufen, H., "Studies on alkali-carbonate reaction," *ACI Material Journals*, Vol. 91, No. 1, pp. 26-29, 1994
- Mindess, S., Young, J.F., and Darwin, A., "Concrete," 2nd Edition, Pearson Education Ltd., 2002
- Mitchell, L.D., Beaudoin, J.J., and Grattan-Bellew, P., "The effects of lithium hydroxide solution on alkali silica reaction gels created with opal," *Cement and Concrete Research*, Vol. 34, No. 4, pp. 641-649, 2004
- Mo, X., Jin, T., Li, G., Wang, K., Xu, Z., and Tang, M., "Alkali-aggregate reaction suppressed by chemical admixture at 80°C," *Construction and Building Materials*, Vol. 19, pp. 473-479, 2005
- Mo, X., Yu, C., and Xu, Z., "Long-term effectiveness and mechanism of Li (OH) in inhibiting alkali-silica reaction," *Cement and Concrete Research*, Vol. 33, pp. 115-119, 2003

- Mo, X., Zhang, Y., Yao, J., Li, G., and Feng, Y., "Influence of various parameters on Li_2CO_3 against alkali-silica reaction," *Construction and Building Materials*, Vol. 22, pp. 1668-1674, 2008
- Mohammed, I., Ronel, S., and Curtil, L., "Influence of composite materials confinement on alkali-aggregate mechanical behavior," *Materials and Structures*, Vol. 39, pp. 479-490, 2006
- Monette, L., Gardner, J., and Grattan-Gellew, P., "Structural effects of the alkali-silica reaction on non-loaded and loaded reinforced concrete beam," 11th International Conference on Alkali-Aggregate Reaction, Quebec, Canada, pp. 999-1008, 2000
- Monteiro, P.J.M., Wang, K., Sposito, G., Santos, M.C., and Andrade, W.P., "Influence of mineral admixtures on the alkali-aggregate reaction," *Cement and Concrete Research*, Vol. 27, No. 12, pp. 1899-1909, 1997
- Nishibayashi, S., Okada, K., Kawamura, M., Kobayashi, K., Kojima, T., Miyagawa, T., Nakano, K., and Ono, K., "Alkali-silica reaction-Japanese experience," Chapter 10 of *The alkali-silica reaction in concrete*, Editor Swamy, Blackie and Son Ltd., Glasgow, London, 1992
- Nixon, P.J., and Bollinghaus, R., "The effect of alkali aggregate reaction on the tensile and compressive strength of concrete," *Durability of Building Materials*, Vol. 2, pp. 243-248, 1985
- Nixon, P., and Sims, I., "Testing aggregates for alkali-reactivity," Report of ILEM TC-106: alkali-aggregate reaction-accelerated tests, *Materials and Structures*, Vol. 29, pp. 323-334, 1996
- Nixon, P.J., and Sims, I., "RILEM TC-106: alkali-aggregate reaction-accelerated tests interim report and summary of national specifications," *Proceeding of the 9th International Conference on alkali-aggregate reaction in concrete*, Vol. 2, published by the Concrete Society, Slough, pp. 731-738, 1992
- Oberholster, R.E., and Davies, G., "An accelerated method for testing the potential reactivity of siliceous aggregates," *Cement and Concrete Research*, Vol. 16, pp. 181-189, 1986
- Ohama, Y., Demura, K., and Kakegawa, M. "Inhibiting alkali-aggregate reaction with chemical admixtures." *Proceedings of the 8th International Conference on Alkali-Aggregate Reaction*, (Ed. K.Okada, S. Nishibayashi, and M. Kawamura), Kyoto, Japan, pp. 253-258, 1989
- Ozol, M. A., "Alkali-carbonate rock reaction," *Significance of tests and properties of concrete and concrete making materials*, ASTM STP 169C, edited by Klieger, Paul,

- and Lamond, Joseph, F., American Society for Testing and Materials, Philadelphia, pp. 372-387, 1994
- PCA IS413, "Diagnosis and control of alkali-silica reaction in concrete," PCA R&D Serial No. 2071, Portland Cement Association, 1997
- Pedneault, A. "Development of testing and analytical procedures for the evaluation of the residual potential of reaction, expansion and deterioration of concrete affected by ASR," M.Sc. Memoir, Laval University, Québec City, Canada, 133 pp., 1996
- Pietruszezak, S., "On the mechanical behavior of concrete subjected to alkali-aggregate reaction," Computers and Structures, Vol. 58, No. 6, pp. 1093-1097, 1996
- Philpotts, A.R., "Principles of igneous and metamorphic petrology," Prentice Hall Publication, ISBN 013691361-X, 1990
- Poole, A.B., "Alkali carbonate reaction in concrete," Proceeding, 5th International Conference on AAR in concrete, Cape Town, S252/34, 9 pp., 1981
- Prezzi, M., Monteiro, Paulo J. M., and Sposito, G., "The alkali-silica reaction, Part I: Use of the Double-Layer Theory to Explain the Behavior of Reaction-Product Gels," ACI Materials Journal, Vol. 94, No. 1, pp. 10-17, 1997.
- Qinghan, B., Nishibayashi, S., Xuequan, W., Yoshino, A., Hong, Z., Tiecheng, W., and Mingshu, T., "Preliminary study of effect of LiNO₂ on expansion of mortars subjected to alkali-silica reaction," Cement and Concrete Research, Vol. 25, No. 8, pp. 1647-1654, 1995
- Ramachandran, V.S., "Alkali-aggregate expansion inhibiting admixtures," Cement and Concrete Composites, Vol. 20, pp. 149-161, 1997
- Ramyar, K., Çopuroğlu, O., Andiç Ö., and Fraaij, A.L.A., "Comparison of alkali-silica reaction products of fly ash of lithium salt bearing mortar under long-term accelerated curing," Cement and Concrete Research, Vol. 34, pp. 1179-1183, 2004
- Rivard, P., and Ballivy, G., "Assessment of the expansion related to alkali-silica reaction by the Damage Rating Index method," Construction and Building Materials, Vol. 19, pp. 83-90, 2005
- Rangaraju, P.R., Sompura, K.R., and Olek, J., "Modified ASTM C 1293 test method to investigate potential of potassium acetate deicer solution to cause alkali-silica reaction," Transportation Research Record, No. 2020, pp. 50-60, 2007
- RILEM Report 7, "Fly ash in concrete: properties and performance," Edited by Wesche, K., ISBN 0419-15790-5, Taylor & Francis Publication, 1990

- Rogers, C.A., "Alkali-Aggregate Reactivity in Canada," *Cement and Concrete Composites*, Vol. 15, No. 1, pp. 13-19, 1993
- Rogers, C.A., "Multi-laboratory study of the accelerated mortar bar test (ASTM C 1260) for alkali-silica reaction," *Cement, Concrete and Aggregates*, CCAGDP, Vol. 21, Is. 2, pp. 185-194, 1999
- Rogers, C.A., and Hooton, R.D., "Reduction in mortar and concrete expansion with reactive aggregates due to alkali leaching," *Cement, Concrete and Aggregates*, CCAGDP, Vol. 13, No. 1, pp. 42-49, 1991
- Rotter, H., "The impact of alkali aggregate reactions on the fracture mechanics of concrete," PhD Dissertation, T-U Vienna Austria, 1996
- Sarkar, S.L., Zollinger, D.G., Mukhopadhyay, A.K., Seungwook, L., and Shon, C.-S., "Handbook for identification of alkali-silica reactivity in airfield pavements," Advisory Circular, No. 150/5380-6, U.S. Department of Transportation, Federal Aviation Administration, 2004 at <http://www.faa.gov/arp/150acs.cfm>
- Savva, A., Manita, P., and Sideris, K.K., "Influence of elevated temperatures on the mechanical properties of blended cement concretes prepared with limestone and siliceous aggregates," *Cement and Concrete Composites*, Vol. 27, pp. 239-248, 2005
- Shehata, M.H., and Thomas, M.D.A., "The effect of fly ash composition on the expansion of concrete due to alkali-silica reaction," *Cement and Concrete Research*, Vol. 30, pp. 1063-1072, 2000
- Shehata, M.H., and Thomas, M.D.A., "Use of ternary blends containing silica fume and fly ash to suppress expansion due to alkali-silica reaction in concrete," *Cement and Concrete Research*, Vol. 32, pp. 341-349, 2002
- Shon, C.-S., Sarkar, S.L., and Zollinger, D.G., "Testing the effectiveness of Class C and Class F fly ash in controlling expansion due to alkali-silica reaction using modified ASTM C 1260 test method," *Journal of Materials in Civil Engineering*, Vol. 16, No. 1, pp. 20-27, 2004
- Shon, C.S., Zollinger, D.G., and Sarkar, S., "Evaluation of modified ASTM C 1260 accelerated mortar bar test for alkali-silica reactivity," *Cement and Concrete Research*, Vol. 32, pp. 1981-1987, 2002a
- Shon, C.-S., Zollinger, D.G., and Sarkar, S.L., "Alkali-silica reactivity resistance of high-volume fly ash cementitious systems," *Journal of the Transportation Research Board*, Vol. 1798, pp. 17-21, 2002b
- Sims, I., "Alkali-silica reaction-UK experience", 1992, in Swamy (1992), Chapter 5

- Smaoui, N., Bérubé, M.A., Fournier, B., Bissonnette, B., and Durand, B., "Effects of alkali addition on the mechanical properties and durability of concrete," *Cement and Concrete Research*, Vol. 35, pp. 203-212, 2005
- Smaoui, N., Bissonnette, B., Berube, M.-A., Fournier, B., and Durand, B., "Mechanical properties of ASR-affected concrete containing fine and coarse aggregates," *Journal of ASTM International*, Vol. 3, No. 3, paper IN JAI12010, 2006
- Stanton, T.E., "Expansion of concrete through reaction between cement and aggregate," *Proceedings of the American Society of Civil Engineers*, Vol. 66, No. 10, pp. 1781-1811, 1940
- Stark, D., "Alkali-silica reactivity in the Rocky mountain region," *Proceedings of the 4th International Conference on effects of alkalis in cement and concrete*, Publication No. CE-MAT-1-78, Purdue University, W. Lafayette, IN, pp. 235-243, 1978
- Stark, D., and Bhatti, M.S.Y., "Alkali-silica reactivity: effect of alkali in aggregate on expansion," *Alkalies in Concrete*, ASTM STP 930, American Society for Testing and Materials, Philadelphia, PA, pp 16-30, 1986
- Stark, D., Morgan, B., Okamoto, P., and Diamond, S., "Eliminating or minimizing alkali-silica reactivity," *Strategic Highway Research Program*, SHRP-P-343, Washington, DC, 49 pp., Jan. 1993
- Stokes, D., "ASR control: testing and material properties," 82nd Annual NESMEA Conference, Newark, DE, USA, 2006
- Stokowski, Jr., Steven, J., and Sarson, J., "Alkali-carbonate reactivity in concrete," *Stone Products Consultants*, Ashland, Massachusetts, USA
http://members.aol.com/CrushStone/fly_acr.htm
- Swamy, R.N., Editor, "The alkali-silica reaction in concrete," Blackie and Son Ltd., Glasgow, London, 1992
- Swamy, R.N., and Al-Asali, M.M., "Influence of alkali-silica reaction on the engineering properties of concrete," *Alkalies in Concrete*, ASTM STP 930, V.H. Dodson, Ed., American Society of Testing and Materials, Philadelphia, pp. 69-86, 1986
- Swamy, R.N., and Al-Asali, M.M., "Engineering properties of concrete affected by alkali-silica reaction," *ACI Materials Journal (Technical Paper)*, Vol. 85, pp.367-374, Sep-Oct., 1988
- Swenson, E.G., and Gillott, J.E., "Alkali reactivity of dolomitic limestone aggregate," *Mazagine of Concrete Research*, Cement and Concrete Association, Vol. 19, No. 59, pp. 95-104, 1967

- Taha, B., and Nounu, G., "Using lithium nitrate and pozzolanic glass powder in concrete as ASR suppressors 2008," *Cement and Concrete Composites*, Vol. 30, pp. 497-505, 2008
- Tambelli, C.E., Schneider, J.F., Hasparyk, N.P., and Monteiro, P.J.M., "Study of the structure of alkali-silica reaction gel by high-resolution NMR spectroscopy," *Journal of Non-Crystalline Solids*, Vol. 352, pp. 3429-3436, 2006
- Tang, M., Deng, M., Lon, X., and Han, S., "Studies of alkali-carbonate reaction," *ACI Materials Journal*, Farmington Hills, Michigan, pp. 26-29, Jan.-Feb., 1994
- Tang, M.S., Lou, Z., and Han, S., "Mechanism of alkali-carbonate reaction," *Proceedings, 7th International conference on concrete alkali-aggregate reactions*, Ottawa, Canada, pp. 275-279, 1986
- Tarek, M.U., Hamada, H., and Yamaji, T., "Alkali-silica reaction-induced strains over concrete surface and steel bars in concrete," *ACI Materials Journal*, Technical Paper, Vol. 100, No. 2, 2003
- Tauma, E.W., Fowler, D.W., and Carrasquillo, R.L., "Alkali-silica reaction in Portland cement concrete: testing methods alternatives," *International Center for Aggregates Research (ICAR), Research Report ICAR-301-1f*, 2001
(http://www.engr.utexas.edu/icar/reports/301_1F/301_1Cvr.pdf accessed on 09/12/2005)
- Technical Overview (Fly Ash Brochure), "Fly ash for concrete," *Headwaters resource*, 16 pp. at http://www.flyash.com/data/upimages/press/HWR_brochure_flyash.pdf assessed on December 9, 2008
- Thomas, M.D.A., Blackwell, B.Q., and Pettifer, K., "Suppression of damage from alkali silica reaction by fly ash in concrete dams," *Proceedings of the 9th International Conference on Alkali-Aggregate Reaction in Concrete*, (held in London, United Kingdom, 1992), Vol. 2, Published by the Concrete Society, Slough, pp. 1059-1066, 1992
- Thomas, M.D.A., and Bleszynski, R.F., "The use of silica fume to control expansion due to alkali-aggregate reactivity in concrete - review," *Materials Science of Concrete*, Eds. J. Skalny and S. Mindess, American Ceramic Society, Vol. 6, 2000
- Thomas, M.D.A., Shehata, M.H., Shashiprakash, S.G., Hopkins, D.S., and Cail, K., "Use of ternary cementitious systems containing silica fumes and fly ash in concrete," *Cement and Concrete Research*, Vol. 29, No. 8, pp. 1207-1214, 1999
- Thomas, M.D.A., and Stokes, D.B., "Use of a lithium-bearing admixture to suppress expansion in concrete due to alkali-silica reaction," *Transportation Research Record*, Vol. 1668, Paper No. 99-1062, pp. 54-59, 1999

- Thomas, M., Fournier, B., Folliard, K., Shehata, M., Ideker, J., and Rogers, C.,
 “Performance limits for evaluating supplementary cementing materials using the
 accelerated mortar bar test,” PCA R&D Serial No. 2892, Portland Cement
 Association, Skokie, Illinois, USA, 22 pp., 2005
- Thomas, M.D.A., and Stokes, D.B., “Use of a lithium-bearing admixture to suppress
 expansion in concrete due to alkali-silica reaction,” Transportation Research Record,
 Vol. 1668, paper no. 99-1062, pp. 54-59, 1999
- Thomas, M.D.A., Fournier, B., Folliard, K.J., Ideker, J.H., and Resendez, Y., “The use of
 lithium to prevent or mitigate alkali-silica reaction in concrete pavements and
 structures,” U.S. Department of Transportation, Federal Highway Administration,
 FHWA-HRT-06-133, 47 pp., 2007
- Touma, W.E., Fowler, D.W., and Carrasquillo, R.L., “Alkali-silica reaction in Portland
 cement concrete: testing methods and mitigation alternatives,” International Center
 for Aggregates Research, Texas, USA, Research Report ICAR 301-1f, 2001
- Touma, W.F., Fowler, D.W., Carrasquillo, R.L., Folliard, K.J., and Nelson, N.R.,
 “Characterizing alkali-silica reactivity of aggregates using ASTM C 1293, ASTM C
 1260 and their modifications,” Transportation Research Record, Record No. 1757,
 pp. 157-165, 2002
- Tremblay, C., Bérubé, M.A., Fournier, B., and Thomas, M.D.A. “Performance of
 Lithium-based Products Against ASR: Effect of Aggregate Type and Reactivity, and
 Reaction Mechanisms,” Proceedings of the 7th CANMET/ACI International
 Conference on Recent Advances in Concrete Technology (suppl. Papers), Las Vegas,
 NV, pp. 247–267, 2004
- Tremblay, C., Berube, M.-A., Fournier, B., Thomas, M.D.A., and Folliard, K.J.,
 “Effectiveness of lithium-based products in concrete made with Canadian natural
 aggregates susceptible to alkali-silica reactivity,” ACI Materials Journal, Vol. 104,
 No.2, pp. 195-205, 2007
- Turanli, L., Shomglin, K., Ostertag, C.P., and Monteiro, P.J.M., “Reduction in alkali-
 silica expansion due to steel microfibers,” Cement and concrete research, Vol. 31, pp.
 825- 827, 2001
- Tuthill, L., "Alkali-silica reaction-40 years later," Concrete International, pp. 32-36, 1982
- Ulm, F.J., Coussy, O., Kefei, L., and Larive, C., “Thermo-chemo-mechanics of ASR
 expansion in concrete structures,” Engineering Mechanics, Vol. 126, No. 3, pp. 233-
 242, 2000

- U.S. Department of Transportation, Federal Aviation Administration, Northwest Mountain Region Revision to AC 150/5370-10B, "Standards for specifying construction of airports," Ann notice B-2 6/06, 2006
- Walker, N., "Chemical reactions of carbonate aggregates in cement paste," American Society for Testing and Materials, ASTM STP 169B, West Conshohocken, PA, USA, pp. 722-734, 1974
- Wang, H., and Gillott, J.E., "Effect of three zeolite-containing natural pozzolanic materials on alkali-silica reaction," Cement and Concrete Research, Vol. 15, pp. 24-30, 1993
- Wang, H., and Gillott, J.E., "The effect of superplasticizers on alkali-silica reactivity," Proceedings of the 8th International Conference on Alkali-Aggregate Reaction, Kyoto, Japan, pp. 187-192, 1989
- Will, J.J., "High-performance concrete using Nevada aggregates," MS Thesis Paper, Department of Civil Engineering, University of Nevada Reno, 2000
- Wood, H., "Durability in concrete construction," Monograph No.4, American Concrete Institute, Detroit, MI, 1968
- Van Aardt, J.H.P., and Visser, S., "Reactions between rocks and the hydroxides of calcium, sodium and potassium." Progress Report Part 2, CSIR Research Report BRR 577, Pretoria, 1982
- Xiang-yin, M., Zhong-zi, X., Ke-ru, W., and Ming-shu, T., "Alkali-silica reaction inhibited by LiOH and its mechanism," Journal of Wudan University of Technology-Material Science Edition, Vol. 18, No. 1, 2003
- Xu, G.J.Z., Watt, D.F., and Hudec, P.P., "Effectiveness of mineral admixtures in reducing ASR expansion," Cement and Concrete Research, Vol. 25, No. 6, pp. 1225-1236, 1995
- Yi, C.K., and Ostertag, C.P., "Mechanical approach in mitigating alkali-silica reaction," Cement and Concrete Research, Vol. 35, pp. 67-75, 2005
- Youssef, M.A., and Moftah, M., "General stress-strain relationship for concrete at elevated temperatures," Engineering Structures, Vol. 29, pp. 2618-2634, 2007
- Zhang, C., Wang, A., Tang, M., Wu, B., and Zhang, N., "Influence of aggregate size grading on ASR expansion," Cement and Concrete Research, Vol. 29, pp. 1393-1396, 1999

VITA

Graduate College
University of Nevada, Las Vegas

Mohammad Shahidul Islam

Local Address:

1525 Pinto Lane, #42
Las Vegas, NV, 89106

Home Address :

C/O: Abdul Halim Mollah
Uttar Tepakhola (Munsi Bari)
Faridpur Sadar, Faridpur 7800
Bangladesh

Degrees:

Bachelor of Science, Civil Engineering, 1999
Bangladesh University of Engineering and Technology (BUET), Bangladesh

Master of Science, Computer Science, 2003
Texas A&M University at Commerce (TAMUC), USA

Special Honors and Awards:

Tau Beta Pi Engineering Honor Society, 2005
Phi Kappa Phi, 2005
Golden Key, 2008
Excellence in Teaching Merit Recognition at UNLV, 2008
International Scholarship at UNLV, 2008-2009
GPSA Research Awards at UNLV, 2006 – 2009
GPSA Service Award at UNLV, 2010
Housing Scholarship at TAMUC, 2001 - 2002
University Scholarship at BUET, 1995 - 1999

Journal Articles:

1. Ghafoori, N. and Islam, M., “Alkali-silica reactivity as affected by the soak solution concentrations,”
2. Ghafoori, N. and Islam, M., “The influence of cement alkalis on alkali-silica reactivity of Portland cement concrete,”
3. Islam, M. and Ghafoori, N., “Use of Class F fly ash in mitigating ASR expansion,”
4. Ghafoori, N. and Islam, M., “Reduction in alkali-silica reactivity by lithium nitrate,”
5. Ghafoori, N. and Islam, M., “Role of alkali-silica reactivity on mechanical properties of Portland cement concrete,”

Conference Proceedings:

1. Ghafoori, N. and Islam, M. "Optimization of fly ash content in suppressing alkali-silica reactivity," The 5th International Structural Engineering and Construction Conference, Las Vegas, NV, September 21-27, pp. 533-538, 2009
2. Ghafoori, N. and Islam, M. "Evaluation of alkali-silica reactivity using mineralogy of aggregates and the expansion tests," The 5th International Structural Engineering and Construction Conference, Las Vegas, NV, September 22-25, pp. 467-472, 2009
3. Ghafoori, N. and Islam, M., "lithium salt for reactive aggregates in Portland cement concrete," 2nd International Conference on Sustainable Construction Materials and Technologies, Ancona, Italy, June 28 - 30, 2010
4. Ghafoori, N. and Islam, M., "Combined use of Class F fly ash and lithium salt for the reduction of alkali-silica reactivity," Sixth International Conference on concrete under severe conditions, Yucatan, Mexico, June 7-9, 2010
5. Ghafoori, N. and Islam, M., "Influence of alkali-silica reactivity in concrete stiffness,"
6. Islam, M. and Ghafoori, N. "Assessing alkali-silica reactivity using the early and extended failure criteria of modified ASTM C 1293,"
7. Islam, M. and Ghafoori, N. "Analysis of expansion test results of ASTM C 1260 for assessing alkali-silica reactivity"

Dissertation Title: "Performance of Nevada's aggregates in alkali-aggregate reactivity of Portland cement concrete"

Dissertation Examination Committee:

Chairperson, Nader Ghafoori, Ph.D.
Committee Member, Samaan Ladkany, Ph.D.
Committee Member, Ying Tian, Ph.D.
Committee Member, Pradip Bhowmik, Ph.D.
Graduate College Faculty Representative, Clay Crow, Ph.D.